ISSN: 0009-7411

CIRUGÍA Y CIRUJANOS

ÓRGANO DE DIFUSIÓN CIENTÍFICA DE LA ACADEMIA MEXICANA DE CIRUGÍA

FUNDADA EN 1933

Contenido

Artículos originales

PERMANYER MÉXICO
www.permanyer.com

Volumen 93, No. 2, Marzo-Abril 2025

Indexada en WoS Core Collection/SCIETM; MEDLINE/PubMed

10985AMEX252

ORIGINAL ARTICLE

The correlation histopathological and conventional/advanced MRI techniques in glial tumors

La correlación histopatológica y la resonancia magnética convencionales/avanzadas en tumores gliales

Selim Seker[1], Tamer Altay[2], Ece Uysal[2], Hidayet S. Cine[3], Ahmed Y. Yavuz[2], and Idris Avci[4]*

[1]Department of Neurosurgery, Istinye University, Liv Hospital; [2]Department of Neurosurgery, University of Health Sciences, Prof. Dr. Cemil Tascioglu City Hospital; [3]Department of Neurosurgery, Istanbul Medeniyet University, Prof. Dr. Suleyman Yalcin City Hospital; [4]Department of Neurosurgery, Spinal Health Center, Memorial Hospital. Istanbul, Turkey

Abstract

Objective: *We aimed to elucidate the histopathological pre-diagnosis of cranial gliomas with magnetic resonance imaging (MRI) techniques in gliomas.* **Method:** *A total of 82 glioma patients were enrolled to our study. Pre-operative conventional MRI images (non-contrast T1/T2/flair/contrast-enhanced T1) and advanced MRI images (DAG and ADC mapping, MRI spectroscopy and perfusion MRI [PMRI]) were analyzed.* **Results:** *Conventional MRI alone is useful in radiological pre-evaluation in low-grade glioma in 54.8% and 86.3% in high-grade glioma. Additional advanced MRI techniques were beneficial in comparing low-grade gliomas in 98% and 83.9% in high-grade glioma. On ROC analysis, ADC cutoff value 0.905 mm²/s (p = 0.001), rCBV cutoff value 1.77 (p = 0.001), Cho/NAA cut-off value 2.20 (p = 0.001), and Cho/Cr cutoff value 2.01 (p = 0.001) were achieved. Significant results were obtained when ADC, Cho/NAA, and Cho/Cr were analyzed into four histopathologically grade groups besides (p = 0.001). NAA/Cr values were not significant in pathological grading. rCBV measurements were statistically significant between Grades I and IV and between II and IV.* **Conclusion:** *Using additional advanced MRI techniques such as PMRI, magnetic resonance spectroscopy, and DWI with conventional MRI could enhance the accuracy of histopathological grading in cranial glioma.*

Keywords: *Glioma. MR spectroscopy. Perfusion MRI. Diffusion-weighted MRI. Histopathological grading.*

Resumen

Objetivo: *Nos propusimos dilucidar el pre-diagnóstico histopatológico de los gliomas craneales con técnicas de resonancia magnética en gliomas.* **Método:** *Un total de 82 pacientes con glioma fueron incluidos en nuestro estudio. Se analizaron imágenes pre-operatorias de RM convencional (T1/T2/flair/contraste realzado T1) e imágenes de RM avanzada (mapeo DAG y ADC, espectroscopia de RM y RM de perfusión).* **Resultados:** *Las técnicas avanzadas adicionales de RM fueron beneficiosas en la comparación de los gliomas de bajo grado en el 98% y en el 83,9% en el glioma de alto grado. En el análisis ROC se alcanzó un valor de corte ADC de 0,905 mm²/s (p = 0,001), un valor de corte rCBV de 1,77 (p = 0,001), un valor de corte Cho/NAA de 2,20 (p = 0,001) y un valor de corte Cho/Cr de 2,01 (p = 0,001). Se obtuvieron resultados significativos cuando se analizaron ADC, Cho/NAA y Cho/Cr en cuatro grupos de grado histopatológico además (p = 0,001). Los valores de NAA/Cr no fueron significativos en la gradación patológica. Las mediciones de rCBV fueron estadísticamente significativas entre*

Correspondence:
Hidayet S. Cine
E-mail: cinesafak@gmail.com

Date of reception: 27-12-2023
Date of acceptance: 13-02-2024
DOI: 10.24875/CIRU.23000648

Cir Cir. 2025;93(2):129-137
Contents available at PubMed
www.cirugiaycirujanos.com

los grados I y IV y entre II y IV. **Conclusión:** *El uso de técnicas avanzadas adicionales de RM como la RMMP, la ERM y la DWI junto con la RM convencional podría mejorar la precisión de la gradación histopatológica en el glioma craneal.*

Palabras clave: *Glioma. Espectroscopia de RM. RM de perfusión. RM ponderada en difusión. Graduación histopatológica.*

Introduction

Imaging methods in gliomas are aimed at pre-operative diagnosis, determining tumor grade and prognosis, radiotherapy and surgical planning, and guiding treatment. The most commonly used imaging method is contrast-enhanced magnetic resonance imaging (MRI). Conventional MRI plays a primary role in evaluating tumor localization, heterogeneity, vascularization, contrast enhancement, peri-tumoral edema, and proximity to important anatomical-functional centers. Secondary tumor findings such as cystic formations, calcification (oligodendroglioma), necrosis (glioblastoma), and hemorrhage (high-grade glioma) are guiding in the differential diagnosis[1,2]. The World Health Organization (WHO) classification is inadequate in important issues such as the anatomical localization of the tumor, its size, degree of surgical accessibility or resectability, biological behavior, and prediction of response to treatment. Similarly, conventional MRI is limited in predicting these criteria. For this reason, the use of various functional MRI methods is preferred to determine the tumor degree[3].

Magnetic resonance spectroscopy (MRS) is a non-invasive functional MRI method that provides biochemical and metabolic information about the tissue. The most important differential diagnosis in this neuroimaging is the distinction between neoplastic-non-neoplastic or low-high-grade tumors[4]. Perfusion MRI (PMRI) is a non-invasive functional MRI method that provides information about tissue blood flow, *in vivo* tumor angiogenesis, and tumor microcirculation at the microscopic level. Increased vascularity corresponds to increased tumor stage and maximum cerebral blood volume (CBV)[5].

Gliomas are the most common brain neoplasm in adults and a major cause of mortality and morbidity. According to the revised WHO classification, central nervous system tumors are grouped based on microscopic imaging. In this classification, neuroepithelial tumors are divided into astrocytic neoplasms, oligodendroglial, oligoastrocytic, ependymal, and choroid plexus tumors. The tumor stage indicates the degree of malignancy and is closely related to survival and prognosis. Staging of gliomas is performed by taking into account histopathologically the presence of mitotic activity, necrosis, and infiltration, which indicate uncontrolled growth and the vascularity of the tumor. The tumor is graded from Grade I to Grade IV: I–II is considered low grade, and III–IV is regarded as high grade. Increased cellularity, atypic cells, and an increase in mitotic activity, endothelial hyperplasia, necrosis, and angiogenesis are additionally observed in Grade IV glioblastomas[6].

In recent years, MRI has changed from the morphological imaging of the tissue to the functional, metabolic, cellular characterization, and secondary biological behavior of the tumor, and to predict the diagnosis, grade, response to treatment, and prognosis with advanced imaging methods. The MRI sequences, including non-contrast T1, T2, FLAIR, contrast-enhanced T1, MRS, PMRI, and diffusion MRI, were performed. Choline (Cho)/N-acetyl aspartate (NAA), NAA/Creatine (Cr), and Cho/Cr ratios, as well as lipid and lactate levels, are utilized as markers, especially useful in the diagnosis of tumoral lesions but provide limited insight into the malignancy level of the tumor[7].

Within the scope of this research, we aimed to elucidate the histopathological pre-diagnosis of cranial gliomas with conventional and advanced MRI techniques (DWI, PMRI, MRS, and ADC values) and investigate the integration of these visual tools in high and low-grade gliomas.

Method

In this research, patients who underwent MRI with the preliminary diagnosis of an intracranial mass were scanned backward from the picture archiving and communication system, and 82 cases with glial tumors between the ages of 15–94 were retrospectively analyzed. Conventional MRI findings, contrast enhancement features, DWI, MRS, PMRI findings, and ADC values were compared with pathology results. All procedures followed were in accordance with the ethical standards of the responsible committee on human experimentation (institutional and national) and with the Helsinki Declaration of 1975, as revised in 2008. Ethics committee approval was granted from our institution

on 27/08/2019 with protocol number 48670771-514.10, and informed consent has been obtained from all participants.

MRI, MRS, PMRI, and ADC measurements

Conventional brain MRI, diffusion, MRS, and PMRI examinations were performed using a 1.5 Tesla MRI device (Magnetom Aera, Siemens, Erlangen, Germany) and a brain coil. The standard brain MRI protocol includes T1-weighted imaging with TR = 426 ms, TE = 99 ms, and slice thickness of 5 mm; T2-weighted imaging with TR = 4350 ms, TE = 102 ms, and slice thickness of 5 mm. In FLAIR sequences, TR = 9000 ms, TE = 86 ms, and slice thickness of 5 mm. For SWI imaging, TR = 49 ms and TE = 40 ms. Contrast-enhanced examinations were performed using 0.5 mmol/ml gadoteric acid. In contrast-enhanced T1-weighted imaging, TR is 402 ms and TE is 5.6 ms.

DWI was taken as TR = 4500 msec, TE = 98 msec, and section thickness as 5 mm. The diffusion-weighted sequence in the axial plane with single-shot echo-planar imaging by applying diffusion-sensitive gradients at three different b values (b = 50, b = 400, and b = 800 mm^2/s) in all three directions (x, y, and z-axis). The device automatically creates ADC maps of isotropic images, and the average ADC values of all lesions were measured manually on these maps. Measurements of the lesions were made as follows: three circular ROIs (Region of Interest) were placed on the ADC map in the axial plane and measurements were made, and the arithmetic average of these measurements was taken. The ROI volume was kept at approximately 15-20 mm^2.

MRS was used for spectroscopic examination using the PRESS (point-resolved spectroscopy) technique. Depending on the size and nature of the mass, a single-voxel or multi-voxel area of 8 cm^3 (2 × 2 × 2 cm) was placed on the intracranial mass. To determine the volume to be selected for examination (volume of interest), axial, coronal, and sagittal images of the mass were obtained using the T2A sequence in the patient's cranial MRI. The spectroscopic voxels taken for examination were made so that the mass remained as far away from the vascular structures and edges of the mass as possible to prevent contamination of the surrounding tissues, and the voxel areas were checked in all three planes. For single-voxel MRS, TE = 135 msec, TR = 2000 msec; For multivoxel MRS, signals from NAA, choline, and creatinine protons were collected within the mass using the parameters TE = 135 msec, TR = 1700 msec. After the spectral data were obtained, the Cho/NAA, Cho/Cr, and NAA/Cr ratios of the masses were obtained using the major peak amplitudes of NAA, Cho, and Cr molecules.

rCBV values were obtained from PMRI as follows: 0.2 mmol/kg Gadoteric acid was administered through an automatic injector, followed immediately by 100 mL isotonic NaCl at a rate of 5 mL/s. Six times in an average of 90 s, consecutive images, each consisting of 20 images, were taken. Spin-echo echo-planar imaging sequences were used in the images taken. The resulting images were transferred to the workstation for post-processing. rCBV maps were obtained with ready-made software programs in the MRI system. When placing the ROI, cystic and non-necrotic areas of the mass and adjacent vascular structures were avoided. The ROI volume was kept at approximately 5-8 mm^3. 3 ROIs were placed on the lesions, and the arithmetic mean of the highest rCBV value was selected. The highest ROI obtained was compared with the white matter in the opposite hemisphere. Relative CBV ratio = rCBV (tumor)/rCBV (normal) was obtained.

Evaluation

While evaluating intracranial masses, radiological findings were reviewed by an experienced radiologist in the following order: lesions were assessed as low and high grade by looking at the features of edema, cyst, hemorrhage, necrosis, and contrast enhancement among conventional MRI findings. Then, considering the predictive values obtained from studies that added diffusion, MRS, and perfusion examination findings from advanced MR imaging methods to conventional MRI were evaluated as low and high grades. Measurements were performed using diffusion, spectroscopy, and perfusion examination, which are advanced MRI examination methods. In the data obtained from the measurements, the importance of ADC, Cho/Cr, Cho/NAA, and rCBV ratios in both low and high-grade discrimination and pathological grading of the lesions was evaluated. All radiological ratings obtained were compared with the pathological results.

Statistical analysis

Patient data collected within the scope of the study were analyzed with the IBM Statistical Package for the Social Sciences (SPSS) for Windows 26.0 (IBM Corp., Armonk, NY) package program. Frequency and percentage for categorical data and mean and standard deviation for continuous data were given as descriptive

values. For comparisons between groups, the "Independent Sample T-test" was used for two groups, and the "Pearson Chi-square test" was used to compare categorical variables. The results were considered statistically significant when the p-value was less than 0.05. ROC analysis for ADC measurements and rCBV ratios in distinguishing low- and high-grade glial tumors.

Results

The presence of edema, hemorrhage, necrosis, cystic focus content, and contrast enhancement characteristics in the lesions were assessed through conventional MRI (Table 1). The results were as follows: edema was detected in 76.8%. When the lesions were examined to determine whether they contained a cystic component, cysts were observed in 50%, hemorrhagic focus and necrosis were detected in 54.9%, and hemorrhage in 45.1%. Additionally, 53.7% of the lesions had no necrosis. A majority of the lesions (84.1%) were contrasted to varying degrees. When the lesions were grouped as low and high grade according to conventional MRI findings, it was seen that 40.2% of the cases were low grade and 59.8% were high grade. The radiological grading based on conventional MRI findings was compatible with the pathological grading. However, the success rate of conventional MRI in detecting low-grade tumors was 54.8%, but high-grade tumors were higher at 86.3% (Fig. 1).

Radiological grading was performed by adding DWI and ADC maps, spectroscopy examination, and PMRI findings. In advanced MRI, the following was taken into consideration: the cutoff point in terms of ADC measurements in distinguishing low and high-grade lesions was 1.1 × 10^{-3} mm^2/s based on studies on the subject, NAA 2.0-2.02 ppm, Cho 3.22 ppm from spectroscopic measurements. The cutoff point for the rCBV ratio was 1.75 from perfusion

MRI findings, with a range of 3.0-3.02 ppm, Cho/NAA ratio between 2-2.5, and Cho/Cr ratio between 2-2.5. The radiological grading was compatible with the pathological results. However, the success of the combination of conventional and advanced MRI in detecting low-grade tumors (83.9%) was better than the grading performed with conventional MRI alone. The detection rate for high-grade tumors was higher (98%) (Table 2).

On ROC analysis, the ADC cutoff value was 0.905 mm^2/s (p = 0.001), rCBV cutoff value 1.77 (p = 0.001), Cho/NAA cutoff value 2.20 (p = 0.001), and Cho/Cr cutoff value 2.01 (p = 0.001) with statistical significance. Significant results were obtained when ADC, Cho/NAA, and Cho/Cr were analyzed into four histopathologically grade groups besides Grade III and IV (p = 0.001). NAA/Cr values were insignificant in pathological grading (p > 0.05).

ROC analysis was performed with rCBV ratios measured in discriminating low and high-grade lesions. The size of the area under the curve was 0.920, and this was statistically significant (p = 0.001). The cutoff value for rCBV ratios was 1.77. The sensitivity value was 94.1%, and the specificity value was 64.5% (Fig. 2).

The rCBV ratios were added to the PMRI findings and the conventional MRI, and the cutoff point for the rCBV ratio was taken as 1.77. The radiological grading

Table 1. Results of conventional radiological characteristics

Demographics	Low-grade	High-grade	p
	n (%)		
Gender	16 (51%)	33 (64%)	
Male	15 (48%)	18 (35%)	
Female			
Tumor grade			
Pathological	31	51	0.189
Conventional MRI	33	49	0.020*
Contrast enhancement	67.70%	94.10%	0.001*
Necrosis	12.90%	66.70%	0.001*
Hemorrhage	12.90%	64.70%	0.325
Cyst	45.20%	52.90%	0.001*
Edema	45.20%	96.10%	0.289
con + adv MRI	83.90%	98%	

*p < 0.05: statistical significance.
con: conventional; adv: advanced; MRI: magnetic resonance imaging.

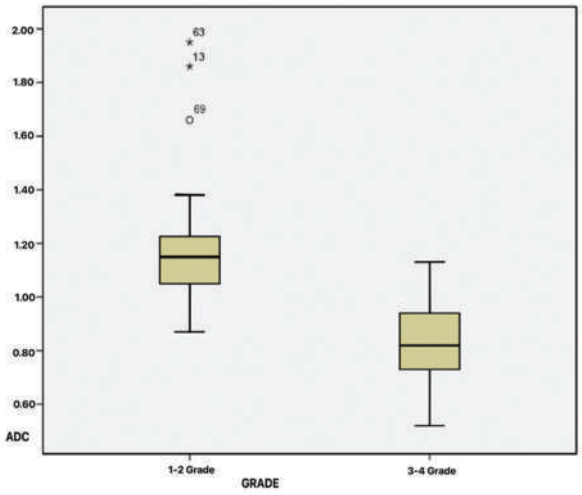

Figure 1. *Comparison of grading according to conventional magnetic resource imaging and ADC association findings with pathological grading.*

Table 2. Comparison of ADC, Cho/NAA, Cho/Cr, NAA/Cr, and NAA/Cr values in distinguishing low- and high-grade lesions

MRI	Grade of tumor	n (%)	Median ± SD (minimum-maximum)	p
ADC	Low	31 (37%)	1.12 ± 0.24 (0.87-1.95)	0.001*
	High	51 (62%)	0.83 ± 0.16 (0.52-1.95)	
Cho/NAA	Low	31 (37%)	3.51 ± 2.70 (0.59-9.60)	0.004*
	High	51 (62%)	5.73 ± 4.06 (0.29-19.53)	
Cho/Cr	Low	31 (37%)	1.97 ± 1.10 (0.52-4.60)	0.001*
	High	51 (62%)	3.99 ± 4.13 (0.63-19.70)	
NAA/Cr	Low	31 (37%)	0.77 ± 0.45 (0.00-1.58)	525
	High	51 (62%)	0.83 ± 0.86 (0.15-4.90)	
rCBV ratio	Low	31 (37%)	1.64 ± 0.72 (0.95-3.58)	0.001*
	High	51 (62%)	3.76 ± 1.66 (1.04-11.22)	

*p < 0.05: statistical significance.
SD: standard deviation; MRI: magnetic resonance imaging; ADC: apparent diffusion coefficient; Cho/NAA: Cholin/N-Asetilaspartat; Cho/Cr: Cholin/Creatin; NAA/Cr: N-asetilaspartat/creatin; rCBV: regional cerebral blood volume.

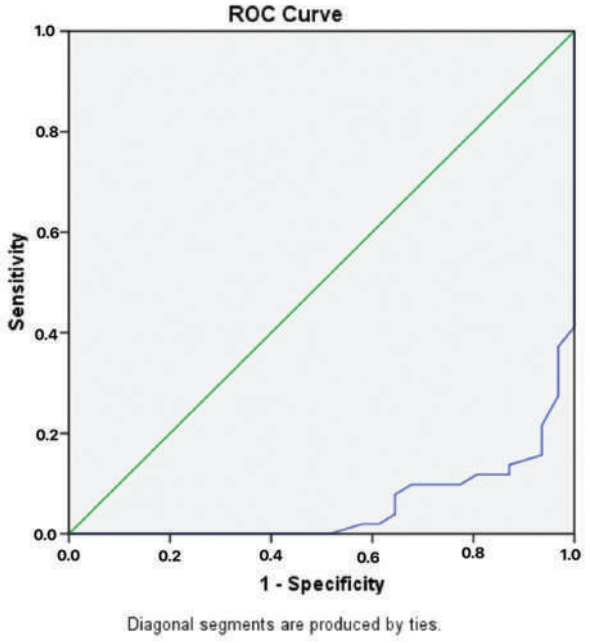

Figure 2. *ROC analysis for ADC measurements in distinguishing low- and high-grade glial tumors.*

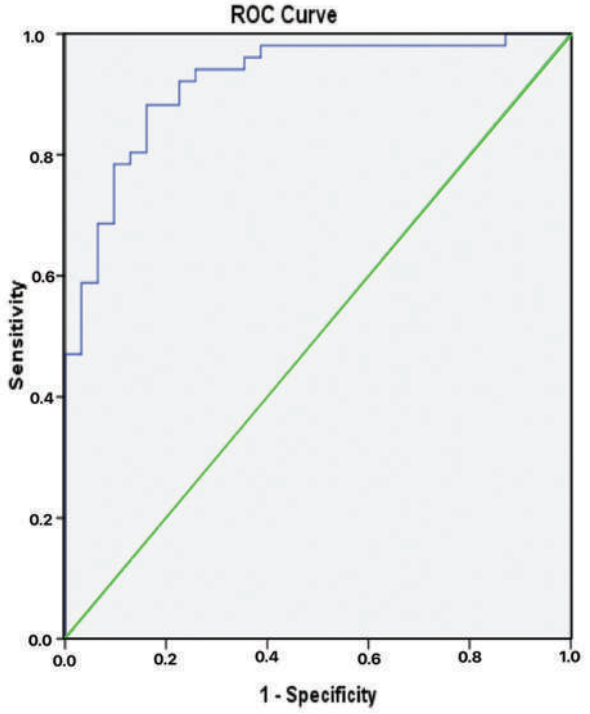

Figure 3. *ROC analysis for rCBV ratios in differentiating low- and high-grade glial tumors.*

was compatible with the pathological results. However, the success rate of the combination of conventional MRI and rCBV findings in detecting low-grade tumors was 74.2%, and the rate of detecting high-grade tumors was higher at 92.2%.

Diffusion MRI and ADC maps were added to conventional MRI findings, and the cutoff point for ADC was taken as 0.905×10^{-3} mm²/s. The radiological grading was compatible with the pathological results. However, while the success rate of combining conventional MRI and ADC findings in detecting low-grade tumors was 64.5%, the rate of detecting high-grade tumors was 73.2%.

Radiological grading was performed again by adding the cutoff points obtained from advanced MRI examinations such as DWI and ADC maps, spectroscopy examination, and PMRI examination to the conventional MRI findings. When the new rating made using the cutoff points, we obtained was compared with the pathological rating, it was seen that the radiological rating was compatible with the pathological rating. However, the success rate of the combination of conventional and advanced MRI in detecting low-grade tumors was 77.4%. The detection rate for high-grade tumors was higher, 98% (Table 3 and Fig. 3).

On ROC analysis, ADC cutoff value 0,905 mm²/s (p = 0.001), rCBV cutoff value 1.77 (p = 0.001), Cho/NAA cutoff value 2.20 (p = 0,001), and Cho/Cr cut-off value 2.01 (p = 0.001) were achieved. Significant results were obtained when ADC, Cho/NAA, and

Table 3. Comparison of ADC, Cho/NAA, Cho/Cr, NAA/Cr, and NAA/Cr values in distinguishing low and high-grade lesions in advanced MRI

MRI	Grade	n	Median ± SD (minimum-maximum)	p
ADC	1	4	1.55 ± 0.33 (1.19-1.95)	KW = 48.41
	2	27	1.15 ± 0.18 (0.87-1.86)	0.001*
	3	17	0.88 ± 0.16 (0.62-1.13)	
	4	34	0.80 ± 0.15 (0.52-1.09)	
Cho/NAA	1	4	1.68 ± 1.91 (0.59-4.55)	KW = 11.54
	2	27	3.78 ± 2.72 (0.80-9.60)	0.009*
	3	17	6.31 ± 3.80 (1.86-13.00)	
	4	34	6.45 ± 4.21 (0.29-19.53)	
Cho/Cr	1	4	1.22 ± 0.46 (0.62-1.74)	KW = 14.39
	2	27	2.08 ± 1.13 (0.52-4.60)	0.002*
	3	17	3.56 ± 1.46 (1.10-6.00)	
	4	34	4.21 ± 4.96 (0.63-19.70)	
NAA/Cr	1	4	1.14 ± 0.56 (0.38-1.58)	KW = 2.62
	2	27	0.71 ± 0.42 (0.00-1.57)	0.453
	3	17	0.74 ± 0.57 (0.20-2.03)	
	4	34	0.88 ± 0.98 (0.15-4.90)	
rCBV ratio	1	4	1.88 ± 0.78 (1.15-2.97)	KW = 40.61
	2	27	1.61 ± 0.71 (0.95-3.58)	0.001*
	3	17	3.61 ± 1.53 (1.04-7.44)	
	4	34	3.83 ± 1.74 (1.64-11.22)	

*p < 0.05: statistical significance.
SD: standard deviation; MRI: magnetic resonance imaging; ADC: apparent diffusion coefficient; Cho/NAA: Cholin/N-Asetilaspartat; Cho/Cr: Cholin/Creatin; NAA/Cr: N-Asetilaspartat/Creatin; rCBV: regional cerebral blood volume; KW: Kruskal–Wallis.

Cho/Cr were analyzed into four histopathologically grade groups besides (p = 0.001). NAA/Cr values were not significant in pathological grading. rCBV measurements were statistically significant between Grades I and IV and between II and IV.

Discussion

In recent years, MRI sequences have been developed that allow us to obtain accurate information about tumor physiology and anatomical information about brain tumors, and these are called "Advanced MR Imaging Methods." Advanced MR imaging methods allow numerically measuring dynamic physiological processes in the brain and providing qualitative information about tissue physiology. Using this qualitative data, the biological behavior of the tumor, the patient's life expectancy, and treatment processes can be predicted before the operation[6-8]. According to the results of our study, MRI techniques have been shown to be useful in grading glial tumors with proper and accurate use of MRI techniques to make pathological diagnoses in advance.

While conventional MRI plays a vital role in determining the localization of intracranial masses, their relationship with critical anatomical structures, and especially the treatment approaches, it can also give us insight into the grading of gliomas[6,7].

Law et al. reported the rate of determining the degree of high-grade gliomas with conventional MRI was 72.5%[9], whereas Arvinda et al. stated 72.7%.[10]. In our study, the conventional MRI findings in detecting low-grade glial tumors were 54.8%; the success rate in detecting high-grade glial tumors was 86.3%, and these results were compatible with the literature.

However, determining the degree of gliomas using conventional MRI has been limited. Moller–Hartmann et al. published that their reliability was between 55.1% and 83.3%[11]. Gene Kondziolka et al. demonstrated a 50% false-positive rate in evaluating supratentorial gliomas[12]. In another study, Lee et al. found that 50% of patients with low-grade astrocytoma detected on conventional MR imaging had high-grade astrocytoma on histopathological examination[13].

In our study, conventional MRI findings such as edema, hemorrhage, necrosis, and contrast enhancement significantly distinguished low and high-grade lesions according to pathological outcomes. A cyst in the lesion was observed in 45.2% of the low-grade lesions and 52.9% of the high-grade lesions.

The contrast enhancement in conventional MRI has an important place in tumor grading in glial tumors, but it is not significant alone in tumor grading. Barker et al. investigated the histopathology results of 31 patients without contrast enhancement, and they found that 32% were Grade III and 4% were Grade IV[14]. In another study, Fan et al. stated that 14% of non-enhancing supratentorial gliomas were high-grade[15]. Dean et al. indicated that the mass effect and necrosis were two crucial determinants of tumor grade. However, they also noted that a high-grade glioma may be confused with a low-grade glioma when it does not have sufficient edema, contrast medium enhancement, necrosis, and mass effect[16]. Considering all these studies and the results of our study, due to the heterogeneous internal structure of tumors and the

inability of conventional MRI to provide detailed information about tumor physiology and metabolites, the correlation of traditional MRI with tumor histopathology remains limited.

Conventional MR imaging with gadolinium-based contrast agents is an accepted tool for characterizing brain tumors. However, DWI, perfusion-weighted imaging, and MRS are relatively newer techniques that provide additional microstructural, microvascular, and biochemical information. These techniques are used to determine the histopathology of glial tumors[17].

DWI and ADC maps, among these advanced MRI techniques, show tumor cellularity. The ADC values obtained are inversely proportional to the tumor grade. Several studies have shown that ADC correlates well with tumor cellularity on histological examination. Calculation of ADC has been demonstrated that it can assist conventional MRI in characterizing glial tumors[18]. In our study, the detection rate of radiological grading with ADC values in addition to conventional MRI, mainly low-grade glial tumors, was higher than the radiological grading by conventional MRI.

Sugahara et al. published that the minimum ADC value correlated well with histological cellularity and was helpful in grading gliomas[19]. However, no significant difference between high-grade and low-grade glial tumors was observed in the studies of Rollin et al. and Lam et al.[20,21]. Lee et al. elaborated that the average ADC values were 1.19 mm^2/s and 1.035 mm^2/s in high- and low-grade gliomas, respectively. Again, in this study, when the cutoff points were examined using the ROC analysis, the result was 1.055 mm^2/s. Contrary to our findings, in significant ADC results between tumor grades could be due to the calculation made on a single section[13]. In our study, significant results were found only by taking diffusion-restricted regions from the tumor area.

Yamasaki et al. conducted measurements in astrocytic tumors and achieved a statistical accuracy of 91.3% between Grade II and high-grade (III and IV) tumors[22]. Server et al. also found a statistical difference between Grade II, Grade III, and Grade IV according to ADC values from tumor areas[23]. In our study, considering the WHO grades in terms of ADC measurements, the difference between the groups was statistically significant. When the measurements were compared in pairs, the difference between Grades I and II, I and III, and I and IV. The difference between Grades II and III and II and IV was significant. Still, no significance was observed between Grades III and IV.

Advanced imaging techniques, such as MRS and PMRI, have been proposed in addition to ADC measurement to predict the grading of pre-operative brain gliomas[24]. PMRI, which allows measurement of regional CBV (rCBV), shows a close correlation with the histopathological grade in gliomas[25]. Schmainda et al. conducted a study on 73 patients with brain glioma and determined the rate of high- and low-grade glial tumors as 96% and 69%, respectively[26]. In our study, when conventional and PMRI were evaluated, the detection rate of high- and low-grade glial tumors was 92.2% and 74.2%, respectively.

Studies conducted with PMRI in brain gliomas have shown that the rCBV cutoff point for distinguishing between high and low-grade glial tumors has not yet been determined[27]. Yoon et al. reported the rCBV cutoff value as 2.44 in a study of 60 patients (12 low grade, 48 high grade), whereas Caulo et al. determined the cutoff value as 2.45 in 118 patients[28]. In our study, the cutoff point was 1.77 (94% sensitivity and 64.5% specificity), similar to the results of Law et al. (1.75 in 120 high- and 40 low-grade glioma patients)[9]. Caulo et al. divided oligodendrogliomas and astrocytomas into degrees and found statistically significant differences between Grade III and Grade IV and Grade II and Grade III oligodendrogliomas. They also found a statistically significant difference between Grade II oligodendroglioma and Grade III astrocytoma[28]. In our study, a significant difference was found only between Grade I and Grade IV and between Grades II and Grade IV, but no difference was found between other grades.

Studies on MRS elaborated that it is a powerful tool in brain tumor grading. Specifically, choline elevation with NAA depression is a reliable indicator in determining the character and metabolic status of the tumor[29]. MRS provided additional information besides conventional MRI in the studies. In our study, when we compared the radiological grading through analyzing the metabolites in MRS in addition to conventional MRI with the pathological results, we recognized that the radiological grading was compatible with the pathological grading.

Law et al. found that Cho/Cr and Cho/NAA metabolite ratios were useful in determining tumor grade (97.5% and 96.7%, respectively)[9]. However, while high specificity was observed in identifying high-grade gliomas, lower specificity was observed in low-grade gliomas due to the smaller number of samples. In our study, in addition to conventional MRI, radiological grading was performed using Cho/NAA and Cho/Cr

ratios one by one, and their superiority over each other was investigated. However, no significance was achieved.

Wang et al. conducted a meta-analysis conducted on 1228 patients and found that MRS was moderately successful in differentiating high-grade from low-grade gliomas. They also stated that the Cho/NAA ratio was superior to the NAA/Cr and Cho/Cr ratios in distinguishing high-grade gliomas from low-grade gliomas[30]. Naveed et al. conducted a study with Grade II and Grade III oligodendrogliomas. They found that the Cho/NAA and Cho/Cr ratios were not statistically different between the two groups[31]. In our study, we have also found that Cho/NAA and Cho/Cr were statistically significant.

Al-Okaili et al. performed a study with conventional MRI and advanced MRI techniques (DWI and ADC maps, MRS, and PMRI) on 111 patients through an algorithm with specific cutoff points. They distinguished high-grade glial tumors from low-grade ones with 90% accuracy and 88% sensitivity[32]. The results of glial tumor grading using the same algorithm in our study were that the detection rate of low-grade glial tumors was 83.9% and high-grade glial tumors 98%.

The limitation of our study is that glial tumors are rare tumors, so larger studies are needed. Furthermore, imaging methods are still insufficient to provide information about the molecular nature of the pathology. Therefore, imaging methods need to be improved. Furthermore, a comparison of this method with the normal population may give more support to the literature.

Conclusion

Using additional advanced MRI techniques such as PMRI, MRS, and DWI, with conventional MRI, could enhance the accuracy of histopathological grading in cranial glioma. A more consistent pre-operative WHO grading is possible when advanced MRI and cutoff points are considered in addition to conventional MRI findings.

Funding

The authors declare that they have not received funding.

Conflicts of interest

The authors declare no conflicts of interest.

Ethical considerations

Protection of humans and animals. The authors declare that the procedures followed complied with the ethical standards of the responsible human experimentation committee and adhered to the World Medical Association and the Declaration of Helsinki. The procedures were approved by the institutional Ethics Committee.

Confidentiality, informed consent, and ethical approval. The authors have followed their institution's confidentiality protocols, obtained informed consent from patients, and received approval from the ethics committee. The SAGER guidelines were followed according to the nature of the study.

Declaration on the use of artificial intelligence. The authors declare that no generative artificial intelligence was used in the writing of this manuscript.

References

1. Wang LM, Englander ZK, Miller ML, Bruce JN. Malignant glioma. Adv Exp Med Biol. 2023;1405:1-30.
2. Palacios-Saucedo GD, Padilla-Martínez JJ, Dávila-Gaytán AG, Herrera-Rivera CG, Vázquez-Guillén JM, Rivera-Morales LG, et al. Factores asociados a sobrevida a un año en pacientes postoperados de glioblastoma. Cir Cir. 2023;91:397-402.
3. Reuss DE. Updates on the WHO diagnosis of IDH-mutant glioma. J Neurooncol. 2023;162:461-9.
4. Moreno-Jiménez S, Martínez-Vaca N, Pérez-Aguilar B, Gómez-Calva B, Díaz-Chávez JJ, Mondragón-Soto MG. Usefulness and safety from stereotactic biopsy in posterior fossa lesions in adult patients. Cir Cir. 2019;87:554-8.
5. Hangel G, Schmitz-Abecassis B, Sollmann N, Pinto J, Arzanforoosh F, Barkhof F, et al. Advanced MR techniques for preoperative glioma characterization: part 2. J Magn Reson Imaging. 2023;57:1676-95. Erratum in: J Magn Reson Imaging. 2023.
6. Seo M, Choi Y, Soo Lee Y, Kim BS, Park JS, Jeon SS. Glioma grading using multiparametric MRI: head-to-head comparison among dynamic susceptibility contrast, dynamic contrast-enhancement, diffusion-weighted images, and MR spectroscopy. Eur J Radiol. 2023;165:110888.
7. Guarnera A, Romano A, Moltoni G, Ius T, Palizzi S, Romano A, et al. The role of advanced MRI sequences in the diagnosis and follow-up of adult brainstem gliomas: a neuroradiological review. Tomography. 2023;9:1526-37.
8. Sacli-Bilmez B, Danyeli AE, Yakicier MC, Aras FK, Pamir MN, Özduman K, et al. Magnetic resonance spectroscopic correlates of progression free and overall survival in "glioblastoma, IDH-wildtype, WHO grade-4". Front Neurosci. 2023;17:1149292.
9. Law M, Yang S, Wang H, Babb JS, Johnson G, Cha S, et al. Glioma grading: sensitivity, specificity, and predictive values of perfusion MR imaging and proton MR spectroscopic imaging compared with conventional MR imaging. AJNR Am J Neuroradiol. 2003;24:1989-98.
10. Arvinda HR, Kesavadas C, Sarma PS, Thomas B, Radhakrishnan VV, Gupta AK, et al. Glioma grading: sensitivity, specificity, positive and negative predictive values of diffusion and perfusion imaging. J Neurooncol. 2009;94:87-96. Retraction in: J Neurooncol. 2013;114:255.
11. Möller-Hartmann W, Herminghaus S, Krings T, Marquardt G, Lanfermann H, Pilatus U, et al. Clinical application of proton magnetic resonance spectroscopy in the diagnosis of intracranial mass lesions. Neuroradiology. 2002;44:371-81.
12. Kondziolka D, Lunsford LD, Martinez AJ. Unreliability of contemporary neurodiagnostic imaging in evaluating suspected adult supratentorial (low-grade) astrocytoma. J Neurosurg. 1993;79:533-6.
13. Lee EJ, Lee SK, Agid R, Bae JM, Keller A, Terbrugge K. Preoperative grading of presumptive low-grade astrocytomas on MR imaging: diagnostic value of minimum apparent diffusion coefficient. AJNR Am J Neuroradiol. 2008;29:1872-7.
14. Barker FG 2nd, Chang SM, Huhn SL, Davis RL, Gutin PH, McDermott MW, et al. Age and the risk of anaplasia in magnetic resonance-nonenhancing supratentorial cerebral tumors. Cancer. 1997;80:936-41.

15. Fan GG, Deng QL, Wu ZH, Guo QY. Usefulness of diffusion/perfusion-weighted MRI in patients with non-enhancing supratentorial brain gliomas: a valuable tool to predict tumour grading? Br J Radiol. 2006;79:652-8.
16. Dean BL, Drayer BP, Bird CR, Flom RA, Hodak JA, Coons SW, et al. Gliomas: classification with MR imaging. Radiology. 1990;174: 411-5.
17. Su Y, Kang J, Lin X, She D, Guo W, Xing Z, et al. Whole-tumor histogram analysis of diffusion and perfusion metrics for noninvasive pediatric glioma grading. Neuroradiology. 2023;65:1063-71.
18. Ke X, Zhao J, Liu X, Zhou Q, Cheng W, Zhang P, et al. Apparent diffusion coefficient values effectively predict cell proliferation and determine oligodendroglioma grade. Neurosurg Rev. 2023;46:83.
19. Sugahara T, Korogi Y, Tomiguchi S, Shigematsu Y, Ikushima I, Kira T, et al. Posttherapeutic intraaxial brain tumor: the value of perfusion-sensitive contrast-enhanced MR imaging for differentiating tumor recurrence from nonneoplastic contrast-enhancing tissue. AJNR Am J Neuroradiol. 2000;21:901-9.
20. Rollin N, Guyotat J, Streichenberger N, Honnorat J, Tran Minh VA, Cotton F. Clinical relevance of diffusion and perfusion magnetic resonance imaging in assessing intra-axial brain tumors. Neuroradiology. 2006;48:150-9.
21. Lam WW, Poon WS, Metreweli C. Diffusion MR imaging in glioma: does it have any role in the pre-operation determination of grading of glioma? Clin Radiol. 2002;57:219-25.
22. Yamasaki F, Kurisu K, Satoh K, Arita K, Sugiyama K, Ohtaki M, et al. Apparent diffusion coefficient of human brain tumors at MR imaging. Radiology. 2005;235:985-91.
23. Server A, Kulle B, Gadmar ØB, Josefsen R, Kumar T, Nakstad PH. Measurements of diagnostic examination performance using quantitative apparent diffusion coefficient and proton MR spectroscopic imaging in the preoperative evaluation of tumor grade in cerebral gliomas. Eur J Radiol. 2011;80:462-70.
24. Su X, Yang X, Sun H, Liu Y, Chen N, Li S, et al. Evaluation of key molecular markers in adult diffuse gliomas based on a novel combination of diffusion and perfusion MRI and MR spectroscopy. J Magn Reson Imaging. 2024;59(2):628-638.
25. Amjad G, Zeinali Zadeh M, Azmoudeh-Ardalan F, Jalali AH, Shakiba M, Ghavami N, et al. Evaluation of multimodal MR imaging for differentiating infiltrative versus reactive edema in brain gliomas. Br J Neurosurg. 2023;37:1031-9.
26. Schmainda KM, Rand SD, Joseph AM, Lund R, Ward BD, Pathak AP, et al. Characterization of a first-pass gradient-echo spin-echo method to predict brain tumor grade and angiogenesis. AJNR Am J Neuroradiol. 2004;25:1524-32.
27. Sanvito F, Raymond C, Cho NS, Yao J, Hagiwara A, Orpilla J, et al. Simultaneous quantification of perfusion, permeability, and leakage effects in brain gliomas using dynamic spin-and-gradient-echo echoplanar imaging MRI. Eur Radiol. 2024;34(5):3087-3101.
28. Caulo M, Panara V, Tortora D, Mattei PA, Briganti C, Pravatà E, et al. Data-driven grading of brain gliomas: a multiparametric MR imaging study. Radiology. 2014;272:494-503.
29. Ankush A, Sardessai S. Role of MRSI major metabolite ratios in differentiating between intracerebral ring-enhancing neoplastic and non-neoplastic lesions, high-grade gliomas and metastases, and high-grade and low-grade gliomas. Cureus. 2022;14:e31841.
30. Wang Q, Zhang H, Zhang J, Wu C, Zhu W, Li F, et al. The diagnostic performance of magnetic resonance spectroscopy in differentiating high-from low-grade gliomas: a systematic review and meta-analysis. Eur Radiol. 2016;26:2670-84.
31. Naveed MA, Goyal P, Malhotra A, Liu X, Gupta S, Mangla M, et al. Grading of oligodendroglial tumors of the brain with apparent diffusion coefficient, magnetic resonance spectroscopy, and dynamic susceptibility contrast imaging. Neuroradiol J. 2018;31:379-85.
32. Al-Okaili RN, Krejza J, Wang S, Woo JH, Melhem ER. Advanced MR imaging techniques in the diagnosis of intraaxial brain tumors in adults. Radiographics. 2006;26 Suppl 1:S173-89.

ORIGINAL ARTICLE

Comparison of cytogenetic and molecular features observed in endometrial cancers: known clinic and difficulties in treatment

Comparación de las características citogenéticas y moleculares observadas en los cánceres de endometrio: clínica conocida y dificultades en el tratamiento

Kemine Uzel[1], Seda E. Keskin[2], Filiz Bilir[3], Merve Gokbayrak[2], Gulhan Demir[2], Naci Cine[2], Gupse Turan[4], Aydın Corakcı[3], and Hakan Savlı[2]*

[1]Department of Obstetrics and Gynecology, Demiroglu Science University, Istanbul; [2]Department of Genetics, Kocaeli University, Faculty of Medicine, Kocaeli; [3]Department of Obstetrics and Gynecology, Kocaeli University, Faculty of Medicine, Kocaeli; [4]Department of Medical Pathology, Kocaeli University, Faculty of Medicine, Kocaeli. Turkey

Abstract

Objective: *Understanding the relationship between genetic structure and the molecular changes involved in endometrial cancer (EC) provides an opportunity to personalize treatments and incorporate targeted therapies.* **Method:** *We compared cytogenetic and molecular features observed in tumoral and adjacent healthy tissue endometrium samples in EC patients.* **Results:** *Non-clonal chromosome aberrations (NCCAs) frequently in patients with EC, especially in 10,15,17,22, X chromosomes and were monitored in 73.7%, clonal chromosomal alterations were observed in 26.3% of the patients. Down POLE gene expression in 42.1%, up p53gene expression in 57.9%, PTEN down-regulation in 47.3%, down ARID1A gene expression in 42.1%, PIK3CA up-regulation was observed in 68% of patients.* **Conclusion:** *The up-regulation of tumor suppressor genes in our study shows that not only these genes are involved but also different pathways and factors play a role in tumorigenesis. Furthermore, an increased number of NCCAs shows an essential role in the development of ECs.*

Keywords: *Endometrial cancer. Genomics. Pathology. Prognostic factors. Targeted therapy.*

Resumen

Objetivo: *Comprender la relación entre la estructura genética y los cambios moleculares involucrados en el cáncer de endometrio brinda la oportunidad de personalizar los tratamientos e incorporar terapias dirigidas.* **Método:** *Comparamos las características citogenéticas y moleculares observadas en muestras de endometrio de tejido sano tumoral y adyacente en pacientes con cáncer de endometrio.* **Resultados:** *Las aberraciones cromosómicas no clonales (NCCA) son frecuentes en pacientes con cáncer de endometrio, especialmente en los cromosomas 10, 15, 17, 22, X y fueron monitoreadas en el 73,7%; se observaron alteraciones cromosómicas clonales en el 26,3% de las pacientes. Disminución de la expresión del gen POLE en el 42,1 %, aumento de la expresión del gen p53 en el 57,9%, disminución de la regulación de PTEN en el 47,3 %, disminución de la expresión del gen ARID1A en el 42,1%, aumento de la expresión de PIK3CA en el 68% de los pacientes.* **Conclusión:** *La regulación positiva de los genes supresores de tumores en nuestro estudio muestra que no solo estos genes están involucrados, sino que diferentes vías y factores juegan un papel en la tumorigénesis. Además, un mayor número de NCCA muestra un papel esencial en el desarrollo de cánceres de endometrio.*

Palabras clave: *Cáncer de endometrio. Genómica. Patología. Factores pronósticos. Terapia dirigida.*

***Correspondence:**
Kemine Uzel
E-mail: kemineuzel@hotmail.com

Date of reception: 25-06-2023
Date of acceptance: 04-10-2024
DOI: 10.24875/CIRU.23000328

Cir Cir. 2025;93(2):138-144
Contents available at PubMed
www.cirugiaycirujanos.com

Introduction

Although cervical cancer is responsible for the highest incidences and deaths of gynecological cancers, endometrial cancers (EC) are still quite common[1]. PTEN is a tumor suppressor gene located in the 10q23.3 chromosome region. PTEN mutations are present in approximately 83% of ECs. Detection of up to 40% of complex hyperplasia suggests that PTEN mutations play a role in early pathogenesis[2]. POLE somatic mutations are found in < 10% of endometrial carcinomas[3]. In EC, p53 mutations are more common in high-grade tumors and it considered among late mutations in pathogenesis[3]. The ARID1A gene has been characterized as a tumor suppressor, and most mutations seen in human cases are frameshift or nonsense mutations. In particular, ARID1A is mutated in all endometrium-associated tumor types, including undifferentiated endometrial carcinomas[4,5]. Activating mutations and amplification of PIK3CA are common in cancer in general. However, the highest rates of PI3K pathway alterations were reported in endometrial malignancies[6].

Five-year survival rates for EC vary according to the stage at diagnosis. The 5-year survival rate in patients with tumors localized in the uterus is ≥ 95% but may decrease to 69% in patients with regional metastases and 17% in patients with distant metastatic disease[7].

Endometrioid and serous EC s were divided into four groups with distinct clinical, pathologic, and molecular features[3]:

– DNA polymerase epsilon (POLE) mutant [ultramutated].

– Microsatellite instability-high (MSI-H)/mismatch-repair deficient (MMR-D) [hypermutated].

– Copy-number low (CN-low) [endometrioid-like].

– Copy-number high (CN-high) [serous-like].

Chromosome breakpoints are a manifestation of chromosomal instability. It has been found that chromosomal deletions in cancer cells often contain tumor suppressor genes. Among the 30 most gene-rich bands, cancer breakpoints localize at 1p36, 1q21, 7q22, 8q24, 11p15, 11q13, 11q23, 12q13, 16p13, and 19p13 sensitive regions[8].

Understanding the relationship between genetic structure and the molecular changes involved in EC provides an opportunity to personalize treatments through facilitating diagnostic testing and incorporating targeted therapies. Therefore, in this study, we aimed to investigate the genetic features of EC s and give clinicians an opinion in this direction.

Method

In this study, endometrial tumoral and adjacent healthy tissue samples were surgically taken from 34 patients diagnosed with EC at University Hospital, Department of Obstetrics and Gynecology. Patient information was obtained from the hospital information system and patients. Tumor sizes and degrees of myometrial invasion were determined by MR imaging. All patients in our study did not receive any neoadjuvant chemotherapy. Primary cell cultures were made as explant cultures or as single-cell suspensions by enzymatic application. Chromosome analysis-prepared preparations were examined under Leica DM2500 optical microscope. Analyzed metaphases were evaluated according to ISCN 2013 (International System for Human Cytogenetic Nomenclature). Metaphases were photographed in an automated imaging (Cytovision) system. In this study, at least 20 metaphases from each patient were examined.

Thirty mg samples were taken from endometrial tissues with scalpel and homogenized by the RNeasy Micro Kit (50) (Qiagen, Germany) protocol, total RNA was isolated. The quantity of RNAs was checked with a spectrophotometer (NanoDrop ND-1000; NanoDrop Technologies, Wilmington, DE). For cDNA synthesis, a cDNA synthesis kit (WisentBioProducts, Canada) and 1μg total RNA were used. Obtained gene expression values were normalized using a housekeeping gene of beta2 microglobulin. Gene expression ratios were compared in tumoral and adjacent healthy tissue groups using REST (Relative Expression Software Tool). The investigated genes in the study are POLE, PTEN, TP53, PIK3CA, and ARID1A. A list of the primers used for the quantitative RT-PCR are presented in table 1.

Statistical analysis

Statistical Package for the Social Sciences (SPSS for Windows, Version 25.0, Chicago, IL, USA) program was used for statistical analysis. Results were presented as the median and interquartile range (25%-75%) for continuous (numeric) data; frequency and percentage for categorical variables. Fisher's exact test was used to

Table 1. List of the primers used for the quantitative RT-PCR

Genes	Primer sequences
POLE (Exon 9)	Forward primer: 5-CTTTTAACAACCAGAGGGAGGT -3 Reverse primer: 5-TTGCTCCCATTCCTGGACTAA-3
PIK3CA (Exon 21)	Forward primer: 5-CATTTGCTCCAAACTGACCA-3 Reverse primer: 5-GATTGGCATGCTGTCGAATA-3
PTEN (Exon 7)	Forward primer: 5-CAGTTTGTGGTCTGCCAGCT-3 Reverse primer: 5-ATCACCACACACAGGTAACG-3
TP53 (Exon 5)	Forward primer: 5-TTGCCAACTGGCCAAGACCT-3 Reverse primer: 5-ACCTCCGTCATGTGCTGTGA-3
ARID1A (Exon 14)	Forward primer: 5-TTCAGTTGGGATCCAGGATGC-3 Reverse primer: 5-ATACTGGGCTGATACCCAGG-3

Table 2. Characteristics of tumors detected in participants

Characteristics of tumors	n	%
Metastasis		
No	30	88.2
Yes	4	11.8
Grade		
1	9	26.5
2	16	47.1
3	9	26.5
Histopathology result		
Non-endometrioid	5	14.7
Endometrioid	29	85.3
Chromosomal abnormality	5	73.7
CCAs	14	26.3
NCCAs		
Myometrial invasion		
< ½	26	76.5
> ½	8	23.5

CCAs: clonal chromosomal alterations; NCCAs: non-clonal chromosome aberrations.

compare categorical variables. For the statistical significance level, $p < 0.05$ was considered sufficient.

Results

While the mean age of the participants was 60.3 ± 1.4 (30-84), the gravida and parity medians were found 3. USG endometrial thickness (mm) was found 16. When the characteristics of the tumors detected in the participants were examined, it was determined that the median tumor size was 4 cm and metastasized in 4 of them. When the laboratory findings of the participants were examined, it was determined that the median of CA 125 was 15.7. In our study, tumors were detected as Stage 1A in 69.7% and Stage 3C in 12.1% of the patients. Characteristics of tumors detected in participants are presented in table 2.

The karyotype analysis results of the participants by tumor type are shown in table 3. Regulation and abnormality situations are presented in table 4.

When the regulation status was compared according to the presence of chromosomal anomaly, no statistically significant difference was found (Table 5).

We analyzed the differential expression of a gene in the tissues affected by the disease, compared with non-affected tissues. In our results, all gene expression values show increases and decreases in pathological tissue compared to healthy tissue.

Discussion

Although we started by using explant and enzymatic methods to produce primary endometrium cancer cell culture, we continued our work with the enzymatic method because, by the explant method, the cell count was less and cultivated for a longer time. Metaphase was observed in only 19 of the 34 patients. This shows a slightly higher rate than the literature, with a success rate of 56%.

About 90% of solid tumors and 75% of hematopoietic cancers have either gained or lost chromosomes[9]. Aneuploidy occurs before or at the same time as malignant transformation[10]. Furthermore, aneuploidy is a feature of cancer caused by increased cell proliferation[11]. Studies on hematologic cancers concluded that the survival of cytopenic patients with non-clonal chromosome aberrations (NCCAs) is worse than cytopenic patients with clonal chromosomal alterations (CCAs) without hematologic malignancies, suggesting that follow-up should be considered for cytopenic patients with both CCAs and NCCAs[12].

Table 3. Karyotype analysis results according to the tumor type of the participants

Histopathology	Karyotype
Endometrioid	41~88, X, -X [5], -4[3], -11[3],19[4] [cp10]/46, XX[7] NCCAs [10]
Carcinosarcoma	46, XX, inv (9)(p11q13)[17] NCCAs[3]
Endometrioid	46, XX[8]/NCCAs[3]
Endometrioid	46, XX[1]/NCCAs[1]
Carcinosarcoma	46, XX[3]/NCCAs[2]
Endometrioid	46, XX[1]/NCCAs[2]
Endometrioid	46, XX[2]/NCCAs[2]
Endometrioid	46, XX[1]/NCCAs[1]
Endometrioid	46, XX[17]/NCCAs[6]
Endometrioid	44~78, XX,+9[2],+19[2],-20[3] [cp5]/46, XX[1] NCCAs[7]
Endometrioid	46, XX[9]/NCCAs[6]
Endometrioid	39~49, XX,-15[3],+16[2][cp5]/46, XX[8]NCCAs[4]
Serous	45, X,-X,[3],-16[3]/46, XX[8] NCCAs[4]
Endometrioid	40~44, X,-X[2]/46, XX[6] NCCAs[7]/46, XX[8]/NCCAs[7]
Endometrioid	46, XX[9]/NCCAs[3]
Endometrioid	46, XX[15]/NCCAs[5]
Endometrioid	46, XX[1]/NCCAs[1]
Endometrioid	46, XX[1]NCCAs[2]
Endometrioid	46, XX[3]/NCCAs[5]

NCCAs: non-clonal chromosome aberrations.

We observed NCCA losses frequently in patients with EC, especially in 10,15,17,22, X chromosomes. On the other hand, polyploidy anomalies were frequently encountered in these patients. CCAs were observed in 26.3% of the patients. NCCAs monitoring in 73.7% of the participants show that these abnormalities cannot be underestimated in cancer cases and play an important role in the development of ECs. At the same time, a decrease in cell differentiation (increased tumor grade) with the numerical anomaly is one of the other results of our study.

POLE mutation status has proven an independent prognostic factor for EC patients. Patients with somatic POLE mutations exhibited a favorable prognosis[13]. POLE low expression has been associated with a favorable prognosis in EC patients[14]. In our results, we observed down POLE gene expression in 42.1% of patients, and Type 1 EC was observed in 78% of these patients, which is associated with a favorable prognosis.

Several studies have shown that p53 overexpression in endometrioid adenocarcinomas of the uterus is significantly higher in serous papillary (75-90% of cases) than in endometrioid endometrial carcinomas (10-35% of cases)[15]. In patients with endometrial carcinoma, overexpression of p53 has been reported largely unfavorable prognostic marker[16]. Up p53gene expression in 57.9% of cases and tumor Grade 2–3 in 63% of these patients is another result of our research, which is related to weaker cell differentiation in these cases, as well as a poor prognosis.

While decreased expression of PTEN is associated with Grade 3, increased PTEN expression is known associated with Grades 1 and 2 endometrial carcinomas[17]. In addition, the association between PTEN expression and the stage of endometrioid endometrial adenocarcinomas has been demonstrated[18]. It has been suggested that since PTEN can increase the chemosensitivity of neoplastic cells, it is an important prognostic indicator of improved overall survival in patients with advanced endometrial carcinoma receiving postoperative chemotherapy[19]. Tumor grade was observed higher in PTEN down-regulated cases. Grade 2–3 was observed in 87% of the patients with down-regulation and down-regulation was observed in 47.3% of the participants.

Considering tumor development and progression, ARID1A loss is associated with deep myometrial invasion in endometrial carcinoma[20]. Studies have shown that ARID1A acts as a tumor suppressor and is involved in tumorigenesis, progression, and apoptosis through the regulation of cellular proliferation in many cancer types, including ECs[21]. Down ARID1A gene expression in 42.1% of patients and deep myometrial invasion was observed in 37.5% of these cases.

PIK3CA mRNA expression was found increased from normal control tissue to EC tissues and endometrioid to non-endometrioid histological type[22]. Furthermore, high PIK3CA mRNA expression is associated with poor prognosis and increased expression in metastases demonstrating the independence of PIK3CA mutational status[23]. We observed PIK3CA up-regulation in 68% of the participants and tumor Grade 2–3 as an indicator of poor prognosis in 66.6% of these patients.

Table 4. Karyotype analysis results, gene regulation and chromosome abnormality status of the participants

Karyotype	Missing or excess chromosome	*POLE 12q24.33*	*PTEN 10q23.31*	*TP53 17q13.1*	*ARIDA 3q26.32*	*PIK3CA 1p35.3*
41~88, X, -X [5], -4[3], -11[3],19[4] [cp10]/46, XX[7] NCCAs [10]	–1, –2, –3, –4, –5, –6, –7, –9, –10, –11, –13, –14, –16, –17, –19, –20, –21, –22, –X, +4, +21	10,014u	87,305u	59,466u	67,6,2u	81,346u
46, XX, inv (9) (p11q13)[17] NCCAs [3]	–6, –12, –17, –X	2,439d	1,312d	1,075u	3,202u	2,542u
46, XX [8]/NCCAs [3]	–10, –15 –22, +2	4,389u	7,454u	9,409u	14,611u	12,346u
46, XX [1]/NCCAs[1]	+8	3,565u	3,753u	4,011u	16,784u	33,498u
46, XX[3]/NCCAs [2]	–1, –8, –9, –10, 11, –12, –15, –17, –18, –21, –X	29,324u	114,405u	58,242u	60,506u	99,457u
46, XX[1]/NCCAs [2]	–2	4,275d	3,143d	2,167d	3,948d	2,556d
46, XX[2]/NCCAs [2]	–14, –X, +13	1,480d	2,864u	2,740u	1,486d	1,533u
46, XX[1]/NCCAs [1]	–7, –8, –9, –10, –13, –20, –X	1,202d	2,709u	2,369u	2,202u	3,173u
46, XX[17]/NCCAs [6]	–6, –8, –9, –10, –14	25,563d	11,096d	5,881d	13,187d	9,409d
44~78, XX,+9[2],+19[2],-20[3] [cp5]/46, XX[1] NCCAs [7]	–14, –16, –19, –20, –21, –22, +2, +5, +7, +8, +9, +11, +12, +13, +14, +18, +19	7,485u	2,852d	2,614d	9,911u	15,412u
46, XX[9]/NCCAs [6]	–3, –4, –15, –17, –22,-X, +8	7,857u	29,000u	18,430u	15,878u	17,101u
39~49, XX,-15[3],+16[2][cp5]/ 46, XX[8] NCCAs [4]	–1, –2, –3, –5, –6, –7, –10, –13, –15, –16, –18, –19, –X, +2, +4, +6, +10+19, +22	21,917u	316,926u	174,127u	179,644u	48,705u
45, X,-X,[3],-16[3]/46, XX[8] NCCAs [4]	–3, –5, –7, –14, –15, –16, –18, –19,-20, –X, +15, polyploidy	2,763d	2,045d	1,334d	1,671d	1,520d
40~44, X,-X[2]/46, XX[6] NCCAs [7]/ 46, XX[8]/NCCAs [7]	–3, –6, –7, –15, –16, –17, –18, –20, –22	98,633u	5,688u	7,130u	342,272u	303,594u
46, XX[9]/NCCAs [3]	–2, –5, –10, –11, –15, –17, –22	9,741u	2,654u	4,608u	2,547u	3,130u
46, XX[15]/NCCAs [5]	–2, –4, –5, –6, –15, –16, –17, –18, –19, –22	1,038u	4,931d	1,262d	2,315d	1,520d
46, XX[1]/NCCAs [1]	–7, –X	20,908d	53,520d	44,818d	39,698d	35,115d
46, XX[1]/NCCAs [2]	–19	4,395d	53,150d	16,178d	16,576d	24,488d
46, XX[3]/NCCAs [5]	–6, –9, –10, –11, –12, –15, –17, –18, –22	2,034u	4,147d	2,275d	1,166d	3,468d

NCCAs: non-clonal chromosome aberrations; u: up-regulation; d: down-regulation; Gene locations: *POLE-12q24.33, PTEN-10q23.31, TP53-17q13.1, PIK3CA-3q26.32, ARID1A-1p35.3*

Although the locations of the genes on the chromosomes are: POLE-12q24.33, PTEN-10q23.31, TP53-17q13.1, PIK3CA-3q26.32, and ARID1A-1p35.3, unfortunately, there is no statistical difference between the cytogenetic findings and the results that we obtained with quantitative reverse transcription polymerase chain reaction (RT PCR). The reason for this is sensitivities of the classical cytogenetic technique and the RT PCR technique is quite different from each other and insufficient to compare these methods, and the changes in gene expression don't depend only on the changes in the copy number of the genes. While large-scale chromosomal abnormalities (insertion/deletion) can be detected with classical cytogenetics, only gene-based examinations with RT PCR are possible. The small number of cells analyzed is an important factor and a major limitation of our study. At the same time, the inability to follow-up on the survival of the patients is another limitation of the study.

Table 5. Comparison of the regulation status according to the presence of a chromosomal abnormality

Gene	Chromosomal abnormality				χ2	p
	NCCAs		CCAs			
	n	%	n	%		
POLE						
Up-regulation	7	50.0	4	80.0	1.360	0.338
Down-regulation	7	50.0	1	20.0		
PTEN						
Up-regulation	7	50.0	3	60.0	0.148	1.000
Down-regulation	7	50.0	2	40.0		
TP53						
Up-regulation	8	57.1	3	60.0	0.012	1.000
Down-regulation	6	42.9	2	40.0		
ARIDA						
Up-regulation	7	50.0	4	80.0	1.452	0.338
Down-regulation	7	50.0	1	20.0		
PIC3CA						
Up-regulation	8	57.1	4	80.0	0.827	0.603
Down-regulation	6	42.9	1	20.0		

χ2: Fisher exact test.

Conclusions

We recommend surgeons and oncologists work with diagnostic methods such as chromosomal microarray and whole genome sequencing since they are more sensitive in the management of targeted therapies. Increased expression of POLE, TP53, and PIK3CA genes is known associated with decreased survival, poor prognosis, and metastasis. We believe that silencing with CRISPR/Cas9-mediated genome editing technology using primary tissue samples may be a potential strategy in the treatment of patients and will be the focus of future research. At the same time, the up-regulation of tumor suppressor genes such as PTEN, TP53, and ARID1A in our study shows that not only these genes are involved but also different pathways and factors play a role in tumorigenesis. The increased number of NCCAs shows that these abnormalities cannot be underestimated in cancer cases and play an important role in the development of ECs, which indicates the need for further research.

Acknowledgments

The authors are especially grateful to all the staff of the Department of Genetics, Kocaeli University.

Funding

This research received support from Kocaeli University within the scope of Scientific Research Projects Funding.

Conflicts of interest

The authors declare no conflicts of interest.

Ethical considerations

Protection of humans and animals. The authors declare that no experiments involving humans or animals were conducted for this research.

Confidentiality, informed consent, and ethical approval. The authors have followed their institution's confidentiality protocols, obtained informed consent from patients, and received approval from the Ethics Committee. The SAGER guidelines were followed according to the nature of the study.

Declaration on the use of artificial intelligence. The authors declare that no generative artificial intelligence was used in the writing of this manuscript.

References

1. Hyuna S, Jacques F, Rebecca LS, Mathieu L, Isabelle S, Ahmedin J, et al. Global cancer statistics 2020: GLOBOCAN estimates of ıncidence and mortality worldwide for 36 cancers in 185 countries. CA Cancer J Clin. 2021;3:209-49.
2. Kanamori Y, Kigawa J, Itamochi H, Shimada M, Takahashi M, Kamazawa S, et al. Correlation between loss of PTEN expression and Akt phosphorylation in endometrial carcinoma. Clin Cancer Res. 2001;7:892-95.
3. Talhouk A, McAlpine JN. New classification of endometrial cancers: the development and potential applications of genomic-based classification in research and clinical care. Gynecol Oncol Res Pract. 2016;3:14.
4. Espinosa I, De Leo A, D'Angelo E, Rosa-Rosa JM, Corominas M, Gonzalez A, et al. Dedifferentiated endometrial carcinomas with neuroendocrine features: a clinicopathologic, immunohistochemical, and molecular genetic study. Hum Pathol. 2018;72:100-6.
5. Toumpeki C, Liberis A, Tsirkas I, Tsirka T, Kalagasidou S, Inagamova L, et al. The role of ARID1A in endometrial cancer and the molecular pathways associated with pathogenesis and cancer progression. *In Vivo*. 2019;33:659-67.
6. Holst F, Werner HM, Mjøs S, Hoivik EA, Kusonmano K, Wik E, et al. PIK3CA amplification associates with aggressive phenotype but not markers of AKT-MTOR signaling in endometrial carcinoma. Clin Cancer Res. 2019;25:334-45.
7. Yen TT, Wang TL, Fader AN, Shih IM, Gaillard S. Molecular classification and emerging targeted therapy in endometrial cancer. Int J Gynecol Pathol. 2020;39:26-35.
8. Musio A, Zambroni D, Vezzoni P, Mariani T. Chromosomes, genes, and cancer breakpoints. Cancer Genet Cytogenet. 2002;139:141-2.
9. Weaver BA, Cleveland DW. Does aneuploidy cause cancer? Curr Opin Cell Biol. 2006;18:658-67. Erratum in: Curr Opin Cell Biol. 2007;2:246.
10. Heselmeyer-Haddad K, Sommerfeld K, White NM, Chaudhri N, MorrisonLE, Palanisamy N, et al. Genomic amplification of the human telomerase gene (TERC) in pap smears predicts the development of cervical cancer. Am J Pathol. 2005;166:1229-38.
11. Hanahan D, Weinberg RA. The hallmarks of cancer. Cell. 2000;100: 57-70.
12. Imataki O, Kubo H, Takeuchi A, Uemura M, Kadowaki N. Nonclonal chromosomal alterations and poor survival in cytopenic patients without hematological malignancies. Mol Cytogenet. 2019;12:46.

13. Imboden S, Nastic D, Ghaderi M, Rydberg F, Rau TT, Mueller MD, et al. Phenotype of POLE-mutated endometrial cancer. PLoS One. 2019;14:e0214318.
14. Li Y, Bian Y, Wang K, Wan XP. POLE mutations improve the prognosis of endometrial cancer via regulating cellular metabolism through AMF/AMFR signal transduction. BMC Med Genet. 2019;20:202.
15. Kurnit KC, Kim GN, Fellman BM, Urbauer DL, Mills GB, Zhang W, et al. CTNNB1 (beta-catenin) mutation identifies low grade, early stage endometrial cancer patients at increased risk of recurrence. Mod Pathol. 2017;30:1032-41.
16. Hirschowitz L, Ganesan R, McCluggage WG. WT1, p53 and hormone receptor expression in uterine serous carcinoma. Histopathology. 2009;55:478-82.
17. Daniilidou K, Frangou-Plemenou M, Grammatikakis J, Grigoriou O, Vitoratos N, Kondi-Pafiti A. Prognostic significance and diagnostic value of PTEN and p53 expression in endometrial carcinoma. A retrospective clinicopathological and immunohistochemical study. J BUON. 2013;18:195-201.
18. Prat J, Gallardo A, Cuatrecasas M, Catasús L. Endometrial carcinoma: pathology and genetics. Pathology. 2007;39:72-87.
19. Terakawa N, Kanamori Y, Yoshida S. Loss of PTEN expression followed by Akt phosphorylation is a poor prognostic factor for patients with endometrial cancer. Endocr Relat Cancer. 2003;10:203-8.
20. Werner HM, Berg A, Wik E, Birkeland E, Krakstad C, Kusonmano K, et al. ARID1A loss is prevalent in endometrial hyperplasia with atypia and low-grade endometrioid carcinomas. Mod Pathol. 2013;26:428-34.
21. Wu JN, Roberts CW. ARID1A mutations in cancer: another epigenetic tumor suppressor? Cancer Discov. 2013;3:35-43.
22. Catasus L, Gallardo A, Cuatrecasas M, Prat J. Concomitant PI3K-AKT and p53 alterations in endometrial carcinomas are associated with poor prognosis. Mod Pathol. 2009;22:522-9.
23. Mjos S, Werner HM, Birkeland E, Holst F, Berg A, Halle MK, et al. PIK-3CA exon9 mutations associate with reduced survival, and are highly concordant between matching primary tumors and metastases in endometrial cancer. Sci Rep. 2017;7:10240.

ORIGINAL ARTICLE

Comparative analysis of PECS-2 and ESP for acute and chronic pain control in breast-conserving surgery. A prospective study

Análisis comparativo de PECS-2 y ESP para el control del dolor agudo y crónico en la cirugía conservadora de mama. Un estudio prospectivo

Hulya Y. Ak[1], Kubra Taskin[1], Merve B. Yediyildiz[1], Irem Durmus[1], Ozlem Sezen[1], Baris Sandal[2], and Banu Cevik[1]*

[1]Department of Anesthesiology and Reanimation, Kartal Dr. Lutfi Kirdar City Hospital; [2]Department of Biostatistics, Istanbul University-Cerrahpasa, Cerrahpaşa Faculty of Medicine. Istanbul, Turkey

Abstract

Objective: *The aim of this study was to compare the effects of Pectoral Nerve Block 2 (PECS-2) and Erector Spinae Plane Block (ESP), which are accepted to have an effect on post-operative pain control after breast cancer surgery, on both acute and chronic pain.* **Method:** *In this double-blind, prospective, randomized study, patients were randomized using a sealed envelope method into two groups: those who underwent PECS-2 (Group P) and those who underwent ESP (Group E) before extubation at the end of the operation. The numerical rating scale (NRS) of patients was queried by a blinded researcher at post-operative 1, 2, 6, 12, and 24 h. In addition, patients were queried for the presence of chronic pain at the 3rd month using NRS.* **Results:** *The NRS scores at 1 h and 2 h in Group P were significantly lower compared to Group E. There was no significant difference in NRS scores at 6 h, 12 h, and 24 h between the groups. The rate of chronic pain was similar between the groups.* **Conclusion:** *In this study examining the effects of ESP and PECS-2 on acute and chronic pain after BCS due to breast cancer, PECS-2 was associated with less post-operative pain.*

Keywords: *Breast-conserving surgery. Chronic post-operative pain. Nerve block. Pain. Post-operative pain. Ultrasonography.*

Resumen

Objetivo: *El propósito de este estudio fue comparar los efectos del pectoral nerve block 2 (PECS-2) y el erector spinae plane block (ESP) en el dolor post-operatorio del cáncer de mama, tanto agudo como crónico.* **Método:** *En este estudio doble ciego, prospectivo y aleatorizado, las pacientes se asignaron aleatoriamente a dos grupos: PECS-2 (grupo P) y BES (grupo E) antes de la extubación al final de la operación. Un investigador ciego evaluó la numerical rating scale (NRS) de las pacientes a las 1, 2, 6, 12 y 24 horas del post-operatorio. Además, se preguntó a las pacientes por la presencia de dolor crónico al tercer mes utilizando la NRS.* **Resultados:** *Las puntuaciones NRS a 1 y 2 horas en el grupo P fueron significativamente menores que las del grupo E. No hubo diferencias significativas en las puntuaciones NRS a las 6, 12 y 24 horas entre ambos grupos. La tasa de dolor crónico fue similar entre ellos.* **Conclusión:** *En este estudio, en el que se examinaron los efectos de ESP y PECS-2 sobre el dolor agudo y crónico después de una BCS por cáncer de mama, el PECS-2 se asoció con menos dolor post-operatorio.*

Palabras clave: *Cirugía conservadora de la mama. Dolor post-operatorio crónico. Bloqueo nervioso. Dolor. Dolor post-operatorio. Ultrasonografía.*

***Correspondence:**
Hulya Y. Ak
E-mail: hulyayilmazak@gmail.com

Date of reception: 17-04-2024
Date of acceptance: 19-06-2024
DOI: 10.24875/CIRU.24000223

Cir Cir. 2025;93(2):145-150
Contents available at PubMed
www.cirugiaycirujanos.com

Introduction

Breast-conserving surgery (BCS) is a surgical method designed to remove cancer by leaving as much of the breast intact as possible. The combination of BCS and sentinel lymph node biopsy has become the standard treatment for patients with early-stage breast cancer. Many patients experience severe acute post-operative pain after breast cancer surgery[1].

Opioid treatment can bring both the pain itself and the accompanying side effects, which can be really distressing for the patient. In addition, acute post-operative pain is a risk factor for chronic post-operative pain and low quality of life after breast cancer surgery[2]. Post-operative chronic pain is defined as pain localized to the surgical area, lasting for at least 3 months, and continuing from acute post-operative pain after excluding other causes of pain[3]. Chronic pain after breast cancer treatment is a significant clinical problem affecting 25-60% of patients. Therefore, the management of post-operative pain is important for outcomes in patients undergoing breast cancer surgery[4].

Perioperative management during breast cancer surgery typically consists of combinations of regional anesthesia techniques combined with general anesthesia. Regional anesthesia also provides better post-operative analgesia, reduced opioid use, and decreased post-operative nausea and vomiting. New regional anesthesia techniques, such as fascial plane blocks have replaced traditional thoracic paravertebral block due to their comparable analgesia with lower complication prevalence[5]. Pectoral Nerve Plane Block 2 (PECS-2) was developed to provide analgesia after breast surgery[6]. This ultrasound-guided block is administered by injecting local anesthetic below the pectoralis minor and serratus anterior muscles at the level of the third rib. Erector Spinae Plane Block (ESP), another commonly used plane block for post-operative pain management, is a relatively simple and safe technique involving the injection of local anesthetic deep into the erector spinae muscle, which can also reduce opioid consumption[7].

The aim of this study is to investigate the effects of two established plane blocks (PECS-2 and ESP) on both acute and chronic pain after BCS in terms of post-operative pain control.

Method

This double-blind, prospective, randomized study was conducted at (Institution name here) between June 2023 and January 2024 after obtaining ethics committee approval (No: 2023/514/250/32, Date: 29 May 2023). Written consent was obtained from all patients. Patient registration and allocation were performed using a consort diagram (Fig. 1). The study included women aged ≥ 18 years who were scheduled for BCS, with or without axillary lymph node clearance and had an ASA physical status of 1-3. Patients who were pregnant, allergic to study drugs, had coagulopathy, injection site infection, chronic pain, or alcohol or drug dependence were excluded from the study. Patients were randomized using a sealed envelope method into two groups: those who underwent PECS-2 (Group P) and ESP (Group E) at the end of the operation. A priori power analysis conducted using GPower 3.1.9.7 software estimated that a minimum sample size of 17 participants per group would be required, assuming an effect size of 1.0, a significance level (α) of 0.05, and 80% power.

Patients were examined and written consent was obtained during the pre-operative period. All operations were performed by the same surgeon. All post-operative blocks were performed under ultrasound guidance (Samsung HM70 EVO) by an anesthesiologist experienced in regional anesthesia (Blocks were applied to all patients by the same anesthesiologist). The anesthesiologists who performed intraoperative patient monitoring and post-operative pain assessment were blinded to the study.

Anesthesia management

All patients received a standard general anesthesia protocol (2 mg/kg IV propofol, 1 μg/kg IV fentanyl, and 0.6-0.8 mg/kg IV rocuronium for intubation). All patients were intubated and connected to the anesthesia machine using volume-controlled ventilation with a tidal volume of 6-8 mL/kg and EtCO2 maintained at 35-45 mmHg. Anesthesia maintenance was achieved with a mixture of 50% oxygen and 50% air and adjusted desflurane and IV remifentanil infusion (0.25-0.5 μg/kg/min) according to 4-6 minimal alveolar concentration. All patients received 10 mg/kg paracetamol and 1 mg/kg tramadol IV at the end of surgery. Based on randomization compliance, a plan block was applied according to the group before extubation.

Ultrasound-guided plan block application

For PECS-2 application in Group P, under sterile conditions, a high-frequency linear ultrasound probe was

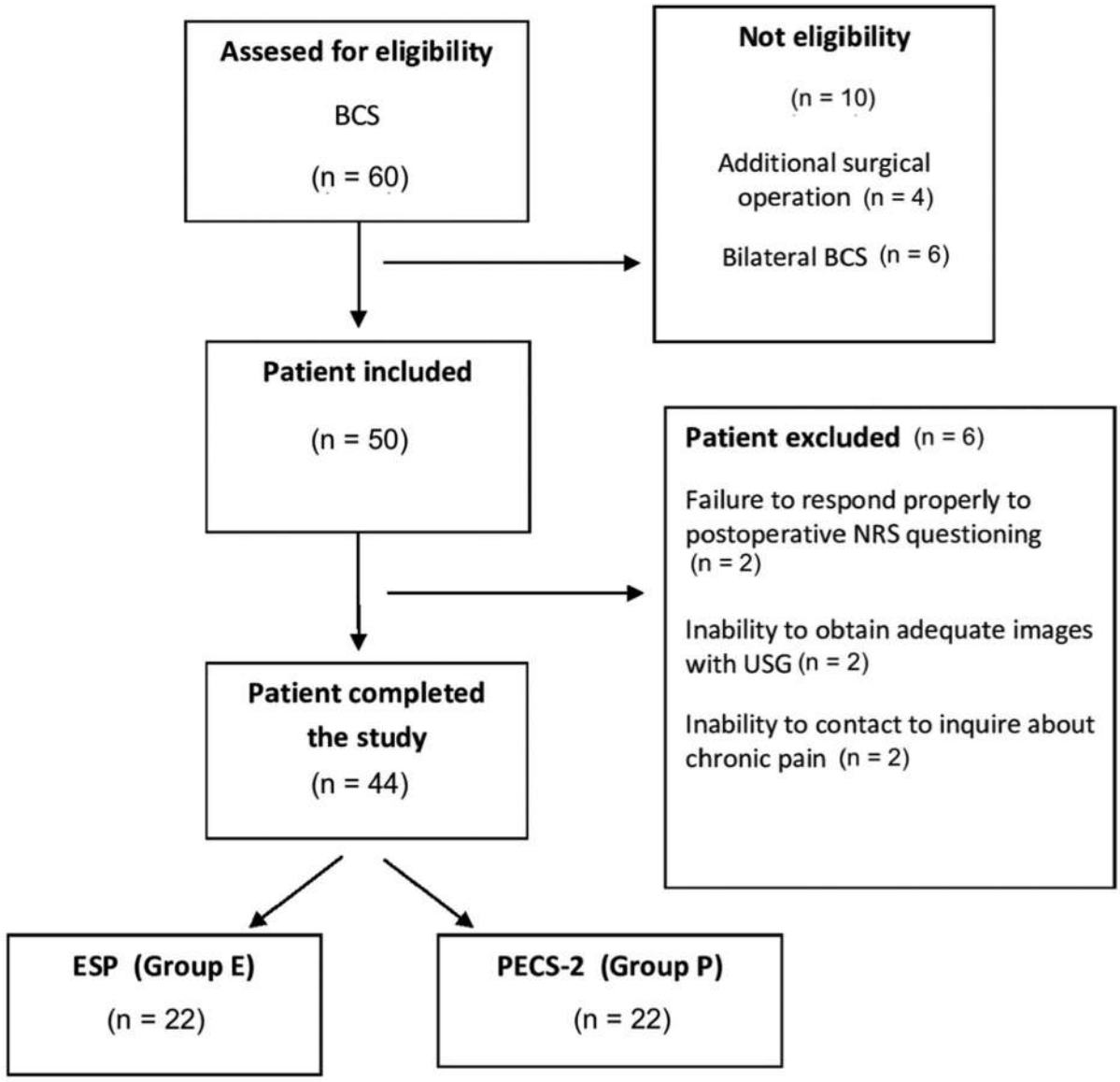

Figure 1. *Flow chart of the consort.*
BCS: breast-conserving surgery; NRS: numerical rating scale; ESP: Erector Spinae Plane; PECS-2: Pectoralis Plane Block 2.

placed in a sagittal plane below the clavicle. A 21-gauge 50 mm isolated facet-tipped needle was inserted from cephalad to caudal under ultrasound guidance and 10 ml of 0.25% bupivacaine was injected between pectoralis minor and major and 20 ml of 0.25% bupivacaine was injected between pectoralis minor and serratus anterior muscles. Bupivacaine was injected slowly with aspiration every 5 ml. For Group E receiving ESP, under ultrasound guidance, a linear USG probe was placed sagittally 2-3 cm lateral to the spine. After identifying the erector spinae muscle and transverse processes, the needle was inserted from the deep aspect of the erector spinae muscle, and 20 ml of 0.25% bupivacaine was applied. A 15-min waiting period was observed for any potential complications. Patients were monitored and followed up for at least 30 minutes in the recovery unit after tracheal extubation.

Post-operative pain assessment

Acute post-operative pain was assessed using the numerical rating scale (NRS) ranging from 0 (no pain) to 10 (worst imaginable pain). In cases where NRS was ≥ 4 at post-operative 30 minutes in the post-anesthetic care unit, patients were given 25 mg IV pethidine as rescue analgesia. Patients requiring

additional analgesia were observed in the post-anesthetic care unit for 1 h.

Post-operative IV analgesia was standardized for all patients. IV Paracetamol 10 mg/kg was administered every 6 h and 25 mg IV Dexketoprofen Trometamol was administered every 12 h. The NRS scores of patients were queried by a blinded researcher at post-operative 1, 2, 6, 12, and 24 h. Each patient was reassessed at post-operative 3 months for the presence of any pain, signs, and symptoms developing or worsening in the breast area (For patients unable to come for follow-up, NRS scores were queried over the phone).

Statistical methods

Descriptive statistics such as mean, standard deviation, median, minimum, maximum, frequency, and ratio values were used to describe the data. Discrete and continuous data were analyzed for normal distribution using the Shapiro-Wilk test. The Independent samples t-test and Mann-Whitney U test were used for the analysis of continuous data which showed normal and skewed distribution. Fisher's exact test or chi-square test was applied to assess statistical significance for discrete and categorical data. All statistical analyses were performed using SPSS Statistics for Windows, version 29.0 (IBM Corp., Armonk, NY, USA). A $p < 0.05$ was considered statistically significant.

Results

A total of 50 patients were included in the study to undergo BCS surgery. The study excluded a total of 6 patients: 2 due to non-cooperation during the NRS assessment, 2 because sufficient ultrasound images couldn't be obtained, and 2 others because communication couldn't be established with them 3 months later. The study was completed with a total of 44 patients (Fig. 1). All patients were female (100%). The mean age was 54.3 ± 7.9 years, and the mean BMI was 28.1 ± 3.5 kg/m². 61.4% of the patients underwent surgery on the left breast, while 38.6% underwent surgery on the right breast.

There were 22 patients in each group. There were no significant differences in age, weight, height, or BMI between Group P and Group E ($p = 0.173$). There was no significant difference between the groups in terms of side (right-left) ($p = 0.353$). The rate of chronic diseases in Group P was significantly higher than in Group E ($p = 0.030$) (Table 1).

There were no significant differences between the groups in terms of pre-operative, intraoperative systolic, and diastolic blood pressure ($p = 0.475$, $p = 0.232$, $p = 0.205$, $p = 0.392$). The pre-operative heart rate in Group P was significantly higher than in Group E ($p = 0.027$). There were no significant differences between the groups in terms of pre-operative and intraoperative saturation and intraoperative heart rate ($p = 0.636$, $p = 0.198$, $p = 0.116$). In addition, surgical duration, anesthesia duration, total fluid, and total bleeding were similar between the groups ($p = 0.162$, $p = 0.490$, $p = 0.811$, $p = 0.382$).

The NRS scores at 1 h and 2 h were significantly lower in Group P compared to Group E ($p < 0.001$, $p < 0.001$). There were no significant differences between the groups in terms of NRS scores at 6 h, 12 h, and 24 h ($p = 0.128$, $p = 0.159$, $p = 0.657$) (Fig. 2). The rate of chronic pain was similar between the groups ($p = 0.294$) (Table 1).

Discussion

In this study, the effect of two different plane blocks applied in the pre-extubation period on post-operative acute and chronic pain was compared in breast cancer patients undergoing BCS. The PECS-2 had significantly lower NRS scores compared to ESP. No difference was observed in NRS scores queried at other times (6, 12, and 24 h) between the groups. We could not detect any difference in the effect of these two plane blocks on post-operative chronic pain.

Gürkan et al. showed a decrease in total morphine consumption in the post-operative period with the ESP applied in the pre-operative period in patients undergoing mastectomy. However, in this study, no difference was observed in NRS scores between patients who did not receive blocks[8]. On the contrary, in a meta-analysis including 679 patients and 11 articles examining recent studies, it was found that ESP performed under USG guidance significantly reduced post-operative pain intensity after breast cancer surgery[9]. In our study, the mean NRS scores at 1, 2, 6, 12, and 24 h remained below 5 in Group E. No complications were encountered during block application.

Yu et al. conducted a comprehensive study with 526 patients undergoing breast cancer surgery, comparing patients who underwent PECS-2 block in the pre-operative period under general anesthesia with those who did not. It was observed that PECS-2 reduced intraoperative remifentanil consumption[10]. In the study by Versyck et al., which compared patients undergoing PECS-2 with those undergoing thoracic paravertebral blocks, no significant difference was found in

Table 1. Comparison of pre and post-operative period data of patients who underwent ESP and PECS-2 procedures

Variable	ESP group		PECS-2 group		p
	Mean ± SD/n-%	Median	Mean ± SD/n-%	Median	
Age (year)	52.6 ± 7.0	52.5	56.0 ± 8.5	58.5	0.150
Weight (kg)	73.4 ± 4.7	73.0	71.8 ± 11.0	70.0	0.534
Height (cm)	161.0 ± 3.6	160.0	160.6 ± 3.2	160.0	0.652
BMI (kg/m^2)	28.4 ± 2.0	28.4	27.9 ± 4.6	27.2	0.173
Side					
Left	12 (54.5%)		15 (68.2%)		0.353
Right	10 (45.5%)		7 (31.8%)		
Chronic disease					
(-)	12 (54.5%)		5 (22.7%)		0.030
(+)	10 (45.5%)		17 (77.3%)		
Chronic pain					
(-)	19 (86.4%)		21 (95.5%)		0.294
(+)	3 (13.6%)		1 (4.5%)		
Systolic blood pressure (mmHg)					
Pre-operative	135.8 ± 9.9	135.5	138.5 ± 10.1	140.0	0.475
Peroperative	126.3 ± 11.4	129.0	122.3 ± 11.6	120.0	0.232
Diastolic blood pressure (mmHg)					
Pre-operative	80.2 ± 8.7	80.0	83.4 ± 7.4	82.0	0.205
Peroperative	74.1 ± 5.0	75.5	75.6 ± 4.6	76.0	0.392
Heart rate (bpm)					
Pre-operative	81.9 ± 5.0	82.0	86.8 ± 7.3	85.0	0.027
Peroperative	78.3 ± 6.0	76.0	81.0 ± 7.6	80.0	0.116
Saturation (%)					
Pre-operative	99.0 ± 1.0	99.0	99.0 ± 1.3	99.5	0.636
Peroperative	99.1 ± 0.8	99.0	99.4 ± 0.5	99.0	0.198
Surgical duration (min)					
Anesthesia duration (min)	114.3 ± 23.1	120.0	104.1 ± 16.4	105.0	0.162
Total fluid (mL)	131 ± 24.9	130.0	123.0 ± 13.9	125.0	0.490
Total blood loss (mL)	1272.7 ± 281.5	1200.0	1220.5 ± 140.3	1200.0	0.811
	64.8 ± 22.2	65.0	59.8 ± 14.3	50.0	0.382
NRS score (h)					
1	4.9 ± 1.0	5.0	2.8 ± 1.1	3.0	< 0.001
2	4.9 ± 1.0	5.0	3.4 ± 0.7	3.0	< 0.001
6	4.2 ± 0.6	4.0	3.9 ± 0.8	4.0	0.128
12	3.6 ± 0.5	4.0	3.3 ± 0.6	3.0	0.159
24	2.9 ± 0.7	3.0	2.8 ± 0.7	3.0	0.657

BMI: body mass index; ESP: erector spinae plane block; PECS-2: pectoral nerve block type 2; NRS: numeric rating scale.

post-operative pain scores, time to first analgesic request, and 24-h opioid consumption. PECS-2, being a less invasive method compared to thoracic paravertebral block, is important in terms of its efficacy in pain management[11]. Barrington et al. found that in patients undergoing a smaller intervention such as BCS, PECS-2, and surgical local infiltration resulted in similar pain scores in terms of post-operative pain in breast cancer patients[12].

In a meta-analysis involving 17 studies with 1069 patients, it was shown that both PECS-2 and ESP blocks were more effective than systemic analgesia in terms of post-operative analgesia following modified radical mastectomy[13]. In the study by Altıparmak et al., PECS-2 effectively reduced post-operative tramadol consumption and pain scores compared to ESP after radical mastectomy[14]. Similarly, in the study by Bakeer et al., total morphine consumption was found to be lower in patients undergoing PECS-2 after mastectomy

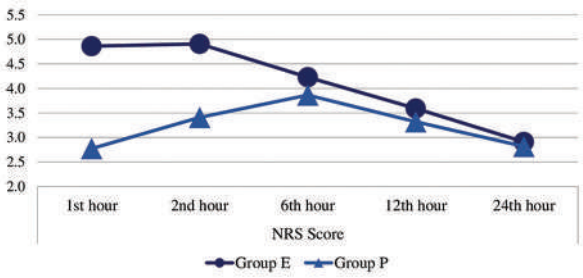

Figure 2. *Comparison of NRS scores between groups. NRS: numeric rating scale.*

compared to ESP. In addition, pain intensity was higher in the ESP group at 1, 2, and 6 h after surgery[15]. In our study, the NRS score in Group P was lower than Group E at 1 and 2 h post-operatively. Unlike this study, there was no difference in NRS scores between groups at other times (6, 12, 24 h) in our study.

In the study by Fujii et al., where they investigated chronic pain after mastectomy, the rate of chronic pain reported 6 months after surgery in patients who underwent PECS-2 was observed to be lower compared to Serratus Plane Block[16]. De Cassai et al. also showed in their study that PECS-2 reduced chronic pain at 3 months after mastectomy[4]. In our study, the rate of chronic pain after BCS was 9.1%. This rate was lower than the reported rates of chronic pain after mastectomy, which range from 20% to 60% in some studies[2]. This may be because BCS is a smaller surgical intervention compared to mastectomy, resulting in a lower rate of chronic pain. In addition, since we applied plane blocks in both groups, the relatively lower incidence of acute pain in the participants could be associated with this. Although three out of four patients with chronic pain were in Group E, we didn't observe a significant difference in terms of chronic pain between PECS-2 and ESP.

Conclusion

In this study, we examined the effects of ESP and PECS-2 on post-operative acute and chronic pain in patients undergoing BCS for breast cancer. According to our findings, PECS-2 was associated with less pain in the post-operative 1st and 2nd h. However, neither block was effective in reducing chronic pain. Our results indicate that PECS-2 is effective in reducing early-stage pain in patients undergoing BCS surgery.

Funding

The authors declare that they have not received funding.

Conflicts of interest

The authors declare no conflicts of interest.

Ethical considerations

Protection of humans and animals. The authors declare that no experiments involving humans or animals were conducted for this research.

Confidentiality, informed consent, and ethical approval. This study was performed in line with the principles of the Declaration of Helsinki. Approval was granted by the Ethics Committee of Kartal Dr. Lutfi Kirdar City Hospital (June 30, 2022/No:2022/514/228/22).

Declaration on the use of artificial intelligence. The authors declare that no generative artificial intelligence was used in the writing of this manuscript.

References

1. Andersen KG, Duriaud HM, Jensen HE, Kroman N, Kehlet H. Predictive factors for the development of persistent pain after breast cancer surgery. Pain. 2015;156:2413-22.
2. Al Ja'bari A, Robertson M, El-Boghdadly K, Albrecht E. A randomised controlled trial of the pectoral nerves-2 (PECS-2) block for radical mastectomy. Anaesthesia. 2019;74:1277-81.
3. Kehlet H, Jensen TS, Woolf CJ. Persistent postsurgical pain: risk factors and prevention. Lancet. 2006;367:1618-25.
4. De Cassai A, Bonanno C, Sandei L, Finozzi F, Carron M, Marchet A. PECS II block is associated with lower incidence of chronic pain after breast surgery. Korean J Pain. 2019;32:286-91.
5. Woodworth GE, Ivie RM, Nelson SM, Walker CM, Maniker RB. Perioperative breast analgesia: a qualitative review of anatomy and regional techniques. Reg Anesth Pain Med. 2017;42:609-31.
6. Blanco R. The "pecs block": a novel technique for providing analgesia after breast surgery. Anaesthesia. 2011;66:847-8.
7. Singh S, Kumar G, Akhileshwar. Ultrasound-guided erector spinae plane block for postoperative analgesia in modified radical mastectomy: a randomised control study. Indian J Anaesth. 2019;63:200-4.
8. Gürkan Y, Aksu C, Kuş A, Yörükoğlu UH, Kılıç CT. Ultrasound guided erector spinae plane block reduces postoperative opioid consumption following breast surgery: a randomized controlled study. J Clin Anesth. 2018;50:65-8.
9. Zhang Y, Liu T, Zhou Y, Yu Y, Chen G. Analgesic efficacy and safety of erector spinae plane block in breast cancer surgery: a systematic review and meta-analysis. BMC Anesthesiol. 2021;21:59.
10. Yu L, Cui X, Song P, Li C, Zhao H, Chang Y. Perioperative pectoral nerve block type II and postoperative recurrence in breast cancer: a randomized controlled trial. BMC Surg. 2022;22:447.
11. Versyck B, van Geffen GJ, Chin KJ. Analgesic efficacy of the Pecs II block: a systematic review and meta-analysis. Anaesthesia. 2019;74:663-73.
12. Barrington MJ, Seah GJ, Gotmaker R, Lim D, Byrne K. Quality of recovery after breast surgery: a multicenter randomized clinical trial comparing pectoral nerves interfascial plane (Pectoral Nerves II) block with surgical infiltration. Anesth Analg. 2020;130:1559-67.
13. Hong B, Bang S, Oh C, Park E, Park S. Comparison of PECS II and erector spinae plane block for postoperative analgesia following modified radical mastectomy: Bayesian network meta-analysis using a control group. J Anesth. 2021;35:723-33.
14. Altıparmak B, Korkmaz Toker M, Uysal Aİ, Turan M, Gümüş Demirbilek S. Comparison of the effects of modified pectoral nerve block and erector spinae plane block on postoperative opioid consumption and pain scores of patients after radical mastectomy surgery: a prospective, randomized, controlled trial. J Clin Anesth. 2019;54:61-5.
15. Bakeer A, Abdallah NM. Erector spinae plane block versus PECS block type II for breast surgery: a randomized controlled trial. Anesthesiol Pain Med. 2022;12:e122917.
16. Fujii T, Shibata Y, Akane A, Aoki W, Sekiguchi A, Takahashi K, et al. A randomised controlled trial of pectoral nerve-2 (PECS 2) block vs. serratus plane block for chronic pain after mastectomy. Anaesthesia. 2019;74:1558-62.

ORIGINAL ARTICLE

Evaluation of the effectiveness of human breast milk exosomes in experimental testicular torsion-detorsion injury model

Evaluación de la eficacia de los exosomas de la leche materna humana en un modelo experimental de lesión por torsión-destorsión testicular

Ünal T. Öztürk[1], Hatice S.Y. Cömert[2], Gül Şalcı[2], Ahmet Alver[3], Sevdegül A. Mungan[4], Neslihan Sağlam[3], Şeniz Erdem[3], Serdar Karakullukçu[5], Mustafa İmamoğlu[2], and Haluk Sarıhan[2]*

[1]Department of Pediatric Surgery, Artvin Public Hospital, Artvin; [2]Department of Pediatric Surgery; [3]Department of Biochemistry; [4]Department of Pathology; [5]Department of Public Health. Faculty of Medicine, Karadeniz Technical University, Trabzon, Turkey

Abstract

Objective: *Our aim was to examine the effectiveness of human breast milk exosomes in treating testicular torsion.* **Methods:** *Rats were divided randomly into three equal groups. Group 1 was our control group. A torsion/detorsion model was created for the rats in Group 2. After the torsion/detorsion model, 1 mg/kg intraperitoneally human breast milk exosomes were given 30 min before detorsion in Group 3. All testicles were removed at the 6th h of the experiment, for biochemical and histopathological examination.* **Results:** *There was a statistically significant decrease in Group 3 MDA values compared to Group 2. When Group 3 and Group 2 SOD and CAT values were compared, it was seen that these values were higher in Group 3. Histopathologically a statistically significant difference was found in Group 3 compared to Group 1 and Group 2 in terms of ischemia/reperfusion injury.* **Conclusion:** *We have shown that human breast milk exosomes in testicular torsion do not completely prevent reperfusion injury but significantly preserve testicular tissue.*

Keywords: *Testicular torsion. Exosome. Ischemia/reperfusion.*

Resumen

Objetivo: *Nuestro objetivo era examinar la eficacia de los exosomas de la leche materna humana en el tratamiento de la torsión testicular.* **Métodos:** *Las ratas se estudiaron en tres grupos iguales. El grupo 1 fue nuestro grupo control. Se creó un modelo de torsión/destorsión para las ratas del grupo 2. Después del modelo de torsión/destorsión, se administró 1 mg/kg de exosomas de leche materna humana por vía intraperitoneal 30 minutos antes de la destorsión en el grupo 3. Todos los testículos se extirparon a la sexta hora del experimento para examen bioquímico e histopatológico.* **Resultados:** *Hubo una disminución estadísticamente significativa en los valores de MDA del grupo 3 en comparación con el grupo 2. Cuando se compararon los valores de SOD y CAT del grupo 3 y del grupo 2, se vio que estos valores eran mayores en el grupo 3. Histopatológicamente se encontró una diferencia estadísticamente significativa en el grupo 3 en comparación con el grupo 1 y el grupo 2 en términos de lesión por isquemia/reperfusión.* **Conclusión:** *Hemos demostrado que los exosomas de la leche materna humana en la torsión testicular no previenen completamente la lesión por reperfusión, pero preservan significativamente el tejido testicular.*

Palabras clave: *Torsión testicular. Exosoma. Isquemia/reperfusión.*

***Correspondence:**
Hatice Sonay Yalçın Cömert
E-mail: sonayyalcin@hotmail.com

Date of reception: 12-09-2023
Date of acceptance: 22-11-2023
DOI: 10.24875/CIRU.23000462

Cir Cir (Eng). 2025;93(2):151-157
Contents available at PubMed
www.cirugiaycirujanos.com

Introduction

Testicular torsion is a surgical emergency that causes cessation of blood flow to the testis and surrounding structures due to the vertical rotation of the spermatic cord in newborns, children, and adolescents[1]. The incidence in men under the age of 25 is 1/4000[2]. Early diagnosis and surgical intervention are required to prevent infertility and subfertility[3]. The diagnosis of testicular torsion should be made within the first 4-6 h. Especially if there is complete spermatic cord torsion, that is if there is a 720-degree rotation, it causes irreversible ischemic damage to the testis and loss of gonads[4].

Ischemic damage during testicular torsion occurs due to oxidative stress and inflammation due to reactive oxygen species (ROS). The primary cause of testicular damage during the ischemic injury period is associated with decreased oxygen supply[5]. Tissue reperfusion should be provided as soon as possible to preserve the viability of ischemia-induced tissues. It is known that after detorsion of the testis, reperfusion also causes cellular damage, which is associated with an increase in ROS production and neutrophil infiltration[6]. The radicals formed in this process cause peroxidation of lipids in the cell membrane, denaturation of proteins, and DNA damage[7].

In recent years, extensive research has sought effective strategies and drugs to minimize or prevent testicular ischemia/reperfusion (I/R) injury. However, other than trying to reduce the temperature of the scrotum, this is the only method that has been successfully applied in clinical practice[8]. Therefore, there is an urgent need to develop new therapeutic agents and a standard treatment protocol to reduce mortality and morbidity rates.

Exosomes are nanoscale cell-derived extracellular vesicles secreted from various cell types and found to contain bioactive components[9]. Exosomes, which can be obtained from saliva, urine, plasma, breast milk, and many other bodily fluids, can be used for therapeutic purposes, as they provide genetic material transfer, immune regulatory roles, and intercellular communication[6,10,11]. Exosomes are natural and, thanks to their very small size, can easily pass through anybody barrier. Considering these benefits, the therapeutic use of exosomes is inevitable[12].

In recent studies, it has been proven that there are high concentrations of exosomes in breast milk, and they have been used in various experimental studies in the literature[13,14]. In this study, we aimed to investigate the protective effect of human breast milk exosomes against I/R damage in testicular torsion and their usability as a treatment modality.

Method

This study was carried out with the contributions of the Departments of Biochemistry and Pathology after being planned by the Department of Pediatric Surgery of Karadeniz Technical University (KTU) Faculty of Medicine, and the ethics committee approval with protocol number 2021/10 was obtained. The surgeries were performed in the KTU Faculty of Medicine Surgical Research Laboratory. Our work was supported by the Scientific Research Projects Coordination Unit.

Study Design

Three groups of 8 Sprague Dawley rats, which were divided randomly and each weighing 250-300 gr, were used in the study. The duration of the experiment was determined as 1 day. Until the study day, the rats were housed in cages with 8 or less sawdust under standard laboratory conditions at 22 ± 2 °C constant room temperature, 60% humidity, and 12 h light/12 h dark. Rats fasted for 24 h before surgery, and only water was given. In all surgical procedures, anesthesia was administered intraperitoneally, 10 mg/kg xylazine hydrochloride (Rompun, Bayer, Turkey) and 50 mg/kg ketamine (Ketalar, Pfizer, Turkey).

Surgical Technique: The operation area was shaved and cleaned with betadine solution. An incision made from the scrotal midline was used in the surgeries. Torsion/detorsion model; the left testis was taken out and rotated 720 degrees counterclockwise. Then, the tunica albuginea was sutured with 6/0 monofilament and fixed to the scrotum so the testis would not be detorsioned again. The scrotum was closed with 4/0 silk, and torsion was performed. After 4 h, the testis was detorted and waited. Orchiectomy was performed on the left testis 2 h after the detorsion procedure.

Group 1: after anesthesia, a vertical incision was made from the scrotal midline; the left testis was taken out by cutting the gubernaculum, then placed in the scrotum in an anatomical position without torsion. The layers were closed with 4/0 silk, and the left orchiectomy was performed 6 h later.

Group 2: a torsion/detorsion model was created for the rats in this group, and left testis orchiectomy was

performed 2 h after detorsion, that is, at the 6th h of the experiment.

Group 3: a torsion/detorsion model was created for rats in this group, and 1 mg/kg ip human breast milk exosomes were given 30 min before detorsion. Left orchiectomy was performed 2 h after detorsion, at the 6th h of the experiment.

The orchiectomy material was divided into two parts. Half of the obtained testicular tissue was immediately frozen with liquid nitrogen and stored at –80 degrees until biochemical analysis. The other half was reserved for histopathological examinations.

Human breast milk collection and exosome isolation

Approximately 200-300 mL of fresh breast milk samples were collected from healthy lactating mothers who applied to the KTU University, Faculty of Medicine, Pediatric Surgery Clinic (Trabzon, Turkey). Milk samples were frozen immediately and kept at –80 °C until used. Exosomes were isolated from breast milk by differential centrifugation and ultracentrifugation. All centrifugations were performed at 4 °C, and breast milk was centrifuged at 3000×g (F0650 rotor, Beckman Coulter Instruments, USA) for 10 min to separate the milk lipid layer. The supernatant was transferred to a new tube, and centrifugation was performed again at 5,000 ×g (F0650 rotor, Beckman Coulter Instruments, USA) for 30 min to eliminate large cellular debris and remaining lipids. Then, the new supernatant was transferred to a new tube, and centrifugation was performed again at 12,000 ×g (F0650 rotor, Beckman Coulter Instruments, USA) for 10 min to remove smaller cellular debris and apoptotic cells. The exosomes were obtained from the new centrifuged milk supernatant by ultracentrifugation at 110,000 ×g for 2 h at 4°C using a JS 24.15 rotor (Beckman Coulter Instruments, USA). After removing the exosome-free supernatant, the crude exosome pellet was suspended in 1000 μL phosphate-buffered saline (PBS, pH 7.4) in a 1.5 mL Eppendorf tube and stored at –80 °C until used for the experiment.

Human breast milk-derived exosome protein extraction and confirmation by western blot

Human breast milk-derived exosomes were lysed in RIPA lysis solution (SE3924401, SERVA) containing protease and phosphatase inhibitor cocktail (PPC1010, SIGMA) was added, and exosomes were kept on ice for 15 min. Afterward, the protein was obtained by centrifugation at 15000 xg, +4°C for 15 min, and its concentrations were analyzed using the Bicinchoninic acid (BCA) kit (LOT: UD282967, Thermo Scientific, USA) and analyzed for total CD63 (positive exosome membrane marker) and calnexin (negative marker) protein expression. Lysate was separated by SDS-PAGE and transferred onto a nitrocellulose membrane. The membranes were probed with antibodies and detected using enhanced chemiluminescence detection. Primary antibodies were as follows: anti-CD63 (1:1000; Abcam, ab68418); and anti-calnexin (1:1000; Abcam, ab213243). The secondary antibody was horseradish peroxidase (HRP)-conjugated goat anti-rabbit (1:5000; Abcam, ab97200).

The protein concentration of the breast milk exosomes used in the experiment was adjusted to 1 μg/mL by the BCA kit.

Biochemical analysis

Testicular tissue was homogenized with 2 mL of cold homogenization buffer in a test tube for about 20 s until the tissues were completely disintegrated and then centrifuged at 3,000 rpm for 10 min. 750 μL of supernatant was placed in 1.5 mL Eppendorf. 600 μL of ethanol-chloroform (2:3) mixture was added to it. It was centrifuged at 10,000 xg for 30 min at +4°C. After centrifugation, protein determination, superoxide dismutase (SOD), and catalase (CAT) activity were measured in the protein phases on the upper part of the Eppendorf. SOD enzyme activity was performed by modifying the method developed by Sun and Oberley[15]. The Aebi method was used to determine CAT enzyme activity[16].

Testicular tissue was homogenized with 2 mL of cold homogenization buffer in a test tube for about 30 s until the tissues were completely disintegrated and then centrifuged at 3,000 rpm for 10 min. The supernatant was taken, and the Malondialdehyde (MDA) level was determined. This method was carried out by modifying the method based on measuring the absorbance at 532 nm of the color of the complex formed by MDA with thiobarbituric acid in an acidic medium[17].

Histopathological assay

Tissues were fixed in Bovine solution for 72 h. Fixed tissue pieces were dehydrated by passing through

70%, 90%, 96%, and 100% graded alcohol series. It was then cleared by passing through a xylene solution. After the paraffin blocks of the tissues were prepared, 5 μm thick sections were taken with a fully automatic microtome. Sections were stained with hematoxylin and eosin (H&E) after deparaffinization. The H&E stained slides were evaluated histopathologically with a light microscope (Olympus BX 51; Olympus Optical Co, Ltd, Tokyo, Japan), by an experienced pathologist unaware of the study groups. Damage to testicular tissues was graded by the Johnsen Testicular Biopsy Score (JTBS). In this scoring system, testicular tissues were evaluated semi-quantitatively in 5 high power fields (HPF) at x200 magnification by light microscopy.

Statistical analysis

SPSS 23.0 statistical package program was used in the analysis of the data. Descriptive statistics of the evaluation results were given as median and quartiles (Q1-Q3). The suitability of the data for normal distribution was checked with the Kolmogorov-Smirnov test. The Kruskal-Wallis test was used to compare the numerical values of three independent groups. A statistically significant level was taken as $p < 0.05$ in the Kruskal-Wallis test. Since significant results were found in the Kruskal-Wallis test, Bonferroni correction was made when making pairwise comparisons. Mann-Whitney U test was used and $p < 0.017$ (0.05/3) was considered significant.

Results

Confirmation of exosomes from mother milk

The presence of exosomes from human breast milk was confirmed by Western blot for the exosome membrane markers cluster of differentiation 63 (CD63) and the negative marker calnexin (Fig. 1).

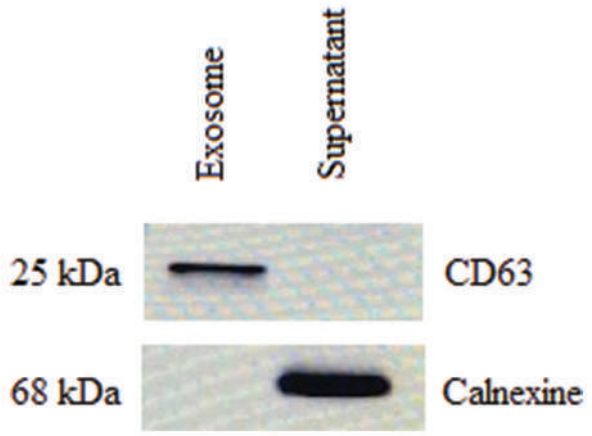

Figure 1. *Confirmation of mother-breast milk exosomes by Western Blot.*

Biochemical analysis

When the tissue MDA, SOD, and CAT values of the three groups were compared, a statistically significant difference was found which is shown in table 1.

When the pairwise MDA values of the groups were compared, a statistically significant difference was found between group 1-group 2 and group 2-group 3 ($p < 0.05$). There was no significant difference between group 1 and group 3.

When the pairwise SOD values of the groups were compared, a statistically significant difference was found between group 2 and group 3 ($p < 0.05$). There was no significant difference between group 1-group 2 and group 1-group 3.

When the pairwise CAT values of the groups were compared, a statistically significant difference was found between group 1 and group 2 ($p < 0.05$). There was no significant difference between group 1-group 3 and group 2-group 3. A pairwise comparison of tissue MDA, SOD, and CAT values is given in table 1.

Histopathological assay

When the left testis JTBS of different groups were compared histopathologically, the difference between them was found to be statistically significant. Values are given in table 2.

A statistically significant difference was found between group 1-group 2 and group 2-group 3 when comparing the JTBS values of the groups in pairs. There was no significant difference between Group 1 and group 3 ($p < 0.05$). Values are given in table 2. Histopathological images in all three groups are shown in figure 2.

Discussion

The primary pathology in testicular torsion is venous occlusion that causes testicular edema and pain. However, this venous occlusion causes hypoxia in the

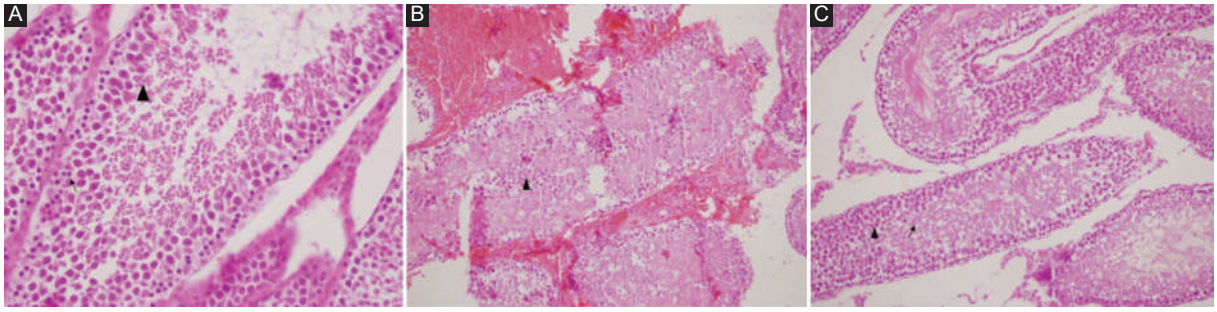

Figure 2. A: *sertoli cell, spermatogonia (↑), and Spermatocyte (▲) in testicle of group 1.* **B***: diffuse fresh bleeding in the interstitial area and exfoliated necrotic cells in seminiferous tubule lumen, few ghost germinal epithelial cells in the left testicular tubule lumen belonging to group 2 (▲) (H&E ×100).* **C:** *Spermatids (↑) and spermatozoons (▲) in the testis belonging to group 3.*

Table 1. The mean values of the biochemical results of the groups

Parameters	Group 1 Median (Q1-Q3)	Group 2 Median (Q1-Q3)	Group 3 Median (Q1-Q3)	p*	*Post-hoc***
MDA (nmol/mg protein)	28.45 (21.03-34.73)	68.74 (44.11-91.00)	22.38 (19.68-22.52)	< 0.001	p^{1-2} = 0.015 p^{2-3} < 0.001
SOD (U/mg protein)	9.83 (8.67-10.65)	10.86 (9.21-13.96)	7.30 (6.78-9.46)	0.012	p^{2-3} = 0.004
CAT (k/g protein)	6.87 (5.54-7.38)	3.33 (2.39-3.84)	5.70 (3.88-6.95)	0.007	p^{1-2} = 0.002

*p < 0.05 was considered statistically significant. The Kruskal-Wallis test was used. **p < 0.017 was considered statistically significant. Bonferroni correction has been made. Mann-Whitney U test was used.
MDA; malondialdehyde; SOD: superoxide dismutase; CAT: catalase.

Table 2. Histopathological assay; JTBS results

Groups	JTBS mean values Median (Q1-Q3)	p*	*Post-hoc***
Group 1	9.5 (9.0-10.0)	< 0.001*	p^{1-2} < 0.001 p^{2-3} = 0.014
Group 2	3.0 (3.0-4.0)		
Group 3	8.0 (7.0-8.0)		

*p < 0.05 was considered statistically significant. Kruskal-Wallis test was used.
**p < 0.017 was considered statistically significant. Bonferroni correction has been made. Mann-Whitney U test was used.
JTBS: Johnsen testicular biopsy score.

testis, just as in other tissues, by disrupting the arterial circulation because the tunica of the testis is not elastic. Thrombi formed at venous, arterial, and capillary levels cause testicular ischemia and subsequent necrosis[18]. By eliminating the factor causing ischemia in reperfusion, blood flow to the ischemic organ can be restored, irreversible damage can be prevented, and lost functions can be restored. However, "reperfusion damage" occurs due to the free oxygen radicals formed and the activated blood cells in the blood. Reperfusion after ischemia damages the tissue more than ischemia[19,20].

Despite the search for alternative medical treatment methods for testicular torsion, emergency surgery is still a valid and widely applied treatment. Although the effect of testicular tissue by torsion is related to the duration and degree of torsion, the efficacy of numerous pharmacological agents and treatments have been evaluated in animal models to prevent testicular reperfusion injury since the primary preventable tissue damage occurs during the post-detorsion reperfusion period[21].

Exosomes are serious cell-cell communication messengers and contain proteins, lipids, and genetic material that can be transported between cells to mediate intercellular communication and immune response[22]. Their existence as natural carriers, high biodistribution and stability in plasma, and relatively small size make them suitable candidates for therapeutic applications[12].

A recent study suggested that exosomes produced from human breast milk may reduce oxidative stress and support immune system development[23], and this encouraged us to use human breast milk exosomes in our study. Admyr et al. showed that exosomes in human breast milk can potentially affect the infant's immune system[14]. To investigate the effect of

exosomes against I/R damage in testicular torsion due to their protective effects in reperfusion injury mentioned above and positive effects on sperm motility and viability, we used exosomes obtained from breast milk, which has not been tested in the literature before.

First, we showed that the presence of human breast milk exosome produced in the Department of Biochemistry of KTU was confirmed by the presence of CD63 and the absence of calnexin using the Western blot method. Then we applied ip low dose (1 cc) exosomes 30 min before detorsion to the torted testis. Studies show that local injection of the damaged testis has no adverse effect on the contralateral testis[24,25]. Our study, in which we obtained statistically significant results, shows that testicular I/R damage and necrosis occur in the testicular tissue.

Keivan et al. have shown that rats' blood serum-derived exosomes inhibit testicular damage, including seminiferous tubule degeneration and loss of interstitial tissue, due to high NO and MDA levels following testicular torsion and NO, MDA, and apoptotic gene expression levels decrease and provide healthy sperm production[26]. Similarly, in our study, when the MDA values of group 2 and group 3 were compared, we found a statistically significant difference between the two groups. Group 3 had significantly lower MDA values. The MDA value does not increase due to the effect of exosomes on reducing tissue damage. In addition, no statistically significant difference was found when the MDA values of group 1 and group 3 were compared.

No statistically significant difference was found when the SOD and CAT values of group 1 and group 3 were compared, and this makes us think that antioxidant enzymes are consumed less in group 3, and instead, the exosome is used as an antioxidant. As a result of these data, we think the exosome is biochemically effective in I/R damage since the MDA and SOD values are significantly different, and the CAT values are higher than Group 2, although there is no statistically significant difference.

Liu et al. showed that caspase-dependent apoptosis pathways are activated after testicular torsion injury, and spermatogenic cells are largely apoptotic, whereas treatment with exosomes significantly reduces the degree of apoptosis in spermatogenic cells[24]. In addition, it has been shown histopathologically that the proliferative effect of the exosomes on spermatogenic cells is not limited to primary spermatocytes, and that it can inhibit spermatogenic cell apoptosis and promote proliferation after testicular torsion-detorsion injury[24]. In our study, when group 2 and group 3 were compared, it was shown that the testicles of group 3 had less damage than group 2, and the difference between them was statistically significant. When group 1 and group 3 were compared, although there were histopathological differences, there was no statistically significant difference. Since exosome application significantly reduced the reperfusion damage in testicular tissue compared to the torsion group in histopathology, it was seen as an expected result that it was not statistically significant. In group 3, spermatids and spermatozoa were preserved, although not as much as normal; it has been shown that there is a significant difference compared to group 2.

Finally, the fact that exosomes were taken from human breast milk, prepared and confirmed with a series of procedures, and the application dose was taken by taking samples from previous experimental studies can be considered among the limitations of our study.

Conclusion

Exosomes are important in diagnostic and therapeutic research as they are natural liposomes. Although studies on exosomes obtained from human breast milk have succeeded and increased in recent years, there is no clinical use in humans yet. We showed that exosomes were significantly protecting the testicular tissue and germ cells compared to the torsion group and new long-term experimental studies with different doses should be needed.

Funding

The authors declare that they have not received funding.

Conflicts of interest

The authors declare no conflicts of interest.

Ethical considerations

Protection of humans and animals. The authors declare that the procedures followed were in accordance with the regulations of the relevant clinical research ethics committee and with those of the Code of Ethics of the World Medical Association (Declaration of Helsinki).

Confidentiality, informed consent, and ethical approval. The authors have followed their institution's confidentiality protocols, obtained informed consent from patients, and received approval from the Ethics Committee. The SAGER guidelines were followed according to the nature of the study.

Declaration on the use of artificial intelligence. The authors declare that no generative artificial intelligence was used in the writing of this manuscript.

References

1. Yilmaz E, Hizli F, Afşarlar ÇE, Demirtaş C, Apaydin S, Karaman İ, et al. Early diagnosis of testicular torsion in rats by measuring plasma d-dimer levels: comparative study with epididymitis. J Pediatr Surg. 2015;50:651-4.
2. Mansour M, Degheili J, Khalifeh I, Tamim H, Jaafar RF, El-Hout Y. Remote ischemic conditioning in a rat model of testicular torsion: does it offer testicular protection? J Pediatr Urol. 2019;15:43.e1-7.
3. Akgür FM, Kilinç K, Aktuğ T. Reperfusion injury after detorsion of unilateral testicular torsion. Urol Res. 1993;21:395-9.
4. Asgari SA, Mokhtari G, Falahatkar S, Mansour-Ghanaei M, Roshani A, Zare A, et al. Diagnostic accuracy of C-reactive protein and erythrocyte sedimentation rate in patients with acute scrotum. Urol J. 2006;3:104-8.
5. Turner TT, Lysiak JJ. Oxidative stress: a common factor in testicular dysfunction. J Androl. 2008;29:488-98.
6. Shiraishi K, Naito K, Yoshida K. Nitric oxide promotes germ cell necrosis in the delayed phase after experimental testicular torsion of rat. Biol Reprod. 2001;65:514-21.
7. Cuzzocrea S, Riley DP, Caputi AP, Salvemini D. Antioxidant therapy: a new pharmacological approach in shock, inflammation, and ischemia/reperfusion injury. Pharmacol Rev. 2001;53:135-59.
8. Visser AJ, Heyns CF. Testicular function after torsion of the spermatic cord. BJU Int. 2003;92:200-3.
9. Miyake H, Lee C, Chusilp S, Bhalla M, Li B, Pitino M, et al. Human breast milk exosomes attenuate intestinal damage. Pediatr Surg Int. 2020;36:155-63.
10. Yildirim C, Yuksel OH, Urkmez A, Sahin A, Somay A, Verit A. Protective effects of Tadalafil and darbepoetin against ischemia - reperfusion injury in a rat testicular torsion model. Int Braz J Urol. 2018;44:1005-13.
11. Becker EJ Jr., Turner TT. Endocrine and exocrine effects of testicular torsion in the prepubertal and adult rat. J Androl. 1995;16:342-51.
12. Kahraman T, Güçlüler G, Gürsel İ. Exosomes: natural nanovesicle candidates used in the diagnosis and treatment. Turk J Immunol. 2014;2:34-40.
13. Lässer C, Alikhani VS, Ekström K, Eldh M, Paredes PT, Bossios A, et al. Human saliva, plasma and breast milk exosomes contain RNA: uptake by macrophages. J Transl Med. 2011;9:9.
14. Admyre C, Johansson SM, Qazi KR, Filén JJ, Lahesmaa R, Norman M, et al. Exosomes with immune modulatory features are present in human breast milk. J Immunol. 2007;179:1969-78.
15. Sun Y, Oberley LW, Li Y. A simple method for clinical assay of superoxide dismutase. Clin Chem. 1988;34:497-500.
16. Aebi HE. Catalase. In: Methods of Enzymatics Analysis. Vol. 3. Weinhem: Verlag Chemie; 1987. p. 273-85.
17. Uchiyama M, Mihara M. Determination of malonaldehyde precursor in tissues by thiobarbituric acid test. Anal Biochem. 1978;86:271-8.
18. Bowlin PR, Gatti JM, Murphy JP. Pediatric testicular torsion. Surg Clin North Am. 2017;97:161-72.
19. Siemionow M, Arslan E. Ischemia/reperfusion injury: a review in relation to free tissue transfers. Microsurgery. 2004;24:468-75.
20. Lysiak JJ, Nguyen QA, Turner TT. Peptide and nonpeptide reactive oxygen scavengers provide partial rescue of the testis after torsion. J Androl. 2002;23:400-9.
21. Shimizu S, Tsounapi P, Dimitriadis F, Higashi Y, Shimizu T, Saito M. Testicular torsion-detorsion and potential therapeutic treatments: a possible role for ischemic postconditioning. Int J Urol. 2016;23:454-63.
22. Wang B, Zhong Y, Gao C, Li J. Myricetin ameliorates scopolamine-induced memory impairment in mice via inhibiting acetylcholinesterase and down-regulating brain iron. Biochem Biophys Res Commun. 2017;490:336-42.
23. Martin C, Patel M, Williams S, Arora H, Brawner K, Sims B. Human breast milk-derived exosomes attenuate cell death in intestinal epithelial cells. Innate Immun. 2018;24:278-84.
24. Liu H, Shi M, Li X, Lu W, Zhang M, Zhang T, et al. Adipose mesenchymal stromal cell-derived exosomes prevent testicular torsion injury via activating PI3K/AKT and MAPK/ERK1/2 pathways. Oxid Med Cell Longev. 2022;2022:8065771.
25. Hsiao CH, Ji AT, Chang CC, Cheng CJ, Lee LM, Ho JH. Local injection of mesenchymal stem cells protects testicular torsion-induced germ cell injury. Stem Cell Res Ther. 2015;6:113.
26. Keivan M, Mansouri Torghabeh F, Davoodi S, Moradi Maryamneghari S, Dadfar R. Single intratesticular injection of blood-serum-derived exosomes can potentially alleviate testopathy following testicular torsion. Animal Model Exp Med. 2022;5:362-8.

ORIGINAL ARTICLE

The relationship between systemic inflammation response index and clinical and histopathological features in gastric cancer

La relación entre el índice de respuesta a la inflamación sistémica y las características clínicas e hitopatológicas en el cáncer gástrico

Hikmet Pehlevan-Özel[1], Tolga Dinç[2], Nermin D. Okay[3], and Mesut Tez[2]*

[1]Department of Surgery, Mamak State Hospital; [2]Department of General Surgery, School of Medicine, University of Health Sciences, Ankara City Hospital; [3]Department of Surgery, General Surgery Clinic, Ankara City Hospital. Ankara, Turkey

Abstract

Objective: *The systemic inflammation response index (SIRI) is a marker used to predict survival. The aim of this study is to examine the relationship between SIRI and clinicopathological features and survival.* **Method:** *The relationship between clinicopathological characteristics and survey and SIRI was retrospectively investigated.* **Results:** *A total of 178 patients were included in the study. Poor prognostic factors such as tumor size, t, T-stage, tumor-node-metastasis (TNM) stage, and CA19-9 level were found to have a statistically significant relationship with patients with high SIRI (p = 0.039, p = 0.001, p = 0.001 and p = 0.013, respectively). A high SIRI was found to be an independent and poor prognostic factor for 3-year and 5-year survival (p = 0.014 and p = 0.027, respectively).* **Conclusions:** *High SIRI was associated with a poor survival rate, as were advanced TNM stage, advanced T stage, larger tumor size, and elevated CA19-9 level; all these are poor prognostic markers for gastric cancer.*

Keywords: *Clinical features. Gastric adenocancer. Gastric adenocancer. Systemic inflammation response index.*

Resumen

Objetivo: *El índice de respuesta inflamatoria sistémica (SIRI) es un marcador utilizado para predecir la supervivencia. El objetivo de este estudio es examinar la relación entre SIRI y las características clinicopatológicas y la supervivencia.* **Método:** *Se investigó retrospectivamente la relación entre las características clinicopatológicas, la encuesta y SIRI.* **Resultados:** *Se incluyeron un total de 178 pacientes. Se encontró que los factores de mal pronóstico como el tamaño del tumor, el estadio T, el estadio TNM y el nivel de CA19-9 tenían una relación estadísticamente significativa con el SIRI elevado (p = 0.039, p = 0.001, p = 0.001 y p = 0.013, respectivamente). Se encontró que un SIRI alto es un factor pronóstico independiente y malo para la supervivencia a tres y cinco años (p = 0.014 y p = 0.027, respectivamente).* **Conclusiones:** *Un SIRI alto se asoció con una tasa de supervivencia deficiente, al igual que el estadio TNM avanzado, el estadio T avanzado, el tamaño del tumor más grande y el nivel elevado de CA19-9; todos estos son marcadores de mal pronóstico para el cáncer gástrico.*

Palabras clave: *Características clínicas. Adenocáncer gástrico. Adenocáncer gástrico. Índice de respuesta inflamatoria sistémica.*

***Correspondence:**
Hikmet Pehlevan-Özel
E-mail: hikmet.pehlevan@gmail.com

Date of reception: 05-05-2023
Date of acceptance: 20-08-2024
DOI: 10.24875/CIRU.23000234

Cir Cir. 2025;93(2):158-165
Contents available at PubMed
www.cirugiaycirujanos.com

Introduction

Gastric cancer is the fifth most common type of cancer and the fourth most common cause of cancer-related death[1]. Gastric cancer is an aggressive disease with a poor prognosis; the 5-year survival was 5.3% for advanced disease and 68.8% for localized disease. The absolute number of diagnosis for gastric cancer has been increased although its global incidence decreases[2]. The treatment strategies of patients are tried to be guided according to the poor prognostic features determined through investigations on the relationship between prognosis and demographic, clinical, and histopathological variables in gastric cancer.

Inflammation in the tumor microenvironment stimulates malignant cell proliferation, angiogenesis, and metastasis, impairs the adaptive immune response, and promotes cancerous tissue survival[3]. Cancer-related inflammation, called the 7th hallmark of cancer, can be measured using cellular (white blood cell counts, neutrophils, lymphocytes, monocytes, and platelets) and humoral components[4]. It was shown that neutrophil (N) has an effect on cancer development and progression, monocyte (M) progression and metastasis, and lymphocyte (L) inhibits the proliferation of cancerous cells. The systemic inflammation response index (SIRI) was developed by incorporating these three parameters as M × N/L[5,6]. The SIRI was developed for the 1st time as a poor prognostic factor in pancreatic cancer, and later it was associated with many cancer types such as hepatocellular cancer, lung cancer, esophageal cancer, breast cancer, and oral squamous cancer[5,7,8]. Studies were shown that SIRI was correlated with some prognostic variables such as stage, tumor size, and lymphovascular invasion (LVI) in cancer patients, and can be a predictor of poor prognosis[7,8]. There are limited studies on the relationship between gastric cancer and SIRI. In these studies, reported from China, SIRI was shown as a poor prognostic factor[6,9,10].

The purpose of this study is to investigate the relationship between SIRI and 3-and 5-year survival as well as to examine its relationship to demographic, clinical, and pathological data of gastric cancer in the Turkish population.

Method

This study consisted of 178 patients who underwent elective gastric surgery with a diagnosis of gastric adenocancer between January 2011 and December 2016 to achieve 5-year survival, retrospectively. This study was performed in line with the principles of the Declaration of Helsinki. Approval was granted by the Local Ethics Committee.

The study included men and women over 18 years of age with gastric adenocancer who were operated under elective conditions. Exclusion criteria were as follows: (1) post-operative mortality in the first 30 days, (2) metastasis, positive surgical margins, or < 15 lymph node extraction (both D1 and D2 lymph node dissection), (3) receiving neoadjuvant therapy, (4) patients with chronic hematological or inflammatory diseases, and known additional cancers dialysis patients, (5) patients had blood transfusions up to 2 months before the operation. Patients' age, gender, preoperative laboratory results (CEA, CA19-9, N, M, and L), tumor location and Borrmann Classifications according to gastroscopy results, type of gastrectomy (total/subtotal), lymph node resection width (D1/D2), post-operative pathology results (tumor size, tumor-node-metastasis [TNM] stage-AJCC), In the 8th edition of the Gastric Cancer Staging System, the degree of differentiation, the presence of LVI, and the presence of perineural invasion (PI) were used in the analyses.

SIRI was calculated using N×M/L formula. The cut-off value was determined for SIRI by performing a Receiver operating characteristic (ROC)-curve analysis. According to this value, the patients were divided into two groups: group 1, which had a SIRI value of low, and group 2, which had a SIRI value of high.

Statistical analyses were performed using SPSS (Statistical Package for the Social Sciences, SPSS Version 15.0, Chicago, IL). The descriptive statistics of the patients were presented as mean ± standard deviation (SD) or median (minimum-maximum) depending on the normality assumption being met for numerical variables and frequency (percentage) for categorical variables, respectively. Comparisons were made using the Independent Samples t-test or Mann-Whitney U test for numerical variables and the Chi-square test for categorical variables. The normality of the numerical variables was assessed with the Kolmogorov-Smirnov test. The Kaplan-Meier method was implemented to construct the 3-and 5-year survival curves, and the equality of the 3-and 5-year survival distributions was compared with the Mantel-Cox (log-rank) test. The effect of the prognostic factors on 3-and 5-year survival was assessed with the Cox Proportional Hazards Model. Variables that had a $p < 0.20$ were included in the Multiple Cox Model, and the

Backward Likelihood Ratio Test methods were used for variable selection. The $p < 0.05$ was considered as statistically significant.

Results

The analyses were conducted using the information of 178 patients who met the criteria. There were 60 (33.7%) female and 118 (66.3%) male patients. The mean age of the patients was 61.74 ± 11.43. In 97 patients (54.5%), a total gastrectomy was performed. There were 20 (11.2%) Stage 1 patient, 45 (25.3%) Stage 2 patients, and 113 (63.5%) Stage 3 patients. Only five out of 178 gastric adenocarcinoma patients had signet ring cell subtypes, while pathological results revealed signet ring cells in 41 (23%) patients whose signet cells were present on final pathology but not enough percentage to be labeled as a signet ring cell subtype. LVI was detected in 112 (68.5%) patients and PNI (66.9%) was detected in 119 patients. When the ROC curve was made for SIRI, the area under the curve was 0.564 and the cut-off point was determined as 1.35. There were 77 (43.3%) patients in the group 1 (SIRI ≤ 1.35) and 101 (56.7%) in the group 2 (SIRI > 1.35).

There was a statistically significant correlation between Group 2 and tumor size, advanced T stage (T3 and T4 disease), advanced disease (Stage 2/Stage 3 disease), and CA 19-9 level ($p = 0.039$, $p = 0.001$, $p < 0.001$, $p = 0.013$, respectively) (Table 1).

The 3-year survival rate was 51.1%, and the 5-year survival rate was 42.7%. The 3-year and 5-year survival rates in group 2 were significantly lower than those in group 1, according to the Kaplan-Meier curve and log-rank test ($p = 0.014$ and $p = 0.027$, respectively) (Figs. 1 and 2).

According to univariate analyses, age, tumor size, T stage, N stage, TNM stage, signet ring cell presence, and PI presence were associated significantly with 3-year survival. SIRI value is also related to 3-year survival (hazard ratio (HR): 1.321, 95% CI: 1.102-1.584, $p = 0.003$) (Table 2). According to univariate analysis, T stage, N stage, TNM stage, signet ring cell presence, and PI presence had a significant correlation with 5-year survival. Furthermore, SIRI was associated with the highest 5-year survival (HR: 1.261, 95%CI: 1.062-1.498, $p = 0.008$) (Table 3).

Age, TNM stage, and signet ring cell presence were found to be associated with 3-year survival after multivariate analyses (Table 2). Multivariate analysis also showed that a high SIRI value was significantly associated with 3-year survival (HR: 1.367, 95% CI: 1.105-1.689 $p = 0.004$) (Tables 2 and 3). According to the multivariate analysis, it was observed that age, TNM stage, and signet ring cell presence were relevant to 5-year survival. The high SIRI value was also significantly associated with 5-year survival (HR: 1.304, 95%CI: 1.069-1.592, $p = 0.009$) (Table 3).

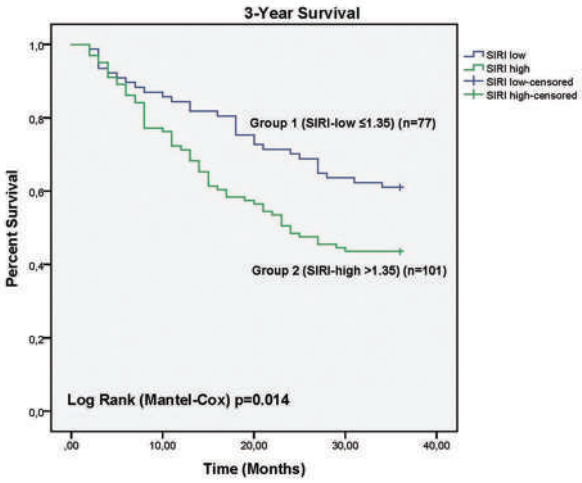

Figure 1. *Systemic inflammation response index low and systemic inflammation response index high Group 3 years follow-up, Kaplan-Meier Analysis.*

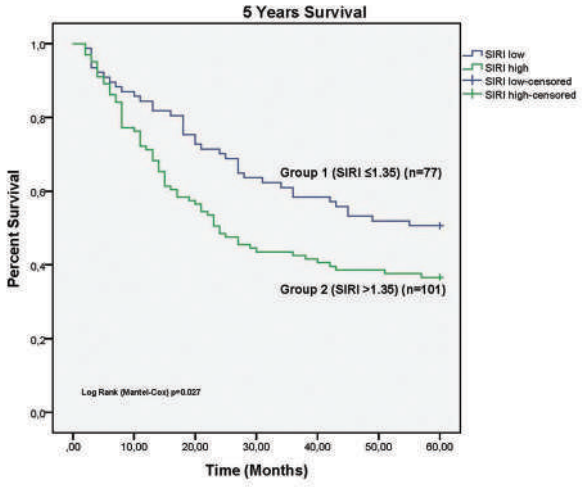

Figure 2. *Systemic inflammation response index low and systemic inflammation response index high Group 5 years follow-up, Kaplan-Meier Analysis.*

Discussions

The severity of cancer-related inflammation can be measured by cells such as neutrophils, lymphocytes, monocytes, and leukocytes in peripheral blood, and

Table 1. Demographic, 0clinical, and pathological data

Variables	Group 1 (SIRI ≤ 1.35) n = 77 (43.3%)	Group 2 (SIRI > 1.35) n = 101 (56.7%)	p
Age (year), mean ± SD	61.32 ± 11.94	62.05 ± 11.07	0.676
Gender			0.342
Female	29 (37.66)	31 (30.69)	
Male	48 (62.34)	70 (69.31)	
Localization			0.470
Kardia	15 (19.48)	25 (24.75)	
Non-kardia	62 (80.52)	76 (75.24)	
Borrmann classification			0.156
Type 1	17 (22.08)	15 (14.85)	
Type 2	26 (33.77)	30 (29.70)	
Type 3	29 (50.65)	44 (43.55)	
Type 4	0	6 (5.95)	
Type 5	5 (6.50)	6 (5.95)	
Surgery			0.879
Total gastrectomy	41 (53.25)	56 (55.45)	
Subtotal gastrectomy	36 (46.75)	45 (44.55)	
Lymph node dissection			1.000
D1	6 (7.79)	9 (8.91)	
D2	71 (92.21)	92 (91.09)	
Tumor size, cm, median (min-max)	5.50 (0.70-25.0)	6.00 (2.00-17.00)	0.039*
T stage			0.001*
T1	14 (18.18)[a]	2 (1.98)[a]	
T2	7 (9.10)[a,b]	5 (4.95)[a,b]	
T3	39 (50.65)[b]	64 (63.37)[b]	
T4	17 (22.07)[b]	30 (29.70)[b]	
N stage			0.554
N0	25 (32.46)	27 (26.73)	
N1	6 (7.79)	12 (11.88)	
N2	13 (16.88)	23 (22.77)	
N3	33 (42.85)	39 (38.62)	
TNM stage			<0.001*
Stage 1	17 (22.08)[c]	3 (2.97)[c]	
Stage 2	12 (15.58)[d]	33 (32.67)[d]	
Stage3	48 (62.34)[d]	65 (64.36)[d]	
Differentiation degree			0.291
Poor	37 (48.05)	57 (56.44)	
Moderate/Well	40 (51.95)	44 (43.56)	
Signet ring cell			0.858
Presence	17 (22.08)	24 (23.76)	
Absence	60 (77.92)	77 (76.24)	
Lymphovascular invasion			0.417
Presence	50 (64.94)	72 (71.29)	
Absence	27 (35.06)	29 (28.71)	
Perineural invasion			0.053
Presence	45 (58.44)	74 (73.27)	
Absence	32 (41.56)	27 (26.73)	
CEA,(U/mL), Median (Min-Max)	1.84 (0.61-65.80)	1.94 (0.37-350.71)	0.376
CA19-9, (U/mL), Median (Min-Max)	9.63 (0.60-4351.00)	16.30 (0.001-460.20)	0.013*

*Statistically significant difference. [ab,cd]: There was a statistically significant difference between those grouped with different letters. SD: standard deviation; cm: centimeter; T: tumor; N: nodal status; TNM: tumor-node-metastasis; CEA: carcinoembryonic antigen; CA 19-9: carbohydrate antigen 19-9.

Table 2. Univariate and multivariate survival analysis for 3 years followed up

Variables	Univariate analysis		Multivariate analysis	
	HR (95% CI)	p	HR (95% CI)	p
Age (year)	1.021 (1.002-1.040)	0.030*	1.024 (1.002-1.047)	0.031*
Male gender	1.312 (0.829-2.077)	0.246		
Non-kardiac localization	1.026 (0.623-1.691)	0.920		
Borrmann classification		0.639		
Type 1	Reference			
Type 2	1.255 (0.645-2.442)	0.504		
Type 3	1.496 (0.798-2.803)	0.209		
Type 4	2.013 (0.656-6.179)	0.222		
Type 5	1.080 (0.385-3.209)	0.884		
Total gastrectomy	1.480 (0.962-2.277)	0.075		
D2 lymph node dissection	0.698 (0.361-1.349)	0.285		
Tumor size, cm	1.054 (1.002-1.108)	0.043*		
T Stage		0.023*		
T1	Reference			
T2	0.286 (0.032-2.556)	0.263		
T3	2.247 (0.813-6.211)	0.119		
T4	3.063 (1.076-8.722)	0.036		
N stage		0.001*		
N0	Reference			
N1	1.263 (0.485-3.287)	0.632		
N2	2.602 (1.321-5.122)	0.006		
N3	3.094 (1.698-5.637)	< 0.001		
TNM stage		< 0.001*		0.001*
Stage 1	Reference		Reference	
Stage 2	1.435 (0.468-4.403)	0.527	0.960 (0.300-3.071)	0.945
Stage 3	3.928 (1.432-10.772)	0.008	2.920 (1.016-8.387)	0.047
Poor differentiation	1.254 (0.821-1.916)	0.295		
Signet ring cell presence	2.013 (1.286-3.153)	0.002*	1.772 (1.074-2.924)	0.025*
Lymphovascular invasion presence	1.571 (0.961-2.568)	0.072		
Perineural invasion presence	1.715 (1.048-2.804)	0.032		
CEA, (U/mL)	1.004 (0.999-1.008)	0.093		
CA19-9, (U/mL)	1.000 (1.000-1.001)	0.562		
SIRI	1.321 (1.102-1.584)	0.003*	1.367 (1.105-1.689)	0.004*

(*) Statistically significant difference. HR: hazard ratios; CI: confidence interval; cm: centimeter; T: tumor; N: nodal status; TNM: tumor-node-metastasis; CEA: carcinoembryonic antigen, CA 19-9: carbohydrate antigen 19-9; SIRI: systemic inflammation response index.

indices created with different combinations of these cells can show the severity of cancer-related inflammation[3,4]. Neutrophils, the first cells of the immune response to inflammation, can promote tumor progression by inducing tumor cell proliferation, stimulating angiogenesis, and deactivating antitumor immunity[11]. Monocytes, which migrate to other tissues in the body and turn into macrophages, and whose number increases in the peripheral circulation with the activation of the immune system, exhibit prognostic value in diseases such as cancer, chronic kidney disease, and pneumonia[12]. After tumor-induced immune regulation, the first line of defense against tumor cells, monocytes and macrophages become tumor-supportive and aid in tumor growth, angiogenesis, invasion, and metastasis[12]. Lymphocytes show an antitumor effect and prevent

Table 3. Univariate and multivariate survival analysis for 5 years followed up

Variables	Univariate analysis		Multivariate analysis	
	HR (95% CI)	p	HR (95% CI)	p
Age (year)	1.017 (1.000-1.035)	0.051	1.021 (1.002-1.041)	0.034*
Male gender	1.299 (0.852-1.982)	0.224		
Non-kardiac localization	0.993 (0.624-1.581)	0.978		
Borrmann classification		0.328		
Type 1	Reference			
Type 2	1.091 (0.590-2.017)	0.781		
Type 3	1.506 (0.854-2.657)	0.158		
Type 4	2.233 (0.816-6.106)	0.118		
Type 5	1.078 (0.422-2.756)	0.875		
Subtotal gastrectomy	0.754 (0.509-1.117)	0.159		
D2 lymph node dissection	0.796 (0.414-1.530)	0.493		
Tumor size, cm,	1.050 (1.002-1.100)	0.043*		
T stage		0.032*		
T1	Reference			
T2	1.140 (0.285-4.558)	0.853		
T3	2.947 (1.072-8.103)	0.036		
T4	3.438 (1.210-9.772)	0.020		
N stage		< 0.001*		
N0	Reference			
N1	1.392 (0.601-3.225)	0.441		
N2	2.622 (1.406-4.888)	0.002		
N3	3.190 (1.842-5.522)	< 0.001		
TNM stage		< 0.001*		< 0.001*
Stage 1	Reference		Reference	
Stage 2	2.070 (0.701-6.118)	0.188	1.464 (0.479-4.476)	
Stage 3	5.003 (1.829-13.685)	0.002	3.702 (1.629-12.786)	0.014
Poor differentiation	1.239 (0.838-1.831)	0.283		
Signet ring cell presence	2.174 (1.435-3.295)	< 0.001*	1.915 (1.210-3.030)	0.006*
Lymphovascular invasion presence	1.510 (0.967-2.359)	0.070		
Perineural invasion presence	1.776 (1.129-2.792)	0.013*		
CEA, (U/mL)	1.004 (0.999-1.008)	0.102		
CA19-9, (U/mL)	1.000 (1.000-1.001)	0.242		
SIRI	1.261 (1.062-1.498)	0.008*	1.304 (1.069-1.592)	0.009*

(*) Statistically significant difference. HR: hazard ratios; CI: confidence interval; cm: centimeter; T: tumor; N: nodal status; TNM: tumor-node-metastasis; CEA: carcinoembryonic antigen; CA 19-9: carbohydrate antigen 19-9; SIRI: systemic inflammation response index.

tumor progression, and studies showed that lymphopenia is associated with low survival in cancers[13]. SIRI was developed using these three parameters, which are known to be associated with the development of cancerous tissue and which are one of the indexes showing the severity of inflammation in cancer[7,8].

In this study, the relationship between SIRI and 3-year survival, and 5-year survival as well as clinical and pathological features of gastric cancer was investigated. The 3- and 5-year survival was better in the SIRI low group. Furthermore, the SIRI highness was found to be significantly associated with the T stage, TNM stage, tumor size, and CA19-9 levels.

SIRI is a parameter that was defined in 2016 and is associated with prognosis in different types of malignancies[5,7,8]. It was shown that high SIRI is associated with poor prognosis when evaluated alone or in combination with parameters such as fibrinogen and albumin when

it is considered specifically for gastric cancer[6,9,10]. However, these studies were of Chinese origin. There were no studies on its effectiveness in different societies. To the best of our knowledge, this is the first study conducted by a Turkish/Western society on gastric cancer. In this study, it was shown that there is a statistically significant relationship between high SIRI and poor prognosis in both 3-year and 5-year survival rates and that SIRI is an independent variable of survival. Furthermore, the statistical relationship between 3-year survival and SIRI appears to be more significant than the statistical relationship between 5-year survival and SIRI, and this can be considered a stronger predictor of SIRI value in post-operative early-period surveillance.

The TNM classification is the most important independent prognostic factor in gastric cancer, and it is the main guiding factor in the treatment of patients[14]. The TNM staging system, published by the American Joint Commission on Cancer, and constantly revised with up-to-date data, was last updated with the 8th edition in 2016[15]. It is tried to reach a prediction about the extent of the tumor in the tissue, the severity of the tumor, and the prognosis of the disease by evaluating the T stage indicating the depth of the tumor in the tissue, the N stage determined by the number of lymph nodes to which the tumor has spread, with at least 15 lymph nodes, and the M stage indicating the distant organ metastasis of the tumor[14,15]. In our study, it was shown that there was a significant difference between SIRI elevation and patients with Stage 1 and Stage 2-3 in the TNM staging system, and the SIRI elevation was higher in Stage 2-3 patients with a worse prognosis. When we looked at the subgroups of TNM staging, it was seen that there was a difference between T1-T2 groups and T3-T4 groups at the T stage, and SIRI was statistically higher in T3-T4 groups. In addition, no relationship was found between the N stage and SIRI elevation in our study, and when patients with distant metastases were not included, the relationship with the M stage and its relationship with patients with TNM Stage 4 could not be evaluated. Consistent with the literature, T stage, N stage, and TNM stage gave significant results in both 3- and 5-year survival in univariate analyses, but when multivariate analyses were examined, only TNM staging for both 3- and 5-year survival gave a statistically significant result.

The effect of gastric cancer tumor size on prognosis is controversial. In previous studies, it was shown that tumor size may increase the depth of tumor invasion and lymph node/distant metastasis, that is, as the size increases, the success of en-bloc resection may decrease. Hence, there may be a significant relationship between tumor size and prognosis[16]. In our study, it was seen that the SIRI is significantly higher in patients with high tumor sizes ($p = 0.009$). Therefore, as the tumor size increases, cancer-related inflammation also increases. In addition, while tumor size was statistically associated with poor prognosis for both 3-year survival and 5-year survival in univariate analysis, this effect could not be seen in multivariate analysis.

CA 19-9 is a Lewis blood group antigen, not secreted in approximately 5-7% of the population, is thought to affect cell adhesion, and can be secreted from normal epithelial cells such as the gallbladder, pancreas, stomach, and prostate[17]. It is known that CA 19-9 is increased in many types of cancer, especially pancreatic adenocarcinoma as well as non-malignant diseases such as cholecystitis, pancreatitis, diabetes mellitus, and autoimmune disorders[17]. The relationship between CA 19-9 and gastric cancer is unclear. Studies are showing that CA19-9 elevation is associated with lymph node metastasis and CA19-9 positivity at the time of recurrence is poor prognostic[18,19]. CA 19-9 might be used as a marker in gastric cancer, especially in advanced cases as a prognostic marker to predict recurrence/metastasis and post-treatment follow-up but cannot be used in early diagnosis and screening[17]. In this study, the relationship between CA 19-9 level and prognosis could not be demonstrated. However, it has been shown that CA 19-9 level is associated with SIRI, which is a poor prognostic factor. The CA 19-9 level is higher in the group with high SIRI.

Some limitations exist in our retrospective study. The surgical records of the patients were used to determine the D1 and D2 lymph node dissections. Furthermore, TNM staging was reported in patients who had more than 15 lymph nodes removal, depending on pathological findings.

Conclusions

In this study, there was a significant relationship between high SIRI and 3- and 5-year survival, and high SIRI was associated with poor survival. In addition, this study was the first in the West for gastric cancer to show a survival relationship with SIRI. Furthermore, a relationship was found between high SIRI and advanced TNM stage, advanced T stage, larger tumor size, and high CA19-9 levels, which are poor prognostic factors of gastric cancer. This is valuable for predicting prognosis before treatment with a low-cost and standardized test.

Acknowledgments

The authors thank all the staff of the surgery and pathology departments in Ankara Numune Research and City Hospital.

Funding

The authors declare that they have not received funding.

Conflicts of interest

The authors declare no conflicts of interest.

Ethical considerations

Protection of humans and animals. The authors declare that no experiments involving humans or animals were conducted for this research.

Confidentiality, informed consent, and ethical approval. The authors have obtained approval from the Ethics Committee for the analysis of routinely obtained and anonymized clinical data, so informed consent was not necessary. Relevant guidelines were followed.

Declaration on the use of artificial intelligence. The authors declare that no generative artificial intelligence was used in the writing of this manuscript

References

1. Sung H, Ferlay J, Siegel RL, Laversanne M, Soerjomataram I, Jemal A, et al. Global cancer statistics 2020: GLOBOCAN estimates of incidence and mortality worldwide for 36 cancers in 185 countries. CA Cancer J Clin. 2021;71:209-49.
2. Chandra R, Balachandar N, Wang S, Reznik S, Zeh H, Porembka M. The changing face of gastric cancer: epidemiologic trends and advances in novel therapies. Cancer Gene Ther. 2021;28:390-9.
3. Mantovani A, Allavena P, Sica A, Balkwill F. Cancer-related inflammation. Nature. 2008;454:436-44.
4. Powell AG, Parkinson D, Patel N, Chan D, Christian A, Lewis WG. Prognostic significance of serum inflammatory markers in gastric cancer. J Gastrointest Surg. 2018;22:595-605.
5. Qi Q, Zhuang L, Shen Y, Geng Y, Yu S, Chen H, et al. A novel systemic inflammation response index (SIRI) for predicting the survival of patients with pancreatic cancer after chemotherapy. Cancer. 2016;122:2158-67.
6. Li S, Lan X, Gao H, Li Z, Chen L, Wang W, et al. Systemic inflammation response index (SIRI), cancer stem cells and survival of localised gastric adenocarcinoma after curative resection. J Cancer Res Clin Oncol. 2017;143:2455-68.
7. Wei L, Xie H, Yan P. Prognostic value of the systemic inflammation response index in human malignancy: a meta-analysis. Medicine (Baltimore). 2020;99:e23486.
8. Zhou Q, Su S, You W, Wang T, Ren T, Zhu L. Systemic inflammation response index as a prognostic marker in cancer patients: a systematic review and meta-analysis of 38 cohorts. Dose Response. 2021;19(4): 1-14.
9. Zhang J, Ding Y, Wang W, Lu Y, Wang H, Wang H, et al. Combining the fibrinogen/albumin ratio and systemic inflammation response index predicts survival in resectable gastric cancer. Gastroenterol Res Pract. 2020;2020:3207345.
10. Liu Z, Ge H, Miao Z, Shao S, Shi H, Dong C. Dynamic Changes in the systemic inflammation response index predict the outcome of resectable gastric cancer patients. Front Oncol. 2021;11:577043.
11. Mollinedo F. Neutrophil degranulation, plasticity, and cancer metastasis. Trends Immunol. 2019;40:228-42.
12. Gouveia-Fernandes S. Monocytes and macrophages in cancer: unsuspected roles. Adv Exp Med Biol. 2020;1219:161-85.
13. Ruffell B, DeNardo DG, Affara NI, Coussens LM. Lymphocytes in cancer development: polarization towards pro-tumor immunity. Cytokine Growth Factor Rev. 2010;21:3-10.
14. Jung H, Lee HH, Song KY, Jeon HM, Park CH. Validation of the seventh edition of the American joint committee on cancer TNM staging system for gastric cancer. Cancer. 2011;117:2371-8.
15. Lu J, Zheng CH, Cao LL, Ling SW, Li P, Xie JW, et al. Validation of the American Joint Commission on Cancer changes for patients with stage III gastric cancer: survival analysis of a large series from a Specialized Eastern Center. Cancer Med. 2017;6:2179-87.
16. Hu K, Wang S, Wang Z, Li L, Huang Z, Yu W, et al. Clinicopathological risk factors for gastric cancer: a retrospective cohort study in China. BMJ Open. 2019;9:e030639.
17. Kotzev AI, Draganov PV. Carbohydrate antigen 19-9, carcinoembryonic antigen, and carbohydrate antigen 72-4 in gastric cancer: is the old band still playing? Gastrointest Tumors. 2018;5:1-13.
18. Feng F, Tian Y, Xu G, Liu Z, Liu S, Zheng G, et al. Diagnostic and prognostic value of CEA, CA19-9, AFP and CA125 for early gastric cancer. BMC Cancer. 2017;17(1):737.
19. Moriyama J, Oshima Y, Nanami T, Suzuki T, Yajima S, Shiratori F, et al. Prognostic impact of CEA/CA19-9 at the time of recurrence in patients with gastric cancer. Surgery Today. 2021;51:1638-48.

ARTÍCULO ORIGINAL

Cambios en la audición de pacientes pediátricos con cáncer tratados con cisplatino

Hearing changes in pediatric cancer patients treated with cisplatin

José L. Olvera-Gómez[1], Yamileth García-Rojas[2], María C. Rojas-Sosa[3], Candy S. Márquez-Ávila[2] y María A. Fierro-Evans[2]*

[1]Coordinación de Planeación y Enlace Institucional, Delegación Sur, Instituto Mexicano del Seguro Social (IMSS); [2]Servicio de Audiología y Foniatría, Hospital Infantil de México Federico Gómez; [3]División de Unidades Médicas de Rehabilitación, Dirección de Prestaciones Médicas, IMSS. Ciudad de México, México

Resumen

Objetivo: *Medir los cambios en la audición evaluada por audiometría tonal y emisiones otoacústicas por productos de distorsión (EOAPD) en niños con cáncer tratados con cisplatino.* **Método:** *Estudio de cohorte retrospectiva. Se incluyeron 42 archivos de niños con cáncer que tenían audiometría tonal (frecuencias convencionales y altas frecuencias) y EOAPD, realizados después de cada dosis de cisplatino. Se comparó la audición con la cantidad de cisplatino y el número de dosis.* **Resultados:** *El 88.1% tuvieron criterios para ototoxicidad (pCCO) y el 11.9% sin criterios (pSCO). La terapia antineoplásica se administró en dos (31%) o tres dosis (69%). En el segundo estudio hubo deterioro superficial en tonos medios y agudos en pCCO ($p < 0.046$). Las altas frecuencias estuvieron afectadas desde la primera dosis en pCCO y hasta la segunda en pSCO; el daño tuvo relación con la dosis acumulada ($r_s = 0.54$; $p = 0.0001$; odds ratio [OR]: 1.125; intervalo de confianza del 95% [IC95%]: 0.893-1.417) con dosis de 300-325 mg/m^2 de superficie corporal. Las EOAPD estuvieron ausentes en el 100% de pCCO en la última dosis (OR: 4.0; IC95%: 0.733-21.838) a 300-325 mg/m^2 de superficie corporal ($p = 0.034$).* **Conclusiones:** *El uso de cisplatino en niños con cáncer se relacionó con daño auditivo entre 2000 y 16,000 Hz desde el inicio del tratamiento y a dosis de 300 mg/m^2 de superficie corporal.*

Palabras clave: *Cisplatino. Cáncer pediátrico. Emisiones otoacústicas. Hipoacusia. Ototoxicidad.*

Abstract

Objective: *To measure changes in hearing assessed by tone audiometry and otoacoustic emissions by product distortions (OAEPD) in children with cancer treated with cisplatin.* **Method:** *Retrospective cohort study. There were 42 files of children with cancer, who had tone audiometry (conventional frequencies and high frequencies) and EOAPD, performed after each dose of cisplatin. Hearing was compared with cisplatin amount and doses number.* **Results:** *Of the 42 subjects, 88.1% were patients with criteria for ototoxicity (pCCO) and 11.9% without criteria (pSCO). Antineoplastic therapy was administered in 2 (31%) and 3 (69%) doses. In the second study, there was superficial damage in medium and high tones in pCCO ($p < 0.046$). The high frequencies were affected from first dose in pCCO and second dose in pSCO; the damage was related with accumulated dose ($r_s = 0.54$; $p = 0.0001$; odds ratio [OR]: 1.125; 95% confidence interval [95%CI]: 0.893-1.417) in doses of 300-325 mg/m^2 of body surface. EOAPD were absent in 100% of pCCO at the last dose (OR: 4.0; 95%CI: 0.733-21.838) at 300-*

***Correspondencia:**
Yamileth García-Rojas
E-mail: yami_garcia80@yahoo.com.mx

Fecha de recepción: 06-07-2023
Fecha de aceptación: 09-09-2023
DOI: 10.24875/CIRU.23000356

Cir Cir. 2025;93(2):166-176
Contents available at PubMed
www.cirugiaycirujanos.com

325 mg/m² of body surface (p = 0.034). **Conclusions:** *The use of cisplatin in children with cancer was associated with hearing damage between 2000 and 16,000 Hz from the start of treatment and at dose of 300 mg/m² of body surface.*

Keywords: *Cisplatin. Pediatric cancer. Otoacoustic emissions. Hearing loss. Ototoxicity.*

Introducción

De acuerdo con la Organización Mundial de la Salud, los tipos de cáncer infantil más comunes son leucemia, cáncer cerebral, linfoma y tumores sólidos como el neuroblastoma y el tumor de Wilms[1]. Según la Agencia Internacional para la Investigación del Cáncer, en 2015 hubo entre 344,543 y 360,114 casos de cáncer infantil en todo el mundo (178.0 por millón), de los que 29,002 casos se ubicaron en América Latina y el Caribe[2]. En México, el cáncer es la segunda causa de muerte en menores de 15 años, debido a que los niños están sobreviviendo hasta los 2-6 años, edad en que la incidencia del cáncer es más alta. En 2007 se inició el Registro Nacional de Cáncer Infantil y se reportó que entre 2007 y 2015 hubo 24,039 casos nuevos tan solo del Seguro Popular, lo que representó un incremento en la incidencia de 133.5 por millón en 2007 a 150.1 por millón en 2015. En nuestro país, la tasa de mortalidad por cáncer es de 8.6/100,000 niños por año entre los 15 y 18 años, con una sobrevivencia global del 75% en instituciones con más de 15 camas y al menos tres oncólogos[3]. En el Instituto Mexicano del Seguro Social, la sobrevivencia global a 5 años fue del 56.1% (mediana de tiempo: 3.4 años) en el periodo de 2006 a 2012[4], y ha continuado con esa tendencia[3].

Debido a los avances en la atención de pacientes con cáncer pediátrico ha mejorado la supervivencia a largo plazo, por lo que la cirugía, la quimioterapia (QT) y la radioterapia (RT) pueden provocar efectos tardíos en los sobrevivientes de cáncer infantil[3,5], creando una población creciente de sobrevivientes que pasarán parte de sus vidas en riesgo de afecciones crónicas y mortalidad tardía, con pérdida potencial de años de vida o viviendo con discapacidad[6]. Entre los efectos discapacitantes se encuentra la pérdida auditiva relacionada con el uso de QT, común en estos niños, ya que se ha detectado que cuando son tratados con RT y QT experimentan una alta incidencia de hipoacusia neurosensorial a lo largo del tiempo como efecto secundario, encontrándose asociación entre la hipoacusia neurosensorial más grave y las dosis recibidas[7]. En particular, la RT ha mostrado que con más dosis mayor será el riesgo y más grave la discapacidad auditiva, como respuesta retardada a la radiación fraccionada. La hipoacusia es permanente cuando se provoca daño irreversible al oído interno, y se ha propuesto que la vuelta basal es más susceptible a la radiación, aunque la cóclea se considera como un órgano completo para el análisis de dosis-respuesta[8].

El cisplatino es de uso común para algunos cánceres frecuentes en los niños, pero en ocasiones se combinan la RT y la QT[9], y aunque existen trabajos que señalan que la dosis de cisplatino supera la importancia de la dosis de RT sobre la cóclea, parece que la irradiación previa reduce el umbral de dosis de cisplatino para la pérdida auditiva[10], por lo que adquiere trascendencia determinar el impacto ototóxico aditivo de la QT que permita a los oncólogos encontrar dosis más seguras para la cóclea[11].

El cisplatino es uno de los más potentes agentes citostáticos antitumorales disponibles, comúnmente utilizado como tratamiento estándar contra una amplia gama de cánceres infantiles, que en regímenes combinados permite un alto índice de cura[12], con el inconveniente de que atraviesa la cóclea y provoca pérdida auditiva neurosensorial permanente, cuya repercusión se refleja en deficiencias en áreas neurocognitivas, que provocan alteraciones en el proceso de aprendizaje y contacto social, y problemas de conducta que afectan la calidad de vida, más evidente cuanto más pequeño sea el niño, por la deprivación del estímulo auditivo sobre el sistema nervioso central[13,14]. El platino reside en el oído durante meses o años después del tratamiento, por lo que el 70% de los niños tratados con platino desarrollan una pérdida auditiva irreversible y el 40% necesitarán audífonos en una etapa temprana[15]. Al igual que la RT, más dosis de cisplatino provocan mayor ototoxicidad, pero existen dudas sobre la dosis acumulada, lo que dificulta desarrollar enfoques ajustados al riesgo para su administración y para orientar mejor los nuevos agentes otoprotectores, como el tiosulfato de sodio[13], lo que apoyaría la prevención de la pérdida auditiva inducida por cisplatino, carboplatino u oxaliplatino, con influencia positiva en la calidad de vida de los supervivientes de cáncer infantil[16]. Cuando los compuestos de platino se generalizaron tenían una mayor incidencia de pérdida auditiva, pero actualmente

parece que la detección de daño se ha estabilizado en los sobrevivientes y se propone que puede ser porque los nuevos regímenes de tratamiento tienen menos radiación ototóxica y los compuestos de platino se dosifican con mayor cuidado[17].

Considerando todo lo anterior, el objetivo del presente trabajo fue medir los cambios en la audición de niños con cáncer manejados con cisplatino en diferentes dosis, mediante la realización de audiometría tonal con frecuencias convencionales y altas frecuencias, así como emisiones otoacústicas por productos de distorsión (EOAPD).

Método

Para lograr el objetivo, se realizó un estudio de cohorte retrospectiva mediante revisión de expedientes de niños con diagnóstico de cáncer y que incluyeron cisplatino como parte de la QT. Los criterios de selección fueron edad entre 4 y 17 años, registro en el expediente de las dosis administradas de QT y un mínimo de dos valoraciones audiológicas relacionadas con la administración de cisplatino en cualquier combinación. Se excluyeron los pacientes que tenían antecedente de hipoacusia antes del diagnóstico de cáncer o del inicio del tratamiento, aquellos con antecedente de RT en cabeza o cuello, antecedente de infección aguda o crónica, o cirugía de oído previa. Las evaluaciones audiológicas fueron audiometría tonal liminar (0.125 Hz a 8 kHz), audiometría tonal de altas frecuencias (10 a 16 kHZ) y EOAPD.

La ototoxicidad se evaluó utilizando los criterios de la *American Speech-Language-Hearing Association* (ASHA), que incluyen:

- Disminución ≥ 20 dB HL nivel de audición (Hearing level), por sus siglas en inglés, en el umbral de tonos puros en una sola frecuencia de prueba.
- Disminución ≥ 10 dB HL en el umbral en dos frecuencias adyacentes.
- Pérdida de respuesta en tres frecuencias consecutivas en las que se obtuvieron respuestas previamente.

Los criterios de la ASHA detectan cambios ototóxicos tempranos antes de la clínica, con existencia de hipoacusia neurosensorial, pero no detectan pérdida auditiva clínicamente significativa en oncología, por lo que cuando se encontró hipoacusia neurosensorial significativa se clasificó la pérdida con el uso de la escala de grados propuesta por Chang para ototoxicidad, específicamente desarrollada para cambios clínicamente significativos inducidos por platino. Los criterios de ototoxicidad de Chang para la gravedad de la pérdida auditiva, son:

- 0 = umbrales ≤ 20 dB en 1, 2 y 4 kHZ.
- 1a = umbrales ≥ 40 dB en 6-12 kHZ.
- 1b = umbrales > 20 y < 40 dB en 4 kHZ.
- 2a = ≥ 40 dB en frecuencias ≥ 4 kHZ.
- 2b = umbrales > 20 y < 40 dB en frecuencias < 4 kHz.
- 3 = ≥ 40 dB en frecuencias ≥ 2 kHZ.
- 4 = umbrales ≥ 40 dB en frecuencias ≥ 1 kHz[18,19].

De acuerdo con los hallazgos en las pruebas audiológicas para umbral tonal, los pacientes se clasificaron utilizando los criterios de Brock para la pérdida auditiva:

- Ninguna: hipoacusia bilateral, menos de 40 dB en todas las frecuencias.
- Leve: hipoacusia bilateral, superior a 40 dB en 8000 Hz.
- Moderada: hipoacusia bilateral, superior a 40 dB desde 6000 Hz.
- Marcada: hipoacusia bilateral, superior a 40 dB desde 4000 Hz.
- Grave: pérdida auditiva bilateral, mayor de 40 dB desde 2000 Hz[20,21].

Resultados

Se revisaron 140 expedientes de niños y adolescentes con cáncer en el Hospital Infantil de México Federico Gómez, tratados con cisplatino en combinación con otros medicamentos, de los cuales 42 cumplieron con los criterios de inclusión (30%). De estos, hubo 22 (52.4%) mujeres y 20 (47.6%) hombres, con una edad promedio de 10.9 ± 3.38 años. En la tabla 1 se muestran el resto de las características generales de los 42 casos y su división en pacientes con criterios para ototoxicidad (pCCO) (n = 37; 88.1%), ubicados en grado 1a, y pacientes sin criterios para ototoxicidad (pSCO) (n = 5; 11.9%), correspondientes al grado 0 de Chang, así como el esquema terapéutico y la dosis de cisplatino prescrita, independientemente del número de administraciones en las que fue otorgada. Se puede observar el predominio de mujeres, sin diferencia significativa en la edad promedio (p > 0.05). El osteosarcoma fue el tipo de cáncer más frecuente (78.6%). Todos recibieron cisplatino como parte del esquema de tratamiento y se puede apreciar que se utilizaron siete diferentes esquemas de QT, siendo cisplatino con adriamicina la combinación más común (71.4%). La administración del medicamento se proporcionó en

Tabla 1. Características generales, esquema terapéutico y dosis otorgada de cisplatino de los 42 pacientes seleccionados y separados de acuerdo con la presencia o ausencia de ototoxicidad

Característica	Variable	Población general (n = 42)	Pacientes con ototoxicidad (n = 37)	Pacientes sin ototoxicidad (n = 5)
Sexo	Masculino, (%)	20 (47.6%)	20 (54.1%)	0
	Femenino, (%)	22 (52.4%)	17 (45.9%)	5 (100%)
Edad (años)	X ± DE	10.9 ± 3.38	10.89 ± 3.35	11 ± 4
Diagnóstico (tipo de cáncer)	Osteosarcoma	33 (78.6%)	29 (78.4%)	4 (80%)
	Meduloblastoma	3 (7.1%)	3 (8.1%)	0
	Rabdomiosarcoma	2 (4.8%)	2 (5.4%)	0
	Tumor germinal	2 (4.8%)	2 (5.4%)	0
	Sarcoma	1 (2.4%)	1 (2.7%)	0
	Adenoma suprarrenal	1 (2.4%)	0	1 (20%)
Esquema de tratamiento	Cisplatino ± adriamicina	30 (71.4%)	27 (73%)	3 (60%)
	Cisplatino ± adriamicina ± doxorrubicina	2 (4.8%)	1 (2.7%)	1 (20%)
	Cisplatino ± etopósido	2 (4.8%)	1 (2.7%)	1 (20%)
	Cisplatino ± adriamicina ± ciclofosfamida	2 (4.8%)	2 (5.4%)	0
	Cisplatino ± adriamicina ± etopósido	1 (2.4%)	1 (2.7%)	0
	Cisplatino ± ciclofosfamida	1 (2.4%)	1 (2.7%)	0
	Cisplatino ± etopósido ± ciclofosfamida	1 (2.4%)	1 (2.7%)	0
	Cisplatino ± doxorubicina	1 (2.4%)	1 (2.7%)	0
	Cisplatino ± doxorubicina ± vincristina	1 (2.4%)	1 (2.7%)	0
	Cisplatino ± etopósido ± doxorubicina	1 (2.4%)	1 (2.7%)	0
Número de fármacos combinados	2	34 (81.0%)	30 (81.1%)	4 (80%)
	3	8 (19.0%)	7 (18.9%)	1 (20%)
Número de dosis recibidas	2	13 (31%)	9 (24.3%)	4 (80%)
	3	29 (69%)	28 (75.7%)	1 (20%)
Primera dosis de cisplatino (mg/m^2 sc)		155.19 ± 37.55	150.48 ± 31.27	190 ± 62.7
Segunda dosis de cisplatino (mg/m^2 sc)		153.57 ± 34.16	152.8 ± 36.16	159 ± 12.4
Tercera dosis de cisplatino (mg/m^2 sc)		155.5 ± 37.5	155.7 ± 38.17	150 ± 0
Dosis acumulada de cisplatino (mg/m^2 sc)		416.1 ± 118.8	421.16 ± 118.9	379 ± 124.56

n: número de pacientes; X±D.E.: promedio y desviación estándar; mg/m^2 sc: miligramos por metro cuadrado de superficie corporal.

tres dosis en la mayoría de los pacientes (69%). También se muestra la dosis administrada de cisplatino, en la población general y dividida en pCCO y pSCO.

En la tabla 2 se puede apreciar que la mayoría recibieron los fármacos en tres dosis (37 pacientes). A pesar de ser pocos los sujetos sin ototoxicidad

Tabla 2. Número de dosis recibidas y cantidad administrada de cisplatino en la población general y en pacientes con y sin criterios de ototoxicidad

Número de dosis de cisplatino recibidas (mg/m² sc)		Población general (n = 42)		Pacientes con ototoxicidad (n = 37)		Pacientes sin ototoxicidad (n = 5)	
Dosis	**X ± DE**	**2 dosis (n = 13)**	**3 dosis (n = 29)**	**2 dosis (n = 9)**	**3 dosis (n = 28)**	**2 dosis (n = 4)**	**3 dosis (n = 1)**
Primera dosis	X ± DE	151.2 ± 19.2	157 ± 43.6	146.1 ± 19.5	151.9 ± 34.4	162.5 ± 14.4	300
Segunda dosis	X ± DE	152.3 ± 18.7	154.1 ± 39.5	148.3 ± 20	154.3 ± 40.2	161.3 ± 13.1	150
Tercera dosis	X ± DE		155.5 ± 37.5		155.7 ± 38.2		150
Dosis acumulada	X ± DE	303.5 ± 34.5	466.7 ± 107.8	294.4 ± 36.8	461.9 ± 106.7	323.8 ± 18.4	600

sc: superficie corporal; X ± DE: promedio y desviación estándar.

(cinco pacientes), en ellos se observaron las mayores dosis promedio por administración en dos y tres dosis (rango: pSCO 150-300 vs. pCCO 146.11-155.71 mg/m² de superficie corporal), y fue estadísticamente significativo entre grupos para la primera dosis administrada (p = 0.025), pero no para la segunda (p = 0.71) y la tercera dosis (p = 0.88), así como para la dosis acumulada (rango: pSCO 294.44-461.89 vs. pCCO 323.75-600) (p = 0.46). Sin embargo, sí hubo significancia en la dosis acumulada al separarlos entre los que recibieron dos y tres dosis, entre los grupos con y sin ototoxicidad (p = 0.0001). En la comparación intragrupo no hubo diferencias para las diferentes dosis administradas.

En la tabla 3 se muestran los umbrales auditivos de los 42 pacientes de la investigación, y separados en pCCO y pSCO. Puede observarse que las frecuencias graves y medias se mantuvieron en promedio dentro de los límites de la normalidad en todos los estudios (< 20 dB), aunque las frecuencias agudas sí mostraron alteraciones mayores en el tercer estudio, en el grupo con ototoxicidad; no obstante, se puede apreciar un incremento promedio en todas las mediciones y los rangos permiten evidenciar que sí había pacientes con deterioro auditivo en cada medición audiológica. El análisis inferencial en pCCO mostró que solo hubo diferencia significativa en el nivel auditivo intragrupo entre el primero y el segundo estudios en las frecuencias medias (p = 0.043) y en las agudas (p = 0.046).

Al separar los grupos considerando el número de dosis (Tabla 4), se encontró que en aquellos que recibieron dos dosis también hubo diferencia significativa en las frecuencias medias (p = 0.043) y altas (p = 0.018) entre los estudios. En los que recibieron tres dosis se encontró diferencia significativa desde las frecuencias bajas entre el primero y el tercer estudios (p = 0.003), y entre el segundo y el tercer estudios (p = 0.010); para las frecuencias medias solo hubo diferencia en los umbrales auditivos entre el segundo y el tercer estudios (p = 0.001); y en las frecuencias agudas, la diferencia se ubicó en todas las comparaciones entre estudios (primero-segundo, primero-tercero y segundo-tercero) (p = 0.0001).

En los pacientes sin ototoxicidad no hubo diferencia intragrupo en los umbrales de las frecuencias graves (p = 0.99), medias (p = 0.141) ni agudas (p = 0.180) entre los estudios de aquellos que recibieron dos dosis (p > 0.05); no fue procedente el análisis en el único paciente con tres dosis.

En la tabla 5 se muestran los hallazgos auditivos en frecuencias supraumbrales (10-16 kHZ), donde se aprecia que desde el primer estudio el umbral promedio se ubicaba arriba de los 20 dB, con un incremento constante en las frecuencias evaluadas en todos los pCCO (dos y tres dosis). En contraste, los pSCO que recibieron dos dosis tuvieron umbrales promedio normales, aunque el análisis al interior de los datos muestra que ya había pacientes con afección > 20 dB en el segundo estudio (20.0 ± 3.4 dB y rango 18-25); así como el único paciente que recibió tres dosis, que desde el segundo estudio mostró un umbral anormal y se incrementó en el tercer estudio. Al comparar a los pCCO se observó mayor daño auditivo cuando se compararon con pSCO, desde el primer estudio, pero solo fue significativo en el segundo (p = 0.004) y el tercer estudios (p = 0.008). La comparación intragrupo evidenció que la diferencia fue significativa para pCCO entre el primero y el segundo estudios (p = 0.0001), y entre el primero y el tercer estudio (p = 0.0001), pero no entre el segundo y el tercer

Tabla 3. Umbral auditivo promedio por frecuencias (graves, medias y agudas) en la población general y separada por pacientes con y sin ototoxicidad

Umbral auditivo por frecuencias	X ± DE/ Rango	Población general (n = 42)	Con ototoxicidad (n = 37)	Sin ototoxicidad (n = 5)	p
Graves dosis 1 (dB)	X ± DE	13.4 ± 3.3	13.7 ± 3.2	11.4 ± 3.3	0.142
	Rango	8-21	8-21	8-15	
Graves dosis 2 (dB)	X ± DE	14.8 ± 6.3	15.27 ± 6.5	11.6 ± 3.6	0.228
	Rango	8-47	8-47	8-16	
Graves dosis 3 (dB)	X ± DE	17.7 ± 8.3	17.6 ± 8.5	19.0	0.874
	Rango	7-56	7-56		
Medias dosis 1 (dB)	X ± DE	14.1 ± 6.6	14.49 ± 6.9	11.4 ± 2.07	0.335
	Rango	7-47	7-47	8-13	
Medias dosis 2 (dB)	X ± DE	13.8 ± 7.6	14.68 ± 7.6	7.4 ± 3.3	0.043
	Rango	4-34	5-34	4-12	
Medias dosis 3 (dB)	X ± DE	12.2 ± 6.9	12.3 ± 7.0	8.0	0.547
	Rango	3-34	3-34		
Agudas dosis 1 (dB)	X ± DE	19.17 ± 12.7	19.8 ± 13.5	14.4 ± 1.1	0.379
	Rango		8-63	13-16	
Agudas dosis 2 (dB)	X ± DE	31.1 ± 18.2	33.16 ± 18.4	16 ± 1.7	0.046
	Rango	10-76	10-76	15-19	
Agudas dosis 3 (dB)	X ± DE	44.6 ± 20.9	45.7 ± 20.3	11.0	0.104
	Rango	11-91	11-91		

X ± DE: promedio y desviación estándar.

estudios (p = 0.319). A pesar del incremento constante en los umbrales de los pSCO, las diferencias no fueron significativas (p > 0.06). Se encontró una correlación entre la dosis acumulada y el umbral auditivo del segundo estudio en tonos graves (r_s = 0.38; p = 0.013), tonos medios (r_s = 0.53; p = 0.0001) y tonos agudos (r_s = 0.32; p = 0.034).

Las alteraciones en las altas frecuencias fueron evidentes desde la primera administración del fármaco en los pCCO, con pérdidas promedio siempre mayores de 20 dB hasta la tercera dosis, aunque fueron significativas solo entre el primero y el segundo estudios (p = 0.0001) y entre el primero y el tercer estudios (p = 0.001) tanto en pacientes con dos como con tres dosis, pero no entre el segundo y el tercer estudios (p = 0.793). En los pSCO apareció alteración leve en la segunda y la tercera dosis, pero no significativa (p > 0.05) (Tabla 5). De igual forma, la comparación entre pCCO y pSCO fue significativa solo en el segundo (p = 0.001) y el tercer estudios (p = 0.006) (Tabla 5). Considerando el daño en las altas frecuencias, hubo diferencia en la tercera dosis (p = 0.001) y con la dosis acumulada (p = 0.0001), y una correlación excelente entre la pérdida auditiva después de la tercera dosis con haber recibido tres dosis (r_s = 0.80; p = 0.0001) y con la dosis acumulada (r_s = 0.54; p = 0.0001), así como una mayor pérdida con dosis superiores a 300 y 325 mg/m^2 de superficie corporal en la segunda dosis (p = 0.036) y en la dosis acumulada (p = 0.009), y también entre el tercer estudio y la dosis acumulada (p = 0.006). Se documentó un riesgo (*odds ratio* [OR]) de 1.125 (intervalo de confianza del 95% [IC95%]: 0.893-1.417) para presentar daño en frecuencias supraumbrales en el tercer estudio con dosis de cisplatino de 300 mg/m^2 de superficie corporal.

Las EOAPD mostraron cambios relacionados con la dosis administrada de cisplatino. En la tabla 6 se puede apreciar que, en el primer estudio, la mayoría de los pacientes tenían respuestas presentes en

Tabla 4. Promedio y desviación estándar, y rango, por frecuencias del umbral auditivo en tonos graves (0.125, 0.250 y 0.500 kHZ), medios (1-2 kHZ) y agudos (4-8 kHZ) en la población general y separada por pacientes con y sin ototoxicidad, considerando el número de dosis recibidas (dos o tres)

		Población general		Con ototoxicidad		Sin ototoxicidad	
Umbral auditivo por frecuencias	**X ± DE/Rango**	**2 dosis (n = 13)**	**3 dosis (n = 29)**	**2 dosis (n = 9)**	**3 dosis (n = 28)**	**2 dosis (n = 4)**	**3 dosis (n = 1)**
Graves dosis 1 (dB)	X ± DE	11.69 ± 2.175	14.2 ± 3.41	12.2 ± 1.64	14.18 ± 3.47	10.5 ± 3.0	15
	Rango	8-15	8-21	10-15	8-21	8-14	
Graves dosis 2 (dB)	X ± DE	11.69 ± 2.17	16.2 ± 7.07	12.2 ± 1.64	16.25 ± 7.2	10.5 ± 3.0	16
	Rango	8-15	8-47	10-15	8-47	8-14	
Graves dosis 3 (dB)	X ± DE		17.8 ± 8.4		17.79 ± 8.56		19
	Rango		7-56		7-56		
Medias dosis 1 (dB)	X ± DE	11.46 ± 2.47	15.3 ± 7.55	11.6 ± 2.69	15.39 ± 7.68	11.0 ± 2.160	13
	Rango	7-16	8-47	7-16	8-47	8-13	
Medias dosis 2 (dB)	X ± DE	8.3 ± 3.75	16.28 ± 7.6	9.0 ± 3.8	16.5 ± 7.67	6.75 ± 3.59	10
	Rango	4-16	6-34	5-16	6-34	4-12	
Medias dosis 3 (dB)	X ± DE		12.5 ± 6.8		12.68 ± 6.89		8
	Rango		3-34		3-34		
Agudas dosis 1 (dB)	X ± DE	16.3 ± 4.49	20.45 ± 14.9	17.0 ± 5.3	20.7 ± 15.15	14.75 ± 0.95	13
	Rango	13-28	8-63	13-28	8-63	14-16	
Agudas dosis 2 (dB)	X ± DE	21.2 ± 9.46	35.5 ± 19.49	23.4 ± 10.7	36.29 ± 19.4	16.25 ± 1.89	15.00
	Rango	14-45	10-76	14-45	10-76	15-19	15
Agudas dosis 3 (dB)	X ± DE		45.38 ± 20.8		46.6 ± 20.13		11.00
	Rango		11-91		11-91		11

X ± DE: promedio y desviación estándar.

Tabla 5. Promedio y desviación estándar, y rango, por frecuencias supraumbral (tonos agudos 10-16 kHZ) en la población general y separada por pacientes con y sin ototoxicidad, considerando el número de dosis recibidas (dos o tres)

		Población general		Con ototoxicidad		Sin ototoxicidad	
Umbral auditivo para altas frecuencias	**X ± DE/ Rango**	**2 dosis (n = 13)**	**3 dosis (n = 29)**	**2 dosis (n = 9)**	**3 dosis (n = 28)**	**2 dosis (n = 4)**	**3 dosis (n = 1)**
Primer estudio (dB) (dosis 1)	X ± DE	22.3 ± 10.7	23.8 ± 16.8	24.7 ± 12.3	24.0 ± 17.0	17.0 ± 1.6	18.0
	Rango	15-53	2-71	17-53	2-71	15-19	
Segundo estudio (dB) (dosis 2)	X ± DE	35.9 ± 18.2	45.0 ± 19.9	43.0 ± 17.6	45.8 ± 19.9	20.0 ± 3.4	23.0
	Rango	18-70	14-87	25-70	14-87	18-25	
Tercer estudio (dB) (dosis 3)	X ± DE	-	58.8 ± 19.8	-	60.0 ± 19.1	-	26.0
	Rango	-	21-102	-	21-102	-	-

X ± DE: promedio y desviación estándar.

Tabla 6. Proporción de pacientes con presencia/ausencia de emisiones otoacústicas por productos de distorsión en la población general y separada por pacientes con y sin ototoxicidad, considerando el número de dosis recibidas (dos o tres)

		Población general		Con ototoxicidad		Sin ototoxicidad	
EOAPD (presentes/ ausentes)	**Presentes/ausentes**	**2 dosis (n = 13)**	**3 dosis (n = 29)**	**2 dosis (n = 9)**	**3 dosis (n = 28)**	**2 dosis (n = 4)**	**3 dosis (n = 1)**
Primer estudio (dosis 1)	Presentes	12	26	8	25	4	1
	Ausentes	1	3	1	3	0	0
Segundo estudio (dosis 2)	Presentes	7	12	4	11	3	1
	Ausentes	6	17	5	17	1	0
Tercer estudio (dosis 3)	Presentes	-	1	0	0	-	1
	Ausentes	-	28	0	28	-	0

EOAPD: emisiones otoacústicas por productos de distorsión.

pCCO (33 pacientes; 89.2%) y pSCO (5 pacientes; 100%). Hubo cambios posterior a la segunda dosis en pCCO, en los que la mayoría no presentaron emisiones (22 pacientes; 60%), pero la variación no fue significativa ($p = 0.11$; χ^2), y para la evaluación después de la tercera dosis todos presentaron ausencia de respuesta (28 pacientes; 100%) ($p = 0.05$). En los pSCO no hubo cambios, pues solo un paciente no tuvo respuesta ($p = 0.34$). El único paciente que recibió tres dosis siempre presentó respuesta en las diferentes mediciones. La presencia/ausencia de respuestas en las EOAPD mostraron una diferencia significativa solo después de la segunda dosis de cisplatino ($p = 0.034$), con una OR de 1.973 (IC95%: 1.097-3.549) para la ausencia de respuestas con dosis superiores a 300 y 325 mg/m^2 de superficie corporal. En los pacientes con tres dosis la diferencia fue significativa, con ausencia de respuestas ($p = 0.0001$). Se encontró una asociación ($r_s = 0.67$; $p = 0.036$) con la dosis acumulada de 300 mg/m^2 de superficie corporal en los pCCO después de la segunda dosis y una OR de 4.0 para la ausencia de respuestas (IC95%: 0.733-21.838) con la misma dosis ($p = 0.034$).

Discusión

Uno de los hallazgos más importantes del presente estudio fue identificar el deterioro auditivo en niños con cáncer tratados con cisplatino en tonos agudos y altas frecuencias (10,000-16,000 Hz) desde la primera dosis de cisplatino, combinado con uno o dos fármacos más (Tablas 3 a 5). Es importante señalar que la prevalencia de pérdida auditiva al término del tratamiento es considerada como el hallazgo primario más importante, pues refleja la toxicidad de la QT al final (Tablas 3 a 5). En esta investigación se encontró que los 37 pCCO (100%) presentaron deterioro en las altas frecuencias desde la primera dosis y tuvieron daño en las agudas a partir de la segunda dosis, de acuerdo con la clasificación de Brock (Tablas 4 y 5), coincidiendo con otras publicaciones[15].

Se ha publicado que la pérdida auditiva ocurre en alrededor del 10% de los sobrevivientes de cáncer infantil en general[22], pero en nuestro trabajo la prevalencia fue mucho mayor (88.1%), más acorde con lo reportado por Diepstraten et al.[15], quienes señalan que hasta el 70% de los niños tratados con platino desarrollan una pérdida auditiva irreversible, y el 40% necesitan usar audífonos en etapa temprana. No obstante, nuestra cifra puede estar sobrecalculada, ya que todos usaron cisplatino y contaban con estudios audiológicos, aunque congruente con el reporte de que las estimaciones de prevalencia de pérdida de audición después de cisplatino varían ampliamente entre diferentes trabajos, debido a factores de riesgo adicionales como el uso de aminoglucósidos y diuréticos de asa, o de otros agentes antineoplásicos que causan hipoacusia[22].

Algunos autores proponen que en la evaluación de estos niños es conveniente el uso de más de un estudio que evalúe la función auditiva, por la credibilidad de los resultados considerando la edad del menor al momento de realizar estudios conductuales. En este trabajo se usó la audiometría tonal y la de altas frecuencias, así como los EOAPD, porque no se consideran relevantes los hallazgos de impedanciometría ni los potenciales auditivos de tallo cerebral[15,23].

De acuerdo con otros autores, encontramos que la dosis acumulada de cisplatino se asoció con la pérdida

de la audición[11], pues las dosis cíclicas más altas pueden aumentar la administración coclear del fármaco a través de la saturación de los mecanismos de transporte activo y pasivo en la cóclea, y una vez en ella, el cisplatino se acumula y se retiene, en particular después de dosis altas repetidas[24]. Fue interesante que una dosis acumulada superior a 300 y 325 mg/m^2 de superficie corporal se relacionó con la presencia de lesión en altas frecuencias y en tonos agudos, y con ausencia de respuesta en las EOAPD ($p < 0.05$)[15].

Keilty et al.[7] encontraron, para el desarrollo de hipoacusia, una OR de 1.48 para la dosis de cisplatino, tomando en cuenta 100 mg/m^2 de superficie corporal ($p < 0.001$), con incrementos en la incidencia acumulada de hipoacusia de alta frecuencia (> 4 kHz) a los 5 años de edad y en todas las frecuencias después de los 5 años[7]. Nuestro análisis permitió evidenciar una OR de 1.125 (IC95%: 0.893-1.417) de presentar daño en altas frecuencias en el tercer estudio con dosis de cisplatino de 300 mg/m^2 de superficie corporal, y una OR de 1.973 (IC95%:1.097-3.549) para la ausencia de respuestas en las EOAPD con dosis por arriba de 300 y 325 mg/m^2 de superficie corporal al término del tratamiento[7,15]. A pesar de que encontramos diferencias significativas en la pérdida de audición entre las dosis administradas, segunda y tercera dosis, así como en la dosis acumulada, parece que no importa el tiempo de duración de las infusiones[16].

Bass et al.[18] identificaron efectos subclínicos de pérdida auditiva después de la exposición a RT en pacientes con cáncer particularmente en el rango de las altas frecuencias y en las EOAPD, mientras la audición se mantuvo normal para las frecuencias convencionales. Nuestros hallazgos son congruentes con este comportamiento, con relación al uso de cisplatino, aunque sin seguimiento a largo plazo (Figs. 1 y 2, y Tabla 6). No obstante, es importante seguir la recomendación del seguimiento durante varios años para controlar los posibles efectos auditivos tardíos[18], por la exposición a ototóxicos con QT o RT. También Moke et al.[13] reportaron que el riesgo para hipoacusia aumentó en un 10-20% por cada 100 mg/m^2 de superficie corporal de dosis acumulada de cisplatino (OR: 1.11; IC95%: 1.01-1.23). Nosotros encontramos un riesgo similar (OR: 1.125; IC95%: 0.893-1.417) con una dosificación de cisplatino de 300 y 325 mg/m^2 de superficie corporal en la segunda dosis ($p = 0.036$), mientras que en el trabajo de Moke et al.[13] la pérdida fue moderada/grave al final del tratamiento con dosis de cisplatino, encontrando que por cada aumento de 50 mg/m2/ciclo, identificaba un OR = 2.16 (IC95%:1.37–3.51). Además, encontramos que diferencias en la dosificación de cisplatino confirieron una OR de 4.0 (IC95%: 0.733-21.838) en pérdida de respuestas en las EOAPD. Si bien se debe considerar que el aumento de la dosis acumulada de cisplatino administrado (± 100 mg/m^2 de superficie corporal) protegió contra la muerte, fue al contrario con la progresión de la enfermedad[13].

Contrario a lo expuesto por Moke et al.[13], se cree que sea probable que el cisplatino retenido solo contribuya a la toxicidad a largo plazo, pues se ha detectado cisplatino circulante en el plasma de sobrevivientes incluso décadas después de la terapia. Por ello, se justifica una mayor investigación sobre las posibles intervenciones para reducir la hipoacusia inducida por cisplatino mediante la alteración de la intensidad de la dosificación de cisplatino con o sin la introducción de agentes otoprotectores, mientras se mantienen la citotoxicidad y el potencial curativo de la dosificación acumulativa, como el uso de amifostina y tiosulfato de sodio en niños como una intervención otoprotectora[13] o el uso de nanopartículas de dexametasona y antioxidantes, que previnieron eficazmente la apoptosis y la producción de especies reactivas de oxígeno causadas por estímulos ototóxicos[25].

Los datos audiológicos encontrados muestran que la pérdida de audición es frecuente en los sobrevivientes de cáncer infantil. Es difícil establecer la relación entre la pérdida de audición y otros antineoplásicos (como la vincristina)[13], debido a que el tratamiento con cisplatino fue un criterio de inclusión, lo que dificulta la identificación de la contribución de otros factores. Sin embargo, las pruebas de audición no son invasivas, son baratas y fáciles de realizar, y cada niño las realiza varias veces durante la infancia con fines de cribado. Por lo tanto, nuestros resultados son congruentes con la necesidad de que los estudios futuros tengan criterios de inclusión más amplios y ofrecer pruebas de audición a todas las personas que recibieron alguna QT, no solo a los que recibieron fármacos que ya se sabe que son ototóxicos[22]. Estudios con criterios más amplios permitirán detectar nuevos factores de riesgo en el paisaje en constante evolución de los tratamientos contra el cáncer[26].

Las pruebas audiológicas precisas y la detección oportuna de la ototoxicidad contribuyen a la detección de hipoacusia en etapa temprana, que puede conducir indirectamente a una mejor calidad de vida. Además, se logró recopilar datos de alta calidad sobre la relación entre el estado de la enfermedad, el tipo de tratamiento y el funcionamiento audiológico en niños con cáncer durante el tratamiento, que en el futuro podrían usarse para identificar a los niños que están en riesgo y que podrían beneficiarse de los agentes otoprotectores[15].

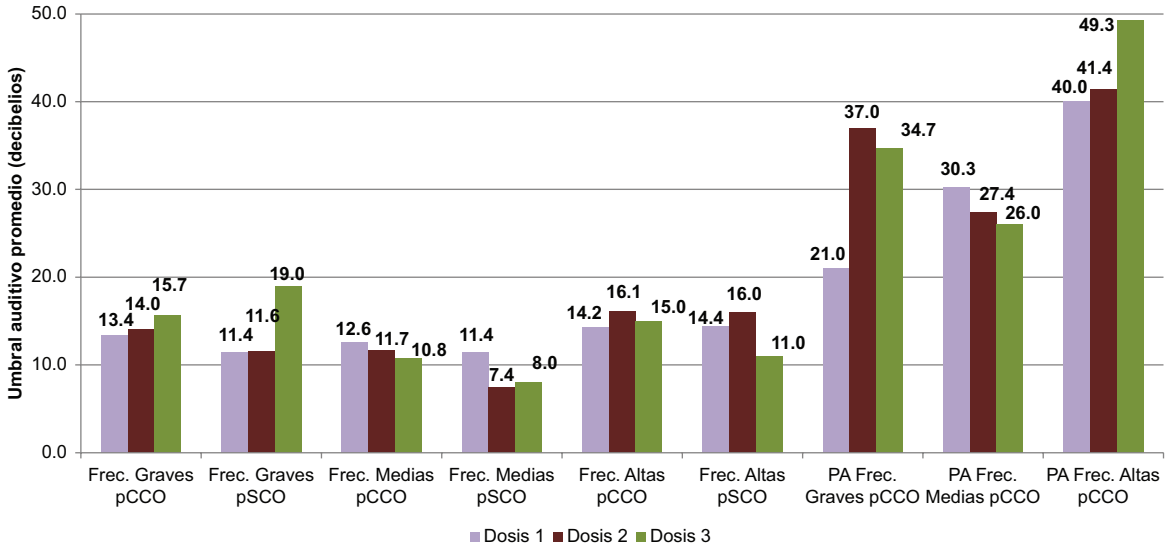

Figura 1. *Comportamiento de los umbrales auditivos, con y sin criterios de ototoxicidad, según número de dosis. PA: pérdida auditiva; pCCO: pacientes con criterios para ototoxicidad; pSCO: pacientes sin criterios para ototoxicidad.*

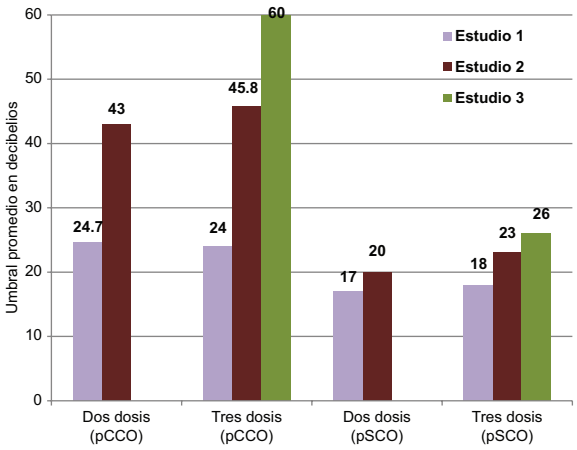

Figura 2. *Comportamiento de las respuestas supraumbral, con y sin criterios de ototoxicidad, de acuerdo al número de estudio. pCCO: pacientes con criterios para ototoxicidad; pSCO: pacientes sin criterios para ototoxicidad.*

También consideramos relevante este trabajo porque algunos autores mencionan que hay una sorprendente falta de trabajos que investiguen específicamente los efectos tardíos en los sobrevivientes de cáncer infantil, considerando que actualmente ha aumentado la cantidad de sobrevivientes[27].

Conclusiones

El cisplatino es un fármaco antineoplásico ampliamente utilizado en el tratamiento del cáncer en la infancia, y la ototoxicidad es uno de sus efectos adversos más frecuentes. Nosotros encontramos un 88.1% de pacientes con deterioro auditivo y hasta un 100% cuando se incluyeron las altas frecuencias en los casos estudiados. Se documentó que la hipoacusia neurosensorial inicia en las altas frecuencias, pero con el incremento en la dosis acumulada de cisplatino (≥ 300 mg/m^2 de superficie corporal) el daño continúa a frecuencias agudas y medias, comprometiendo el área del lenguaje después de la segunda y la tercera dosis. Evaluar la función auditiva de los niños con cáncer durante su tratamiento con cisplatino puede permitir la detección oportuna del deterioro de los umbrales auditivos. La audiometría tonal de altas frecuencias y los EOAPD mostraron ser útiles, ya que revelaron de manera temprana cambios en la función auditiva con respecto a la audiometría tonal en las frecuencias convencionales, por lo que los protocolos de monitorización auditiva en los pacientes tratados con cisplatino deben incluir, por lo menos, estos estudios audiológicos.

En conclusión, debido a que el número de sobrevivientes de cáncer infantil ha incrementado en las últimas décadas, es de suma importancia establecer protocolos de cribado y monitorización de ototoxicidad en pacientes tratados con cisplatino y otros agentes potencialmente ototóxicos para conocer la función auditiva desde las etapas iniciales del tratamiento, y poder intervenir oportunamente con la rehabilitación auditiva, ya que la hipoacusia en este grupo de población tiene

repercusiones en el lenguaje, el aprendizaje, la integración social y el desarrollo de la personalidad.

Agradecimientos

Los autores agradecen al personal de Oncología y Audiología-Foniatría, por su participación en la realización de este proyecto. Al Hospital Infantil de México, por fomentar la realización de la investigación.

Este estudio es parte del trabajo de ingreso por el autor principal a la Academia Mexicana de Cirugía, para el sitial de Comunicación, Audiología, Otoneurología y Foniatría, en la convocatoria 2023.

Financiamiento

Este trabajo no recibió financiamiento externo de ninguna entidad pública ni privada.

Conflicto de intereses

Los autores declaran no tener ningún conflicto de intereses.

Consideraciones éticas

Protección de personas y animales. Los autores declaran que para esta investigación no se han realizado experimentos en seres humanos ni en animales.

Confidencialidad, consentimiento informado y aprobación ética. Los autores han obtenido la aprobación del Comité de Ética para el análisis de datos clínicos obtenidos de forma rutinaria y anonimizados, por lo que no fue necesario el consentimiento informado. Se han seguido las recomendaciones pertinentes.

Declaración sobre el uso de inteligencia artificial. Los autores declaran que no utilizaron ningún tipo de inteligencia artificial generativa para la redacción de este manuscrito.

Bibliografía

1. Organización Panamericana de la Salud, Organización Mundial de la Salud. Cáncer en la niñez y la adolescencia. 2017. (Consultado el 02-10-2022.) Disponible en: https://www.paho.org/es/temas/cancer-ninez-adolescencia.
2. Johnston WT, Erdmann F, Newton R, Steliarova-Foucher E, Schüz J, Roman E. Childhood cancer: estimating regional and global incidence. Cancer Epidemiol. 2021;71:101662.
3. Rivera-Luna R, Zapata-Tarres M, Shalkow-Klincovstein J, Velasco-Hidalgo L, Olaya-Vargas A, Finkelstein-Mizrahi N, et al. The burden of childhood cancer in Mexico: implications for low- and middle-income countries. Pediatr Blood Cancer. 2017;64(6).
4. Castro-Ríos A, Martínez-Valverde S. Childhood cancer survival, 2006-2012 cohorts of Mexican Institute of Social Security beneficiaries at the Central-South Region of Mexico. Front Oncol. 2022;12:1-9.
5. Palmer JD, Hall MD, Mahajan A, Paulino AC, Wolden S, Constine LS. Radiotherapy and late effects. Pediatr Clin North Am. 2020;67:1051-67.
6. Ryder-Burbidge C, Diaz RL, Barr RD, Gupta S, Nathan PC, McKillop SJ, et al. The burden of late effects and related risk factors in adolescent and young adult cancer survivors: a scoping review. Cancers (Basel). 2021;13):4870.
7. Keilty D, Khandwala M, Liu ZA, Papaioannou V, Bouffet E, Hodgson D, et al. Hearing loss after radiation and chemotherapy for CNS and head-and-neck tumors in children. J Clin Oncol. 2021;39:3813-21.
8. Hua C, Bass JK, Khan R, Kun LE, Merchant TE. Hearing loss after radiotherapy for pediatric brain tumors: effect of cochlear dose. Int J Radiat Oncol Biol Phys. 2008;72:892-9.
9. Yock TI, Murphy B, Bass JK, Ronckers CM, Kremer L, Baliga S, et al. Modeling the risk of hearing loss from radiotherapy in childhood cancer survivors: initial results from the Pediatric Normal Tissue Effects in the Clinic (PENTEC) Hearing Loss Task Force. Int J Radiat Oncol Biol Phys. 2019;105:S191.
10. Scobioala S, Parfitt R, Matulat P, Kittel C, Ebrahimi F, Wolters H. Impact of radiation technique, radiation fraction dose, and total cisplatin dose on hearing: retrospective analysis of 29 medulloblastoma patients. Strahlenther Onkol. 2017;193:910-20.
11. Cohen-Cutler S, Wong K, Mena V, Sianto K, Wright MA, Olch A, et al. Hearing loss risk in pediatric patients treated with cranial irradiation and cisplatin-based chemotherapy. Int J Radiat Oncol Biol Phys. 2021;110:1488-95.
12. Generotti C, Cox BC, Singh J, Hamilton D, McKenzie E, O'Malley BW Jr, et al. Subclinical diagnosis of cisplatin-induced ototoxicity with biomarkers. Sci Rep. 2022;12:18032.
13. Moke DJ, Luo C, Millstein J, Knight KR, Rassekh SR, Brooks B, et al. Prevalence and risk factors for cisplatin-induced hearing loss in children, adolescents, and young adults: a multi-institutional North American cohort study. Lancet Child Adolesc Health. 2021;5:274-83.
14. Rajput K, Edwards L, Brock P, Abiodun A, Simpkin P, Al-Malky G. Ototoxicity-induced hearing loss and quality of life in survivors of paediatric cancer. Int J Pediatr Otorhinolaryngol. 2020;138:110401.
15. Diepstraten FA, Meijer AJ, van Grotel M, Plasschaert S, Hoetink AE, Fiocco M, et al. A Study on Prevalence and Determinants of Ototoxicity During Treatment of Childhood Cancer (SOUND): protocol for a prospective study. JMIR Res Protoc. 2022;11:e34297.
16. van As JW, van den Berg H, van Dalen EC. Different infusion durations for preventing platinum-induced hearing loss in children with cancer. Cochrane Database Syst Rev. 2020;(1):CD010885.
17. Weiss A, Sommer G, Kasteler R, Scheinemann K, Grotzer M, Kompis M, et al; Swiss Pediatric Oncology Group (SPOG). Long-term auditory complications after childhood cancer: a report from the Swiss Childhood Cancer Survivor Study. Pediatr Blood Cancer. 2017;64:364-73.
18. Bass JK, Huang J, Hua CH, Bhagat SP, Mendel LL, Onar-Thomas A, et al. Auditory outcomes in patients who received proton radiotherapy for craniopharyngioma. Am J Audiol. 2018;27:306-15.
19. Chang KW, Chinosornvatana N. Practical grading system for evaluating cisplatin ototoxicity in children. J Clin Oncol. 2010;28:1788-95.
20. Coze C, Hartmann O, Michon J, Frappaz D, Dusol F, Rubie H, et al. NB87 induction protocol for stage 4 neuroblastoma in children over 1 year of age: a report from the French Society of Pediatric Oncology. J Clin Oncol. 1997;15:3433-40.
21. Brock PR, Bellman SC, Yeomans EC, Pinkerton CR, Pritchard J. Cisplatin ototoxicity in children: a practical grading system. Med Pediatr Oncol. 1991;19:295-300.
22. Strebel S, Waespe N, Kuehni CE. Hearing loss in childhood cancer survivors. Lancet Child Adolesc Health. 2021;5:e17.
23. Meijer AJM, van den Heuvel-Eibrink MM, Brooks B, Am Zehnhoff-Dinnesen AG, Knight KR, Society of Paediatric Oncology Supportive Care Committee, et al. Recommendations for age-appropriate testing, timing, and frequency of audiologic monitoring during childhood cancer treatment: an International Society of Paediatric Oncology Supportive Care Consensus Report. JAMA Oncol. 2021;7:1550-8.
24. Breglio AM, Rusheen AE, Shide ED, Fernandez KA, Spielbauer KK, McLachlin KM, et al. Cisplatin is retained in the cochlea indefinitely following chemotherapy. Nat Commun. 2017;8:1654.
25. Barbara M, Margani V, Covelli E, Filippi C, Volpini L, El-Borady OM, et al. The use of nanoparticles in otoprotection. Front Neurol. 2022;13:912647.
26. Clemens E, van den Heuvel-Eibrink MM, Mulder RL, Kremer LCM, Hudson MM, Skinner R, et al. Recommendations for ototoxicity surveillance for childhood, adolescent, and young adult cancer survivors: a report from the International Late Effects of Childhood Cancer Guideline Harmonization Group in collaboration with the PanCare Consortium. Lancet Oncol. 2019;20:e29-41.
27. Friend AJ, Feltbower RG, Hughes EJ, Dye KP, Glaser AW. Mental health of long-term survivors of childhood and young adult cancer: a systematic review. Int J Cancer. 2018;143:1279-86.

ORIGINAL ARTICLE

Complications in transgender patients undergoing vaginoplasty procedure

Complicaciones en pacientes transgénero sometidas a procedimiento de vaginoplastia

Francisco Delgado-Guerrero
Servicio de Urologia, Hospital General de Tlahuac, Mexico City, Mexico

Abstract

Objective: *To report the statistics of complications in gender reassignment surgery (vaginoplasty) observed in the first surgical center in Mexico for public transgender surgery.* **Method:** *We conducted a descriptive, observational study of patients treated and postoperatively underwent vaginoplasty surgery in the period 2019 to 2022. Intraoperative, immediate and late complications were evaluated. Intraoperative complications were taken as: rectal perforation and bleeding. Immediate complications: wound dehiscence, hematoma, and necrosis of the vaginal segment. Late complications: urethrovaginal fistula, rectovaginal fistula, and stenosis of the vaginal introitus.* **Results:** *Twenty-two patients who underwent vaginoplasty with inversion of the foreskin were evaluated. Regarding immediate complications, the most frequent were alterations in scarring and tissue integration, being necrosis of the vaginal segment the most frequent. As for late complications, only vaginal prolapse and urethral stricture were found.* **Conclusion:** *Foreskin inversion vaginoplasty is the most widely used and safest technique worldwide, above colovaginoplasty and peritoneal vaginoplasty techniques, and fortunately serious complications are rare. In our report, tissue alterations were the common ones and that is secondary alteration of vascular integration and devascularization factors during the dissection.*

Keywords: *Transgender health. Post-operative complications. Reconstructive surgical procedure.*

Resumen

Objetivo: *Reportar la estadística de complicaciones en cirugía de reasignación de genero (vaginoplastia) observadas, en el primer centro quirúrgico en México de cirugía transgénero público.* **Método:** *Realizamos un estudio descriptivo y observacional de las pacientes tratadas y post-operadas de cirugía de vaginoplastia en el periodo de 2019 a 2022. Se evaluaron las complicaciones: intraoperatorias, inmediatas y tardías. Se consideraron complicaciones intraoperatorias la perforación rectal y el sangrado. Complicaciones inmediatas: dehiscencia de herida, hematoma y necrosis del segmento vagina. Complicaciones tardías: fístula uretrovaginal, fístula rectovaginal y estenosis del introito vaginal.* **Resultados:** *Se evaluaron 22 pacientes a las que se les realizó vaginoplastia con inversión del prepucio. En cuanto a las complicaciones inmediatas, las más frecuentes fueron las alteraciones en la cicatrización y la integración tisular, siendo la necrosis del segmento vaginal la más frecuente. En cuanto a las complicaciones tardías, solo se encontraron prolapso vaginal y estenosis uretral.* **Conclusión:** *La vaginoplastia con inversión de prepucio es la técnica más usada mundialmente y la más segura, por arriba de las técnicas de colovaginoplastia y vaginoplastia peritoneal, y las complicaciones graves son pocos comunes, afortunadamente. En nuestro reporte las alteraciones tisulares fueron las comunes y eso es secundario a la alteración de la integración vascular y los factores de desvascularización durante la disección.*

Palabras clave: *Salud transgénero. Complicaciones postoperatorias. Procedimiento quirúrgico reconstructivo.*

Correspondence:
Francisco Delgado-Guerrero
E-mail: delgadoguerrero11@hotmail.com

Date of reception: 25-07-2023
Date of acceptance: 25-10-2023
DOI: 10.24875/CIRU.23000380

Cir Cir. 2025;93(2):177-180
Contents available at PubMed
www.cirugiaycirujanos.com

Introduction

The performance of gender-affirming procedures has become increasingly common, reflecting a changing social and political climate of equality for gender identity. Although many transgender patients do not choose to undergo the surgical transition process, gender-affirming procedures remain an option for those who wish to further align physical appearances with their identified gender. Vaginoplasty with foreskin inversion is commonly performed for female transgender patients in which the foreskin and scrotum are used to create a natural-appearing vulva and vaginal canal.

Despite these positive results, penile inversion for vaginoplasty is associated with a high rate of functional and cosmetic complications, most of which are self-limited or treated on an outpatient basis without the need for surgical procedures. Large series report that 70% of patients experience some type of postoperative complications such as altered skin tissue flap integration (26%) and less commonly but more consistently neo vaginal stenosis (4%) and rectovaginal fistula (2%). In addition, up to 33.7% of patients undergo procedures for secondary correction of esthetic conditions and function[1-3].

In this article, we present our experience and management of patients with post-surgical complications in patients undergoing vaginoplasty procedure.

Method

A descriptive and observational study was performed, of patients attended and post-operated of vaginoplasty in the period from 2019 to 2022, patients with complete surgical protocol and previous assessments by endocrinology and psychiatry, of clínica Condesa, in addition to hormonal interruption 2 months before surgical procedure, all patients with strict compliance with the criteria of World Professional Association for Transgender Health, such as: majority of age, hormonal treatment for at least 2 years, assessment by 2 mental health professionals (psychiatry), 24/7 life experience with chosen sex.

The technique performed was the penis-scrotal inversion technique, which consists of a series of procedures such as: penectomy, orchiectomy, clitoroplasty, and vaginoplasty. The creation of vaginoplasty involves inversion of the penile skin and is perhaps the most studied and used today. For most surgeons, it is the technique of choice. It uses the inverted penile skin that functions as a tube that becomes the neovagina. It has been described that the average vaginal depth ranges from 10 to 13.5 cm; the average width of the neovagina is 3 to 4 cm.

Table 1. Characteristics of the patients who underwent vaginoplasty

Variable	p
Total patients (n)	22
Age (years)	36.2 (19-55)
Diabetes Mellitus	2
Arterial hypertension	1
Years of hormonal treatment	7 (2-18)
Previous orchiectomy	2
Body mass index	28.0 kg/m^2
History of circumcision.	2
Smoking	3

An evaluation of the complications in the patients operated in the period from 2019 to 2022, with vaginoplasty technique with inversion of the foreskin was carried out, three groups were divided: intraoperative, immediate, and late. The immediate complications were: rectal perforation, bleeding with necessity, and transfusion. As for immediate complications: wound dehiscence, hematoma, vaginal segment necrosis, vaginal edema, abscess, urethral necrosis, clitoral necrosis, and urinary tract infection. Late complications were taken as: urethrovaginal fistula, rectovaginal fistula, vaginal introitus stenosis, vaginal prolapse, urethral meatus stenosis, and urethral prolapse.

Results

The total number of patients studied were 22 postoperative patients of vaginoplasty procedure with foreskin inversion, performed by a single surgeon in our institution, the mean age was 36 years, 2 patients with a history of previous orchiectomy, mean body mass index 28.0 kg/m² (range, 20.2-39.4 kg/m²), mean use of hormonal treatment of 6 years, with follow-up during each month for 6 months (Tables 1 and 2).

Of the 22 patients operated on, intra-operative complications were found as intraoperative bleeding in only one patient, secondary to a sacral bleeding >500cc, indication for transfusion by the anesthesiology service. As for immediate complications, the most common was alterations in healing and tissue integration, being necrosis of the vaginal segment, the others were: hematoma, wound dehiscence, abscess, wound infection, and edema (Figs. 1 and 2). Finally, the late

Table 2. Complications percentage intraoperative

Time complication	%
Intraoperative	
Rectal perforation.	-
Bleeding	1 (4.5)
Immediate	
Wound dehiscence	2 (9.0)
Hematoma	2 (9.0)
Vaginal segment necrosis	4 (18)
Abscess	1 (4.5)
Urethral necrosis	-
Wound infection	1 (4.5)
Edema.	2 (9.0)
Necrosis of the clitoris	-
Late	
Urethrovaginal fistula	-
Rectovaginal fistula.	-
Introitovaginal stenosis	-
Vaginal prolapse	1 (0.45)
Meatourethral stenosis	1 (0.45)
Urethral prolapse	-

Figure 1. A*: severe edema after vaginoplasty surgery.* **B***: vaginal fundal prolapse.*

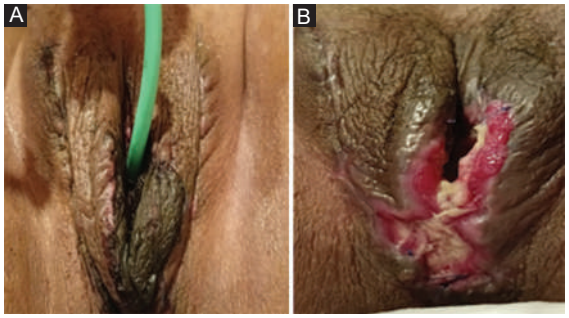

Figure 2. A*: vaginal border necrosis.* **B***: vaginal border granulation.*

complications presented were: vaginal prolapse secondary to severe edema and partial stenosis of meatal urethral stenosis.

Discussion

Minor wound healing problems are commonly reported after vaginoplasty (range 3.3%-33%), and many resolve without surgical intervention. Wound dehiscence, especially in areas of increased tissue tension (i.e., introitus and labia majora), most commonly occurs within the 1st month after surgery[4,5]. In the observed results, most of the complications observed were of the immediate type the most common, with impaired healing as well as the presence of partial necrosis of vaginal tissue, Ferrando reported that of the 17% of her patients (n = 76 patients) who experienced complications, more than 50% of these complications involved wound dehiscence or wound separation. Most studies consistently report that post-operative wound dehiscence is treated with local wound care and does not require surgical intervention[6,7].

Tissue loss may be associated with wound dehiscence and occurs most frequently at points of maximal tissue tension, such as the vaginal introitus. Minor tissue necrosis (i.e., resolved without reoperation under general anesthesia) representing the highest incidence reported in some studies[8,9]. Minor cases of tissue necrosis can often be treated with local wound care, whereas more significant tissue loss may require surgical debridement. The most common major complication (17%) was tissue necrosis along the lower edge of the wound. García MM et al. reported that of the patients requiring reoperation, 25% were related to tissue necrosis[10,11].

Pre-operative patient optimization (smoking cessation, control of diabetes, and cardiopulmonary status) is important, as these concomitant conditions may be independent predictors of post-operative tissue necrosis.

Conclusion

Complications arising from surgery are defined as an unexpected or undesired outcome of surgical treatment that causes, in addition to a difficult situation for the surgeon, a lengthening of the hospital stay, vary in severity and some can be easily treated with conservative management strategies and/or small revision surgeries, whereas other events are considered true complications and require and/or surgery to treat the problem.

Foreskin inversion vaginoplasty is the most widely used and safest technique worldwide, above

colovaginoplasty and peritoneal vaginoplasty techniques, and fortunately serious complications are rare. In our report, tissue alterations were the common ones and that is secondary alteration of vascular integration and devascularization factors during the dissection.

Funding

The authors declare that they have not received funding.

Conflicts of interest

The authors declare no conflicts of interest.

Ethical considerations

Protection of humans and animals. The authors declare that the procedures followed complied with the ethical standards of the responsible human experimentation committee and adhered to the World Medical Association and the Declaration of Helsinki. The procedures were approved by the institutional Ethics Committee.

Confidentiality, informed consent, and ethical approval. The authors have obtained approval from the Ethics Committee for the analysis of routinely obtained and anonymized clinical data, so informed consent was not necessary. Relevant guidelines were followed.

Declaration on the use of artificial intelligence. The authors declare that no generative artificial intelligence was used in the writing of this manuscript.

References

1. Ferrando CA. Complications of vaginoplasty CA. Clin Plast Surg. 2018;45:361-8.
2. Ding C, Khondker A, Goldenberg MG, Kwong JC, Lajkosz K, Potter E, et al. Urinary complications after penile inversion vaginoplasty in transgender women systematic review and meta-analysis. Can Urol Assoc J. 2023;17:121-8.
3. Amies Oelschlager AM, Kirby A, Breech L. Evaluation and management of vaginoplasty complications. Curr Opin Obstet Gynecol. 2017;29:316-21.
4. Drinane JJ, Santucci R. What urologists need to know about male-to-female genital confirmation surgery (vaginoplasty): techniques, complications, and how to treat them. Minerva Urol Nefrol. 2020;72:162-72.
5. Gaither TW, Awad MA, Osterberg EC, Murphy GP, Romero A, Bowers ML, et al. Postoperative complications following primary penile inversion vaginoplasty among 330 male-to-female transgender patients. J Urol. 2018;199:760-5.
6. Russell CB, Hong CX, Fairchild P, Bretschneider CE. Complications after orchiectomy and vaginoplasty for gender affirmation: an analysis of concurrent versus separate procedures using a national database. Urogynecology (Phila). 2023;29:202-8.
7. Raigosa M, Avvedimento S, Yoon TS, Cruz-Gimeno J, Rodriguez G, Fontdevila J. Male-to-female genital reassignment surgery: a retrospective review of surgical technique and complications in 60 patients. J Sex Med. 2015;12:1837-45.
8. Buncamper ME, van der Sluis WB, van der Pas RS, Özer M, Smit JM, Witte BI, et al. Surgical outcome after penile inversion vaginoplasty: a retrospective study of 475 transgender women. Plast Reconstr Surg. 2016;138:999-1007.
9. Wangjiraniran B, Selvaggi G, Chokrungvaranont P. Male-to-female vaginoplasty: preecha's surgical technique. J Plast Surg Hand Surg. 2015;49:153-9.
10. Ives GC, Fein LA, Finch L, Sluiter EC, Lane M, Kuzon WM, et al. Rvaluation of BMI as a risk factor for complications following gender-affirming penile inversion vaginoplasty. Plast Reconstr Surg Glob Open. 2019;7:e2097.
11. Garcia MM, Shen W, Zhu R, Stettler I, Zaliznyak M, Barnajian M, et al. Use of right colon vaginoplasty in gender-affirming surgery. Surg Endosc. 2021;35:5643-54.

ORIGINAL ARTICLE

Rehabilitation effect of manual lymphatic drainage on pain threshold and tolerance, tactile sensation, and strength

Efecto de rehabilitación del drenaje linfático manual en el umbral y tolerancia al dolor, sensación táctil y fuerza

Emine Cihan[1] and Cansu S. Pirinççi[2]*

[1]Department of Therapy and Rehabilitation, Selcuk University, Vocational School of Health Sciences, Konya; [2]Department of Cardiopulmonary Physiotherapy and Rehabilitation, Gulhane Physiotherapy and Rehabilitation Faculty, University of Health Sciences, Ankara. Turkey

Abstract

Objective: *This study evaluates the acute therapeutic effect of manual lymphatic drainage (MLD).* **Method:** *Eighty-two individuals (164 upper limbs) participating in the study were divided into two groups: MLD and sham. Before and after treatment, measurements of pressure pain threshold (PPT), pain tolerance, muscle strength (using a hand dynamometer and pinchmeter), and two-point discrimination (2PD) with an esthesiometer were conducted.* **Results:** *Age, height, weight, body mass index, gender, and dominant extremity of the participants showed similar characteristics ($p > 0.05$). There was a difference hypothenar PPT ($p = 0.038$) and pain tolerance ($p = 0.009$), thenar PPT ($p = 0.021$) and pain tolerance ($p = 0.001$), mid-ulnar PPT ($p = 0.028$), biceps PPT ($p < 0.001$), pain tolerance ($p < 0.001$), and grip strength ($p = 0.030$) between the groups after the therapy. When comparison was made between the groups at baseline and after the treatment all were found to differ ($p < 0.05$).* **Conclusions:** *MLD reduced PPR, pain tolerance, hand grip, and pinch strength in young adults. However, in this population, the distance felt in 2PD evaluation with MLD decreased.*

Keywords: *Manual lymphatic drainage. Pain threshold. Pain tolerance. Tactile sense. Muscle strength.*

Resumen

Objetivo: *Este estudio evalúa el efecto terapéutico agudo del drenaje linfático manual (DLM).* **Método:** *Ochenta y dos individuos (164 miembros superiores) que participaron en el estudio se dividieron en dos grupos: DLM y DLM simulado. Antes/después del tratamiento, mediciones de umbral de dolor por presión (PPT) y tolerancia al dolor, mediciones de fuerza muscular con dinamómetro de mano y pinchómetro, y evaluación de discriminación de dos puntos (2PD) con un estesiómetro.* **Resultados:** *La edad, talla, peso, índice de masa corporal, sexo y extremidad dominante de los participantes mostraron características similares ($p > 0.05$). Hubo diferencia entre PPT hipotenar ($p = 0.038$) y tolerancia al dolor ($p = 0.009$), PPT tenar ($p = 0.021$) y tolerancia al dolor ($p = 0.001$), PPT mediocubital ($p = 0.028$), PPT de bíceps ($p < 0.001$) y tolerancia al dolor ($p < 0.001$), fuerza de agarre ($p = 0.030$) entre los grupos después de la terapia. Cuando se hizo la comparación entre los grupos al inicio y después del tratamiento, se encontró que todos diferían ($p < 0.05$).* **Conclusiones:** *El DLM redujo la PPT, la tolerancia al dolor, el agarre manual y la fuerza de pellizco en adultos jóvenes. Sin embargo, en esta población, la distancia sentida en la evaluación 2PD con DLM disminuyó.*

Palabras clave: *Drenaje linfático manual. Umbral del dolor. Tolerancia al dolor. Sentido táctil. Fuerza muscular.*

***Correspondence:**
Emine Cihan
E-mail: pteminecihan@gmail.com

Date of reception: 05-03-2024
Date of acceptance: 09-10-2024
DOI: 10.24875/CIRU.24000129

Cir Cir. 2025;93(2):181-189
Contents available at PubMed
www.cirugiaycirujanos.com

Introduction

Manual lymphatic drainage (MLD), one of the components of complex decongestive physiotherapy, is a gentle massage technique with proven positive effects on lymphatic circulation. MLD can be applied to different parts of the body (e.g., arms, legs, neck, abdomen, and trunk), with a different technique for each region (stationary circle, scoop, pump, and rotary)[1]. It has disease-specific application principles, and its efficacy can be further increased by respiration[2]. MLD is effective in mobilizing lymph fluid, promoting lymphangiomotor activity and venous return, and supporting the immune system. With these effects, MLD has been proven to reduce edema in the extremities[3].

Although the efficacy of MLD is frequently investigated in patients with lymphedema/chronic venous insufficiency, it has been reported that this application has different effects on the body other than edema reduction in different patient populations and healthy individuals[4-6].

Various studies conducted with different populations have shown that soft touch activates different receptors on the skin through, not only increases stimulation in nerve endings but also activates inhibitory nerve endings, causes changes in tactile sensation, provides the activation of the parasympathetic system, increases muscle strength, results in changes in systolic and diastolic blood pressure, and reduces heart rate[7,8].

However, it is not known whether these effects are due to the MLD technique or the general therapeutic effectiveness of soft touches. Explaining the effects of MLD in every aspect can provide more effective management of the technique on diseases and pave the way for its use in different areas. Therefore, its effects on healthy individuals need to be known and defined. In this study, the effects of MLD technique and random soft touches on pain threshold, pain tolerance, muscle strength, and tactile sense were investigated.

Method

Patients and study protocol

Ninety-six healthy individuals participated in this 2-arm randomized controlled study. Fourteen individuals that used corticosteroid drugs within the past 2 months, and a further five that did not accept to participate in the study were excluded from the study. As a result, 82 (MLD group: 41, sham group: 41) volunteers were included in the study that November 2023.

The participants were randomly divided into two groups as the study and sham groups. The randomization procedure was performed using a coin toss. The participants were blinded to the group allocation. Ethical approval was obtained from the Non-Pharmaceutical and Medical Device Research Ethics Committee of blinded (decision number: blinded), and the study was conducted in accordance with the principles of the Declaration of Helsinki. Individuals were explained about the measurements and the reason for the study. Consent forms were obtained. It was explained to the participants that if they wanted to leave the study, they could leave the study at any time. The patients' demographic data were questioned. MLD application was made by lymphedema physiotherapist. The research was conducted in the physiotherapy course laboratory at Selcuk University.

This is prospective randomized controlled study and randomization was carried out by a different researcher Cansu Sahbaz Pirinççi (CSP), who did not apply the intervention, using a computer program. A researcher (EC) performed the assessments and treatments in this study. The participants were blinded to the group allocation.

Age, gender, height, weight, body mass index (BMI), and dominant extremity were recorded. MLD was applied to both extremities of the participants (a total of 164 upper extremities). Before and after MLD, the same physiotherapist performed pressure pain threshold (PPT) measurements, hand dynamometer (Jamar) and pinchmeter evaluations (Baseline), and tactile sensation evaluation with an esthesiometer.

Inclusion criteria

- Being aged 18-30 years
- Did not have any communication disorders.

Exclusion criteria

- Having any skin disease
- Having a history of neurological and/or orthopedic disease
- Having a significant scar or burn tissue in the upper extremity
- Having any condition that would prevent communication
- Steroid users.

Procedures

Manual Lymphatic Drainage (MLD)

MLD was limited to the upper extremities. During the MLD application, when the volunteers were in the supine hook position, blood hemodynamics and lower extremity motor function were increased through active bilateral shoulder rotation combined with breathing after first effleurage. Cervical lymph nodes were stimulated. The suction power in the thoracic duct was increased with breathing exercises. After the stimulation of central lymph nodes, the axillo-axillary collateral path was activated by stimulating the axillary lymph nodes in the contralateral region, and axillo-inguinal lymph nodes were activated by stimulating inguinal lymph nodes in the ipsilateral region. Then, upper extremity drainage was applied to the participants in this position. Following the drainage of the proximal part of the upper extremity, it was distally proceeded. The lymph fluid was drained by returning from the distal to the proximal and moved to axillary and inguinal lymph nodes through collateral pathways. The MLD session took an average of 30 min for each volunteer[9].

Sham Manual Lymphatic Drainage (MLD)

Similar to the MLD group, the physiotherapist applied random soft touches to similar areas. The touches were not in the order appropriate to any manual technique. Treatment duration and frequency for individuals in the sham MLD group were quite similar to their counterparts in the MLD group.

Outcome measures

Pressure Pain Threshold (PPT) and pain tolerance measurement

Quantitative PPT measurements were performed using a 1-cm^2 surface algometer (Baseline, USA), which was found to be valid and reliable by previous studies[10]. This algometer consists of a metal piston attached to a dial that can measure pressure in kilograms (kg) and pounds (Lb). The algometer was positioned vertically and placed on the thenar, hypothenar, mid-ulnar, and biceps regions using the marked points. Measurements were repeated 3 times with a rest period of 10 s. The average of these three measurements was used for analysis. Pain tolerance was measured once at the same points. The highest tolerable pressure was used in the measurement and it was recorded.

Evaluation of hand and finger grip strength

The Jamar dynamometer recommended by the American Association of Hand Therapists was used to measure hand grip strength. A pinchmeter (Baseline) was used to measure finger grip strength. Hand grip and finger grip strength was measured using the recommended standard position, with the patients sitting, with their shoulders in adduction, elbows in 90° flexion and mid-rotation, and wrists in neutral position. Three measurements were made at 1-min intervals, and the average values were recorded[11,12].

Two-point discrimination (2PD)

This evaluation was performed using an esthesiometer (Instrument Company, Lafayette, IN, USA), with the participants in the sitting position with their eyes closed. Evaluation was made from the biceps medial to the elbow[13]. Starting from the range where two points could be easily distinguished, the distance between the two points was reduced in 1-mm increments until the two points were felt as one point. Then, starting with two-point stimulation at the minimum interval that was felt as a single point, the distance between the two points was increased in 1-mm intervals until the distance between the two points was felt separately as two points again. The contact time of the two-point stimulation was adjusted to be approximately 1-2 s, and approximately 3-5 s was waited between each stimulation. The shortest distance felt between two points provided the static 2PD value.

Statistical analysis

G*Power software package (G*Power, Version 3.0.10, Franz Faul, Universität Kiel, Germany) was used to calculate the sample size. Ten participants from each group were randomly recruited for the pilot study. The effect size corresponding to this value was 0.632. It was calculated that to achieve 80% power with α = 0.05 type I error, 41 patients were required for each group. Frequency tables and descriptive statistics were used to interpret the findings. The conformity of the variables to the normal distribution was examined using visual (histogram and probability graphs) and analytical (Shapiro-Wilk test) methods.

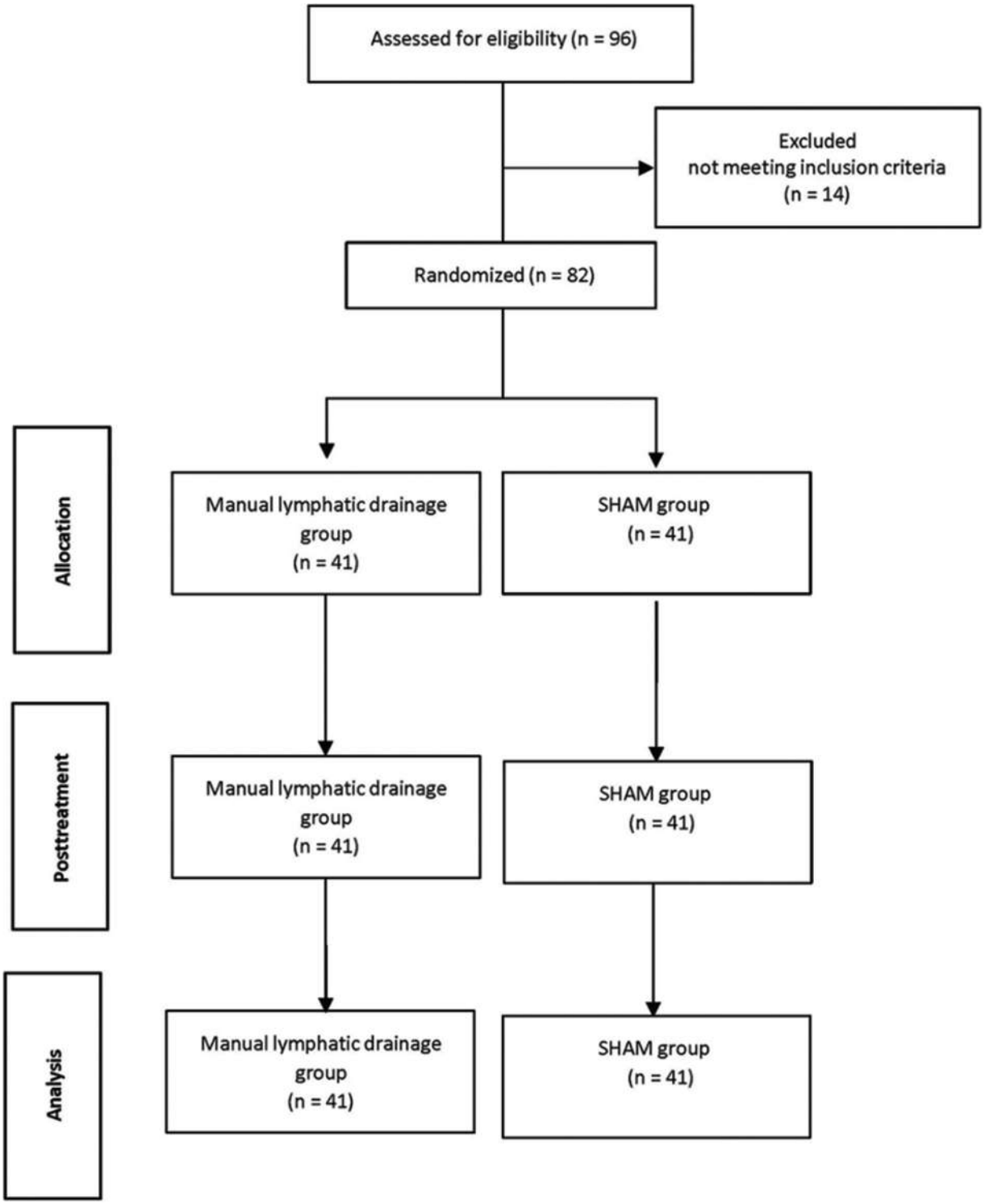

Figure 1. *CONSORT flow diagram.*

Related-samples t-test (Wilcoxon test) was used to evaluate the parameters that did not show a normal distribution and the paired-samples t-test was used to evaluate the parameters with a normal distribution within the groups. In the intergroup evaluations, Mann-Whitney U-test was used for the data that did not show normal distribution. The effect size (d) was calculated by Cohen's guidelines. In all statistics,

Table 1. Demographic data of the participants

Variables	MLD Group (n = 41)		Sham group (n = 41)		x^2, z	p
	X ± SD	n (min-max)	X ± SD (n = 41)	n (min-max)		
Age (years)	20.07 ± 1.52	20 (18-24)	19.97 ± 1.90	19 (18-25)	–0.919	0.358
Height (cm)	166.61 ± 8.05	165 (153-186)	169.73 ± 7.87	168 (158-186)	–1.779	0.075
Weight (kg)	64.27 ± 12.11	62 (42-95)	63.43 ± 13.69	65 (45-89)	–0.605	0.545
BMI (kg/m^2)	23.02 ± 3.12	22.67 (17.94-31.02)	21.78 ± 3.15	21.95 (18-28.41)	–1.648	0.099
	n	%	n	%		
Gender						
Male	14	34.1	20	48.8	1.809	0.179
Female	27	65.9	21	51.2		
Dominant extremity						
Right	33	80.5	28	68.3	1.6	0.206
Left	8	19.5	13	31.7		

cm: centimeter; kg: kilogram; m: meter; X: mean; SD: standard deviation; n: number of participants; min: minimum; max: maximum; %: percentage; BMI: body mass index.

p significance value was accepted as $p < 0.05$. Statistical analyses were performed using IBM SPSS Statistics version 24.0 package 61 (IBM Corp. Released 2016. IBM SPSS Statistics for Windows, Version 24.0. Armonk, NY: IBM Corp.).

Results

A total of 82 (MLD group: 41, Sham group: 41) people participated in the study. No side effects were observed in participant during and after application. There was no loss during the study (Fig. 1). Age, height, weight, BMI, gender, and dominant extremity of the participants showed similar characteristics ($p > 0.05$). Changes of the participant's demographic data are shown in table 1.

In the comparison between the groups, all the parameters were similar before the therapy ($p > 0.05$). There was a difference hypothenar PPT ($p = 0.038$) and pain tolerance ($p = 0.009$), thenar PPT ($p = 0.021$) and pain tolerance ($p = 0.001$), mid-ulnar PPT ($p = 0.028$), biceps PPT ($p < 0.001$), and pain tolerance ($p < 0.001$) between the groups after the therapy. In the MLD group, all parameters changed after the treatment ($p < 0.05$). In SHAM group, hypothenar PPT ($p = 0.008$), mid-ulnar pain tolerance ($p = 0.007$), and biceps pain tolerance ($p = 0.005$) changed after the treatment. Changes in PPT and pain tolerance are shown in table 2.

In the comparison between the groups, all the parameters were similar before the treatment ($p > 0.05$). There was a difference grip strength ($p = 0.030$) between the groups after the treatment. In the MLD group, all parameters changed after the treatment ($p < 0.05$). In SHAM group, grip strength ($p = 0.008$ changed after the treatment. Changes in muscle strength and 2PD are shown in table 3.

When comparison was made between the groups at baseline and after the treatment all were found to differ (Table 4).

Discussion

On completion of the study, we conducted with healthy young adults, we found that MLD caused a decrease in PPT and pain tolerance, reduced grip and pinch strength, and increased their tactile sensation in 2PD.

MLD is part of complex decongestive therapy, which is considered as the gold standard in the treatment of lymphedema[14]. In the past decade, the efficacy of MLD on edema and pain has been investigated in different patient groups. In a study including MLD in exercise therapy for complex regional pain syndrome, Uher et al. reported that MLD improved pain, edema, and range of motion, but the results were similar to the exercise-only group[15]. Similarly, Kim (2014) found that MLD had a curative effect on pain, but this was not statistically significant. The author also noted that PPT significantly increased after MLD treatment[8]. There are also studies showing that the increase in PPT and pain tolerance has clinical significance[16].

The effect of MLD on pain can be explained by different theories: MLD nociceptive receptors can increase parasympathetic responses by reducing

Table 2. Changes in PPT and pain tolerance

Variables	Variables	MLD Group (n = 82)		Sham group (n = 82)		z	p	d
		Mean ± SD	Median (min-max)	Mean ± SD	Median (Min-Max)			
Hypothenar	BT-PPT	6.54 ± 2.28	6 (3-14)	6.06 ± 2.49	6 (3-12)	−1.828	0.068	
	AT-PPT	5.60 ± 2.27	5 (2-13)	6.40 ± 2.48	6 (3-12)	−2.075	0.038	0.336
	t, z		−3.301		−2.668			
	p		0.001		0.008			
	d		0.413		0.136			
	BT-pain tolerance	10.82 ± 5.13	10 (3-30)	10.34 ± 4.82	9.75 (5-30)	−0.670	0.503	
	AT-pain tolerance	8.62 ± 3.37	8 (2-17)	10.73 ± 5.22	10 (3-30)	−2.621	0.009	0.480
	t, z		−4.496		−1.178			
	p		< 0.001		0.239			
	d		0.057		0.077			
Thenar	BT-PPT	6.54 ± 2.72	6 (2-15)	6.13 ± 2.12	6 (2-14)	−0.678	0.498	
	AT-PPT	6.52 ± 7.22	5 (2-55)	6.16 ± 2.11	6 (2-14)	−2.300	0.021	0.067
	t, z		−3.174		−1.633			
	p		0.002		0.102			
	d		0.003		0.014			
	BT-Pain tolerance	9.43 ± 3.95	8.75 (4-25)	9.18 ± 3.37	8.75 (4-20)	−0.187	0.852	
	AT-Pain tolerance	7.29 ± 2.74	7 (2-16)	9.07 ± 3.40	8.5 (4-20)	−3.383	0.001	0.576
	t, z		−4.885		−1.807			
	p		< 0.001		0.071			
	d		0.629		0.032			
Mid-Ulnar	BT-PPT	5.77 ± 2.18	5 (1-13)	5.54 ± 1.92	5 (1-12)	−0.577	0.564	
	AT-PPT	5 ± 1.80	5 (2-13)	5.44 ± 1.93	5 (1-12)	−2.193	0.028	0.235
	t, z		−2.795		−1.841			
	p		0.005		0.066			
	d		0.385		0.051			
	BT-Pain tolerance	8.68 ± 3.04	8 (4-16)	8.21 ± 2.85	8 (4-15)	−1.049	0.294	
	AT-Pain tolerance	7.55 ± 2.72	7 (2-15)	7.90 ± 2.67	8 (4-15)	−0.791	0.429	0.129
	t, z		−3.620		−2.692			
	p		< 0.001		0.007			
	d		0.391		0.112			
Biceps	BT-PPT	5.22 ± 1.66	5 (2-10)	5.49 ± 1.77	5 (2-12)	−0.89	0.373	
	AT-PPT	4.36 ± 1.62	4 (1-9)	5.30 ± 1.86	5 (2-12)	−3.751	< 0.001	0.538
	t, z		−4.178		−1.897			
	p		< 0.001		0.058			
	d		2.626		0.104			

(Continues)

Table 2. Changes in PPT and pain tolerance *(continued)*

Variables	Variables	MLD Group (n = 82)		Sham group (n = 82)		z	p	d
		Mean ± SD	Median (min-max)	Mean ± SD	Median (Min-Max)			
	BT-Pain tolerance	7.82 ± 2.79	7.75 (3-15)	8.06 ± 2.74	8 (3.5-15)	–0.556	0.578	
	AT-Pain tolerance	5.89 ± 2.46	5 (2-13)	7.71 ± 2.80	8 (3.5-15)	–4.201	< 0.001	3.341
	t, z		–5.282		–2.823			
	p		< 0.001		0.005			
	d		0.733		0.126			

BT: before treatment; AT: after treatment; PPT: pressure pain threshold; MLD: manual lymph drainage; X: mean; SD: standard deviation; n: number of extremities; min: minimum; max: maximum; p < 0.05.

Table 3. Changes in muscle strength and two-point discrimination

Variables	MLD Group (n = 82)		Sham Group (n = 82)		z	p	d
	Mean ± SD	Median (min-max)	Mean ± SD	Median (min-max)			
BT-Grip strength	29.20 ± 9.68	26.6 (16.3-58.3)	28.36 ± 9.70	26.45 (11-55)	–0.406	0.685	
AT-Grip strength	25.70 ± 9.31	21.6 (10-46)	28.06 ± 9.55	25.80 (11-55)	–2.169	0.030	0.250
t, z		–6.738		–2.668			
P		< 0.001		0.008			
D		0.368		0.031			
BT-Pinch Strength	4.34 ± 1.71	4.1 (1.6-9.6)	4.19 ± 1.70	4 (1.6-9)	–0.628	0.530	
AT-Pinch Strength	3.84 ± 1.47	3.55 (1.5-7.6)	4.04 ± 1.73	3.6 (1.6-9)	–0.313	0.754	0.124
t, z		–3.375		–1.728			
P		0.001		0.084			
D		0.340		0.087			
BT-Two-point discrimination	13.97 ± 2.10	15 (1-15)	13.59 ± 2.35	14 (1-15)	–1.452	0.146	
AT-Two-point discrimination	13.54 ± 1.84	14 (8-18)	13.85 ± 1.37	14 (9-15)	–0.703	0.482	0.191
t, z		–2.563		–0.885			
P		0.010		0.376			
D		0.217		0.135			

BT: before treatment; AT: after treatment; MLD: manual lymph drainage; X: mean; SD: standard deviation; n: number of extremities; min: minimum; max: maximum; p < 0.05.

sympathetic nervous system activation through rhythmic stimulation. According to the gate control theory of pain, MLD can reduce the activity of A delta and C fibers through the soft touches that it contains or it can regulate pain intensity by helping increase neurotransmitter release[8,17,18].

Contrary to the literature, in the present study, we found that MLD caused a significant decrease in PPT and pain tolerance. This may be due to the criteria that we used in sample selection. We only included individuals with a pain level of < 1 according to the Visual Analog Scale, which may actually be evidence that the pain-reducing mechanisms of these individuals were deactivated. We consider that this mechanism of action of MLD on pain has not yet been explained.

The results we obtained from the 2PD evaluation indicate that MLD may have increased sensitivity in fibers carrying pressure sensation. Static 2PD assessment tests the slowly adapting type I afferent Aβ fiber system in the skin and is received by Merkel receptors.

Table 4. Comparison of differences between groups at baseline and after treatment

Variables	MLD group (n = 82)		Sham group (n = 82)		z	p	d
	Mean ± SD	Median (Min-Max)	Mean ± SD	Median (Min-Max)			
Hypotenar PPT	−0.93 ± 2.67	−1 (−9-6.5)	0.34 ± 1.11	0 (0-5.5)	−5.161	< 0.001	0.621
Hypotenar pain tolerance	−2.20 ± 4.51	−2 (−20-7)	0.39 ± 2.89	0 (−2-25)	−5.858	< 0.001	0.683
Thenar PPT	−0.02 ± 7.50	−1 (−10-49)	0.03 ± 0.16	0 (0-1)	−4.09	< 0.001	0.009
Thenar pain tolerance	−2.14 ± 3.91	−2 (−19-4)	−0.10 ± 0.54	0 (−3-1)	−4.893	< 0.001	0.730
Mid-ulnar PPT	−0.77 ± 2.21	−1 (−7-4)	−0.09 ± 0.51	0 (−4-0)	−2.551	0.011	0.423
Mid-ulnar pain tolerance	−1.13 ± 2.57	−1 (−9-4)	−0.31 ± 0.97	0 (−4-0)	−2.561	0.010	0.422
Biceps PPT	–	−1 (−6-4)	−0.18 ± 0.91	0 (−5-1.5)	−4.188	< 0.001	0.474
Biceps pain tolerance	−1.93 ± 2.72	−2 (−9-5)	−0.34 ± 1.03	0 (−5-0)	−5.631	< 0.001	0.773
Grip strength	−3.50 ± 4.13	−2.65 (−17-8)	−0.30 ± 0.99	0 (−6-0)	−7.771	< 0.001	1,06
Pinch strength	−0.49 ± 1.31	−0.3 (−5-2.9)	−0.15 ± 0.79	0 (−3.5-2)	−3.24	0.001	0.314
Two-point discrimination	−0.42 ± 2.67	0 (−7-13)	0.26 ± 1.64	0 (−2-8)	−2.797	0.005	0.306

PPT: pressure pain threshold; MLD: manual lymph drainage; X: mean; SD: standard deviation; n: number of extremities; min: minimum; max: maximum; p < 0.05.

While only myelinated thick afferents were previously considered to be tactile sensory receptors, recent studies have shown that C fibers also contribute to tactile sensation. These are unmyelinated low-threshold C afferents that respond strongly to the pleasant sensation caused by a light and soft touch[19]. C afferents carrying delayed pain[20] may make the skin sensitive to touch by acting as tactile receptors for pleasant touches in the absence of pain. Thus, increased tactile sensitivity may heighten the "pressure"[21] factor based on the working mechanism of the algometer. We consider that in painless and healthy tissue that becomes sensitive to pressure, this may cause a decrease in PPT and pain tolerance.

MLD generally provides an increase in muscle strength when used in cases that develop lymphedema after cancer. An increase in muscle strength with increased function as a result of reduced edema is an expected result[11]. It has been reported that MLD supports the regeneration of muscle strength in the post-exercise period in athletes engaged in Far Eastern sports, MLD has been suggested to be one of the important elements of therapeutic methods to reduce the risk of injury[22]. However, these studies reporting improvement in muscle strength performed evaluations in the regeneration period. In studies investigating classical massage applications, massage is not recommended before performance because it may reduce performance in activities, such as sprinting and vertical jumping, that require muscle strength[23]. Massage, whether superficial or deep, affects neuromotor and neuromuscular components and changes the internal tension of structures[24]. In our study, grip and pinch strength significantly decreased after MLD, which may be due to the reaction of muscles to changes in internal tension or the increase in muscle relaxation as a result of heightened parasympathetic responses with the suppression of the sympathetic system[8]. Increased parasympathetic activity may have caused a decrease in readiness for action.

Conclusion

MLD applied to healthy individuals causes a decrease in muscle strength. However, it enhances tactile sensation and results in increased sensitivity in 2PD. It reduces PPT and pain tolerance. In this case, MLD can be thought that the activity in pain and sensory receptors increases. The decrease in muscle strength emphasizes the reducing effect of MLD on the internal tension of the muscle. Based on these findings, the clinical usage areas of MLD can be rearranged.

Limitations

Due to the similar ages of the participants, we only evaluated a certain age group. The use of this method in different populations may show age-related variations

in terms of efficacy. In addition, laboratory studies should be included in the future to make the results more objective.

Funding

The authors declare that they have not received funding.

Conflicts of interest

The authors declare no conflicts of interest.

Ethical considerations

Protection of humans and animals. The authors declare that the procedures followed complied with the ethical standards of the responsible human experimentation committee and adhered to the World Medical Association and the Declaration of Helsinki. The procedures were approved by the institutional Ethics Committee.

Confidentiality, informed consent, and ethical approval. The authors have obtained approval from the Ethics Committee for the analysis of routinely obtained and anonymized clinical data, so informed consent was not necessary. Relevant guidelines were followed.

Declaration on the use of artificial intelligence. The authors declare that no generative artificial intelligence was used in the writing of this manuscript.

Ethical approval

The study was approved by the Non-Pharmaceutical and Medical Device Research Ethics Committee of Konya Chamber of Commerce Karatay University (decision number: 2022/009)

References

1. Johnson G. Dr Vodder's manual lymph drainage. A practical guide. NZJ Physiother. 2011;39:103-4.
2. Bakar Y, Berdici B, Şahin N, Pala ÖO. Lymphedema after breast cancer and its treatment. J Breast Health. 2014; 10: 6-14.
3. Ezzo J, Manheimer E, McNeely ML, Howell DM, Weiss R, Johansson KI, et al. Manual lymphatic drainage for lymphedema following breast cancer treatment. Cochrane Database Syst Rev. 2015;2015:CD003475.
4. Provencher AM, Giguere-Lemieux E, Croteau E, Ruchat SM, Corbin-Berrigan LA. The use of manual lymphatic drainage on clinical presentation of musculoskeletal injuries: A systematic review. Complement Ther Clin Pract 2021;45:101469.
5. Pichonnaz C, Bassin JP, Lécureux E, Christe G, Currat D, Aminian K, et al. Effect of manual lymphatic drainage after total knee arthroplasty: a randomized controlled trial. Arch Phys Med Rehabil. 2016;97:674-82.
6. Ekici G, Bakar Y, Akbayrak T, Yuksel I. Comparison of manual lymph drainage therapy and connective tissue massage in women with fibromyalgia: a randomized controlled trial. J Manipulative Physiol Ther. 2009;32:127-33.
7. Schingale FJ, Esmer M, Küpeli B, Ünal D. Investigation of the less known effects of manual lymphatic drainage: a narrative review. Lymphat Res Biol. 2022;20:7-10.
8. Kim SJ. Effects of manual lymph drainage on the activity of sympathetic nervous system, anxiety, pain, and pressure pain threshold in subjects with psychological stress. Phys Ther Korea. 2014;26:391-7.
9. Földi M, Földi E, Ströβenreuther R, Kubik S. Földi's Textbook of Lymphology: for Physicians and Lymphedema Therapists. Netherlands: Elsevier Health Sciences; 2012.
10. Reeves JL, Jaeger B, Graff-Radford SB. Reliability of the pressure algometer as a measure of myofascial trigger point sensitivity. Pain. 1986;24:313-21.
11. Cho Y, Do J, Jung S, Kwon O, Jeon JY. Effects of a physical therapy program combined with manual lymphatic drainage on shoulder function, quality of life, lymphedema incidence, and pain in breast cancer patients with axillary web syndrome following axillary dissection. Support Cancer Ther. 2016;24:2047-57.
12. Halpern CA, Fernandez JE. The effect of wrist and arm postures on peak pinch strength. J Hum Ecol (Tokyo). 1996;25:115-30.
13. Han J, Park S, Jung S, Choi Y, Song H. Comparisons of changes in the two-point discrimination test following muscle fatigue in healthy adults. J Phys Ther Sci. 2015;27:551-4.
14. Zasadzka E, Trzmiel T, Kleczewska M, Pawlaczyk M. Comparison of the effectiveness of complex decongestive therapy and compression bandaging as a method of treatment of lymphedema in the elderly. Clin Interv Aging. 2018;13:929-34.
15. Uher EM, Vacariu, Schneider B, Fialka V. Comparison of manual lymph drainage with physical therapy in complex regional pain syndrome, type I. A comparative randomized controlled therapy study. Wien Klin Wochenschr. 2000;112:133-7.
16. Keser I, Esmer M. Does manual lymphatic drainage have any effect on pain threshold and tolerance of different body parts? Lymphat Res Biol. 2019;17:651-4.
17. Priganc VW, Ito MA. Changes in edema, pain, or range of motion following manual edema mobilization: a single-case design study. J Hand Ther. 2008;21:326-35.
18. Cihan E, Yildirim NÜ, Bilge O, Bakar Y, Doral M. Outcomes with additional manual lymphatic drainage to rehabilitation protocol in primary total knee arthroplasty patients: preliminary clinical results. SDÜ Sağlık Bilimleri Derg. 2021;12:319-29.
19. Olausson H, Wessberg J, McGlone F, Vallbo Å. The neurophysiology of unmyelinated tactile afferents. Neurosci Biobehav Rev. 2010;34:185-91.
20. Koga K, Furue H, Rashid MH, Takaki A, Katafuchi T, Yoshimura M. Selective activation of primary afferent fibers evaluated by sine-wave electrical stimulation. Mol Pain. 2005;1:1-11.
21. Manafi-Khanian B, Arendt-Nielsen L, Frøkjær JB, Graven-Nielsen T. Deformation and pressure propagation in deep somatic tissue during painful cuff algometry. Eur J Pain. 2015;19:1456-66.
22. Zebrowska A, Trybulski R, Roczniok R, Marcol W. Effect of physical methods of lymphatic drainage on postexercise recovery of mixed martial arts athletes. Clin J Sport Med. 2019;29:49-56.
23. Mine K, Lei D, Nakayama T. Is pre‐performance massage effective to improve maximal muscle strength and functional performance? A systematic review. Int J Sports Phys Ther. 2018;13:789-99.
24. Abrantes R, Nunes S, Monteiro E, Fiuza A, Cesar Cunha J, Ribeiro M, et al. Massage acutely increased muscle strength and power force. J Exerc Physiol Online. 2019;22:100-9.

ORIGINAL ARTICLE

Evaluation of the presence of sarcopenia and the relationship with disease activity in fibromyalgia

Evaluación de la presencia de sarcopenia y su relación con la actividad de la enfermedad en la fibromialgia

Pınar Ö. Başaran and Dilek E. Büyükşireci*

Department of Physical Medicine and Rehabilitation, Hitit University Erol Olçok, Education and Research Hospital, Çorum, Turkey

Abstract

Objective: *The objective of this study was to investigate the presence of sarcopenia in fibromyalgia and whether there is any relationship between physical performance, disease activity, pain levels, and the existence of sarcopenia.* **Method:** *Fifty female patients diagnosed with fibromyalgia syndrome (FMS) based on the classification criteria of the 2016 American College of Rheumatology and 50 healthy controls were admitted. Disease activity was evaluated with the Fibromyalgia Impact Questionnaire (FIQ) and pain level was evaluated with the Numerical Rating Scale. Sarcopenia was screened by the SARC-F questionnaire and the presence of sarcopenia was evaluated according to ISarcoPRM criteria. Furthermore, right-hand grip strength was evaluated with a dynamometer. Ultrasound was used to measure the anterior thigh muscle thickness on the quadriceps femoris.* **Results:** *SARF-C scores were significantly higher in patients with FMS ($p < 0.001$). The presence of sarcopenia was found as 20 (40%) in FMS patients and 6 (12%) in healthy controls ($p < 0.001$). Right-hand grip strength was significantly different in patients with FMS ($p = 0.007$). Right anterior thigh muscle thickness was similar in the two groups ($p = 0.875$). A positive correlation was observed between FIQ score and SARF-C score in FMS patients with sarcopenia ($r = 0.708$, $p < 0.001$).* **Conclusion:** *Sarcopenia was thought of as a common problem in patients with FMS. Evaluating sarcopenia in patients with FMS could enhance the effectiveness of FMS treatment.*

Keywords: *Disease activity. Fibromyalgia. Sarcopenia. Ultrasonography.*

Resumen

Objetivo: *Investigar la presencia de sarcopenia en la fibromialgia y si existe alguna relación entre el rendimiento físico, la actividad de la enfermedad, los niveles de dolor y la existencia de sarcopenia.* **Método:** *Ingresaron 50 mujeres diagnosticadas de síndrome de fibromialgia (SFM) según los criterios de clasificación del American College of Rheumatology de 2016 y 50 mujeres sanas como controles. La actividad de la enfermedad se evaluó con el Fibromyalgia Impact Questionnaire (FIQ) y el nivel de dolor con la Numerical Rating Scale. La sarcopenia se detectó mediante el cuestionario SARC-F y su presencia se evaluó según los criterios ISarcoPRM. También se evaluó la fuerza de prensión de la mano derecha con un dinamómetro. Se utilizó ecografía para medir el grosor muscular de la cara anterior del muslo en el cuádriceps femoral.* **Resultados:** *Las puntuaciones SARC-F fueron significativamente mayores en las pacientes con SFM ($p < 0.001$). Se detectó presencia de sarcopenia en 20 (40%) de las pacientes con SFM y en 6 (12%) de las controles sanas ($p < 0.001$). La fuerza de prensión de la mano derecha fue significativamente diferente en las pacientes con SFM ($p = 0.007$). El grosor del músculo anterior derecho del muslo fue similar en los dos grupos ($p = 0.875$). Se observó una correlación positiva entre las puntuaciones FIQ y SARC-F en las*

***Correspondence:**
Pınar Ö. Başaran
E-mail: pinarozge@yahoo.com

Date of reception: 26-06-2024
Date of acceptance: 08-12-2024
DOI: 10.24875/CIRU.24000354

Cir Cir. 2025;93(2):190-196
Contents available at PubMed
www.cirugiaycirujanos.com

pacientes con SFM y sarcopenia (r = 0.708; p < 0.001). **Conclusiones:** *La sarcopenia se consideró un problema común en las pacientes con SFM. La evaluación de la sarcopenia en pacientes con SFM podría mejorar la eficacia del tratamiento del SFM.*

Palabras clave: *Actividad de la enfermedad. Fibromialgia. Sarcopenia. Ultrasonografía.*

Introduction

Fibromyalgia syndrome (FMS) is a chronic rheumatic condition characterized by numerous symptoms, including tenderness in specific areas of the body, reduced pain threshold, fatigue, psychological issues, and sleep disturbances[1]. FMS affects approximately 2% of the general population, predominantly middle-aged women[2]. In a study conducted with 1930 females in Türkiye, the prevalence of fibromyalgia was found to be 3.6%[3]. Patients were diagnosed with FMS based on the 2016 diagnostic criteria established by the American College of Rheumatology (ACR)[4]. The etiology and pathogenesis of FMS are not fully known. Furthermore, genetic disorders, and causal factors such as the occurrence of trauma, the inflammation process, mental stress, and infections may change the neuroendocrine mechanisms related to pain or can trigger deterioration[5].

Sarcopenia is characterized as a progressive and generalized musculoskeletal disorder involving accelerated muscle mass decline and functional impairment[6]. It is a relatively uncommon condition in the musculoskeletal spectrum. The European Working Group on Sarcopenia in Older People (EWGSOP)[6] established a consensus definition and clinical diagnostic criteria for sarcopenia in 2010, later updated as EWGSOP2 in January 2019[7]. There is limited research exploring the association between fibromyalgia and sarcopenia. Within the International Society of Physical and Rehabilitation Medicine (ISPRM) framework, Kara et al.[8] determine the diagnostic algorithm for sarcopenia (ISarcoPRM). And also Kara et al.[9] used the ultrasonographic evaluation to clarify the diagnoses of sarcopenia.

Because of widespread body pain, physical activity level decreases in FMS. A small number of studies in the literature have examined the relationship between fibromyalgia and sarcopenia[10,11]. Our study aims to explore the prevalence of sarcopenia in fibromyalgia patients using the new ISarcoPRM criteria and to investigate potential correlations between physical performance, disease activity, pain levels, and sarcopenia presence.

Method

This cross-sectional study was conducted in the Turkish population and included 50 female patients diagnosed with FMS based on the 2016 ACR criteria, along with 50 healthy controls matched for age and sex. The participants were recruited from the Physical Medicine and Rehabilitation outpatient clinic for routine health check-ups, including physical examinations and hemogram measurements, between August 2023 and December 2023. The study received ethical approval from the Local Ethics Committee of the University (decision number 114, 2023) and adhered to the principles of the Declaration of Helsinki. All participants provided informed consent before enrollment, and they were thoroughly briefed about the study protocol.

Female subjects between 25-65 years old, diagnosed with fibromyalgia for at least 6 months were included in the study. Patients undergoing physical therapy in the past 3 months, had a history of concomitant rheumatic disease, diabetes mellitus, hypertension, myopathies, diseases that affect ambulation such as lower extremity operations, peripheral or central nervous system disease, severe lung or heart failure, kidney or liver diseases, malignancy, pregnancy or breastfeeding or any psychiatric disorder, and any medications that could influence muscle function, such as steroids were excluded from the study. After the demographic characteristics of the patients were recorded, physical examinations were performed and body mass indexes (BMI) were noted. All evaluations were made by the same physician.

The Fibromyalgia Impact Questionnaire (FIQ) was used to evaluate the disease activity and it comprises ten items organized into three domains: functional, physical symptoms, and mental symptoms. Each item is rated on a scale (0-10), where lower scores indicate better disease activity. Sarmer et al.[12] established the reliability of the FIQ in the Turkish population.

The numerical rating scale (NRS)[13] was employed to evaluate pain levels, where patients rated their pain on a scale from 0 to 10, high scores describe more severe pain.

Sarcopenia was screened by the SARC-F questionnaire[14]. It includes five questions, each question scores 0-2 points. Five domains are rising from chair strength, stair climbing, walking ability, and history of falls. A score of 4 points or higher is indicative of sarcopenia.

The presence of sarcopenia was evaluated according to ISarcoPRM[8]. According to ISarcoPRM diagnostic algorithm for sarcopenia, the first hand grip strength was measured with a Jamar dynamo meter in kilograms (Saehan hydraulic hand dynamometer)[15]. Patients performed the test 3 times with each hand, with 30 s rest between trials then an average of three trials calculated separately for the right and left hands. Results under 19 kg were assessed as probable sarcopenia. Then, anterior thigh muscle thicknesses were evaluated with ultrasonography. Ultrasound was used to measure the anterior thigh muscle thickness on the quadriceps femoris. All measurements were conducted by the same researcher. A multi-frequency probe (6-12 MHz: Philips purewave) was utilized for ultrasound examinations. Participants were positioned supine with legs extended and muscles relaxed, and images were captured midway between the superior border of the patella and the anterior superior iliac spine. Sonographic Thigh Adjustment Ratio (STAR) is already suggested for the diagnosis of sarcopenia[8]. If the ratio was under 1.0 in females, this was accepted as sarcopenia. The presence of sarcopenia was recorded.

Physical performance was assessed with the test of five times sit-to-stand test (FTSST) and usual gait speed with 6 meters walk test (6MWT). At FTSST subjects sit down without touching the back of the chair and stand up fully for 5 times and time was measured in seconds[16]. The 6MWT, a 6-m flat path, was marked on the hospital corridor, participants walked on the path and walking time was measured in seconds[17]. Above 15 s was accepted as a disability according to the ISarcoPRM diagnostic algorithm[8].

Statistical analysis

SPSS for Windows version 16.0 software was used for statistical analysis. The normal distribution of variables was assessed visually and with the Kolmogorov–Smirnov test. Continuous data were presented as mean ± standard deviation or median with interquartile range, while categorical data were summarized as frequencies and percentages. Parametric data were compared using the Student t-test, and non-parametric data using the Mann-Whitney U-test. Correlations between patient characteristics and clinical parameters were evaluated using Spearman and Pearson correlation coefficients. Statistical significance was set at $p < 0.05$

Results

Age, weight, height, and BMI were similar in FMS patients and the control group (Table 1). SARF-C score, 6MWT, and FTSST tests were significantly higher in patients with FMS ($p < 0.001$). The presence of sarcopenia was found as 20 (40%) in FMS patients and 6 (12%) in healthy controls according to ISarcoPRM criteria ($p < 0.001$). Right-hand grip strength was significantly different in patients with FMS ($p = 0.007$). Right anterior thigh muscle thickness is similar in the two groups ($p = 0.875$). FTSST and 6MWT were significantly decreased in FMS patients ($p < 0.001$).

NRS and FIQ scores were not different between FMS patients with sarcopenia and FMS patients without sarcopenia (Table 2). A positive correlation was found between FIQ score and SARF-C score in FMS patients with sarcopenia ($r = 0.708$, $p < 0.001$). However, FIQ score was not correlated with anterior thigh muscle thickness, hand grip strength, 6MWT, and FTSST tests (Table 3).

Discussion

This study revealed an elevated prevalence of sarcopenia among patients with FMS. Although there is no difference in anterior thigh muscle thickness measured by USG, we evaluated a loss in physical performance and hand grip muscle strength in patients with FMS. We identified a correlation between the severity of fibromyalgia symptoms and the presence of sarcopenia.

There are a few studies investigating the frequency of sarcopenia in FMS[11,12]. An important point about our study was that we used the US for diagnosing sarcopenia. Dual X-ray absorptiometry (DXA), magnetic resonance imaging (MRI), computerized tomography (CT), ultrasonography (US), and bio-electrical impedance analysis (BIA) can be used for evaluating muscle mass. In addition to the radiation to which the patient is exposed, specific muscle mass cannot be evaluated by DXA. CT and MRI are the gold standard methods for quantifying muscle mass but they are expensive and time-consuming procedures. The US is portable, easier, and cheaper. Because of that, we used the US

Table 1. Demographic and clinical features of the participants

Patients' characteristics	Fibromyalgia group (n = 50)	Healthy controls (n = 50)	p
Age (year)	46.70 ± 8.78	43.82 ± 8.71	0.103
Height (cm)	156.55 ± 6.51	159.21 ± 6.94	0.051
Weight (kg)	69.6 (64.62-78.52)	67.1 (63.5-75.32)	0.285
BMI (kg/m2)	29.56 ± 4.55	27.77 ± 4.70	0.057
NRS	9 (6-10)		
Fibromyalgia Impact Questionnaire (FIQ)	74.8 (53.96-85.65)		
SARF-C	4.8 ± 2.31	1.40 ± 1.65	***< 0.001***
SARF-C, n (%)	37 (74%)	10 (20%)	***< 0.001***
6MWT (s)	11.64 ± 2.61	7.47 ± 1.43	***< 0.001***
FTSST (s)	14.40 ± 3.56	8.01 ± 1.27	***< 0.001***
Right hand grip strength (kg)	21.02 ± 7.33	24.60 ± 5.37	0.007
Right anterior thigh muscle thickness (mm)	16.3 ± 4.2	16.4 ± 3.5	0.875
Presence of sarcopenia, n (%)	20 (40%)	6 (12%)	0.001

BMI: body mass index; NRS: numeric rating scale; SARF-C: a simple questionnaire to rapidly diagnose sarcopenia; 6MWT: 6 m walk test; FTSST: five times sit-to-stand test. n: number. Numerical data are given as mean ± standard deviation or median (interquartile range) values. p values in bold and italics indicate statistically significant.

Table 2. Clinical features of fibromyalgia patients with sarcopenia and without sarcopenia

Variables	Patients with sarcopenia (n = 20)	Patients without sarcopenia (n = 30)	p
Age	46.85 ± 9.12	46.6 ± 8.7	0.923
NRS	8.20 ± 2.11	7.53 ± 2.37	0.315
Fibromyalgia Impact Questionnaire (FIQ)	76.57 (68.02-89.06)	73.9 (53.32-84.0)	0.373
SARF-C	5.85 ± 2.39	4.10 ± 2.0	***0.007***
6MWT (s)	15.87 ± 3.33	13.43 ± 3.43	***0.016***
FTSST (s)	12.78 ± 2.72	10.89 ± 2.28	***0.011***
Right anterior thigh muscle thickness (mm)	1.68 ± 0.43	1.55 ± 0.41	0.573
Right hand grip strength (kg)	14.1 ± 3.5	25.63 ± 5.2	***< 0.001***

NRS: numeric rating scale; SARF-C: a simple questionnaire to rapidly diagnose sarcopenia; 6MWT: 6 m walk test; FTSST: five times sit-to-stand test; n: number. Numerical data are given as mean ± standard deviation or median (interquartile range) values. p values in bold and italics indicate statistically significant.

for evaluating the muscle mass in our study according to ISarcoPRM criteria.

In a previous study[18], quadriceps femoris muscle mass, evaluated by ultrasonography, was found to be significantly lower in FMS patients. However, this study did not investigate the relationship between muscle mass, muscle strength, and physical performance. In a larger study[19], muscle mass was assessed using BIA, revealing no differences between FMS patients and healthy controls. Our study found similar anterior thigh muscle mass thickness between FMS patients and healthy participants. Despite no observed loss of muscle mass, our research identified reduced muscle strength in patients with FMS. Unlike these two studies, we utilized ultrasound for evaluation, employing a more detailed methodology.

Table 3. Correlation between sarcopenia criteria and clinical features in fibromyalgia patients with sarcopenia

Variables	SARF-C	6MWT (s)	FTSST (s)	Right anterior thigh muscle thickness (mm)	Right hand grip strength (kg)
Age*	r = 0.192 p = 0.418	r = 0.402 p = 0.079	r = 0.405 p = 0.077	r = –0.168 p = 0.479	r = –0.272 p = 0.245
NRS*	r = 0.204 p = 0.389	r = 0.056 p = 0.815	r = 0.401 p = 0.080	r = –0.221 p = 0.348	r = –0.222 p = 0.346
Fibromyalgia Impact Questionnaire (FIQ)	r = ***0.708*** p = ***0.000***	r = 0.132 p = 0.578	r = 0.059 p = 0.806	r = –0.063 p = 0.791	r = –0.100 p = 0.675

SARF-C: a simple questionnaire to rapidly diagnose sarcopenia; 6MWT: 6 m walk test; FTSST: five times sit-to-stand test; NRS: numeric rating scale; *Pearson correlation.
Values in bold and italics indicate statistically significant.

Some studies showed that muscle strength and physical performance reductions were found in FMS patients similar to our study[6,20,21]. These studies also showed a relationship between disease activity and quadriceps femoris muscle strength[21-23]. We found decreased hand grip strength in patients with FMS. However, we did not evaluate the quadriceps femoris muscle strength and we did not find a relationship between hand grip strength and disease activity in our study.

We did not classify patients according to the duration of fibromyalgia diagnosis or age range. Muscle strength may decrease more over time in patients with long-term disease[10]. At the same time, if patients were classified according to their age range, different results related to muscle strength may be obtained. In the previous study, patients with FMS were examined at 10-year age intervals and hand strength decreased significantly every 10 years, although muscle mass remained the same[19]. Devrimsel et al.[23] found higher hand disability scores in patients with FMS than in healthy populations. This shows that the assessment of hand strength is not only useful for screening sarcopenia but also may help to prevent disability. According to the results of our study, it is useful to be vigilant for sarcopenia in FMS patients with low hand grip muscle tests.

The previous study conducted in patients who developed sarcopenia after COVID-19 infection showed that high-intensity exercise increases hand grip strength, physical performance, and quality of life compared to low-intensity exercise[24]. Likewise, in the previous studies, we also found a significant loss in physical performance in FMS patients compared to healthy controls[6,20,21]. It is debatable whether fibromyalgia itself reduces physical performance or whether physical activity and, therefore, poor performance trigger fibromyalgia. In conclusion, the increased prevalence of sarcopenia and poor physical performance which we found in fibromyalgia patients may be due to lack of physical activity. In this case, an increased frequency of sarcopenia in fibromyalgia patients seems to be an expected result. This study once again emphasizes the importance of exercise and strategies to prevent sarcopenia and improve the quality of life in patients with fibromyalgia. Another study conducted in elderly adults found that patients with sarcopenia had higher mortality during in-hospital follow-up[25]. A meta-analysis involving women with ovarian cancer showed that sarcopenia and low muscle mass were associated with poor survival and high mortality[26]. This suggests that sarcopenia is not only associated with quality of life but also with mortality in later life. For this reason, it is important to be diagnosed and treated at a young age.

Some studies were found that patients with FMS had significantly decreased muscle strength, functional performance, and exercise capacity compared with healthy individuals[27-29]. Also in some studies, the values of the fat mass percentage were found higher in FMS patients[30]. In FMS, insulin-like growth factor I levels decrease, and proinflammatory cytokines IL-1beta, and TNF-a are increased[31]. These cytokines are also thought that they be associated with the development of sarcopenia[32]; on all these facts, there may be a connection between sarcopenia and FMS.

Chronic muscle pain has a great impact on the performance of daily activities. Being aware that the pain occurs with isokinetic movements has been reported among the possible causes of poor muscle performance in patients with FMS[28,29]. In our study, there was no relationship between sarcopenia and pain level in patients with FMS. This may suggest that there are more different factors than pain that play a role in muscle mass and strength in fibromyalgia.

FMS occurs in young women of reproductive age. In patients who develop sarcopenia at this age, not only functionality is affected but it alos can cause serious morbidity in patients at older ages. Sarcopenia in the elderly is an expected outcome, but affecting women of this age may also cause socioeconomic problems. So far, no complete protocol has been applied in previous studies on sarcopenia in patients with FMS. In a study, sarcopenia was assessed only by muscle strength, in the other only by the US or by functional status. In our study, we used both the SARC-F questionnaire, upper and lower extremity performance, and at the end US as an objective assessment parameter. This was a valuable study because there are a few studies about FMS and sarcopenia in the literature and sarcopenia is common in young women with FMS. However, there are some limitations in our study. Only female FMS patients were invited to our study and we did not comment on male FMS patients. Second, we did not know the other conditions that can affect sarcopenia such as physical activity levels, and nutritional status.

Conclusion

As a result of this study, we think that sarcopenia is common in patients with FMS. Hand strength is useful for suspecting sarcopenia. Assessing the presence of sarcopenia in FMS patients may improve the success of FMS treatment by improving the exercise program.

Funding

The authors declare that they have not received funding.

Conflicts of interest

The authors declare no conflicts of interest.

Ethical considerations

Protection of humans and animals. The authors declare that the procedures followed complied with the ethical standards of the responsible Human Experimentation Committee and adhered to the World Medical Association and the Declaration of Helsinki. The procedures were approved by the Institutional Ethics Committee.

Confidentiality, informed consent, and ethical approval. The authors have followed their institution's confidentiality protocols, obtained informed consent from patients, and received approval from the Ethics Committee. The SAGER guidelines were followed according to the nature of the study.

Declaration on the use of artificial intelligence. The authors declare that no generative artificial intelligence was used in the writing of this manuscript.

References

1. Wolfe F, Ross K, Anderson J, Russell IJ, Hebert L. The prevalence and characteristics of fibromyalgia in the general population. Arthritis Rheum. 1995;38:19-28.
2. Macfarlane GJ, Kronisch C, Dean LE, Atzeni F, Häuser W, Fluß E, et al. EULAR revised recommendations for the management of fibromyalgia. Ann Rheum Dis. 2017;76:318-28.
3. Topbas M, Cakirbay H, Gulec H, Akgol E, Ak I, Can G. The prevalence of fibromyalgia in women aged 20-64 in Turkey. Scand J Rheumatol. 2005;34:140-4.
4. Wolfe F, Clauw DJ, Fitzcharles MA, Goldenberg DL, Häuser W, Katz RL, et al. 2016 Revisions to the 2010/2011 fibromyalgia diagnostic criteria. Semin Arthritis Rheum. 2016;46:319-29.
5. Clauw DJ. Fibromyalgia: update on mechanisms and management. JCR J Clin Rheumatol. 2007;13:102-9.
6. Cruz-Jentoft AJ, Sayer AA. Sarcopenia. Lancet. 2019;29:2636-46.
7. Cruz-Jentoft AJ, Bahat G, Bauer J, Boirie Y, Bruyère O, Cederholm T, et al. Sarcopenia: revised European consensus on definition and diagnosis. Age Ageing. 2019;48:16-31.
8. Kara M, Kaymak B, Frontera W, Ata AM, Ricci V, Ekiz T, et al. Diagnosing sarcopenia: functional perspectives and a new algorithm from the ISarcoPRM. J Rehabil Med. 2021;53:jrm00209.
9. Kara M, Kaymak B, Ata AM, Özkal Ö, Kara Ö, Baki A, et al. STAR-sonographic thigh adjustment ratio: a golden formula for the diagnosis of sarcopenia. Am J Phys Med Rehabil. 2020;99:902-8.
10. Kapuczinski A, Soyfoo MS, De Breucker S, Margaux J. Assessment of sarcopenia in patients with fibromyalgia. Rheumatol Int. 2022;42:279-84.
11. Koca I, Savas E, Ozturk ZA, Boyaci A, Tutoglu A, Alkan S, et al. The evaluation in terms of sarcopenia of patients with fibromyalgia syndrome. Wien Klin Wochenschr. 2016;28:816-21.
12. Sarmer S, Ergin S, Yavuzer G. The validity and reliability of the Turkish version of the fibromyalgia impact questionnaire. Rheumatol Int. 2000;20:9-12.
13. Hjermstad MJ, Fayers PM, Haugen DF, Caraceni A, Hanks GW, Loge JH, et al. Studies comparing numerical rating scales, verbal rating scales, and visual analogue scales for assessment of pain intensity in adults: a systematic literature review. J Pain Symptom Manage. 2011;41:1073-93.
14. Malmstrom TK, Morley JE. SARC-F: a simple questionnaire to rapidly diagnose sarcopenia. J Am Med Dir Assoc. 2013;14:531-2.
15. Innes E. Handgrip strength testing: a review of the literature. Aust Occup Ther J. 1999;46:120-40.
16. Lord SR, Murray SM, Chapman K, Munro B, Tiedemann A. Sit-to-stand performance depends on sensation, speed, balance, and psychological status in addition to strength in older people. J Gerontol A Biol Sci Med Sci. 2002;57:539-43.
17. Tan DM, McGinley JL, Danoudis ME, Iansek R, Morris ME. Freezing of gait and activity limitations in people with Parkinson's disease. Arch Phys Med Rehabil. 2011;92:1159-65.
18. Umay E, Gundogdu I, Ozturk EA. What happens to muscles in fibromyalgia syndrome. Ir J Med Sci. 2020;189:749-56.
19. Latorre-Román PÁ, Segura-Jiménez V, Aparicio VA, Santos E Campos MA, García-Pinillos F, et al. Ageing influence in the evolution of strength and muscle mass in women with fibromyalgia: the al-Ándalus project. Rheumatol Int. 2015;35:1243-50.
20. Sener U, Ucok K, Ulasli AM, Genc A, Karabacak H, Coban NF, et al. Evaluation of health-related physical fitness parameters and association analysis with depression, anxiety, and quality of life in patients with fibromyalgia. Int J Rheum Dis. 2016;19:763-72.
21. Norregaard J, Bulow PM, Lykkegaard JJ, Mehlsen J, Danneskiold-Samsoe B. Muscle strength, working capacity and effort in patients with fibromyalgia. Scand J Rehabil Med. 1997;29:97-102.
22. Aparicio VA, Ortega FB, Heredia JM, Carbonell-Baeza A, Sjöström M, Delgado-Fernandez M. Handgrip strength test as a complementary tool in the assessment of fibromyalgia severity in women. Arch Phys Med Rehabil. 2011;92:83-8.

23. Devrimsel G, Turkyilmaz AK, Beyazal MS, Karkucak M. Assessment of hand function and disability in fibromyalgia. Z Rheumatol. 2019;78: 889-93.
24. Ibrahim AA, Dewir IM, Abu El Kasem ST, Ragab MM, Abdel-Fattah MS, Hussein HM. Influences of high vs. low-intensity exercises on muscle strength, function, and quality of life in post-COVID-19 patients with sarcopenia: a randomized controlled trial. Eur Rev Med Pharmacol Sci. 2023;27:9530-9.
25. Tufan A, Tolu T, Senturk Durmus N, Alkac C, Can B. FRAIL Scale: an independent predictor of in-hospital mortality among older adults. Eur Rev Med Pharmacol Sci. 2023;27:10396-402.
26. Ge HP, Song DF, Wu P, Xu HF. Impact of sarcopenia and low muscle attenuation on outcomes of ovarian cancer: a systematic review and meta-analysis. Eur Rev Med Pharmacol Sci. 2023;27:4544-562.
27. Maquet D, Croisier JL, Renard C, Crielaard JM. Muscle performance in patients with fibromyalgia. Joint Bone Spine. 2002;69:293-9.
28. Góes SM, Leite N, Shay BL, Homann D, Stefanello JM, Rodacki AL. Functional capacity, muscle strength and falls in women with fibromyalgia. Clin Biomech (Bristol). 2012;27:578-83.
29. Larsson A, Palstam A, Bjersing J, Löfgren M, Ernberg M, Kosek E, et al. Controlled, cross-sectional, multi-center study of physical capacity and associated factors in women with fibromyalgia. BMC Musculoskelet Disord. 2018;19:121.
30. Lobo MM, Paiva ED, Andretta A, Schieferdecker ME. Body composition by dual-energy X-ray absorptiometry in women with fibromyalgia. Rev Bras Reumatol. 2014;54:273-8.
31. Salemi S, Rethage J, Wollina U, Michel BA, Gay RE, Gay S, et al. Detection of interleukin 1beta (IL-1beta), IL-6, and tumour necrosis factor-alpha in skin of patients with fibromyalgia. J Rheumatol. 2003;30:146-50.
32. Beaudart C, McCloskey E, Bruyère O, Cesari M, Rolland Y, Rizzoli R, et al. Sarcopenia in daily practice: assessment and management. BMC Geriatr. 2016;16:170.

ARTÍCULO ORIGINAL

Modelos anatómicos tridimensionales y de realidad aumentada para el estudio de la neuroanatomía

Three dimensional models and augmented reality for the study of neuroanatomy

Juan S. Davidson-Córdoba[1], Diana P. Duarte-Mora y Laura C. Martínez-Camargo[2]*

[1]Servicio de Neurocirugía, Centro Hospitalario Serena del Mar, Cartagena; [2]Servicio de Neurocirugía, Universidad Militar Nueva Granada, Hospital Militar Central, Bogotá. Colombia

Resumen

Objetivo: *Crear modelos anatómicos tridimensionales y de realidad aumentada para el estudio de la neuroanatomía, a partir de modelos cadavéricos por medio de fotogrametría para su reconstrucción tridimensional, comparando dos software, uno totalmente automatizado y otro semiautomatizado, con los libros clásicos para el estudio de la neuroanatomía.* **Método:** *Se crearon modelos anatómicos tridimensionales mediante la técnica de fotogrametría por medio de dos software. Los objetos fueron evaluados por los residentes de neurocirugía.* **Resultados:** *Se crearon tres modelos anatómicos tridimensionales a partir de fotogrametría por cada programa y se evaluaron con una encuesta aplicada a 23 residentes de neurocirugía.* **Conclusiones:** *No hay diferencia significativa entre la herramienta 3DF Zephyr© 2021 3Dflow para la creación de objetos tridimensionales anatómicos de forma semiautomatizada y el Autodesk ReCap Photo 22.1 Automated Software© 2021 Autodesk, Inc. Los residentes consideran que los modelos realizados en el presente trabajo son útiles en el aprendizaje de la neuroanatomía.*

Palabras clave: *Neuroanatomía. Fotogrametría. Imágenes de realidad aumentada. Tridimensional. Modelos anatómicos. Anatomía.*

Abstract

Objective: *Create three-dimensional anatomical and augmented reality models for the study of neuroanatomy, from cadaveric models using photogrammetry for three-dimensional reconstruction, comparing two software, one fully automated and the other semi-automated with classic books for the study of neuroanatomy.* **Method:** *Three-dimensional anatomical models were created through the photogrammetry technique and by means of two software. The objects were evaluated by the neurosurgery residents.* **Results:** *Three three-dimensional anatomical models were created from photogrammetry for each program and evaluated with a survey applied to 23 neurosurgery residents.* **Conclusions:** *There is no significant difference between the 3DF Zephyr© 2021 3Dflow tool for creating anatomical three-dimensional objects in a semi-automated way compared to Autodesk ReCap Photo 22.1 Automated Software© 2021 Autodesk, Inc. The residents consider that the models made in this work are useful in learning neuroanatomy.*

Keywords: *Neuroanatomy. Photogrammetry. Augmented reality images. Three-dimensional. Anatomical models. Anatomy.*

***Correspondencia:**
Juan S. Davidson-Córdoba
E-mail: juanse_davidson@icloud.com

Fecha de recepción: 08-04-2023
Fecha de aceptación: 30-10-2023
DOI: 10.24875/CIRU.23000184

Cir Cir. 2025;93(2):197-201
Contents available at PubMed
www.cirugiaycirujanos.com

Introducción

El conocimiento de la anatomía humana es uno de los pilares de la medicina y del desarrollo de la neurocirugía, contando para su estudio con textos específicos, aunque en el presente existen descripciones muy precisas e imágenes que permiten su comprensión. Por consideraciones éticas y escasez de programas de donación es cada vez menor la exposición de los estudiantes de medicina a especímenes cadavéricos[1-3], y adicionalmente, para los residentes de neurociencias, la posibilidad de acceder a modelos anatómicos precisos es baja y los especímenes cadavéricos existentes en anfiteatros pueden presentar un deterioro significativo por el uso y el tiempo[4], por lo que la creación de modelos anatómicos tridimensionales y de realidad aumentada por medio de técnicas automatizadas, como la fotogrametría, se convierte en una herramienta de mayor precisión anatómica para los residentes de neurocirugía y mejora el aprendizaje de la neuroanatomía[4].

Método

Se adquirieron múltiples fotografías de los especímenes cadavéricos neuroanatómicos disponibles en el laboratorio de anatomía de la Universidad El Bosque con una cámara semiprofesional Canon EOS Rebel T5i, bajo los parámetros modo automático y manual ISO 100, con exposiciones oscilantes f8-f29 y apertura de diafragma de 4 a 10 segundos de todos los especímenes (360°), siguiendo las recomendaciones establecidas en los tutoriales en línea de 3Dflow Academy. Luego, con la técnica de fotogrametría, la cual a partir de múltiples imágenes previamente captadas por fotografía permite crear modelos tridimensionales por medio de *software*[5], en este caso Autodesk ReCap Photo 22.1© 2021 Autodesk, Inc. y 3DF Zephyr© 2021 3Dflow, se realizó la reconstrucción tridimensional de las imágenes. El primero de los programas solo requirió la carga de las imágenes en sus servidores, ya que el proceso es automatizado. Con el programa 3DF Zephyr© 2021 3Dflow es necesario contar con un equipo capaz de realizar el procesamiento de dichas imágenes; en nuestro caso se utilizó un computador con especificaciones Intel(R) Core(TM) i9-10980XE CPU @ 3.00GHz, RAM 64,0 GB (63.7 GB utilizable) y tarjeta gráfica NVIDIA GeForce RTX™ 3090 Founders Edition. Se procedió a realizar el proceso semiautomatizado, que consta de una fase previa manual opcional de enmascaramiento de las imágenes para limpiar defectos de la imagen y permitir un mejor emparejamiento de las fotografías, lo cual es realizado por el usuario, y una fase automática posterior para el proceso de creación del objeto tridimensional. Cada modelo fue valorado por un fotógrafo profesional (Juan Manuel Martínez Segura) que evidenció unas condiciones óptimas de luz para poder ser procesados en dichos *software.*

Finalmente se compararon dichas herramientas para definir cuál era el mejor modelo tridimensional y de realidad aumentada que contara con una precisión óptima para el estudio de sus componentes, basándose en una encuesta realizada a los residentes de neurocirugía de la Universidad del Bosque, la Universidad Militar Nueva Granada y el Hospital General de México, comparando los modelos anatómicos creados entre ellos, las imágenes de fotografía cadavérica y los esquemas plasmados en los libros guía de neuroanatomía (Fig. 1).

Posteriormente se tabularon los datos en una matriz realizada en Excel, de la cual se realizó una estadística descriptiva de las primeras ocho variables de la encuesta y se aplicó el coeficiente de correlación de Pearson para la comparación entre los modelos anatómicos realizados en el programa Autodesk ReCap Photo y los realizados en el programa 3DF Zephyr.

Resultados

Se adquirieron imágenes fotográficas con múltiples parámetros de exposición, apertura de diafragma, en ISO 100, de tres especímenes cadavéricos (hemisferio cerebral, base de cráneo y vértebra C1), en un rango entre 52 y 100 fotos dependiendo de la cantidad de áreas con formas irregulares, las cuales requieren una mayor cantidad de imágenes, como las apófisis y los forámenes en la base del cráneo y la superficie cerebral. Luego se procesaron las imágenes en cada uno de los *software* para la creación de modelos tridimensionales a prueba, obteniendo tres modelos anatómicos por cada programa, es decir, seis en total (Figs. 2 a 4).

Se aplicó una encuesta para evaluar y comparar los modelos anatómicos a 23 residentes de neurocirugía, de los cuales el 82.6% eran hombres, con edades entre 27 y 40 años, con un promedio de edad de 30.3 años (Tabla 1).

En cuanto a las preferencias de literatura para el aprendizaje de neuroanatomía en el cráneo, el 66.6% de los residentes usan el libro de Rhoton y

Figura 1. *Montaje para toma de fotografías de especímenes cadavéricos.*

Figura 2. *Modelos 1 y 2: hemisferio cerebral.*

Figura 3. *Modelos 1 y 2: vértebra C1 (Atlas).*

el 33% usan Rhoton, Netter y Latarjet. Respecto a las preferencias para el estudio de neuroanatomía en la columna, los residentes en su mayoría prefieren Latarjet (44.4%), seguido de *Anatomy Atlas and Interpretation of Spine Surgery* (22.22%) y Latarjet-Carpenter, Springer y Netter, con un 11.11% cada uno[6-10].

El 50% de los residentes han tenido la oportunidad de usar modelos anatómicos tridimensionales y de realidad aumentada para el aprendizaje de neuroanatomía, y el 11.1% no usaría los modelos para su formación. Sin embargo, el 100% de los residentes considera que los modelos realizados en el

Figura 4. *Modelos 1 y 2: base de cráneo (óseo).*

Tabla 1. Población de estudio

	n (%)
Sexo	
Femenino	4 (17.39)
Masculino	19 (82.6)
Año de residencia	
1	2 (8.69)
2	6 (26.08)
3	7 (30.43)
4	5 (21.73)
5	3 (13.04)
Promedio de edad	30.3 años

presente trabajo son útiles en el aprendizaje de la neuroanatomía.

Referente a la pregunta «Comparando con los modelos cadavéricos que ha tenido a su disposición, ¿considera que los modelos anatómicos tridimensionales y de realidad aumentada son una mejor herramienta para el aprendizaje de neuroanatomía?», el 26% de los residentes consideran que no hay diferencia, el 21.7% que son una mejor herramienta y el 47.8% que son una peor herramienta para el aprendizaje de neuroanatomía.

Al comparar los modelos realizados (modelos 1 en el programa Autodesk ReCap Photo y modelo 2 en el programa 3DF Zephyr) con las figuras plasmadas en los libros escogidos por los residentes como su guía bibliográfica, para el modelo de hemisferio cerebral el 47.8% de los residentes prefirieron el modelo 1, el 13% el modelo 2 y el 30.4% la imagen del libro de Rhoton. Para el modelo de la vértebra C1, el 43.4% prefirieron el modelo 1, el 43.4% el modelo 2 y el 8.6% prefirieron Latarjet. Para el modelo de la base del cráneo, el 60.8% escogieron el modelo 2, el 60.8% el modelo 2 y el 17.3% la imagen de Netter.

Para comparar la definición y la precisión anatómica percibida por los residentes, de los modelos

Tabla 2. Análisis de precisión anatómica y definición de la imagen

	Definición de la imagen	Precisión anatómica
Promedio		
Modelo 1 Hemisferio (Autodesk ReCap Photo)	3.27	3.36
Modelo 2 Hemisferio (3DF Zephyr)	3.04	3.09
p	0.580593089	0.508693651
Promedio		
Modelo 1 Atlas (Autodesk ReCap Photo)	3.45	3.31
Modelo 2 Atlas (3DF Zephyr)	3.45	3.22
p	0.682692308	0.822045998
Promedio		
Modelo 1 Base de cráneo (Autodesk ReCap Photo)	4	2.3
Modelo 2 Base de cráneo (3DF Zephyr)	3.22	3.18
p	0.42014774	0.399507359

realizados en el presente trabajo se asignó un valor a cada variable dispuesta en la encuesta, siendo 5 muy buena, 4 buena, 3 aceptable, 2 mala y 1 muy mala. Se aplicó el coeficiente de correlación de Pearson y se evidenció que no hay diferencias significativas en la definición ni en la precisión anatómica entre los programas Autodesk ReCap Photo y 3DF Zephyr para todos los modelos anatómicos realizados (Tabla 2).

Discusión

A lo largo de la historia se ha tratado de refinar el conocimiento acerca de la composición del cuerpo humano. Los primeros aportes se encuentran en los papiros de Smith, Ebers y Brugsch («el gran papiro de Berlín»), escritos entre los años 3000 y 2500 a.C., cuyos contenidos describen estructuras craneales. Posteriormente, Alcmeón de Crotona e Hipócrates de Cos, en los siglos V y IV a.C., respectivamente, realizan otras descripciones anatómicas. Por otra parte, de Hipócrates se cuenta con 72 libros y 59 tratados, y así mismo Aristóteles, en esa misma época, brinda en sus escritos información sobre anatomía comparativa y embriología[1,11,12].

Entre los años 310 y 250 a.C., Herófilo de Calcedonia y Erasístrato de Ceos realizaron importantes trabajos de investigación, enriqueciendo el conocimiento obtenido hasta ese momento sobre el sistema nervioso y los vasos sanguíneos y linfáticos. En la época de los antiguos romanos, comprendida entre los años 670 a.C. y 480 d.C., la mayor fuente de conocimiento anatómico provenía de los gladiadores heridos, siendo Claudio Galeno Nicon el principal representante de ese tiempo[11,12].

Tras el fin del Imperio Romano, el estudio del cuerpo humano se trasladó al Medio Oriente durante la edad dorada islámica, entre los años 701 y 1300 d.C. En el Renacimiento, muchos dibujos atómicos fueron aportados por artistas, entre los que destaca Leonardo da Vinci (1452-1519), quien describió por primera vez las meninges cerebrales[1,11,13,14].

Desde finales del siglo XX se ha planteado la necesidad imperiosa de realizar modificaciones a la enseñanza tradicional de la anatomía humana, por lo que se ha impulsado el desarrollo de bases de datos y simuladores con los que se puedan realizar interacciones más estrechas y un real afianzamiento del conocimiento teórico-práctico en los estudiantes tanto de ciencias básicas como de residencias médico-quirúrgicas, sin perder el realismo y la riqueza de información que podría proveer un modelo cadavérico. Dentro de las técnicas actuales que emplean el estudio anatómico tridimensional se incluyen, en orden cronológico de aparición, la estereoscopia (1920), la tomografía computarizada y la resonancia magnética (1970), y los modelos de simulación o *software* tridimensionales (1986)[15-18]. La característica esencial de estos últimos es que permiten la materialización y la integración de imágenes digitales obtenidas a través de registros fotográficos, tomográficos o por resonancia magnética, que posteriormente son modelados y editados en computadores tridimensionales, y finalmente impresos[19,20].

La implementación de modelos anatómicos tridimensionales en el aprendizaje de los estudiantes de medicina puede llegar a proporcionar un diagnóstico oportuno y así mismo generar mayor análisis de diferentes patologías previo a la realización de laboratorios o imagenología, debido al conocimiento integral de la anatomía[21,22]. Igualmente son de gran ayuda en cuanto a la preparación de los estudiantes antes de iniciar prácticas en exploraciones cadavéricas[23-25].

La fotogrametría permite crear imágenes tridimensionales con características de un modelo real, por lo que logra ser de gran ayuda para la formación de estudiantes de medicina o de residentes, tanto en habilidad quirúrgica[17] y razonamiento espacial, en comparación con los métodos convencionales[26],

como en apoyo en la presentación de casos clínicos, foros o congresos.

Conclusiones

En el presente estudio se evidencia que no hay diferencia en la calidad visual ni en la percepción por parte de los residentes entre los modelos tridimensionales creados con dos aplicaciones distintas. Adicionalmente, los residentes prefirieron el uso de modelos anatómicos tridimensionales sobre las figuras de los textos guía.

Aunque aún no se ha logrado implementar los modelos tridimensionales como base del aprendizaje de los estudiantes, en este caso los residentes de neurocirugía consideraron que son de gran utilidad en su formación académica. Se espera, en un futuro cercano, lograr su implementación para estudiantes de neurociencias, debido a que pueden ser un gran complemento de diferentes referencias bibliográficas para ayudar a comprender y retener información anatómica[27].

Financiamiento

Este estudio no requirió financiamiento.

Conflicto de intereses

Los autores declaran no tener conflicto de intereses.

Consideraciones éticas

Protección de personas y animales. Los autores declaran que para esta investigación no se han realizado experimentos en seres humanos ni en animales.

Confidencialidad, consentimiento informado y aprobación ética. El estudio no involucra datos personales de pacientes ni requiere aprobación ética. No se aplican las guías SAGER.

Declaración sobre el uso de inteligencia artificial. Los autores declaran que no utilizaron ningún tipo de inteligencia artificial generativa para la redacción de este manuscrito.

Bibliografía

1. Habbal O. The science of anatomy: a historical timeline. Sultan Qaboos Univ Med J. 2017;17:e18-22.
2. Moore KL, Dalley AF, Agur AMR. Anatomía con orientación clínica. Barcelona: Lippincott Williams & Wilkins; 2018.
3. Rhoton Jr. AL. The cerebrum. Neurosurgery. 2007;61(Suppl_1):SHC- 37-119.
4. Habbal O. The state of human anatomy teaching in the medical schools of Gulf Cooperation Council Countries: present and future perspectives. Sultan Qaboos Univ Med J. 2009;9:24-31.
5. De Jesús-Luis AS, Ordóñez-Velázquez S, Pineda-Martínez D, Brenes-Solano B, González-Fernández J. Fotogrametría: cómo crear modelos tridimensionales de bajo costo, con características realistas y fácil manipulación, para su uso en la enseñanza y el diagnóstico médico. Invest Educ Med. 2019;(32):100-11.
6. Peris-Celda M, Martínez-Soriano F, Rhoton Jr AL, editores. Rhoton's Atlas of head, neck, and brain. 2D and 3D images. New York: Thieme; 2017.
7. Latarjet M, Ruiz Liard A. Anatomía humana. Tomos I y II. 5.a ed. Buenos Aires: Médica Panamericana; 2018.
8. Tamraz JC, Comair Y. Atlas of regional anatomy of the brain using MRI: with functional correlations. 2nd ed. Berlin: Springer; 2011.
9. Carpenter MB. Neuroanatomia: fundamentos. 4.a ed. Madrid: Médica Panamericana; 1998.
10. Rubin MG, Safdieh JE. Netter. Neuroanatomía esencial. Barcelona: Elsevier-Masson; 2008.
11. Standring S. A brief history of topographical anatomy. J Anat. 2016;229:32-62.
12. Katz L. Medicine in the time of Hippocrates. Revista Médica de la Universidad Veracruzana. 2007;7:59-62.
13. Vicențiu Săceleanu M, George Mohan A, Alexandru Marinescu A, Marinescu A, Vlad Ciurea A. Leonardo da Vinci — ingenious anatomist: 500 years since the death of the famous erudite. Romanian Journal of Morphology and Embryology. 2019;60:1391-5.
14. Vigo V, Hirpara A, Yassin M, Wang M, Chou D, de Bonis P, et al. Immersive surgical anatomy of the craniocervical junction. Cureus. 2020;12:e10364.
15. Spitzer VM, Whitlock DG. The visible human dataset: the anatomical platform for human simulation. Anat Rec. 1998;253:49-57.
16. Garg A, Norman GR, Spero L, Maheshwari P. Do virtual computer models hinder anatomy learning? Acad Med. 1999;74(10 Suppl):S87-9.
17. Erolin C. Interactive 3D digital models for anatomy and medical education. En: Rea PM, editor. Biomedical visualisation. Vol. 2. Cham: Springer; 2019. p. 1-16.
18. Rea P, editor. Biomedical visualisation. Vol. 7. Cham: Springer; 2020.
19. Ye Z, Dun A, Jiang H, Nie C, Zhao S, Wang T, et al. The role of 3D printed models in the teaching of human anatomy: a systematic review and meta-analysis. BMC Med Educ. 2020;20:335.
20. De Benedictis A, Nocerino E, Menna F, Remondino F, Barbareschi M, Rozzanigo U, et al. Photogrammetry of the human brain: a novel method for three-dimensional quantitative exploration of the structural connectivity in neurosurgery and neurosciences. World Neurosurg. 2018;115:e279-91.
21. Jones DG. Anatomy in a post-covid-19 world: tracing a new trajectory. Anat Sci Educ. 2021;14:148-53.
22. Jacquesson T, Simon E, Dauleac C, Margueron L, Robinson P, Mertens P. Stereoscopic three-dimensional visualization: interest for neuroanatomy teaching in medical school. Surg Radiol Anat. 2020;42:719-27.
23. Hanna SJ, Freeston JE. Importance of anatomy and dissection: the junior doctor's viewpoint. Clin Anat. 2002;15:377-8.
24. Fleming C, Sadaghiani MS, Stellon MA, Javan R. Effectiveness of three-dimensionally printed models in anatomy education for medical students and resident physicians: systematic review and meta-analysis. J Am Col Radiol. 2020;17:1220-9.
25. Rubio RR, Shehata J, Kournoutas I, Chae R, Vigo V, Wang M, et al. Construction of neuroanatomical volumetric models using 3-dimensional scanning techniques: technical note and applications. World Neurosurg. 2019;126:359-68.
26. Petriceks AH, Peterson AS, Angeles M, Brown WP, Srivastava S. Photogrammetry of human specimens: an innovation in anatomy education.
27. Kournoutas I, Vigo V, Chae R, Wang M, Gurrola J 2nd, Abla AA, et al. Acquisition of volumetric models of skull base anatomy using endoscopic endonasal approaches: 3D scanning of deep corridors via photogrammetry. World Neurosurg. 2019;129:372-7.

ORIGINAL ARTICLE

Do the ınflammatory markers have a prognostic role in an elderly patient population diagnosed with non-muscle ınvasive bladder cancer?

¿Tienen los marcadores inflamatorios un papel pronóstico en una población de pacientes ancianos diagnosticados con cáncer de vejiga no invasivo?

Aykut Demirci, Tuncel Uzel, Abdullah Bolat, and Halil Başar*
Department of Urology, Dr. Abdurrahman Yurtaslan Ankara Oncology Training and Research Hospital, Ankara, Turkey

Abstract

Objective: *To evaluate whether the systemic immune-inflammation index (SII), neutrophil–lymphocyte ratio (NLR), platelet–lymphocyte ratio (PLR), and De–Ritis ratio (DRR) are determinants of progression-free survival (PFS), recurrence-free survival (RFS) and overall survival (OS) in patients aged ≥ 70 years diagnosed with non-muscle invasive bladder cancer (NMIBC).* **Method:** *The study included 173 elderly patients diagnosed with NMIBC between January 2015 and March 2022. The clinical and pathological data of the patients were examined. Cox regression analysis was performed.* **Results:** *The patient's mean age was 75.6 ± 4.57 years. A statistically significant correlation was determined between higher mean NLR, PLR, and SII values and PFS (p = 0.04, p = 0.009, and p = 0.007, respectively) and OS (p = 0.001, p = 0.003, and p < 0.001, respectively). The multivariate analysis results showed that tumor size (≥ 3 cm) and PLR (> 144.6) were independent risk factors for PFS (HR: 2.09, p = 0.03; HR:3.2, p = 0.01, respectively), the presence of multiple tumors for RFS (HR: 1.73, p = 0.01), and comorbid diseases for OS (HR: 2.18, p = 0.006).* **Conclusion:** *Inflammatory parameters were found to have no independent effects on RFS and OS in patients of advanced age with NMIBC, and only PLR could be used to predict PFS.*

Keywords: *Bladder Cancer. Systemic immune-inflammation index. The neutrophil–lymphocyte ratio. Platelet–lymphocyte ratio. De–Ritis ratio.*

Resumen

Objetivo: *El objetivo de este estudio fue evaluar si el índice de inmunoinflamación sistémica (SII), la relación neutrófilo-linfocito (NLR), la relación plaqueta-linfocito (PLR) y la relación De-Ritis son determinantes de la supervivencia sin progresión (SSP), la supervivencia sin recurrencia (SSR) y la supervivencia global (SG) en pacientes de 70 años o más diagnosticados con cáncer de vejiga invasor no músculo (CVNM).* **Método:** *Se incluyeron en el estudio un total de 173 pacientes ancianos diagnosticados con CVNM entre enero de 2015 y marzo de 2022. Se registraron datos clínicos y patológicos. Se realizó un análisis de regresión de Cox.* **Resultados:** *La edad media de los pacientes fue de 75.6 ± 4.57 años. Los resultados revelaron una asociación estadísticamente significativa entre valores medios más altos de NLR, PLR y SII y la SSP (p = 0.04, p = 0.009 y p = 0.007, respectivamente) y la SG (p = 0.001, p = 0.003 y p < 0.001, respectivamente). El análisis multivariante identificó el tamaño del tumor (≥ 3 cm) y la PLR (> 144.6) como factores de riesgo independientes para la SSP (hazard ratio [HR]: 2.09, p = 0.03; HR: 3.2, p = 0.01, respectivamente), la presencia de múltiples tumores para la SSR (HR: 1.73, p = 0.01) y las*

***Correspondence:**
Aykut Demirci
E-mail: draykutdemirci@hotmail.com

Date of reception: 30-05-2023
Date of acceptance: 08-11-2023
DOI: 10.24875/CIRU.23000278

Cir Cir. 2025;93(2):202-210
Contents available at PubMed
www.cirugiaycirujanos.com

enfermedades concomitantes para la SG (HR: 2.18, p = 0.006). **Conclusión:** *Se encontró que los parámetros inflamatorios no tienen efectos independientes en la SSR y la SG en pacientes de edad avanzada con CVNM, y solo la PLR podría usarse para predecir la SSP.*

Palabras clave: *Cáncer de vejiga. Índice de inflamación inmunitaria sistémica. Relación neutrófilo-linfocito. Relación plaqueta-linfocito.*

Introduction

Although the incidence of bladder cancer varies according to country, it has been reported to be the 10th most frequently seen cancer type with approximately 573,000 new patients per year worldwide[1]. Cases of non-muscle invasive bladder cancer (NMIBC) constitute 75% of these patients. Patients with NMIBC are at risk of recurrence at the rate of 70% and progression at 30%. This causes patients to undergo repeated surgery and creates a risk of impaired bladder functions[2,3]. Models have been formed to evaluate various clinical and pathological markers to determine prognostic risk groups of NMIBC patients, and developments are ongoing[4,5].

The distribution of cells playing a role in inflammation and the developing microenvironment is thought to have an impact on the development and proliferation of tumor cells[6]. Previous studies in the literature have attempted to show that the neutrophil-lymphocyte ratio (NLR), platelet-lymphocyte ratio (PLR), and systemic immune-inflammation index (SII), which are calculated according to the relative status of these cell counts to each other, and the De-Ritis ratio (DRR), which is calculated from the serum activity values of liver enzymes such as aspartate aminotransferase (AST) and alanine aminotransferase (ALT) which are thought to be a marker of tumor metabolism, could be used to determine tumor behavior in NMIBC patients[7,8].

Although the calculation of these ratios is simple and low-cost, there are inconsistencies in the results between studies, and their place in clinical use remains a matter of debate. In addition, there is no study showing what the role of these ratios could be in the prognostic determination of NMIBC patients of advanced age, who are expected to have reduced immune capacity together with aging[9].

The aim of this study was to evaluate the relationship of the NLR, PLR, SII, and DRR with progression, recurrence, and overall survival in an elderly patient population diagnosed with NMIBC.

Method

Patient selection

This retrospective study was approved by the Ethics Committee of Dr. Abdurrahman Yurtaslan Oncology Training and Research Hospital (Decision no: 2022-02/51). The study sample comprised 173 patients aged ≥ 70 years who were diagnosed with NMIBC following transurethral bladder tumor resection (TURBT) in our clinic between January 2015 and March 2022. The study exclusion criteria were defined as non-attendance of clinic follow-up appointments, incomplete data, a diagnosis of a muscle-invasive bladder tumor or benign pathology as a result of a pathological examination, or a history of hematological disease, a diagnosis of pneumonia within 3 months before admission, severe hepatic or renal diseases, or an active infection within 2 weeks before admission (Fig. 1).

Management and follow-up

The demographic and clinical data of each patient were recorded, including age, gender, comorbid diseases, duration of follow-up, smoking status, pre-operative laboratory examinations (hemogram, serum creatinine level, NLR, PLR, DRR, and SII values), and pathological data such as number and size of tumors, clinical T stage (cT) according to the 2017 Tumor, Node, Metastasis (TNM) classification, tumor grade according to the WHO 2016 classification, and the presence of carcinoma *in situ*.

Recurrence was defined as the determination of a tumor of the same pathological grade and progression as the determination of a tumor of a more advanced grade during the follow-up period. A record was made of the total duration of follow-up (months), the time from first diagnosis to progression and/or recurrence if any (months), and survival status. The NLR was calculated by dividing the neutrophil count by the lymphocyte count, the PLR by dividing the platelet count by the lymphocyte count, the SII by

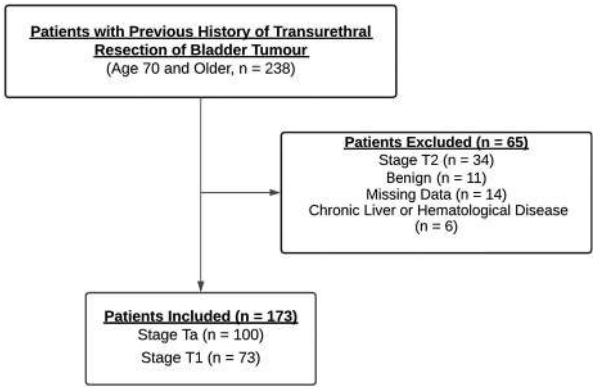

Figure 1. *Flowchart of the study design.*

dividing the neutrophil by the lymphocyte count then multiplying by the platelet count, and the DRR by dividing AST by ALT.

Following the transurethral resection of bladder tumor (TURBT) procedure, patients were classified according to the EAU NMIBC 2021 scoring system. Low-risk patients were administered a single dose of intravesical treatment early after the operation, then if no tumor was determined on cystoscopy at 3 months, follow-up consisted of cystoscopy at 9 months, then annually for 5 years thereafter. Patients evaluated as high-risk or very high-risk who refused radical cystectomy were applied with thoracoabdominal computed tomography (CT) once a year, intravesical Bacillus Calmette-Guerin (BCG) treatment for up to a year together with cystoscopy and urinary cytology at 3 months, and if no tumor was determined, this was repeated once every 3 months for 2 years, then once every 6 months for up to 5 years, and annually thereafter. The follow-up protocol for moderate-risk patients was made on an individual basis combining the elements of the low-risk and high-risk patient groups[2].

Statistical analysis

Statistical analyses of the study data were performed using SPSS version 22.0 software (SPSS, Chicago, IL, USA). The Shapiro-Wilk test was applied to assess the conformity of data to normal distribution. Continuous data were reported as mean ± standard deviation or median (interquartile range) values, and categorical data as number (n) and percentage (%). The Mann-Whitney U-test was applied in the comparisons of two groups of independent, non-parametric data. The cutoff values with the highest sensitivity and specificity were determined with ROC curve analysis. Survival status was examined using Kaplan-Meier analysis. The independent effect of variables on progression, recurrence, and overall survival, was determined through univariate and multivariate Cox regression analyses. Statistical significance was set at the level of $p < 0.05$.

Results

The evaluation was made of 173 patients comprising 86.7% males and 13.3% females with a mean age of 75.6 ± 4.57 years, and a median follow-up of 25 (36) months. Progression was observed in 30.1% of the patients at a median of 11.5 (28) months. Recurrence was observed in 46.2% of the patients at a median of 9 (13) months. The clinical and demographic data of the patients are summarized in table 1.

A statistically significant difference was determined between progression and the inflammatory parameters of NLR ($p = 0.04$), PLR ($p = 0.009$), and SII ($p = 0.007$). No significant difference was observed between recurrence and the inflammatory parameters ($p > 0.05$). A statistically significant difference was determined between overall survival and NLR ($p = 0.001$), PLR ($p = 0.003$), and SII ($p < 0.001$) (Table 2).

The cutoff values with the highest sensitivity and specificity were determined to be NLR: 2.8 ($p = 0.04$), PLR: 144.6 ($p = 0.009$), and SII: 697.35 ($p = 0.007$). For the determination of OS, the best cutoff points were determined to be NLR: 2.84 ($p = 0.001$), PLR: 136.05 ($p = 0.003$), and SII: 656.03 ($p < 0.001$) (Fig. 2 and Table 3).

In the Kaplan-Meier analysis examining the PFS and OS curves of the low and high NLR, PLR, and SII groups according to the determined cutoff values. Significant differences were determined between the high and low groups of NLR, PLR, and SII for PFS (log-rank $p = 0.002$, $p < 0.001$, $p = 0.03$, respectively) and OS (log-rank $p = 0.04$, $p = 0.02$, $p = 0.004$, respectively) (Fig. 3).

In the univariate Cox regression analysis, tumor size ($p = 0.01$), tumor stage ($p = 0.003$), tumor grade ($p = 0.01$), NLR ($p = 0.003$), PLR ($p < 0.001$), and SII ($p = 0.04$) values were seen to be significantly associated with progression (Table 4a). Age ($p = 0.006$) and the number of tumors ($p = 0.04$) were found to be associated with recurrence (Table 4b). A significant relationship was determined between OS and the variables of age ($p = 0.01$), comorbidities ($p = 0.03$), tumor stage ($p = 0.001$), tumor grade ($p = 0.001$), PLR ($p = 0.02$), and SII ($p = 0.005$) (Table 4c).

Table 1. Demographic and clinical characteristics of the patients

All patients (n = 173)	
Age*	75.6 ± 4.57
Sex, n (%)	
Male	150 (86.7)
Female	23 (13.3)
Follow-up period (months)**	25 (36)
Chronic diseases, n (%)	
None	71 (35.1)
DM	37 (18.3)
HT	56 (27.7)
CAD	24 (11.8)
COPD	14 (6.9)
Smoking, n (%)	
Yes	46 (26.6)
No	79 (45.7)
Ex-smoker	48 (27.7)
sCR (mg/dL)**	1.01 (0.44)
WBC (10^9/L)*	8.05 ± 2.46
Number of tumors, n (%)	
Single	102 (59,0)
Multiple	71 (41.0)
Diameter, n (%)	
< 3 cm	70 (40.5)
≥ 3 cm	103 (59.5)
Category, n (%)	
cTa	100 (57.8)
cT1	73 (42.2)
Concomitant CIS, n (%)	
Yes	15 (8.7)
No	158 (91.3)
Grade (WHO, 2016), n (%)	
Low grade	88 (50.9)
High grade	85 (49.1)
Adjuvant treatment, n (%)	
Yes	77 (44.5)
No	96 (55.5)
Progression, n (%)	
Yes	52 (30.1)
No	121 (69.9)
Recurrence, n (%)	
Yes	80 (46.2)
No	93 (53.8)
Overall survival, n (%)	
Alive	111 (64.2)
Dead	62 (35.8)

*(Mean ± SD); **(Median [IQR])
DM: diabetes mellitus; HT: hypertension; CAD: coronary artery disease; CVA: cerebrovascular accident; COPD: chronic obstructive pulmonary disease; CIS: carcinoma *in situ*; sCR: serum creatinine level; WBC: white blood cells; cT: clinical T stage.

In the multivariate analysis, predictive factors were determined to be tumor size (≥ 3 cm) and PLR (> 144.6) for progression (p = 0.03, p = 0.01, respectively, Table 4a), advanced age and the presence of multiple tumors for recurrence (p = 0.002, p = 0.01, respectively, Table 4b), and age and comorbidities for OS (p = 0.03, p = 0.006, respectively) (Table 4c).

Discussion

In previous studies in literature, NLR, PLR, SII, and DRR are among the markers usually evaluated to predict the survival of cancer patients[10]. The aim of this retrospective study was to examine the effect of these values on prognosis in an elderly patient population diagnosed with NMIBC following TURBT, and the results showed that with the exception of DRR, an increase in the other parameters had a negative effect on both progression and overall survival. However, the results of the multivariate analyses including other clinical and pathological data showed that only PLR was determined to be a significant marker for progression.

Inflammation and the subsequent host response formed against cancer cells play a significant role in both the development of tumors and antitumoral activity and this status affects the oncological results[11,12]. The determination of white blood cell distribution in the complete blood count is a frequently used method in the evaluation of inflammation[13]. Inflammatory markers such as NLR, PLR, and SII are examined to determine prognosis in most cancer types[14-16]. The effect of these parameters has become more important with the knowledge of the role played by inflammation in the development of bladder tumors[17]. Although development is from the same epithelial cell type, in contrast to upper urinary system tumors, there are still no recommended inflammatory parameters in routine use for NMIBC patients[2].

In a study of 122 patients which examined the effect of NLR on the prognosis of NMIBC patients, a cutoff value of 2.41 for NLR was determined to be an independent predictor of disease progression and recurrence[18]. In another study of patients with a median age of 69.27 years (63.78-79.44), the best NLR cutoff value was determined to be 3 and this was reported to be an independent risk factor for recurrence but not progression[19]. In contrast to these results, there are also studies showing that there is no effect of NLR in the determination of progression or recurrence[7,20]. The results of a study of 1551 patients diagnosed with NMIBC showed that PLR (cutoff point:124) was correlated with overall

Table 2. Inflammatory parameters according to the prognosis of patients

Variables	Progression		p†	Recurrence		p†	Overall status		p†
	Yes (n = 52)	No (n = 121)		Yes (n = 80)	No (n = 93)		Alive (n = 111)	Dead (n = 62)	
NLR*	3.6 ± 1.8	3.34 ± 2.55	**0.04**	3.31 ± 2.12	3.51 ± 2.53	0.83	3.05 ± 2.12	4.07 ± 2.6	**0.001**
PLR*	181.59 ± 88.2	153.12 ± 99.9	**0.009**	156.9 ± 76.8	165.7 ± 112.05	0.8	149.8 ± 99.4	182.8 ± 89.9	**0.003**
SII*	1023.7 ± 690.3	881.75 ± 1239.5	**0.007**	903.8 ± 973.7	942.1 ± 1208.8	0.97	793.7 ± 1071.2	1158.5 ± 1129.8	**< 0.001**
De–Ritis Ratio*	1.34 ± 0.57	1.28 ± 0.47	0.56	1.28 ± 0.49	1.31 ± 0.51	0.5	1.29 ± 0.46	1.29 ± 0.57	0.96

*Mean ± standard deviation
†Mann-Whitney U test
NLR: neutrophil-lymphocyte ratio; PLR: platelet-lymphocyte ratio; SII: systemic immune-inflammation index.
Significant values were shown in bold (p < 0.05).

Table 3. ROC curve analysis

Variables	Progression					Overall survival				
	Cut-point	AUC (95%CI)	Sensitivity	Specificity	p	Cut-point	AUC (95%CI)	Sensitivity	Specificity	p
NLR	2.8	0.596 (0.5-0.68)	0.71	0.55	**0.04**	2.84	0.647 (0.55-0.73)	0.67	0.56	**0.001**
PLR	144.6	0.625 (0.53-0.71)	0.69	0.62	**0.009**	136.05	0.63 (0.55-0.72)	0.67	0.57	**0.003**
SII	697.35	0.62 (0.53-0.72)	0.59	0.58	**0.007**	656.03	0.66 (0.58-0.75)	0.71	0.61	**< 0.001**

AUC: area under the ROC curve; 95% CI: 95% confidence interval; NLR: neutrophil-lymphocyte ratio; PLR: platelet-lymphocyte ratio; SII: systemic immune-inflammation index.
Significant values were shown in bold (p < 0.05).

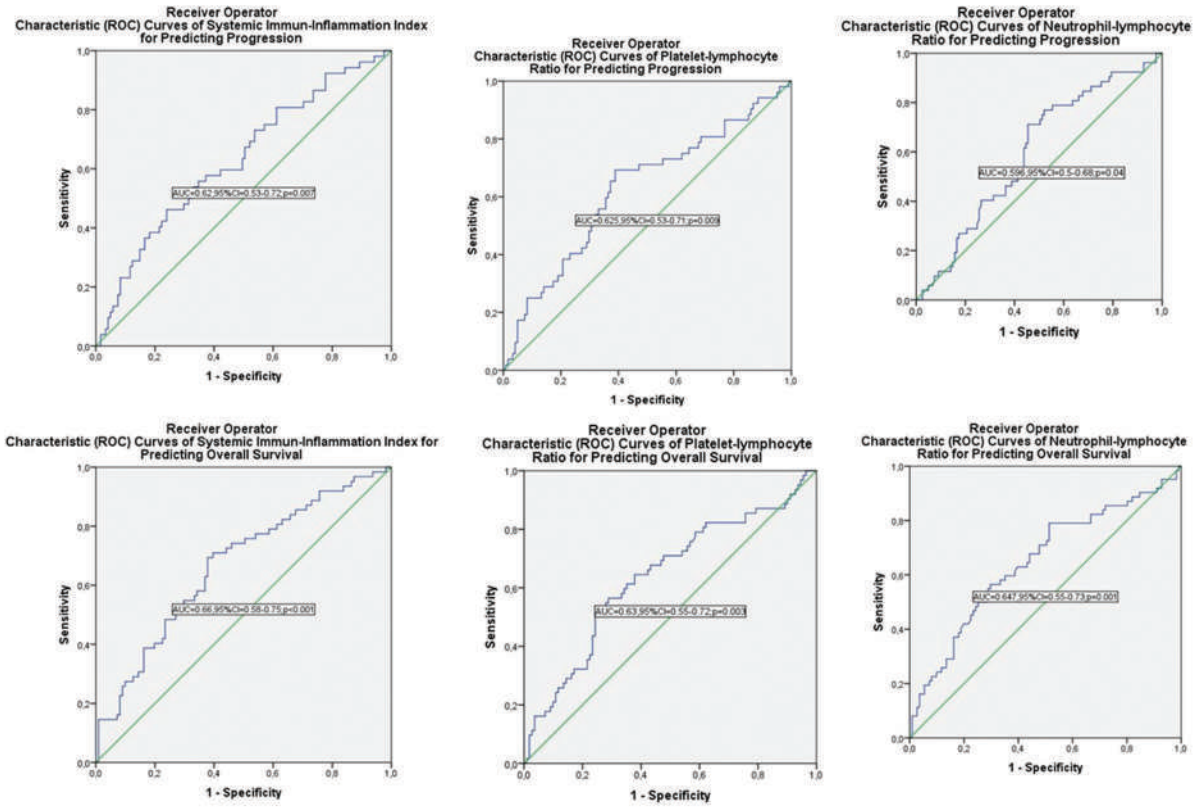

Figure 2. *Receiver operator characteristic curve analysis.*

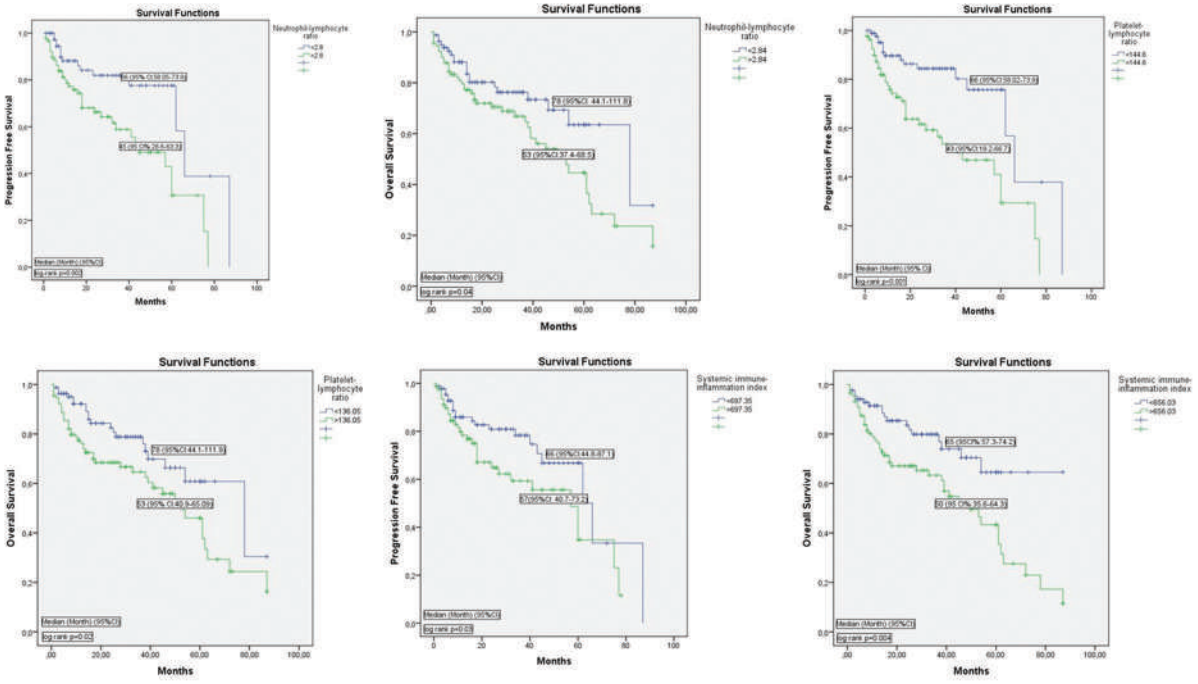

Figure 3. *Kaplan-Meier analysis.*

Table 4a. Cox regression analysis of progression predictors

Variables	Univariate analysis			Multivariate analysis		
	HR	95% CI	p	HR	95% CI	p
Age (continuous variable)	1.04	0.98-1.11	0.17	-	-	-
Number of tumors (single vs. multiple)	1.31	0.75-2.28	0.33	-	-	-
Tumor size (< 3 cm vs. ≥ 3 cm)	2.23	1.18-4.21	**0.01**	2.09	1.05-4.16	**0.03**
Tumor stage (cTa vs. cT1)	2.34	1.34-4.09	**0.003**	1.59	0.65-3.91	0.3
Concurrent CIS (yes vs. no)	1.09	0.43-2.77	0.84	-	-	-
Tumor grade (low vs. high)	2.02	1.14-3.55	**0.01**	1.002	0.41-2.42	0.99
Adjuvant treatment (yes vs. No)	1.26	0.72-2.2	0.4	-	-	-
NLR (< 2.8 vs. ≥ 2.8)	2.56	1.38-4.74	**0.003**	1.6	0.66-3.91	0.29
PLR (< 144.6 vs. ≥ 144.6)	2.96	1.62-5.42	**< 0.001**	3.2	1.3-7.86	**0.01**
SII (< 697.35 vs. ≥ 697.35)	1.80	1.02-3.18	**0.04**	0.48	0.2-1.14	**0.09**
De-Ritis ratio (continuous variable)	1.57	0.85-2.88	0.14	-	-	-

CIS: carcinoma *in situ*; NLR: neutrophil-lymphocyte ratio; PLR: platelet-lymphocyte ratio; SII: systemic immune-inflammation index.
Significant values were shown in bold (p < 0.05).

survival but was not significant for PFS or RFS[21]. In another study of NMIBC patients aged ≥65 years, higher PLR values were determined in those with more advanced stage pT1 than in those with pTa stages, but there was no evaluation of the prognosis of patients and multivariate analyses were not performed[22]. As the studies conducted for PLR have been more with muscle-invasive bladder cancer patients, it is difficult to reach a conclusion for NMIBC patients[23]. The SII has started to be used in recent

Table 4b. Cox regression analysis of recurrence predictors

Variables	Univariate analysis			Multivariate analysis		
	HR	95% CI	p	HR	95% CI	p
Age (continuous variable)	1.06	1.01-1.11	**0.006**	1.07	1.02-1.12	**0.002**
Number of tumors (single vs. multiple)	1.56	1.006-2.42	**0.04**	1.73	1.1-2.71	**0.01**
Tumor size (< 3 cm vs. ≥ 3 cm)	0.98	0.62-1.53	0.93	-	-	-
Tumor stage (cTa vs. cT1)	1.38	0.89-2.16	0.14	-	-	-
Concurrent CIS (yes vs. no)	1.72	0.85-3.46	0.12	-	-	-
Tumor grade (low vs. high)	1.15	0.74-1.79	0.52	-	-	-
Adjuvant treatment (yes vs. no)	1.21	0.78-1.88	0.38	-	-	-
NLR (continuous variable)	1.03	0.93-1.14	0.54	-	-	-
PLR (continuous variable)	1.000	0.99-1.002	0.88	-	-	-
SII (continuous variable)	1.000	1.000-1.000	0.59	-	-	-
De-Ritis ratio (continuous variable)	0.87	0.55-1.39	0.58	-	-	-

CIS: carcinoma *in situ*; NLR: neutrophil-lymphocyte ratio; PLR: platelet-lymphocyte ratio; SII: systemic immune-inflammation index.
Significant values were shown in bold (p < 0.05).

Table 4c. Cox regression analysis of overall survival predictors

Variables	Univariate analysis			Multivariate analysis		
	HR	95% CI	p	HR	95% CI	p
Age (continuous variable)	1.06	1.01-1.12	**0.01**	1.06	1.004-1.128	**0.03**
Comorbidity (yes vs. no)	1.76	1.05-2.95	**0.03**	2.18	1.25-3.82	**0.006**
Number of tumors (single vs. multiple)	1.56	0.95-2.58	0.07	-	-	-
Tumor size (< 3 cm vs. ≥ 3 cm)	1.66	0.96-2.86	0.06	-	-	-
Tumour stage (cTa vs. cT1)	2.39	1.43-4.00	**0.001**	1.33	0.66-2.66	0.41
Concurrent CIS (yes vs. no)	0.34	0.08-1.42	0.14	-	-	-
Tumor grade (low vs. high)	2.37	1.40-4.01	**0.001**	1.5	0.74-3.02	0.25
Adjuvant treatment (yes vs. no)	0.69	0.41-1.16	0.16	-	-	-
NLR (< 2.84 vs. ≥ 2.84)	1.7	0.99-2.91	0.051	-	-	-
PLR (< 136.05 vs. ≥ 136.05)	1.82	1.06-3.11	**0.02**	0.99	0.43-2.28	0.98
SII (< 656.03 vs. ≥ 656.03)	2.19	1.26-3.80	**0.005**	1.78	0.75-4.19	0.18
De-Ritis ratio (continuous variable)	1.02	0.62-1.65	0.93	-	-	-

CIS: carcinoma *in situ*; NLR: neutrophil-lymphocyte ratio; PLR: platelet-lymphocyte ratio; SII: systemic immune-inflammation index.
Significant values were shown in bold (p < 0.05).

years to obtain more information about the host inflammatory response using both the neutrophil and platelet counts together[24]. In a multicenter study which examined 1117 patients, there was determined to be no significant effect of SII (cutoff point:580) on OS, and although the effect was significant on PFS and RFS, this effect was not seen in subgroup analyses[16].

In addition to increasing comorbid diseases together with aging, there has also been reported to be a higher risk of autoimmune diseases and malignant diseases. This causes a deterioration in the body's homeostasis, which is important in the fight against cancer[25]. In particular, a decrease in the number of T lymphocytes, which are responsible for cellular immunity and antitumoral activity, contributes to this[9]. However, in elderly patients, the platelet cells in the blood remain relatively higher than other white blood cells[26]. By surrounding tumor cells circulating in the blood, platelet cells prevent apoptosis of the tumor cells, and the ongoing secretion of growth factors and cytokines increases angiogenesis, causing an increase in the tumorogenic effect[27]. The cutoff values determined in the current study for PLR and SII were higher than those reported in previous studies. Moreover, although it was determined that NLR, PLR, and SII could have a significant effect on progression and overall survival, PLR was seen to be more significant for PFS. In accordance with these results, it can be considered that in the evaluation of advanced-age NMIBC patients, platelet cells have an important role in survival, and this should be kept in mind in the approach to this group of patients.

With the rapid proliferation and destruction of cancer cells, the level of AST enzymes in the blood can increase, and the DRR is obtained with the thought that cancer metabolism can be determined by dividing the AST value by ALT, which is an enzyme specific to the liver[28]. With the use of DRR in the evaluation of prognosis in most cancer types, studies in recent years have started to show what contribution is made in NMIBC patients. In the most comprehensive study of 1117 patients, a cutoff value of 1.2 was determined for DRR and it was shown to be associated only with RFS[8]. Despite a statistically significant correlation determined between DRR and progression in another study, Batur et al. found no significant relationship between DRR and progression or recurrence[29,30]. The results of the current study were similar to those of Batur et al., and no relationship was determined between OS and DRR, therefore, no cutoff value was formed for DRR. Although patients with hepatitis and hematological diseases were not included in the current study, which could change the DRR results, there is the possibility that the results were affected by multiple drug use, which is common at advanced ages. These points must be taken note of in the clinical use of DRR.

This study had some limitations that should be considered. The study design was retrospective, the follow-up period was short, the patient number was relatively low, and other known values showing inflammation such as C-reactive protein and erythrocyte sedimentation rate, were not available from the patient records. As the patient population was aged ≥ 70 years, it was not possible to form a healthy control group to compare the parameters. As some patients could not tolerate adjuvant treatments and/or because of the "stay at home" regulation during the COVID-19 pandemic, some patients could not go to pharmacies, so the full effect of adjuvant therapy could not be reflected in the results[31].

Conclusion

Despite following the necessary treatment and follow-up protocols, there is a risk of developing recurrence and progression for patients diagnosed with bladder cancer. In addition to age, comorbidities, and tumor characteristics in the determination of the prognosis of elderly NMIBC patients, the inflammatory parameters seem to be promising. When evaluated with other clinical and pathological variables, the inflammation parameters showed no significance for recurrence and overall survival in an elderly population diagnosed with NMIBC but PLR was determined to be an independent marker in the determination of progression-free survival.

Funding

The authors declare that they have not received funding.

Conflicts of interest

The authors declare no conflicts of interest.

Ethical considerations

Protection of human and animal subjects. The authors declare that no experiments involving humans or animals were conducted for this research.

Confidentiality, informed consent, and ethical approval. The authors have obtained approval from the Ethics Committee for the analysis of routinely obtained and anonymized clinical data, so informed consent was not necessary. Relevant guidelines were followed.

Use of artificial intelligence for generating text. The authors declare that no generative artificial intelligence was used in the writing of this manuscript.

References

1. Bray F, Ferlay J, Soerjomataram I, Siegel RL, Torre LA, Jemal A. Global cancer statistics 2018: GLOBOCAN estimates of incidence and mortality worldwide for 36 cancers in 185 countries. CA Cancer J Clin. 2018;68:394-424. Erratum in: CA Cancer J Clin. 2020;70:313.
2. Babjuk M, Burger M, Compérat EM, Gontero P, Mostafid AH, Palou J, et al. European Association of Urology guidelines on non-muscle-invasive bladder cancer (TaT1 and carcinoma *ın situ*) -2019 update. Eur Urol. 2019;76:639-57.
3. Demir DO, Doluoglu OG, Yildiz AK, Kacan T, Yazar VM, Demirbas A, et al. Effect of Re-TUR time on recurrence and progression in high-risk non-muscle-invasive bladder cancer. Cir Cir. 2022;90:6-12.
4. Demirci A, Ordu M. The prognostic effect of ımmunohistochemical staining rates in patients with non-muscleınvasive bladder cancer. Indian J Pathol Microbiol. 2023;66:502-10.
5. Tataroğlu ÖD. Bladder cancer: a mini review. Unicos Rev. 2022;1:1-4.
6. Diakos CI, Charles KA, McMillan DC, Clarke SJ. Cancer-related inflammation and treatment effectiveness. Lancet Oncol. 2014;15:e493-503.
7. Yıldız HA, Değer MD, Aslan G. Prognostic value of preoperative inflammation markers in non-muscle invasive bladder cancer. Int J Clin Pract. 2021;75:e14118.
8. Laukhtina E, Mostafaei H, D'Andrea D, Pradere B, Quhal F, Mori K, et al. Association of De Ritis ratio with oncological outcomes in patients with non-muscle invasive bladder cancer (NMIBC). World J Urol. 2021;39:1961-8.
9. Sharma R, Kapila R, Haq MR, Salingati V, Kapasiya M, Kapila S. Age-associated aberrations in mouse cellular and humoral immune responses. Aging Clin Exp Res. 2014;26:353-62.
10. Zhang J, Zhou X, Ding H, Wang L, Liu S, Liu Y, et al. The prognostic value of routine preoperative blood parameters in muscle-invasive bladder cancer. BMC Urol. 2020;20:31.
11. Aggarwal BB, Vijayalekshmi RV, Sung B. Targeting inflammatory pathways for prevention and therapy of cancer: short-term friend, long-term foe. Clin Cancer Res. 2009;15:425-30.
12. Chen J, Hao L, Zhang Z, Zhang S, Zhang Y, Dong B, et al. Activation hypoxia inducible factor-1α gene affected the tumor microenvironment and induced recurrence and invasion of bladder cancer *in vitro*. Cir Cir. 2022;90:588-95.
13. Riesco A. Five-year cancer cure: relation to total amount of peripheral lymphocytes and neutrophils. Cancer. 1970;25:135-40.
14. Guthrie GJ, Charles KA, Roxburgh CS, Horgan PG, McMillan DC, Clarke SJ. The systemic inflammation-based neutrophil-lymphocyte ratio: experience in patients with cancer. Crit Rev Oncol Hematol. 2013; 88:218-30.
15. Li B, Zhou P, Liu Y, Wei H, Yang X, Chen T, et al. Platelet-to-lymphocyte ratio in advanced cancer: review and meta-analysis. Clin Chim Acta. 2018;483:48-56.
16. Katayama S, Mori K, Pradere B, Laukhtina E, Schuettfort VM, Quhal F, et al. Prognostic value of the systemic immune-inflammation index in non-muscle invasive bladder cancer. World J Urol. 2021;39:4355-61.
17. Wigner P, Grębowski R, Bijak M, Saluk-Bijak J, Szemraj J. The ınterplay between oxidative stress, ınflammation and angiogenesis in bladder cancer development. Int J Mol Sci. 2021;22:4483.
18. Mano R, Baniel J, Shoshany O, Margel D, Bar-On T, Nativ O, et al. Neutrophil-to-lymphocyte ratio predicts progression and recurrence of non-muscle-invasive bladder cancer. Urol Oncol. 2015;33:67.e1-7.
19. Favilla V, Castelli T, Urzì D, Reale G, Privitera S, Salici A, et al. Neutrophil to lymphocyte ratio, a biomarker in non-muscle invasive bladder cancer: a single-institutional longitudinal study. Int Braz J Urol. 2016;42:685-93.
20. Albayrak S, Zengin K, Tanik S, Atar M, Unal SH, Imamoglu MA, et al. Can the neutrophil-to-lymphocyte ratio be used to predict recurrence and progression of non-muscle-invasive bladder cancer? Kaohsiung J Med Sci. 2016;32:327-33.
21. Kang M, Jeong CW, Kwak C, Kim HH, Ku JH. Preoperative neutrophil-lymphocyte ratio can significantly predict mortality outcomes in patients with non-muscle invasive bladder cancer undergoing transurethral resection of bladder tumor. Oncotarget. 2017;8:12891-901.
22. Atik YT, Cimen HI, Gul D, Arslan S, Kose O, Halis F. Are the preoperative neutrophil/lymphocyte ratio and platelet/lymphocyte ratio predictive for lamina propria invasion in aging patients? Aging Male. 2020;23:1528-32.
23. Li DY, Hao XY, Ma TM, Dai HX, Song YS. The prognostic value of platelet-to-lymphocyte ratio in urological cancers: a meta-analysis. Sci Rep. 2017;7:15387.
24. Wang Q, Zhu SR, Huang XP, Liu XQ, Liu JB, Tian G. Prognostic value of systemic immune-inflammation index in patients with urinary system cancers: a meta-analysis. Eur Rev Med Pharmacol Sci. 2021;25:1302-10.
25. Zhang HG, Grizzle WE. Aging, immunity, and tumor susceptibility. Immunol Allergy Clin North Am. 2003;23:83-102, vi.
26. Li C, Li J, Li Y, Lang S, Yougbare I, Zhu G, et al. Crosstalk between platelets and the immune system: old systems with new discoveries. Adv Hematol. 2012;2012:384685.
27. Vallet-Regi M, Manzano M, Rodriguez-Manas L, Checa Lopez M, Aapro M, Balducci L. Management of cancer in the older age person: an approach to complex medical decisions. Oncologist. 2017;22:335-42.
28. Vander Heiden MG, Cantley LC, Thompson CB. Understanding the Warburg effect: the metabolic requirements of cell proliferation. Science. 2009;324:1029-33.
29. Fukui-Kawaura S, Kawahara T, Araki Y, Nishimura R, Uemura K, Namura K, et al. A higher De Ritis ratio (AST/ALT) is a risk factor for progression in high-risk non-muscle invasive bladder cancer. Oncotarget. 2021;12:917-22.
30. Batur AF, Aydogan MF, Kilic O, Korez MK, Gul M, Kaynar M, et al. Comparison of De Ritis Ratio and other systemic inflammatory parameters for the prediction of prognosis of patients with transitional cell bladder cancer. Int J Clin Pract. 2021;75:e13743.
31. Yildiz AK, Ozgur BC, Bayraktar AS, Demir DO, Doluoglu OG. How has the COVID-19 pandemic affected patients with primary bladder cancer? Cir Cir. 2023;91:204-11.

ARTÍCULO DE REVISIÓN

La disfunción autonómica en la enfermedad por reflujo gastroesofágico. El eje neurogastro-cardiaco: ¿amigo o enemigo?

Autonomic dysfunction in gastroesophageal reflux disease. The neurogastro-cardiac axis: friend or foe?

Sergio Sobrino-Cossío[1,2], Jorge Cossío-Aranda[3], Elymir S. Galvis-García[1,4], Gualberto Mateos-Pérez[1,2], Óscar Teramoto-Matsubara[2,5], Jesús A. González-Hermosillo[6], Juan C. López Alvarenga[7], Mustafa Azizoglu[8,9] y José M. Remes-Troche[10]*

[1]Departamento de Gastroenterología, Hospital Ángeles del Pedregal; [2]Unidad Gástrica, Centro Avanzado en Endoscopia y Estudios Funcionales; [3]Departamento de Cardiología, Hospital Ángeles del Pedregal; [4]Departamento de Gastroenterología y Consulta Externa, Hospital General de México Dr. Eduardo Liceaga; [5]Departamento de Gastroenterología, Centro Médico ABC; [6]Clínica de Disautonomías, Instituto Nacional de Cardiología. Ciudad de México, México; [7]University of Texas Rio Grande Valley, Edimburg, Texas, Estados Unidos de América; [8]Deparment of Pediatric Surgery, Esenyurt Necmi Kadioglu State Hospital, Istanbul, Turkey; [9]Department of Stem Cell and Tissue Enginering, Health Sciences Institute, Istinye University, Istanbul, Turkey; [10]Instituto de Investigaciones Médico-Biológicas, Universidad Veracruzana, Veracruz, México

Resumen

La enfermedad por reflujo gastroesofágico (ERGE) es una condición compleja y altamente prevalente. El deterioro de la comunicación intestino-cerebro está asociado a la disfunción autonómica. La modulación del sistema nervioso autónomo controla las funciones gastrointestinales. En la ERGE se han reportado una disminución del tono vagal (actividad parasimpática) y un aumento de la actividad simpática, con el equilibrio autónomo desplazado hacia el sistema simpático. Los cuestionarios clínicos y la medición de la variabilidad de la frecuencia cardiaca, método no invasor, pueden ser útiles en los pacientes con ERGE para detectar la disfunción autonómica. La restauración de la actividad del sistema parasimpático (principalmente neuromodulación), con la subsecuente mejoría de la actividad parasimpática, disminuirá la intensidad de los síntomas autonómicos y de la ERGE, mejorando la calidad de vida.

Palabras clave: *Sistema nervioso autónomo. Variabilidad de la frecuencia cardíaca. Enfermedad por reflujo gastroesofágico. Disfunción autonómica.*

Abstract

Gastroesophageal reflux disease (GERD) is a complex and highly prevalent entity. Impaired gut-brain communication is associated with autonomic dysfunction. Modulation of the autonomic nervous system controls gastrointestinal functions. In GERD, a decrease in vagal tone (parasympathetic activity) and an increase in sympathetic activity with autonomic balance shifted towards the sympathetic system have been reported. Clinical questionnaires and non-invasive measurement of heart rate variability may be useful in patients with GERD to detect autonomic dysfunction. Restoration of parasympathetic system activity (mainly neuromodulation), with subsequent improvement of parasympathetic activity, will reduce the intensity of autonomic symptoms and GERD, improving quality of life.

Keywords: *Autonomic nervous system. Heart rate variability. Gastroesophageal reflux disease. Autonomic disfunction.*

***Correspondencia:**
Sergio Sobrino-Cossío
E-mail: ssobrinocossio@gmail.com

Fecha de recepción: 10-01-2025
Fecha de aceptación: 21-01-2025
DOI: 10.24875/CIRU.25000022

Cir Cir. 2025;93(2):211-220
Contents available at PubMed
www.cirugiaycirujanos.com

Introducción

La enfermedad por reflujo gastroesofágico (ERGE) es una condición clínica compleja en la que el reflujo del contenido gastroduodenal hacia el esófago provoca síntomas o complicaciones, afección en la calidad de vida y un alto costo del manejo que supera los 12,000 millones de dólares anuales en los Estados Unidos de América[1-4].

En Latinoamérica, su prevalencia se ha descrito entre el 15% y el 25%[5]. En los Estados Unidos de América, la ERGE es el trastorno gastrointestinal más prevalente y afecta a un tercio de la población adulta[6]. En el mundo occidental, la prevalencia en los adultos se ha reportado en un 20%[6,7].

El reflujo gastroesofágico (RGE) es un fenómeno fisiológico. El consenso de Lyon 2.0 definió la «ERGE comprobada» cuando existe evidencia concluyente de RGE, incluida la presencia de esofagitis erosiva (grados B, C y D de la clasificación de Los Ángeles), el esofágo de Barrett y la estenosis péptica, y un tiempo de exposición al ácido en el esófago distal > 6% medido por monitorización ambulatoria del pH e impedanciometría de 24 horas. La ausencia de esofagitis significativa y un tiempo de exposición al ácido en el esófago < 4% descartan la enfermedad. Sin embargo, es importante aclarar que la evidencia objetiva de ERGE tiene poca correlación con la frecuencia y la intensidad de los síntomas, ya que estos no solo dependen de la intensidad del estímulo esofágico, sino también del grado de sensibilidad esofágica de cada individuo[4,5].

Patogénesis de la enfermedad por reflujo gastroesofágico

La fisiopatología de la ERGE es compleja (Fig. 1)[8]. La exposición constante del esófago al RGE (ácido gástrico, bilis, pepsina y enzimas pancreáticas) puede causar daño de la mucosa esofágica (inicialmente relacionado con la pepsina y luego con la respuesta inflamatoria mediada por las citocinas y la infiltración leucocitaria)[9].

Los mecanismos que más contribuyen al desarrollo de ERGE son: 1) el incremento en el número de las relajaciones transitorias del esfínter esofágico inferior (EEI), 2) el aumento de la presión abdominal y 3) la presión disminuida del EEI. La fisiopatología de la ERGE incluye un mal funcionamiento de la unión esofagogástrica, una disminución del aclaramiento esofágico y alteraciones en la integridad de la mucosa esofágica[2].

La barrera antirreflujo está compuesta por el EEI y el diafragma crural. El EEI tiene un componente intrínseco, formado por las fibras musculares esofágicas bajo un control neurohormonal, y otro extrínseco, formado por los pilares diafragmáticos y el ligamento frenoesofágico, los cuales proporcionan el soporte anatómico al EEI y mayor protección contra el RGE[3,10,11].

Síntomas típicos y manifestaciones extraesofágicas

Los síntomas típicos y más comunes de ERGE son pirosis (sensación de ardor subesternal) y regurgitación (retorno sin esfuerzo del contenido gástrico hacia la boca). La diana terapéutica en las enfermedades relacionadas con el ácido es la supresión farmacológica de la secreción ácida del estómago. El control del pH intragástrico está relacionado con la curación de la mucosa y el alivio sintomático[1]. La escala de pH es logarítmica (valores de 0 a 14), siendo un pH 4 diez veces menos ácido que un pH 2, cien menos que un pH 3 y mil menos que un pH 1[11]. Aunque la pirosis y la regurgitación son síntomas comunes de la ERGE, son pobres predictores de la presencia de esofagitis grave. Estos síntomas por sí solos no son suficientes para confirmar o descartar la presencia de esofagitis. La sensibilidad y la especificidad diagnósticas para la pirosis se han reportada en un 30-76% y un 62-96%, respectivamente[12].

Para entender la enfermedad, el Consenso de Montreal dividió la ERGE en síndromes[13]:

- Esofágicos:
  - Sintomáticos: reflujo típico y dolor torácico por reflujo.
  - Daño de la mucosa esofágica (esofagitis por reflujo, estenosis por reflujo, esófago de Barrett y adenocarcinoma).
- Extraesofágicos:
  - Asociación establecida: tos crónica, asma, laringitis y erosiones dentales por RGE.
  - Asociación propuesta: laringitis, sinusitis, otitis media recurrente, fibrosis pulmonar idiopática.

En la ERGE, los pacientes con daño de la mucosa tienen mayor probabilidad de tener una anormal exposición del esófago al ácido (71% vs. 40%). En el fenotipo erosivo se ha reportado mayor dilatación de los espacios intercelulares. La disminución en la

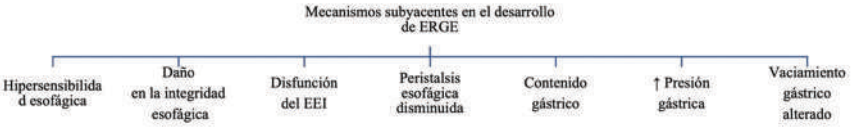

Figura 1. *Mecanismos subyacentes en el desarrollo de enfermedad por reflujo gastroesofágico (ERGE)[8]. EEI: esfínter esofágico inferior.*

resistencia tirular, el aumento en la permeabilidad y el paso de los iones H^+ están asociados con una mayor respuesta inflamatoria, sensibilización de las terminaciones nerviosas sensoriales aferentes y disfunción neural[14,15]. El fenotipo erosivo puede subdividirse en tres grupos:

- Alteración del aclaramiento esofágico debido a una motilidad esofágica alterada.
- Disfunción de la unión esofagogástrica o de la barrera antirreflujo debido a hipotensión del EEI, relajaciones transitorias del EEI o disinergia entre el EEI y el diafragma crural (p. ej., presencia de hernia de hiato).
- Factores gástricos posteriores, incluido el retraso en el vaciado gástrico y la presencia de una bolsa de ácido gástrico[7].

La enfermedad por reflujo no erosiva (ERNE) es el fenotipo más común y representa hasta el 70% de los casos de ERGE, mientras que la esofagitis erosiva representa aproximadamente el 30% y el esófago de Barrett un 6-8% de la población de pacientes con ERGE[7].

El fenotipo no erosivo es un grupo extraordinariamente heterogéneo que incluye tres subgrupos (después de las mediciones objetivas del reflujo) de pacientes: 1) verdadero reflujo ácido (exposición anormal al ácido [EAA] positiva en 50%), 2) esófago hipersensible (EAA negativa e índice de síntomas > 50%) y 3) pirosis funcional (EAA negativa e índice de síntomas < 50%)[16]. El índice de síntomas es la relación entre la pirosis y el número de episodios de reflujo ácido. El fenotipo no erosivo es más refractario al tratamiento, ya que incluye afecciones no relacionadas con el ácido (50%)[17]. En la ERNE, las predicciones de la respuesta a los inhibidores de la bomba de protones (IBP) son difíciles, por lo que una prueba con un supresor más potente permitiría estratificar a los pacietes respondedores. La falla al tratamiento puede ser explicada porque el diagnóstico está basado en los síntomas, la persistencia de eventos de reflujo débilmente ácidos con extensiones al esófago proximal y la hipersensibilidad visceral[1]. Sin embargo, cuando se seleccionan pacientes con evidencia objetiva de reflujo ácido (impedanciometría intraluminal multicanal con pH-metría de 24 h), la tasa de respuesta a los IBP es similar en los fenotipos erosivos y en la ERNE verdadera (72% vs. 73%)[18]. La pirosis funcional y la hipersensibilidad al reflujo representan más del 90% de los pacientes con pirosis sin respuesta al tratamiento con IBP dos veces al día[18].

Los mecanismos subyacentes a las manifestaciones de las vías respiratorias extraesofágicas aún no se conocen bien. Se han propuesto dos hipótesis: 1) el contacto directo del ácido gástrico con las vías respiratorias superiores y 2) un reflejo vagal provocado por la acidificación del esófago distal, que provoca broncoespasmo[13]. La sensibilización del árbol pulmonar puede hacer que las vías respiratorias se vuelvan reactivas a otros estímulos, lo que produce broncoespasmo a través de un mecanismo vagal[19,20].

Es importante destacar que se ha reportado una mayor frecuencia de disfunción (disautonomías) del sistema nervioso autónomo (SNA) en los pacientes con síntomas de ERGE; la fisiopatología de la ERGE se ha relacionado con alteraciones en la actividad del SNA[21,22].

Los pacientes refieren que los síntomas de ERGE ocurren con mayor frecuencia en el período posprandial. Se ha reportado que existen factores precipitantes de los síntomas en la ERGE (material refluido) y factores que modifican la respuesta al tratamiento, como un aclaramiento esofágico alterado y la sensibilidad de la mucosa. Se estima que entre el 10% y el 40% de los pacientes con ERGE tienen una respuesta incompleta o nula a una dosis estándar de IBP[1].

Aunque no hay datos que confirmen la mayor frecuencia de síntomas autonómicos en el posprandio temprano o tardío en los pacientes con ERGE, muchos aparecerán después de la ingesta de grasa o de condimentos (mayor volumen), incluso en pacientes bajo tratamiento con supresores del ácido. Durante la evaluación de la ERGE, la presencia y la intensidad de los síntomas autonómicos (sequedad de la mucosa oral, hipersalivación, alteraciones en

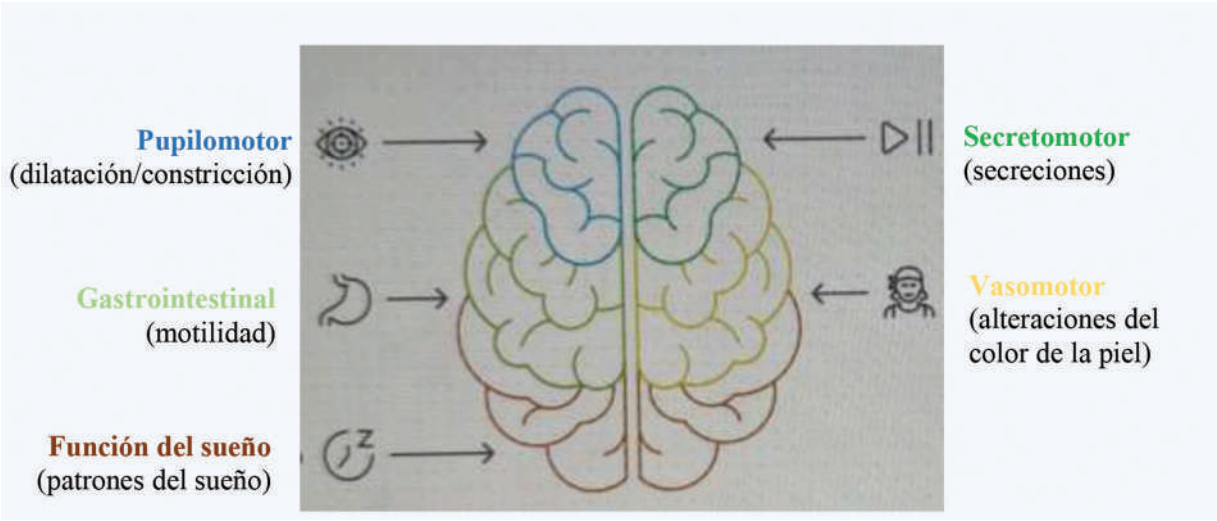

Figura 2. *Efectos del sistema nervioso autónomo*[22-26].

el ritmo cardiaco, disnea súbita, ansiedad, depresión, intolerancia ortostática, estado de alerta o hipervigilancia, y dolor torácico) no suelen ser considerados.

Sistema nervioso autónomo y enfermedad por reflujo gastroesofágico

El SNA está compuesto anatómicamente y funcionalmente por dos divisiones: 1) el sistema nervioso simpático (SNS) y 2) el sistema nervioso parasimpático (SNPS) (Figs. 2-4 y Tabla 1). Ambos son tónicamente activos y proporcionan una frecuencia variable de entradas neuronales (aumento o disminución) a los tejidos (potenciación o disminución). Esta característica mejora la capacidad para regular con mayor precisión la actividad funcional de un tejido. Sin la actividad tónica, la entrada neural a un tejido podría aumentar. El SNS y el SNPS trabajan en forma coordinada y, en general, tienen efectos opuestos[23].

Las fibras simpáticas (principalmente esplácnicas), como las parasimpáticas (vagales), inervan el EEI, siendo esencial la actividad parasimpática para su relajación reflexiva. Los aferentes sensoriales vagales provienen desde el EEI y el esófago distal, y hacen sinapsis en el núcleo del tracto solitario del rombencéfalo. Los eferentes vagales se originan en el núcleo motor dorsal y hacen sinapsis con el plexo mientérico del sistema nervioso entérico. El SNPS contribuye a las neuronas inhibidoras y excitadoras. Las fibras excitatorias surgen de la porción rostral del núcleo motor dorsal y las inhibidoras surgen de la porción caudal. El núcleo motor dorsal y el núcleo del tracto solitario forman un complejo vagal dorsal en el rombencéfalo que coordina el control reflejo del EEI[23].

Milovanovic et al.[21] reportaron que los pacientes con síntomas de ERGE tienen distorsión de los componentes del SNS y del SNPS. La función parasimpática deteriorada se ha asociada con la ERGE. La asociación entre síntomas gastrointestinales y arritmias cardíacas, como uno de los deterioros del SNA en la ERGE, se ha descrito como síndrome gastrocardíaco. El SNA tiene efectos en los diferentes sistemas; la neuropatía autonómica puede manifestarse en casi cualquier sistema. La hipotensión ortostática una de las manifestaciones más comunes de la disautonomía autonómica, pero pueden presentarse otras[24].

Disautonomía

El SNA controla las funciones corporales vitales (presión arterial, respiración, sistema gastrointestinal, frecuencia cardiaca, control de la temperatura corporal y actividad de la vejiga). El sistema nervioso central proporciona sus entradas al sistema nervioso entérico modulando el SNA para controlar las funciones gastrointestinales. El SNA está compuesto por una red controlada por los sistemas fisiológicos a través de entradas (interna y externa) para mantener la homeostasis. La red del sistema nervioso central, junto con el SNS y el SNPS, regulan las funciones

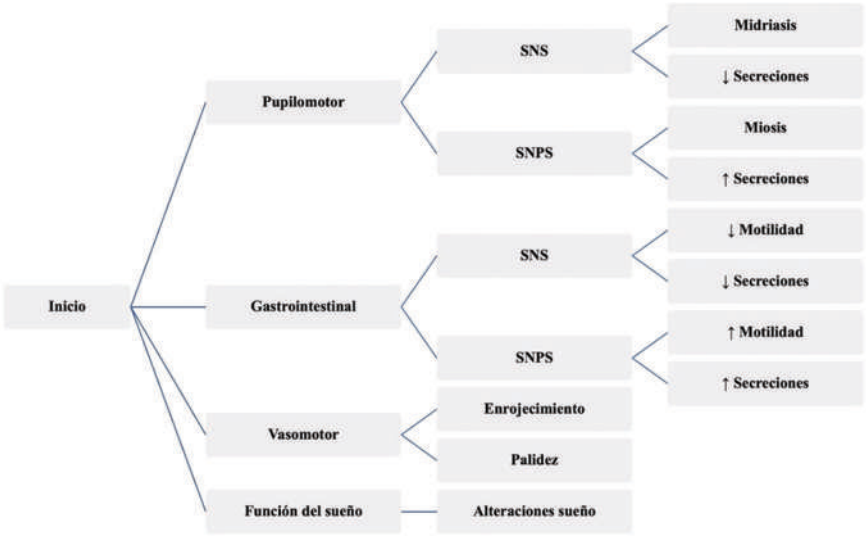

Figura 3. *Efectos sobre sistemas específicos[22-26]. SNPS: sistema nervioso parasimpático; SNS: sistema nervioso simpático.*

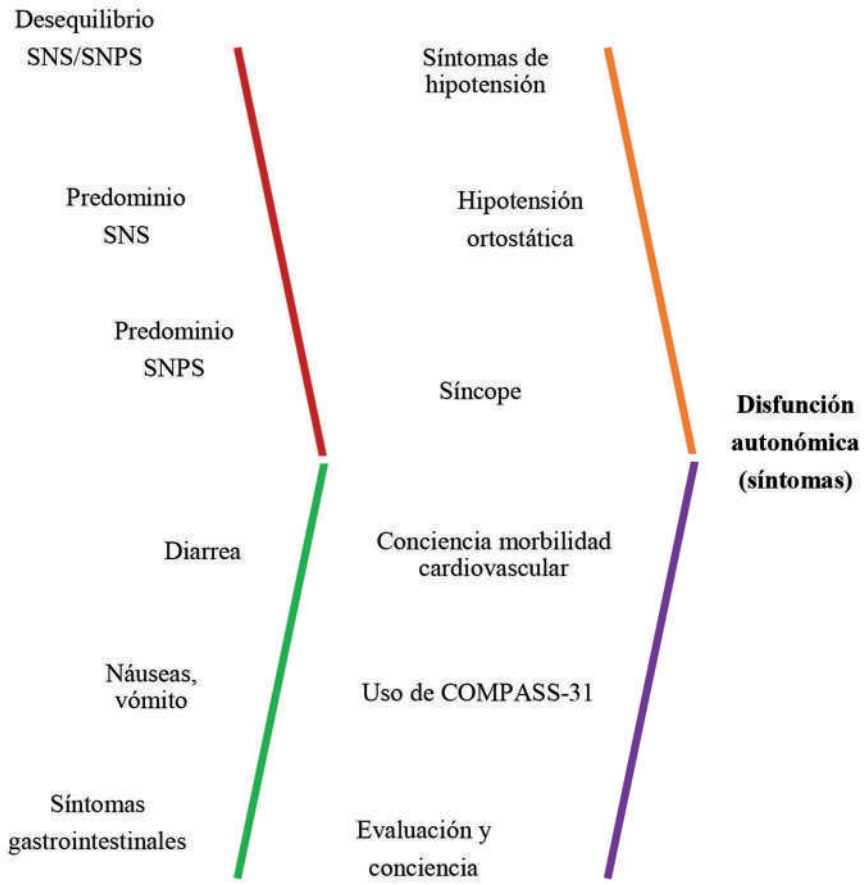

Figura 4. *Comprendiendo la disfunción autonómica[22-26]. SNPS: sistema nervioso parasimpático; SNS: sistema nervioso simpático.*

corporales, y cuando falla se expresa por diversas manifestaciones clínicas[22-25] (Tabla 1):

- Cardiovasculares: frecuencia cardiaca fija, hipotensión postural, taquicardia en reposo.
- Gastrointestinales: disfagia, gastroparesia, náuseas, vómitos, plenitud abdominal, constipación.
- Genitourinarias: atonía de la vejiga.

Tabla 1. Síntomas simpáticos y parasimpáticos que afectan al ser humano[23-25]

	Efecto de la estimulación	
Sistema/órgano	**Simpática**	**Parasimpática**
Ojo	Contracción del músculo radial del iris (dilatación de pupila: midriasis)	Contracción del músculo esfínter del iris (constricción de la pupila: miosis)
	Relajación del músculo ciliar (visión lejana)	Contracción del músculo ciliar (visión cercana)
Corazón	↑ frecuencia cardiaca	↓ frecuencia cardiaca
	↑ fuerza de contracción	
	↑ tasa de conducción	
Vasos sanguíneos	Vasoconstricción (mayoría de vasos sanguíneos), ↑ presión arterial	Vasodilatación (ciertos vasos sanguíneos)
Tracto gastrointestinal	↓ motilidad y secreciones	↑ motilidad y secreciones
Vejiga	Relajación del músculo detrusor	Contracción del músculo detrusor
Glándulas sudoríparas	↑ sudoración (diaforesis)	Sin efecto directo
Músculos piloerectores	Contracción (piel de gallina)	Sin efecto directo
Bronquios	Relajación (broncodilatación)	Contracción (broncoconstricción)
Pupilomotor	Dilatación pupila (midriasis)	Constricción pupila (miosis)
Gastrointestinal	↑ motilidad y secreciones, lo que puede llevar a estreñimiento	↑ motilidad y secreciones, facilitando la digestión
Secretomotor	↓ secreciones (excepto sudor)	↑ secreciones
Vasomotor	Cambios de color de la piel (enrojecimiento, palidez)	
Genitourinario	Dificultad en la erección	Función sexual normal
Función del sueño	Alteraciones del sueño	

- Pupilares: reflejos luminosos ausentes o retrasados, disminución del tamaño de la pupila.
- Sexuales: disfunción eréctil, eyaculación retrógrada.
- Sudomotoras: anhidrosis, salivación.
- Vasomotoras: extremidades frías (debido a la pérdida de respuestas vasomotoras), edema (debido a la pérdida del tono vasomotor y al aumento de la permeabilidad capilar).

Los síntomas más frecuentes de disautonomía son hipotensión ortostática, confusión, visión de túnel y malestar en la cabeza, el cuello o el tórax. Puede presentarse concomitantemente con hipertensión en decúbito supino debido al aumento de la resistencia periférica, que induce natriuresis, exacerbando la hipotensión ortostática. Hay muchos otros estímulos más benignos que pueden disminuir la presión arterial (bipedestación, deglución, maniobra de Valsalva, deshidratación, ejercicio, hiperventilación, calor, etc.) o aumentarla (reposo en decúbito supino, ingesta de agua o café, inclinación de la cabeza hacia abajo, hipoventilación, etc.)[25].

Se ha observado que los síntomas autonómicos son más frecuentes en los pacientes con ERGE que en voluntarios sanos. En el estudio de Milovanovic et al.[21] se detectó una disfunción autonómica grave en el 44.4 % de los pacientes con ERGE, comparado con el 7.9% de los controles ($p < 0.001$). Así mismo, la medición de la presión arterial ambulatoria de 24 h mostró valores significativamente más altos de presión arterial sistólica y presión del pulso en el grupo con ERGE comparado con el grupo de control[21].

Se ha sugerido que la disfunción parasimpática no es solo una consecuencia de la inflamación esofágica crónica, sino también el factor principal en la etiología de la ERGE. Las alteraciones en la actividad del SNA afectan tanto la contracción como la relajación transitoria del EEI (que actúa como una barrera de

reflujo), lo que lleva a la aparición y la progresión de la ERGE[23,26].

El esófago distal y el corazón comparten la inervación vagal aferente, lo cual dificulta distinguir entre la isquemia por dolor torácico del esófago y la cardiaca; el dolor esofágico imita el malestar cardiaco isquémico. En los contextos clínicos, esto conduce al diagnóstico erróneo de dolor torácico por RGE como angina de pecho, y viceversa[27]. La presencia de ERGE puede predisponer a la isquemia miocárdica al alterarse el equilibrio simpático-parasimpático por una función parasimpática alterada. Este mecanismo podría desencadenar un reflejo esofagogástrico-cardiaco, dando como resultado una disminución de la perfusión miocárdica. La ERGE y los trastornos de la interacción cerebro-intestino podrían estar asociados con una disfunción autonómica, que puede identificarse mediante la variabilidad de la frecuencia cardiaca[28].

El SNA con sus dos ramas, el SNS y el SNPS, también desempeña un papel fundamental en la modulación de las funciones cardiacas, como la arritmogénesis. Existe evidencia de que la hiperactividad del SNPS puede desencadenar arritmias «vagotónicas» (p. ej., fibrilación atrial paroxística, síndrome de Brugada, fibrilación ventricular idiopática)[29].

La variabilidad en la frecuencia cardiaca es menor en los pacientes con síntomas ERGE en comparación con los controles, lo cual indica una disfunción autonómica grave. Los pacientes con síntomas más graves exhiben una mayor dominancia simpática[29]. Otros autores reportan datos similares[30,31].

Basándose en un análisis de la variabilidad de la frecuencia cardiaca, Ali y Chen[32] reportaron que los trastornos de la interacción cerebro-intestino (antes trastornos funcionales gastrointestinales) y la ERGE estaban asociados con una disminución de la actividad parasimpática y un aumento de la actividad del SNS con el equilibrio autónomo desplazado hacia el sistema simpático. Estas afecciones fueron asociadas con disfunción autonómica, principalmente debido a la supresión del tono vagal y un simpático hiperactivo. Puede evaluarse de forma no invasiva utilizando las mediciones de la variabilidad en la frecuencia cardiaca.

Disautonomía, enfermedad por reflujo gastroesofágico y síntomas de COVID-19 prolongada

Una revisión sistemática informó que el análisis de la variabilidad de la frecuencia cardiaca fue consistente para detectar la reducción de la actividad parasimpática y la dominancia simpática en pacientes con trastornos del eje cerebro-intestino. Algunos estudios han reportado las relaciones de la frecuencia cardiaca (máxima/mínima) durante el cambio postural, la maniobra de Valsalva, el agarre manual y la respiración profunda para registrar la variabilidad del ritmo cardiaco en lugar de parámetros en el dominio del tiempo o la frecuencia. Seis de 15 estudios concluyeron que los pacientes tenían baja variabilidad de la frecuencia cardiaca en comparación con los controles. Cuatro estudios informaron una disminución de la actividad del SNPS y del SNS[33]. Djeddi et al.[33] estudiaron la actividad autónoma antes, durante y después del evento de RGE, y encontraron que la actividad del SNPS se suprime significativamente antes del evento de reflujo. Jones et al.[34] indicaron que un mejor control de la disfunción autónoma tiene un efecto positivo sonre la mejoría sintomática en la ERGE.

Los síntomas típicos incluyen fatiga crónica, síntomas gastrointestinales, confusión mental, taquicardia ortostática y disnea de esfuerzo. Estos pueden ser graves y debilitantes, y muchos pacientes quedan con incapacidad o independencia modificada. Las causas subyacentes de las denominadas secuelas posagudas del síndrome de SARS-CoV-2 (PASC, *postacute sequelae of SARS-CoV-2 infection*) aún no están aclaradas, pero ante la evidencia de la similitud entre la clínica de los fenotipos de PASC y el síndrome de taquicardia ortostática postural se ha postulado que la disautonomía puede desempeñar un papel en su fisiopatología. La activación compensatoria del sistema nervioso simpático en el síndrome de taquicardia ortostática postural puede causar taquicardia, insomnio, disfunción gastrointestinal y ansiedad, síntomas también comunes en las PASC[35].

Las PASC se presentan en muchas formas y afectan a todos los órganos del cuerpo. Esta presentación heterogénea sugiere la participación del SNA. Hasta ahora, los estudios sobre la desregulación del SNA en personas con PASC han sido en gran medida observacionales y descriptivos, basados en inventarios de síntomas o en medidas objetivas, pero indirectas, de la función cardiovascular, y han prestado poca atención a los componentes adrenomedular, hormonal y nervioso entérico del SNA[36].

La detección temprana (presencia e intensidad) de los síntomas disautonómicos en los pacientes con síntomas de ERGE crónicos, cuya prevalencia en nuestro país es alta, independientemente del riesgo

cardiometabólico, puede mejorar la respuesta al tratamiento con fármacos supresores ácidos, procinéticos o neuromoduladores, en especial en los pacientes con una exposición esofágica normal al ácido (hipersensibilidad al reflujo), lo cual puede contribuir a mejorar su calidad de vida.

El equilibrio entre el SNS y el SNPS es crucial para mantener la homeostasis y prevenirc las arritmias cardiacas. El desequilibrio puede manifestarse con una variedad de síntomas, y su identificación y tratamiento pueden ser importantes en el manejo de diversas condiciones clínicas.

Los síntomas autonómicos se presentan con mayor frecuencia en el periodo posprandial en los pacientes con ERGE crónica. Nuestro grupo considera que este es un fenotipo diferente en la ERGE que no ha sido evaluado de manera adecuada. El incremento en la frecuencia y en la intensidad de las alteraciones autonómicas en la ERGE (no erosiva, diabéticos, obesos, post-COVID-19) producido por el desequilibrio entre el SNS y el SNPS requiere la realización de estudios clínicos con cuestionarios clínicos y mediciones de la variabilidad de la frecuencia cardiaca) cardiaca para evaluar el impacto sobre la salud, la respuesta a tratamiento y la calidad de vida. El Consenso de Montreal debería considerar los fenómenos disautonómicos como un subtipo especial.

Escenarios clínicos

La figura 5 muestra el abordaje diagnóstico en escenarios clínicos de pacientes con ERGE y síntomas autonómicos.

Síntomas autonómicos aislados

Cualquier sujeto sano o con ERGE leve puede manifestar síntomas autonómicos posterior a una abundante ingesta de alimentos (chile, grasa o condimentos), los cuales son infrecuentes, de corta duración y baja intensidad. Las medidas higiénico-dietéticas y el adecuado control de la supresión ácida serán suficientes para aliviar los síntomas.

ERGE crónica con síntomas autonómicos

Los pacientes pueden referir mayor intensidad de síntomas autonómicos en el posprandio mediato (asociado al volumen y al tipo de alimento), de aparición súbita, difíciles de explicar y que desencadenan ansiedad ante el miedo de sufrir una enfermedad cardiaca (dolor torácico, taquicardia o bradicardia, disnea, sequedad de boca o confusión mental) o complicaciones de la ERGE (odinofagia, disfagia, distensión y dolor abdominal epigástrico, cáncer). Generalmente están asociados con factores detonantes (cambios bruscos de dieta, ayuno prolongado, ingesta de fármacos analgésicos, antiinflamatorios, esteroides u hormonales, y estrés postraumático). Estos síntomas pueden manifestarse de manera ocasional o persistente.

Si los síntomas autonómicos son persistentes, se deberá considerar el uso de cuestionarios clínicos y la prueba de variabilidad de la frecuencia cardiaca[21]. Los síntomas son desencadenados por la supresión del tono vagal y un simpático hiperactivo[21,22,24]. Los fármacos supresores del ácido neutralizan el pH intragástrico, pero no tienen efecto significativo para paliar los síntomas. En este grupo debe considerarse lo siguiente:

- Síntomas típicos de la ERGE (pirosis y regurgitación): incremento en la duración y la intensidad, incluso con la ingesta de agua o de alimentos no irritantes.
- Dolor torácico opresivo: es complejo distinguir el origen cardiaco del esofágico, ya que tienen la misma inervación. El dolor puede ser desencadenado con la ingesta de agua o de alimentos no irritantes. Muestra carácter difuso (difícil localización), pobre relación con la enfermedad (o la intensidad del estímulo) que lo origina, capacidad de producir respuestas autonómicas de gran intensidad y capacidad de generar sensaciones referidas (dolor referido). En el tracto gastrointestinal, la relación entre daño tisular y dolor no es obvia; estímulos relativamente leves (contracción tónica de la musculatura lisa, inflamación leve de la mucosa o isquemia leve) pueden producir reacciones intensas de dolor[37].
- Dispepsia: uno de los síntomas más frecuentes es la saciedad temprana, seguida de distensión abdominal con o sin dolor epigástrico, náuseas y eructos.
- Disfagia con o sin *globus.*
- Sobreposición sintomática.

En este grupo deben considerarse las mediciones objetivas del RGE (endoscopia e impedanciometría intraluminal multicanal con pH-metría de 24 h)[16,18] y la optimización de los fármacos supresores del ácido, procineticos, agentes para mejorar la acomodación gástrica o neuromoduladores.

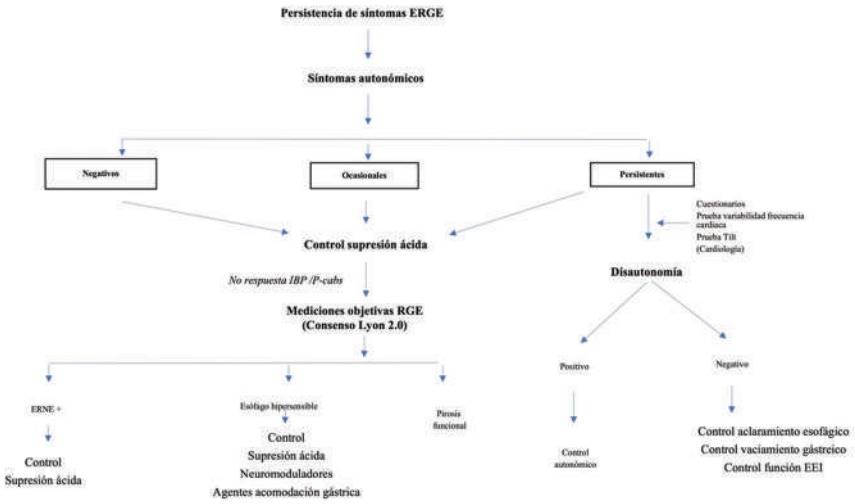

Figura 5. *Propuesta de abordaje en pacientes con enfermedad por reflujo gastroesofágico (ERGE) y síntomas autonómicos. EEI: esfínter esofágico inferior; ERNE: enfermedad por reflujo no erosiva; IBP: inhibidores de la bomba de protones.*

Disautonomía (prueba diagnóstica: tilt test)

Los síntomas más frecuentes de disautonomía son hipotensión ortostática, confusión, visión de túnel y malestar en la cabeza, el cuello o el tórax[26]. El estrés, el calor, el ayuno prolongado, el desvelo, la deshidratación y la falta de apego al tratamiento cardiológico pueden ocasionar un incremento en la frecuencia, la duración y la intensidad de los síntomas en los diferentes sistemas. Los mecanismos fisiopatológicos en la ERGE (alteraciones en el EEI, vaciamiento esofágico alterado y retraso del vaciamiento gástrico) son controlados por el SNA (fibras vagales). La inervación parasimpática desempeña un papel importante en la regulación del tono del EEI[38], y este se incrementa con un mal control de la disautonomía. En estos casos, es difícil tratar de comprobar la causalidad, pero son enfermedades asociadas que influyen en una mala calidad de vida. Un buen control de los síntomas de ERGE mejorará el control autonómico, y viceversa.

Conclusiones

La vida humana depende del SNA, pues controla funciones corporales involuntarias, como la presión arterial, el sistema gastrointestinal, la frecuencia cardiaca y la actividad de la vejiga. Por lo anterior, se sugiere evaluar la frecuencia y la intensidad de los síntomas autonómicos en los sujetos con ERGE, y la presencia de manifestaciones esofágicas y extraesofágicas en pacientes con síntomas autonómicos persistentes y disautonómicos.

Financiamiento

Los autores declaran no haber recibido financiamiento para este estudio.

Conflicto de intereses

Los autores declaran no tener conflicto de intereses.

Consideraciones éticas

Protección de personas y animales. Los autores declaran que para esta investigación no se han realizado experimentos en seres humanos ni en animales.

Confidencialidad, consentimiento informado y aprobación ética. El estudio no involucra datos personales de pacientes ni requiere aprobación ética. No se aplican las guías SAGER.

Declaración sobre el uso de inteligencia artificial. Los autores declaran que no utilizaron ningún tipo de inteligencia artificial generativa para la redacción de este manuscrito.

Bibliografía

1. Katz PO, Dunbar KB, Schnoll-Sussman FH, Greer KB, Yadlapati R, Spechler SJ. ACG clinical guideline for the diagnosis and management of gastroesophageal reflux disease. Am J Gastroenterol. 2022:117: 27-56.

2. Iwakiri K, Fujiwara Y, Manabe N, Ihara E, Kuribayashi S, Akiyama J, et al. Evidence-based clinical practice guidelines for gastroesophageal reflux disease 2021. J Gastroenterol. 2022;57:267-85.
3. Jung HK, Tae CH, Song KH, Kang SJ, Park JK, Gong EJ, et al.; Korean Society of Neurogastroenterology and Motility. 2020 Seoul consensus on the diagnosis and management of gastroesophageal reflux disease. J Neurogastroenterol Motil. 2021;27:453-81.
4. Gyawali CP, Yadlapati R, Fass R. Updates to the modern diagnosis of GERD: Lyon consensus 2.0. Gut. 2024;73:361-71.
5. Olmos JA, Pandolfino JE, Piskorz MM. Latin American consensus on diagnosis of gastroesophageal reflux disease. Neurogastroenterol Motil. 2024;36:e14735.
6. El-Serag HB, Sweet S, Winchester CC. Update on the epidemiology of gastro-oesophageal reflux disease: a systematic review. Gut. 2014;63:871-80.
7. Woo JY, Pikov V, Chen JDZ. Neuromodulation for gastroesophageal reflux disease: a systematic review. J Trabsl Gastroenterol. 2023;1:47-56.
8. Sharma, P, Yadlapati, R. Pathophysiology and treatment options for gastroesophageal reflux disease: looking beyond acid. Ann NY Acad Sci. 2021;1486:3-14.
9. Tack J. The role of bile and pepsin in the pathophysiology and treatment of GERD. APT. 2006;24:10-6.
10. Rosen RD, Winters R. Physiology, lower esophageal sphincter. [Updated 2023 Mar 17]. En: StatPearls. Treasure Island (FL): StatPearls Publishing; 2023.
11. Bajwa SA, Toro F, Kasi A. Physiology, esophagus. En: StatPearls. Treasure Island (FL): StatPearls Publishing; 2023.
12. Sobrino-Cossío S, Teramoto-Matsubara O, Mateos-Pérez G, Abdo-Francis JM, Tawil J, Olguín-Ramírez C, et al. In search of the grail: a race for acid suppression. Rev Gastroenterol Mex. 2019;84:344-56.
13. Vakil N, van Zanten SV, Kahrilas P, Dent J, Jones R. The Montreal definition and classification of gastroesophageal reflux disease: a global evidence-based consensus. Am J Gastroenterol. 2006;101:1900-20.
14. Boeckxstaens GEE. Review article: the pathophysiology of GERD. Aliment Pharm Ther. 2008;26:149-60.
15. Tack J. The role of bile and pepsin in the pathophysiology and treatment of GERD. Aliment Pharm Ther. 2006;24:10-6.
16. Bredenoord AJ, Hemmink GJ, Smout AJ. Relationship between gastro-oesophageal reflux pattern and severity of mucosal damage. Neurogastroenterol Motil. 2009;21:807-12.
17. Scarpignato C. Poor effectiveness of proton pump inhibitors in non-erosive reflux disease: the truth in the end! Neurogastroenterol Motil. 2012;24:697-704.
18. Hunt RH, Cederberg C, Dent J. Optimizing acid suppression for treatment of acid-related diseases. Dig Dis Sci. 1995;40:24S-49S.
19. Hampel H, Abraham NS, El-Serag HB. Meta-analysis: obesity and the risk for gastroesophageal reflux disease and its complications. Ann Intern Med. 2005;143:199-211.
20. El-Serag HB, Ergun GA, Pandolfino J, Fitzgerald S, Tran T, Kramer JR. Obesity increases oesophageal acid exposure. Gut. 2007;56:749-55.
21. Milovanovic B, Filipovic B, Mutavdzin S, Zdravkovic M, Gligorijevic T, Paunovic J, et al. Cardiac autonomic dysfunction in patients with gastroesophageal reflux disease. World J Gastroenterol. 2015;21:6982-9.
22. Lee YC, Wang HP, Lin LY, Chuang KJ, Chiu HM, Wu MS, et al. Circadian change of cardiac autonomic function in correlation with intra-esophageal pH. J Gastroenterol Hepatol. 2006;21:1302-8.
23. McCorry LK. Physiology of the autonomic nervous system. Am J Pharm Educ. 2007;71:1-11.
24. Waxenbaum JA, Reddy V, Varacallo M. Anatomy, autonomic nervous system. En: StatPearls. Treasure Island (FL): StatPearls Publishing; 2025.
25. Valenti VE, Vanderlei LCM, Godoy MF. Editorial: Understanding the role of the autonomic nervous system in health and disease. Front Neurosci. 2024;18:1446832.
26. Amarasiri DL, Pathmeswaran A, de Silva HJ, Ranasinha CD. Response of the airways and autonomic nervous system to acid perfusion of the esophagus in patients with asthma: a laboratory study. BMC Pulm Med. 2013;13:33.
27. Liuzzo JP, Ambrose JA. Chest pain from gastroesophageal reflux disease in patients with coronary artery disease. Cardiol Rev. 2005;13:167-73.
28. Dobrzycki S, Baniukiewicz A, Korecki J, Bachórzewska G, Prokopczuk P, Musial W, et al. Does gastro-esophageal reflux provoke the myocardial ischemia in patients with CAD? Int J Cardiol. 2005;104:67-72.
29. Wang H-M, Huang P-Y, Yang S-C, Wu M-K, Tai WC, Chen, CH, et al. Correlation between psychosomatic assessment, heart rate variability, and refractory GERD: a prospective study in patients with acid reflux esophagitis. Life. 2023;13:1862.
30. Roman S, Keefer L, Imam H, Korrapati P, Mogni B, Eident K, et al. Majority of symptoms in esophageal reflux PPI non-responders are not related to reflux. Neurogastroenterol Motil. 2015;27:1667-74.
31. Barlow WJ, Orlando RC. The pathogenesis of heartburn in nonerosive reflux disease: a unifying hypothesis. Gastroenterology. 2005;128:771-8.
32. Ali MK, Chen JDZ. Roles of heart rate variability in assessing autonomic nervous system in functional gastrointestinal disorders: a systematic review. Diagnostics. 2023;13:293.
33. Djeddi DD, Kongolo G, Stéphan-Blanchard E, Ammari M, Léké A, Delanaud S, et al. Involvement of autonomic nervous activity changes in gastroesophageal reflux in neonates during sleep and wakefulness. PLoS One. 2013;8:e83464.
34. Jones EL, Perring S, Khattab A, Allenby-Smith O. The effects of proton pump inhibitors on autonomic tone in patients with erosive and non-erosive esophagitis. Neurogastroenterol Motil. 2016;28:659-64.
35. Chung TH, Azar A. Autonomic nerve involvement in post-acute sequelae of SARS-CoV-2 syndrome (PASC). J Clin Med. 2022;12:73.
36. Goldstein DS. Post-COVID dysautonomias: what we know and (mainly) what we don't know. Nat Rev Neurol. 2024;20:99-113.
37. Boeckxstaens G, Camilleri M, Sifrim D, Houghton LA, Elsenbruch S, Lindberg G, et al. Fundamentals of neurogastroenterology: physiology/motility – sensation. Gastroenterology. 2016;150:1292-304.e2.
38. Triki L, Gammoudi N, Chtourou L, Gallas S, Tahri N, Zouari HG. Dysfunction of the autonomic nervous system in gastro-esophageal reflux disease: consequences for the cardiovascular system. Neurophysiol Clin. 2024;54:103009.

CASO CLÍNICO

A rare cause of intestinal obstruction: sock ingestion

Una causa rara de obstrucción intestinal: ingestión de calcetines

Mustafa Azizoğlu[1], Salih Bayram[2], Bahattin Aydoğdu[1], and Mehmet H. Okur[1]*

[1]Department of Pediatric Surgery Dicle University Medical School, Diyarbakır; [2]Department of Pediatric Surgery, Mardin Training and Research Hospital, Mardin. Turkey

Abstract

Although most foreign bodies leave the gastrointestinal tract spontaneously without causing serious injuries such as bleeding and obstruction, they can sometimes occlude the intestine and may present with symptoms of ileus. A 14-year-old boy with cerebral palsy was admitted to our center due to persistent bilious vomiting. A foreign body (sock) was seen in the jejunal loops at laparotomy. Enterotomy and enterostomy were performed.

Keywords: *Socks ingestion. Foreign body. Children.*

Resumen

Aunque la mayoría de los cuerpos extraños abandonan el tracto gastrointestinal de forma espontánea sin causar lesiones graves como sangrado y obstrucción, a veces pueden ocluir el intestino y pueden presentarse con síntomas de íleo. Un niño de 14 años con parálisis cerebral ingresó en nuestro centro por vómitos biliosos persistentes. Se observó un cuerpo extraño (calcetín) en las asas yeyunales en la laparotomía. Se realizó enterotomía y enterostomía.

Palabras clave**:** *Ingestión de calcetines. Cuerpo extraño. Niños.*

Introduction

Foreign body ingestion is one of the common problems among children[1]. Of the many kinds of objects found in such cases, which include coins, pins, button batteries, magnets, and many others, the most common objects found in most countries were coins[1,2]. Ingested foreign bodies can lodge anywhere in the gastrointestinal (GI) tract, including the proximal esophagus, distal esophagus, and stomach. The diversity of the foreign bodies and lodging positions can cause different severities of complications such as bledding and obstruction[2,3] A plain radiography can be the most useful investigation. The radiograph demonstrates the location, number, size, and shape of any foreign bodies[3].

Case report

A 14-year-old boy with cerebral palsy and medical history of foreign body ingestion was admitted to the emergency department due to intractable vomiting. The patient presented with a 2-day history of the inability to defecate, retch, nausea, bilious vomiting, restlessness, and abdominal pain. On abdominal examination, tenderness was observed. There was no gas and stool output after the rectal enema. At the admission, body

***Correspondence:**
Mustafa Azizoğlu
E-mail: mdmazizoglu@gmail.com

Date of reception: 12-04-2022
Date of acceptance: 04-05-2022
DOI: 10.24875/CIRU.22000216

Cir Cir. 2025;93(2):221-223
Contents available at PubMed
www.cirugiaycirujanos.com

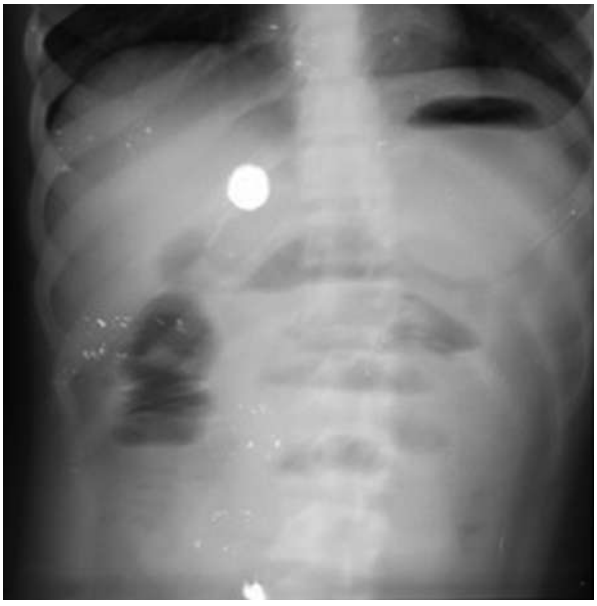

Figure 1. *X-ray shows several air-fluid levels.*

Figure 2. *Computed tomography; the foreign body observed in bowel loop.*

temperature: 37.5°C, blood pressure: 110/76 mmHg, heart rate: 96/min, C-reactive protein: 1.25 mg/dL, WBC: 22.74, and NEU: 20.9. The X-ray revealed an air-fluid level with partial obstruction (Fig. 1).

The CT reports noted intestinal obstruction and ileus secondary to foreign body ingestion (Fig. 2).

Then, the patient underwent a laparotomy. All bowel loops were checked. We found that proximal intestinal loops were dilated. The foreign body (sock) was palpable at 110 cm of the ligament of traits (Fig. 3). Enterotomy was performed at this point of the intestine on the antimesenteric face and the sock was removed. And then, the intestine was repaired with a double layer of continuous stitching. Endoscopy was performed on the patient, and after making sure that there was no other foreign body. The surgical intervention was completed without complications.

Oral feeding was started at the post-operative 48th h. The patient was discharged uneventfully at the 72nd h postoperatively.

Discussion

Foreign body ingestion is a pediatric emergency disease that is very common in children, especially in mentally retarded individuals, and does not require surgery in the vast majority, but the surgical situation varies according to the location of the foreign body[1]. Although the majority of foreign bodies leave the GI tract spontaneously, especially large foreign bodies with the potential to adhere to the intestines cannot leave, and surgical intervention is required for these[2,3]. Some of these foreign bodies can be life-threatening[2]. When we look at the overall event, approximately 10-20% of cases of foreign body ingestion require endoscopic removal, while < 1% needs surgery to take out the foreign body or to treat complications[4]. Abdominal radiography is the first preferred radiological study in foreign body ingestion[4,5]. For this patient too, at admission, abdominal radiography was performed firstly. CT can be performed only in patients with suspected complications and for differential diagnosis[4-6]. Therefore, we performed CT for differential diagnosis of other causes of ileus. Laparotomy was performed on the patient after abdominal CT was reported as having intestinal obstruction due to a foreign body. For the patient with a history of foreign body, endoscopy was also performed; in case, there was a foreign body in the stomach. The main complications of the FBI in the bowel involve mucosal bleeding, intestinal obstruction, and perforation[1,4,7]. In this patient, we thought intestinal obstruction was due to a foreign

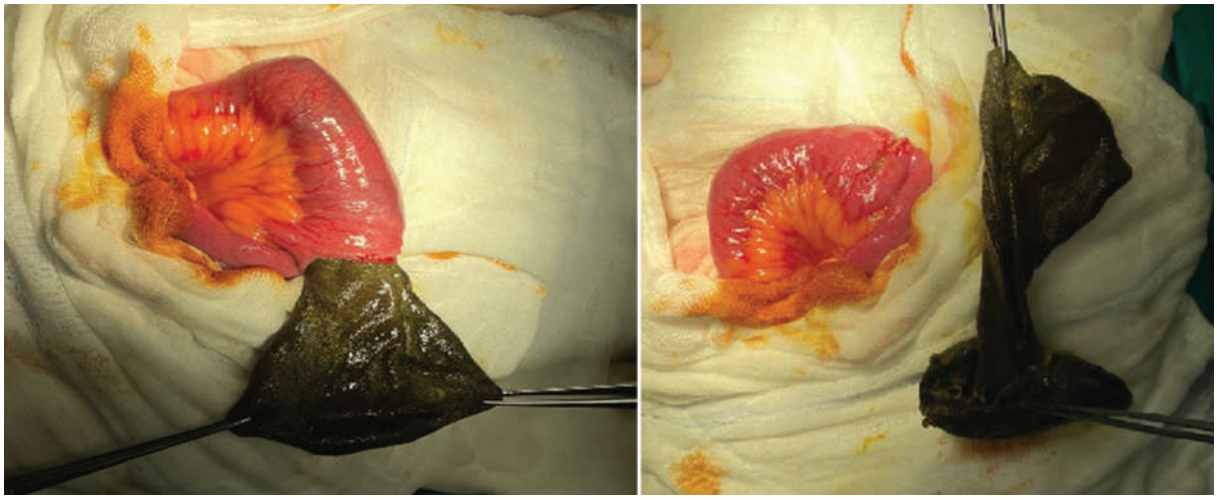

Figure 3. *The sock was clearly seen in the bowel loop.*

body, and therefore, we performed a laparotomy. Foreign bodies impacted in the intestine can be removed by performing enterotomy[8]. Thus, we performed an enterotomy and successfully removed the foreign body.

Conclusion

Especially when mentally retarded patients present with intestinal obstruction, it should be considered that they may have swallowed a foreign body, and CT may be performed to confirm the diagnosis in these patients. At the same time, considering that these patients may swallow more than one foreign body, endoscopy may be performed during the surgery.

Funding

The authors declare that they have not received funding.

Conflicts of interest

The authors declare no conflicts of interest.

Ethical considerations

Protection of humans and animals. The authors declare that no experiments involving humans or animals were conducted for this research.

Confidentiality, informed consent, and ethical approval. The authors have followed their institution's confidentiality protocols, obtained informed consent from patients, and received approval from the Ethics Committee. The SAGER guidelines were followed according to the nature of the study.

Declaration on the use of artificial intelligence. The authors declare that no generative artificial intelligence was used in the writing of this manuscript.

References

1. Kramer RE, Lerner DG, Lin T, Manfredi M, Shah M, Stephen TC, et al. Management of ingested foreign bodies in children: a clinical report of the NASPGHAN endoscopy committee. J Pediatr Gastroenterol Nutr. 2015;60:562-74.
2. Liew AN, Suhardja TS, Arachchi A, Lim J. Plastic bread clip impacted in gastrointestinal tract: a case report and review of the literature. Clin J Gastroenterol. 2019;12:441-6.
3. Wang X, Zhao J, Jiao Y, Wang X, Jiang D. Upper gastrointestinal foreign bodies in adults: a systematic review. Am J Emerg Med. 2021;50:136-41.
4. Birk M, Bauerfeind P, Deprez PH, Häfner M, Hartmann D, Hassan C, et al. Removal of foreign bodies in the upper gastrointestinal tract in adults: European Society of Gastrointestinal Endoscopy (ESGE) Clinical Guideline. Endoscopy. 2016;48:489-96.
5. Crain MA, Lakhani DA, Kuhnlein R, Balar AB, Neptune S, Parrish D, et al. Small bowel obstruction from hollow foreign body ingestion: a case report and brief review of literature. Radiol Case Rep. 2021;16:1628-32.
6. Kumar D, Nair AV, Nepal P, Za Alotaibi T, Al-Heidous M, Macdonald DB. Abdominal CT manifestations in fish bone foreign body injuries: what the radiologist needs to know. Acta Radiol Open. 2021;10:1-8.
7. Volpi A, Laforgia R, Lozito C, Panebianco A, Punzo C, Ialongo P, et al. Ingestion of foreign bodies among prisoners: a ten years retrospective study at University Hospital of Southern Italy. G Chir. 2017;38:80-3.
8. Tewari S, Chigicherla S, Sharma RD, Redkar R. Multidisciplinary management for intestinal obstruction by Gel Ball ingestion. J Indian Assoc Pediatr Surg. 2021;26:120-2.

CASO CLÍNICO

Traqueoplastia *slide* sin *bypass* cardiopulmonar para el tratamiento de la estenosis congénita larga y compleja: reporte de caso y revisión de la literatura

Slide tracheoplasty without cardiopulmonary bypass for the treatment of long and complex congenital stenosis: case report and review of the literature

Rogelio Sancho-Hernández, Rubén E. Carlos-Corona y Lizbéth Solorio-Rodríguez*

Servicio de Cirugía Torácica Pediátrica; Servicio de Cirugía Cardiovascular; Servicio de Neonatología. Instituto Nacional de Pediatría, Ciudad de México, México

Resumen

La estenosis traqueal congénita es una afección que causa obstrucción aguda de la vía aérea y asocia unas altas morbilidad y mortalidad ante el retraso diagnóstico y por sus comorbilidad acompañante. La traqueoplastia slide es el procedimiento de elección y requiere tradicionalmente el uso de bypass cardiopulmonar para facilitar la técnica de reconstrucción traqueal. No existen reportes nacionales de esta traqueoplastia. Con una modificación a la descripción original se describe la técnica quirúrgica y se reporta un caso sin uso de bypass cardiopulmonar. Se propone una revisión de la literatura que permita orientar un abordaje y un tratamiento integrales.

Palabras clave: *Traqueoplastia. Traqueoplastia slide. Estenosis traqueal congénita. Broncoscopia.*

Abstract

Congenital tracheal stenosis is an entity that causes acute airway obstruction and is associated with high morbidity and mortality due to diagnostic delay and its accompanying comorbidity. Slide tracheoplasty is the procedure of choice that traditionally requires the use of cardiopulmonary bypass to facilitate the tracheal reconstruction technique. There are no national reports of this tracheoplasty. With a modification to the original description, the surgical technique is described and a case report executed without the use of cardiopulmonary bypass. A review of the literature is proposed to guide the comprehensive approach and treatment.

Keywords: *Tracheoplasty. Slide tracheoplasty. Congenital tracheal stenosis. Bronchoscopy.*

***Correspondencia:**
Rogelio Sancho-Hernández
E-mail: rogeliosanchohernandez@gmail.com

Fecha de recepción: 09-06-2022
Fecha de aceptación: 10-10-2022
DOI: 10.24875/CIRU.22000311

Cir Cir. 2025;93(2):224-230
Contents available at PubMed
www.cirugiaycirujanos.com

Introducción

La estenosis traqueal congénita (ETC) es una afección urgente que causa obstrucción aguda de la vía aérea y asocia una alta morbimortalidad ante el retraso diagnóstico y por la comorbilidad acompañantes. La ETC larga y compleja se caracteriza por la presencia de anillos traqueales completos a lo largo del segmento estenótico, lo que determina una estrechez fija del lumen traqueal que se expresa con estridor y dificultad respiratoria en la lactancia temprana. Las anormalidades cardiovasculares se presentan en un 69% de los casos, siendo las anomalías vasculares como el *sling* (anillo) de la arteria pulmonar las que determinan el pronóstico y la sobrevida. La broncoscopia es el estándar diagnóstico y la principal estrategia para la planeación quirúrgica y el seguimiento[1]. Desde su primera descripción por Tsang et al.[2] en 1989, la traqueoplastia *slide* es considerada el procedimiento de elección para la ETC larga, y requiere tradicionalmente el uso de *bypass* cardiopulmonar (BCP) para facilitar la técnica de reconstrucción traqueal. No existen reportes nacionales de esta traqueoplastia por deslizamiento *(slide)* para el tratamiento de la ETC. Con una modificación a la técnica original se describe el procedimiento quirúrgico y se reporta un caso de traqueoplastia *slide* ejecutada sin uso de BCP. Se propone una revisión de la literatura que permita orientar el tratamiento de esta emergencia congénita de la vía aérea.

Caso clínico

Varón de 3 meses de edad con trisomía 21 y retraso del crecimiento intrauterino, con estridor bifásico y dificultad respiratoria al nacimiento. Se logra la intubación con cánula endotraqueal (CET) de 3.5 mm que se detiene en el cuello sin lograr avanzar distal a la carina. Intubado por 1 mes y hospitalizado por 2 meses por neumonía, es egresado. Acude al servicio de urgencias con dificultad respiratoria grave y se estabiliza nuevamente con intubación endotraqueal de 3.5 mm con la punta de la CET a nivel del cuello. La ecocardiografía muestra un defecto septal atrial de 3 mm. Presenta hipertensión pulmonar de 50 mmHg y volumen espiratorio forzado del 65%, sin cardiopatías estructurales y estado de falla cardíaca secundario a un aumento en las resistencias de la vía aérea. Se realiza evaluación con broncoscopio flexible inicial de 2.8 mm, encontrando estenosis traqueal fija en el segundo anillo traqueal, extensa e infundibular de anillos completos, que no permite el paso del equipo. Se decide realizar dilatación traqueal rígida y asegurar la vía aérea con una CET de 3 mm hasta la carina. Con mejoría de las condiciones hemodinámicas, se realiza una tomografía computarizada con reconstrucción aérea que advierte estenosis traqueal larga, compleja, con colapso inspiratorio en el bronquio izquierdo. Con el paciente estable, se interviene para traqueoplastia *slide* (deslizamiento traqueal) a los 4 meses edad (Fig. 1).

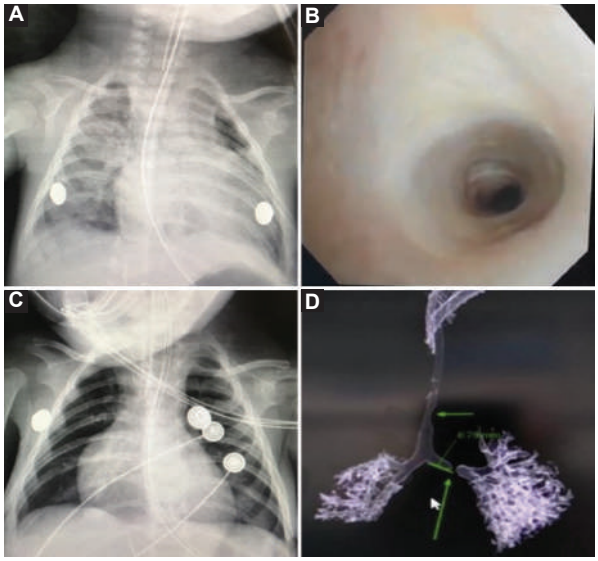

Figura 1. A: *lactante con estridor y dificultad respiratoria con cánula endotraqueal (CET) de 3 mm que se detiene a nivel de la vía aérea cervical.* **B:** *presencia de estenosis crítica infundibular de anillos completos a partir del segundo anillo traqueal que confirma el diagnóstico de estenosis traqueal congénita (ETC) por broncoscopia.* **C:** *avance distal hasta la carina de una CET de 3 mm posterior a la dilatación rígida traqueal que mejora las condiciones hemodinámicas y respiratorias.* **D:** *ETC de larga extensión con colapso inspiratorio en bronquio izquierdo en una reconstrucción tomográfica de la vía aérea.*

Técnica quirúrgica

Con intubación con CET de 3 mm en la carina se realiza esternotomía media con extensión cervical, disección con preservación de vasos supraaórticos hasta exponer totalidad de la tráquea hasta la carina y emergencias bronquiales, se transecciona la tráquea en el punto medio de la estenosis longitudinal y se resecan dos anillos traqueales completos y centrales, con la estrechez más crítica incluida, para evaluación patológica. Se realiza un corte longitudinal medial y anterior en el *slide* traqueal distal o inferior que permite la ventilación con CET de 3 mm con globo (esta modificación de la técnica original permitió la reconstrucción sin BCP convencional

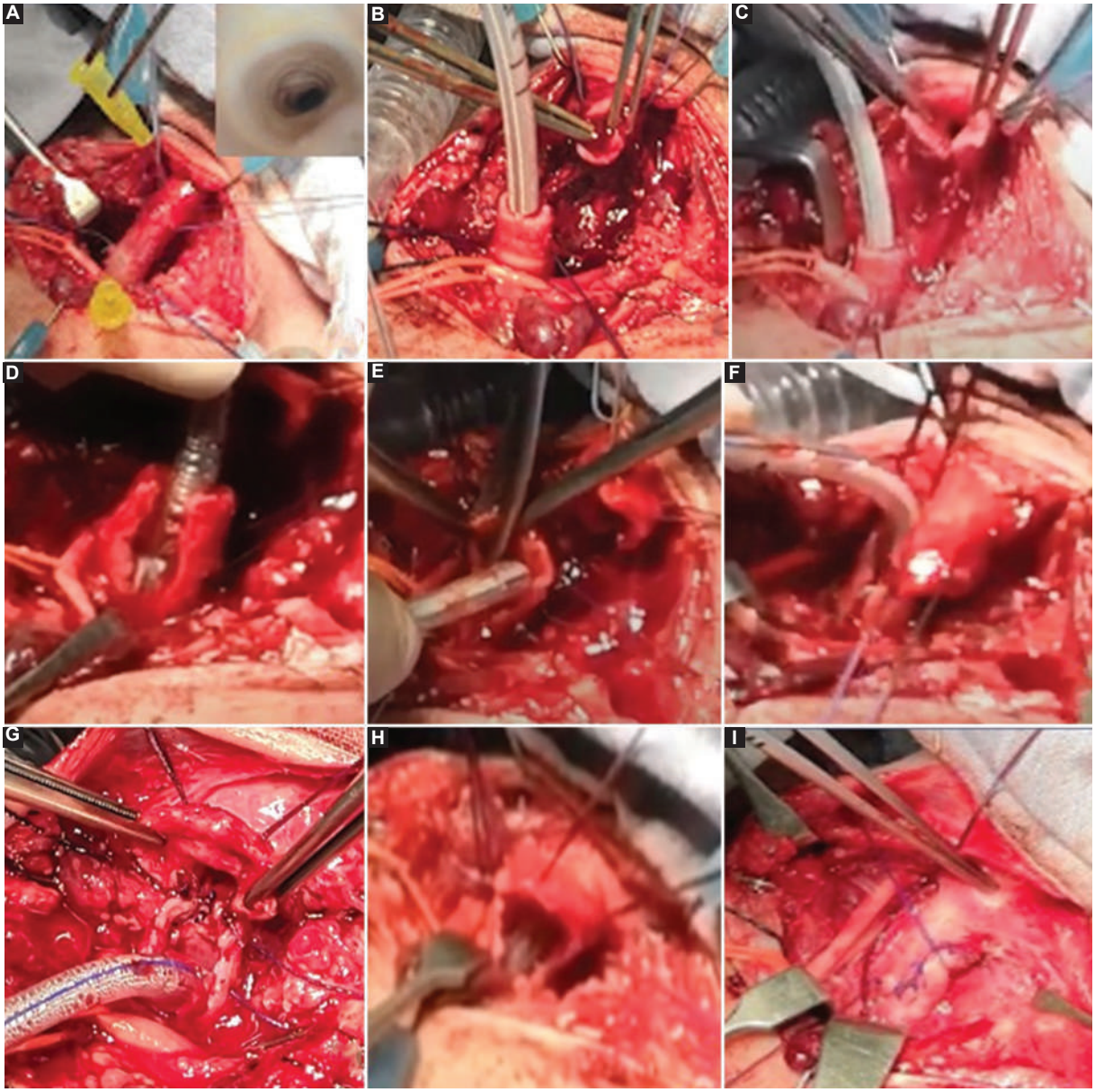

Figura 2. A: *esternotomía media y cervical con conservación de vasos supraaórticos exponiendo la totalidad de la tráquea. Se determina por broncoscopia transoperatoria la extensión de la estenosis traqueal congénita (ETC) y se marcan con dos agujas los extremos de la estenosis crítica. Obsérvese la grave reducción del calibre de la tráquea.* **B:** *transección de la ETC en el punto medio longitudinal entre las dos agujas cefálica y caudal previamente marcadas. Se corrobora la presencia diagnóstica de anillos traqueales completos con ausencia de tráquea membranosa en ambos cabos traqueales y se inicia la ventilación con cánula endotraqueal (CET) de 3 mm en el cabo traqueal distal.* **C:** *se prepara el cabo traqueal proximal como slide posterior: insición longitudinal media en la tráquea posterior con extensión al segundo anillo traqueal estenótico.* **D:** *preparación del cabo traqueal distal como slide anterior: insición longitudinal media de la pared traqueal anterior con extensión a la emergencia bronquial izquierda sobre la CET de 3 mm con globo inflado para ventilación transoperatoria. E: se espatulan los extremos triangulares de ambos slides para lograr una disposición en forma de «lengua».* **F:** *se corrobora el deslizamiento sin tensión de ambos slides sobrepuestos.* **G:** *anastomosis traqueal posterior iniciando en el vértice de ambos slides. La ventilación por slide distal prosiguió durante el transoperatorio.* **H:** *anastomosis y reconstrucción de la neotráquea anterior. Se avanza una CET de 3.5 mm para su edad.* **I:** *disposición final de la traqueoplastia slide (la pinza de disección señala el cartílago cricoides). Se corrobora la integridad de la reconstrucción traqueal bajo visión broncoscópica.*

durante todo el operatorio). Se prepara el cabo proximal o superior como *slide* posterior con un corte longitudinal medial y posterior, se espatulan los bordes de ambos *slides* traqueales hasta alcanzar una dispocisión en forma de lengua, se corrobora la aproximación de ambos cabos sobrepuestos sin tensión y con adecuada irrigación se completa la anastomosis por sobreposición de ambos *slides* o cabos traqueales preformados con sutura absorbible de Vicryl 4-0. Previamente completada la anastomosis

posterior, se avanza una CET de 3.5 mm sin globo, se completa la anastomosis anterior y se corrobora con una breve extubación y broncoscopia transoperatoria la integridad de la traqueoplastia *slide,* con aceptable aumento del calibre de su lumen y avance del equipo hacia la segmentación pulmonar, se aspiran las secreciones y se reintuba con CET de 3.5 mm por arriba de la neocarina. Es trasladado a cuidados intensivos sin drenajes (Fig. 2). En el seguimiento posoperatorio se realiza a los 7 días una extubación exitosa, con egreso a los 40 días del posquirúrgico. Cursa con reingresos por eventos sépticos asociados a su inmunodeficiencia que requieren intubación endotraqueal con CET para su edad en tres ocasiones sin incidentes. Al año de edad presenta granuloma y estenosis traqueal concéntrica y fibrosa del 50% en sitio de vértices de la traqueoplastia refractaria a manejo endoscópico. Se realiza traqueoplastia para resección de dos anillos traqueales en el tercio medio traqueal con anastomosis término-terminal sin complicaciones. Se advierte evidente crecimiento en longitud y lumen aéreo *post-slide,* con vía íntegra broncoscópica y asintomático a 2 años de seguimiento (Fig. 3).

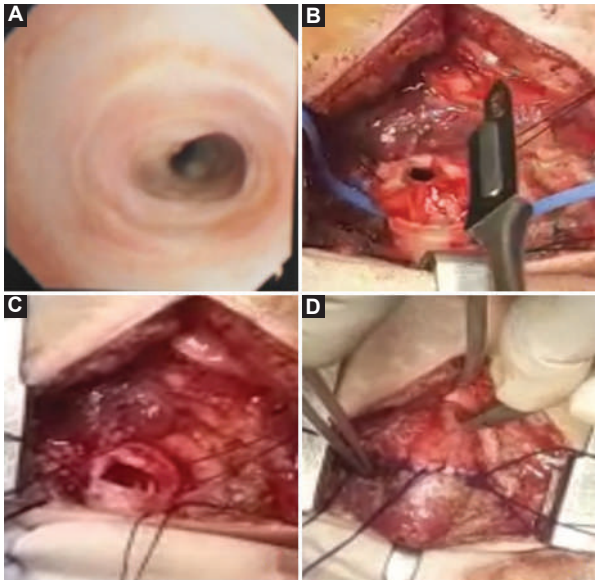

Figura 3. A: *estenosis intrínseca adquirida en la neotráquea post-slide refractaria a manejo endoscópico. Adviértase el incremento del lumen traqueal.* **B:** *sexto anillo traqueal estenótico resecado.* **C:** *traqueoplastia con anastomosis término-terminal sin tensión con cánula endotraqueal para su edad.* **D:** *se advierte la neotráquea post-slide con incremento diametral y longitudinal superior a la estenosis traqueal congénita en la figura 2A.*

Discusión

Se han descrito numerosas técnicas para la reconstrucción quirúrgica de la ETC: resección y anastomosis término-terminal traqueales, traqueoplastia de aumento con parche pericárdico o cartílago costal autólogos, y traqueoplastia *slide* o por deslizamiento. Desde su primera descripción por Tsang et al.[2] en 1989, la traqueoplastia *slide* se ha aceptado como la técnica de reconstrucción preferida, con mayores ventajas pronósticas y quirúrgicas sobre otros métodos: reconstrucción traqueal definitiva y rígida, con estabilidad en la vía aerea con tejido traqueal vascularizado y preservado que impacta en una reconstrucción traqueobronquial sin excesiva tensión, duplica la circunferencia traqueal y aumenta hasta cuatro veces el área traqueal, extubación temprana con reducción en la formación de tejido de granulación y con un potencial crecimiento traqueal en el posquirúrgico y el seguimiento[3]. La broncoscopia es la estrategia diagnóstica más importante, pues corrobora, como en nuestro paciente, la presencia característica de anillos traqueales cartilaginosos completos, así como la ausencia de tráquea membranosa; además, permite decidir la estrategia quirúrgica ante malformaciones aerodigestivas asociadas, como la compresión pulsatil en la vía aérea de algún anillo vascular acompañante y las lesiones adquiridas resultantes del trauma en la intubación endotraqueal y el escenario de intervenciones endoscópicas o quirúrgicas previas. La broncoscopia asistió la dilatación rígida terapéutica y aseguró la vía aérea para mejorar las condiciones hemodinámicas y preoperatorias del paciente. Cuando la evaluación endoscópica distal de la vía aérea no es posible por la estrechez crítica del lumen traqueal, la tomografía computarizada con reconstrucción tridimensional de la vía aérea permite graduar la extensión y la gravedad de la vía aérea comprometida; así mismo, descarta la presencia de malformaciones cardiovasculares asociadas evaluadas funcionalmente durante la ecocardiografía. Ambos elementos complementan la elección de la estrategia quirúrgica más apropiada[4].

La mitad de los pacientes con ETC acompañan un anillo vascular tipo *sling* de la arteria pulmonar, por lo que su reconocimiento preoperatorio es obligado para realizar convencionalmente la reimplantación vascular de la arteria pulmonar izquierda a la porción troncal de la arteria pulmonar principal simultánea, junto con la traqueoplastia *slide,* en el 60% con asistencia del BCP[5]. La ventilación preoperatoria previa es requerida, como en nuestro caso, en el 31% de los pacientes

ante la presencia de estridor y dificultad respiratoria en la sala de reanimación neonatal. La dificultad para avanzar una CET de 3.5 mm en el recién nacido de término hacia la vía aérea distal debe advertir al pediatra de la posibilidad de una obstrucción congénita de la vía aérea. Abocar inmediatamente por debajo de las cuerdas vocales la CET o una menor de 3 mm suficiente para ventilar al paciente son medidas aceptables para asegurar la vía aérea y evitar el trauma adquirido agregado a las maniobras de intubación que empeoran el pronóstico de la ETC. La broncoscopia es obligada, pues este abordaje evitará la realización errónea de una traqueostomía como conducta inadvertida. Los días de ventilación mecánica y la estancia hospitalaria promedian los 7 y 20 días, respectivamente. Se ha encontrado que la mortalidad hospitalaria estaba relacionada con el inicio de oxigenación con membrana extracorpórea [ECMO]) preoperatoria más que el uso concomitante de BCP. La estancia hospitalaria prolongada está influenciada por la complejidad de la malformación en la vía aérea y por los efectos sistemicos en la duración del soporte con BCP, sin influenciar en la sobrevida; esta última se ve afectada por la necesidad de una cirugía intracardíaca simultánea. Entonces, las ETC aisladas sin *sling* pulmonar o sin malformaciones intracardíacas podrían beneficiarse, como en nuestro caso, de la traqueoplastia *slide* posterior a los 3 meses de edad sin los factores de riesgo asociados al BCP: hemorragia intraoperatoria con incremento en la transfusión de hemoderivados, efectos sistémicos de la heparinización y la sobrecarga hídrica, este último con impacto en la generación de edema y riesgo de dehiscencia en la línea de sutura de la anastomosis traqueal.

La duración prolongada de la ventilación mecánica posoperatoria se ha asociado a reintervenciones en la vía aérea, esto favorecido quizás por el trauma endotraqueal que agrega daño local durante las estrategias de intubación endotraqueal. Así mismo, la complejidad de la ETC y la edad menor de 3 meses al momento de la traqueoplastia *slide* son otros factores asociados a mortalidad hospitalaria[6].

Grillo et al.[7] publicaron los primeros reportes en torno a la traqueoplastia *slide* sin uso de BCP, corroborando también el crecimiento satisfactorio de la vía aérea a largo plazo posterior a la intervención. Al igual que en nuestro caso, se modificó la descripción original de Tsang et al.[2] preparando inicialmente con una incisión medial y longitudinal en la cara anterior de la porción distal traqueal un *slide* anterior que permite ventilar con una CET con globo para la edad del paciente la vía aérea y pulmonar durante el transoperatorio, contrario a la recomendación original de incidir el segmento proximal anteriormente y el segmento distal posteriormente bajo el apoyo de la circulación con BCP. Iniciamos la anastomosis superiormente en la pared posterior, no encontramos dificultades para culminar la anastomosis y no hubo necesidad de retirar y reinsertar la CET para facilitar la anastomosis del *slide* traqueal[7]. La otra modificación fue espatular los bordes libres de los cabos preformados de tal manera que se lograra una sobreposición hermética y perfecta con forma de «lengua» de ambos *slides*[2,8], en lugar de la disposición triangular de las incisiones originales que predisponían a una línea de sutura sobreponiendo los cabos y fomentando la característica deformidad en «ocho» de la visión broncoscópica. Creemos también que esta modificación evita la exposición cartilaginosa intraluminal de dicha deformidad como predisponente de reestenosis recurrentes y refractarias. Se ha documentado la seguridad de esta técnica, reservando el uso de BCP con canulación bicaval con moderada hipotermia y cardioplejia para acompañar los procedimientos intracardíacos o aquellos con fisiología cardíaca limítrofe. En ausencia de una reparación intracardíaca, la canulación venosa simple con BCP en normotermia es suficiente[8]. Se recomiendan las actuales tendencias de extubacion temprana desde el posoperatorio inmediato e inclusive las técnicas de ventilación no invasiva (ventilación nasal de alto flujo, presión positiva con dos niveles de presión [BiPAP], presión positiva continua en la vía respiratoria [CPAP]), que generan menor daño local y edema sobre la anastomosis.

Para optimizar la estrategia quirúrgica más recomendable para cada paciente basada en los pronósticos de mortalidad y anomalías cardiovasculares asociadas se han propuesto tres grupos:

- Con una ETC larga aislada, la traqueoplastia *slide* podría ser recomendada con o sin el uso de soporte de BCP; grupo de mortalidad baja.
- Con una ETC larga con anomalías vasculares y cardíacas no complejas (*sling* de la arteria pulmonar, defectos septales y atriales, etc.), la traqueoplastia *slide* y la anomalía intracardíaca simple podrían ser corregidas simultáneamente.
- Con una ETC larga y anomalías cardíacas y vasculares complicadas (estenosis pulmonar crítica, tetralogía de Fallot con ausencia de válvula pulmonar, bloqueo al flujo de salida del ventrículo derecho, etc.), en las que la duración del BCP es el principal factor pronóstico de mortalidad, se sugiere

una estrategia quirúrgica en etapas: estabilización de la vía aérea inicial (como en nuestro caso), traqueoplastia *slide* y corrección de la cardiopatía intracardíaca en tiempos quirúrgicos diferentes.

En las ETC con extensión menor del 20% de la longitud traqueal total es recomendable la resección y anastomosis término-terminal traqueal. En nuestro caso fue posible practicarla como reoperación de una lesión adquirida local de estenosis secundaria al trauma de intubación y tejido de granulación asociados. Se puede corroborar durante la traqueoplastia de reintervención el crecimiento traqueal transversal y longitudinal, radiológico y endoscópico, documentado en varios reportes posteriores a la traqueoplastia *slide*[9]. Deben realizarse, desde el posquirúrgico inmediato hasta el tardío, la detección y corrección de las complicaciones mayores y menores. Las complicaciones mayores justifican las intervenciones oportunas y tempranas; por ejemplo, la dehiscencia anastomótica en los primeros 10 días posoperatorios con datos de sepsis y fuga aérea que requerirá una broncoscopia inmediata diagnóstica y estabilizar la vía aérea con una intubación endotraqueal videoasistida, con insuflación temporal de un globo distal a la dehiscencia, o la intubación bronquial selectiva para mejorar las condiciones para una inmediata reoperación idónea. La broncoscopia, en todos los casos, como una intervención menor garantiza el potencial éxito del manejo conservador con terapia tópica antiinflamatoria y terapia nebulizada con broncodilatación de algunas secuelas tempranas asociadas a la intubación endotraqueal y ventilación mecánica desde el edema, evaluación de malacia y traqueoendobronquitis hasta la resección endoscópica temprana de granulomas inflamatorios. Las complicaciones menores, como la formación subaguda o tardía de tejido de granulación, podrían requerir, como en nuestro caso, la remoción de tejido de granulación con fórceps o dilatación traqueal neumática con esteroide local y sistémico. Ante la recurrencia fibrótica y la reestenosis traqueal por tejido de granulación y la refractariedad en el manejo endoscópico previo están justificadas las intervenciones tardías y mayores para resección estenótica y anastomosis término-terminal traqueal, como ocurrió en el presente caso.

A medida que la mortalidad intrahospitalaria previa al egreso y posterior a la traqueoplastia *slide* ha disminuido desde un 30% hasta un 6% secundario al manejo multidisciplinario con reconocimiento temprano y tratamiento de las complicaciones, la mejoría en las variables de la técnica quirúrgica y los cuidados intensivos de la vía aérea, entre otros, la mortalidad tardía posterior al egreso permanece estable en un 10%, siendo la reestenosis recurrente de la vía aérea la causa principal. En nuestro caso, la reestenosis recurrente y refractaria secundario a la formación de tejido de granulación fue la principal razón de reintervención (presente hasta en un 23% de las revisiones, incluida la malacia traqueobronquial). Hemos adoptado la recomendación de reconocer los datos clínicos de estridor y el aumento en las secreciones bronquiales y la evaluación broncoscópica secuencial entre la extubacion y los 10 días, a 1, 3 y 6 meses, y anual posterior a la traqueoplastia *slide* para el reconocimiento y la intervención temprana de estas complicaciones tardías[10].

Conclusiones

La traqueoplastia *slide* es el tratamiento quirúrgico de elección para la ETC compleja. La broncoscopia es la herramienta diagnóstica y de seguimiento idónea, junto a la angiotomografía y la evaluación de la comorbilidad asociada. Se puede ofrecer una estrategia quirúrgica aceptable; con una modificación a la descripción original es posible, en nuestro medio, ofertar la reconstrucción traqueal por deslizamiento sin los factores de riesgo asociados al BCP y con la participación de un equipo multidisciplinario.

Agradecimientos

Los autores agradecen el profesionalismo del personal médico asistencial y de enfermería en las unidades de cuidados intensivos críticos, endoscópicos y anestésicos del Intituto Nacional de Pediatría, por su apoyo en esta publicación, en especial a su equipo de cirugía pediátrica.

Financiamiento

Los autores declaran no haber recibido ningún financiamiento.

Conflicto de intereses

Los autores declaran no tener ningún conflicto de intereses.

Consideraciones éticas

Protección de personas y animales. Los autores declaran que para esta investigación no se han realizado experimentos en seres humanos ni en animales.

Confidencialidad, consentimiento informado y aprobación ética. Los autores han seguido los protocolos de confidencialidad de su institución, han obtenido el consentimiento informado de los pacientes, y cuentan con la aprobación del Comité de Ética. Se han seguido las recomendaciones de las guías SAGER, según la naturaleza del estudio.

Declaración sobre el uso de inteligencia artificial. Los autores declaran que no utilizaron ningún tipo de inteligencia artificial generativa para la redacción de este manuscrito.

Bibliografía

1. Sengupta A, Murthy RA. Congenital tracheal stenosis and associated cardiac anomalies: operative management and techniques. J Thorac Dis. 2020;12:1184-93.
2. Tsang V, Murday A, Gillbe C, Goldstraw P. Slide tracheoplasty for congenital funnel-shaped tracheal stenosis. Ann Thorac Surg. 1989;48:632-5.
3. Manning PB, Rutter MJ, Lisec A, Gupta R, Marino BS. One slide fits all: the versatility of slide tracheoplasty with cardiopulmonary bypass support for airway reconstruction in children. J Thorac Cardiovasc Surg. 2011;141:155-61.
4. Stephens EH, Wiedermann J, Dearani JA. Expert technique: pediatric tracheal surgery. World J Pediatr Congenit Heart Surg. 2021;12:414-7.
5. Butler CR, Speggiorin S, Rijnberg FM. Outcomes of slide tracheoplasty in 101 children: a 17-year single-center experience. J Thorac Cardiovasc Surg. 2014;147:1783-9.
6. Wu Y, Wang G, Dai J. Slide tracheoplasty for congenital tracheal stenosis repair: a systematic review and meta-analysis. Laryngoscope. 2022;132:1532-41.
7. Grillo H, Wright C, Vlahakes JV. Management of congenital tracheal stenosis by means of slide tracheoplasty or resection and reconstruction, with long-term follow-up of growth after slide tracheoplasty. J Thorac Cardiovasc Surg. 2002;123:145-52.
8. Zhang H, Wang S, Lu Z. Slide tracheoplasty in 81 children: improved outcomes with modified surgical technique and optimal surgical age. Medicine (Baltimore). 2017;96:e8013.
9. OkamotoT, Nishijima E, Maruo A. Congenital tracheal stenosis: the prognostic significance of associated cardiovascular anomalies and the optimal timing of surgical treatment. J Pediatr Surg. 2009;44:325-8.
10. Antón-Pacheco JL, Comas JV, Luna C. Treatment strategies in the management of severe complications following slide tracheoplasty in children. Eur J Cardiothorac Surg. 2014;46:280-5.

Sinus pilonidal de localización perianal. Difícil diagnóstico diferencial con fístula perianal

Pilonidal sinus of perianal location. Difficult differential diagnosis with perianal fistula

Laura Rubio-López, Silvia Benito-Barbero, Paloma Guillamot-Ruano y Javier Páramo-Zunzunegui*
Servicio de Cirugía General y del Aparato Digestivo, Hospital Universitario de Móstoles, Móstoles, Madrid, España

Resumen

La enfermedad pilonidal generalmente surge en el área sacrococcígea en varones jóvenes. Se presenta el caso de un varón de 39 años con diagnóstico inicial de fístula perianal. A pesar de la exploración clínica y la resonancia magnética pélvica, solo durante la cirugía se evidenció que el origen de la fístula se encontraba en una enfermedad pilonidal perianal. El sinus pilonidal perianal es muy raro en la literatura. A menudo se confunde con otras enfermedades perianales, como la fístula anal. Por ello, la enfermedad pilonidal perianal debe tenerse en cuenta en el diagnóstico diferencial de la fístula perianal.

Palabras clave: *Sinus pilonidal. Fístula. Ano.*

Abstract

Pilonidal disease usually arises in the sacrococcygeal area in young men. We present a case of a 39-year-old male with an initial diagnosis of perianal fistula. Despite clinical examination and pelvic magnetic resonance image, only during surgery was revealed that the origin of the fistula was in perianal pilonidal disease. Perianal pilonidal sinus are very rare in the literature. It is often confused with other perianal diseases such as anal fistula. Thus, perianal pilonidal disease should be considered in the differential diagnosis of perianal fistula.

Keywords: *Pilonidal sinus. Fistula. Anus.*

***Correspondencia:**
Laura Rubio-López
E-mail: lrubiol@salud.madrid.org

Fecha de recepción: 11-06-2022
Fecha de aceptación: 29-06-2022
DOI: 10.24875/CIRU.22000314

Cir Cir. 2025;93(2):231-233
Contents available at PubMed
www.cirugiaycirujanos.com

Introducción

La enfermedad pilonidal es una patología supurativa que afecta con mayor frecuencia a varones de entre 15 y 30 años. Se caracteriza por un quiste de contenido piloso, localizado en la región sacrococcígea, que puede infectarse y fistulizar a la piel[1]. La presencia de sinus pilonidales localizados en la región perianal es muy infrecuente.

Caso clínico

Varón de 39 años, sin cirugías anales previas ni otros antecedentes de interés, valorado en consulta por un cuadro de supuración perianal intermitente de 1 año de evolución. En la exploración física presentaba un orificio fistuloso externo (OFE) localizado a las 2 horas, a 3 cm del margen anal en posición de litotomía, con supuración activa y sin alteraciones en el tacto rectal. Las imágenes ponderadas en T2 de la resonancia magnética (RM) pélvica (Fig. 1), aparentemente, mostraron una fístula transesfinteriana anterior con una pequeña colección hiperintensa en el pliegue interglúteo. Ante la sospecha de fístula anal se realizó una exploración quirúrgica (Fig. 2), observando un OFE localizado a las 2 horas, con signos de abscesificación, y otro OFE a las 7 horas en litotomía. Así mismo, asociaba un orificio pilonidal en la región coccígea. Se canularon los OFE y se inyectó peróxido de hidrógeno, sin evidenciar comunicación con el canal anal en la anuscopia, al contrario de lo que sugería la RM. El OFE a las 2 horas comunicaba con la cavidad abscesual y el OFE de las 7 horas comunicaba con la fosita pilonidal posterior. Se realizaron fistulotomías, que mostraron cavidades pilonidales crónicas, con gran contenido piloso y de granulación (Fig. 3). Se efectuaron escisiones completas de las cavidades pilonidales y posterior marsupialización de los bordes para favorecer el cierre por segunda intención. Al mes y medio de la intervención (Fig. 4), el paciente se encontraba asintomático, con una correcta cicatrización de las heridas quirúrgicas. Tras 2 años de seguimiento, el paciente no muestra datos de recidiva.

Discusión

El diagnóstico de sinus pilonidal suele ser sencillo. Es un diagnóstico clínico, basado en la presencia de un orificio pilonidal en la parte superior del surco interglúteo, a 4-10 cm del margen anal[1]. La enfermedad pilonidal crónica se presenta con cicatrices y fístulas que se comunican con la piel, limitándose casi exclusivamente a la región sacrococcígea y sin comunicar con el canal anal. Sin embargo, en la literatura científica se han publicado reducidos casos de enfermedad pilonidal de localización perianal, en los que, como en nuestro paciente, no se llega al diagnóstico correcto hasta la exploración quirúrgica[2-8].

La RM pélvica es la prueba de imagen de elección para el diagnóstico diferencial de la enfermedad perianal, presentando una sensibilidad del 100% y una especificidad del 98% para el diagnóstico de fístula perianal, y resulta de gran utilidad en la planificación preoperatoria[9]. No obstante, tal como defiende Sert[2], no es útil en el diagnóstico diferencial entre fístula perianal y enfermedad pilonidal perianal, lo cual pensamos que se debe, en parte, al bajo índice de sospecha de esta última.

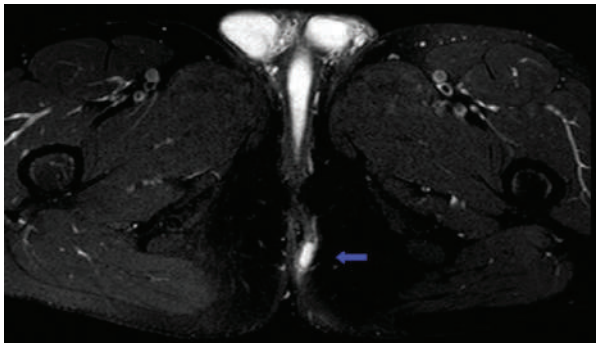

Figura 1. *Resonancia magnética pélvica (imagen ponderada en T2) que muestra una fístula transesfinteriana anterior con una pequeña colección hiperintensa en el pliegue interglúteo (flecha).*

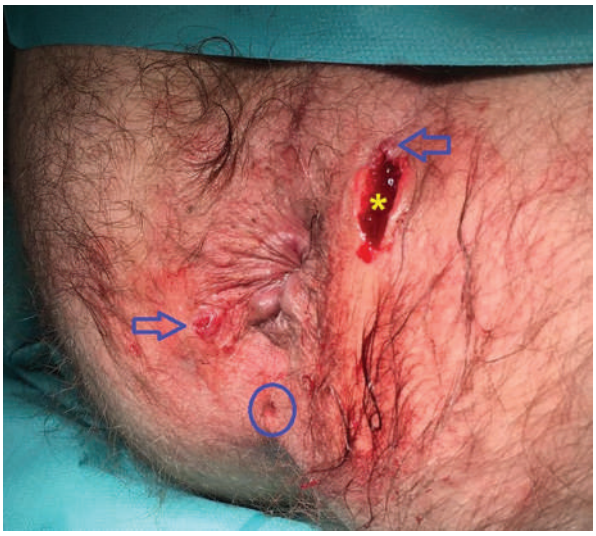

Figura 2. *Exploración quirúrgica. Se observan dos orificios fistulosos externos, uno localizado a las 2 horas (flecha), con signos de abscesificación (asterisco), y otro a las 7 horas en litotomía (flecha). Así mismo, asociaba un orificio pilonidal en la región coccígea (círculo).*

Figura 3. *Fistulotomías que muestran unas cavidades pilonidales crónicas, con contenido piloso y de granulación.*

Figura 4. *Cicatrización de las heridas quirúrgicas al mes y medio de la intervención.*

Autores como Eberspacher et al.[3] y Aggarwal et al.[4] reportan que, de manera infrecuente, la enfermedad pilonidal perianal puede producir abscesos que fistulicen al canal anal. En nuestro paciente, aunque el quiste pilonidal no presentaba aparente relación con los esfínteres, ni evidencia de fístula anal, existiría el riesgo de que a largo plazo la hubiera desarrollado.

El tratamiento de la enfermedad pilonidal perianal se basa en los mismos principios que en la localización sacrococcígea, teniendo especial cuidado en la obliteración del trayecto fístuloso y la preservación de los esfínteres. Sert[2] realizó manejo conservador mediante incisión y fenolización, pero la técnica más empleada en los casos publicados ha sido la escisión, con o sin cierre primario[3,5,7,8]. En nuestro paciente se realizó una escisión amplia con marsupialización de los bordes y cierre por segunda intención, con buenos resultados durante el seguimiento.

Conclusiones

El sinus pilonidal de localización perianal es muy infrecuente en la práctica clínica, pero debe tenerse en cuenta en el diagnóstico diferencial de la fístula perianal, sobre todo en aquellos pacientes con diagnóstico simultáneo de sinus pilonidal. Por último, consideramos que nuestro paciente puede ser agregado a los escasos casos clínicos publicados.

Financiamiento

Los autores declaran no haber recibido ningún tipo de financiamiento.

Conflicto de intereses

Los autores no presentan conflicto de intereses.

Consideraciones éticas

Protección de personas y animales. Los autores declaran que para esta investigación no se han realizado experimentos en seres humanos ni en animales.

Confidencialidad, consentimiento informado y aprobación ética. Los autores han obtenido la aprobación del Comité de Ética para el análisis de datos clínicos obtenidos de forma rutinaria y anonimizados, por lo que no fue necesario el consentimiento informado. Se han seguido las recomendaciones pertinentes

Declaración sobre el uso de inteligencia artificial. Los autores declaran que no utilizaron ningún tipo de inteligencia artificial generativa para la redacción de este manuscrito.

Bibliografía

1. de Parades V, Bouchard D, Janier M, Berger A. Pilonidal sinus disease. J Visc Surg. 2013;150:237-47.
2. Sert OZ. Pilonidal sinus of the perianal region: difficult to diagnose. Int J Surg Case Rep. 2020;72:96-8.
3. Eberspacher C, Mascagni D, Fralleone L, Grimaldi G, Antypas P, Mascagni P, et al. Pilonidal disease mimicking anterior anal fistula and associated with posterior anal fistula: a two-step surgery. Case report. G Chir. 2017;38:313-7.
4. Aggarwal K, Jain BK, Sharma N, Goel S. Pilonidal sinus of anal canal: a possible unique diagnosis. ANZ J Surg. 2015;85:693-4.
5. Iqbal CW, Gasior AC, Snyder CL. Pilonidal disease mimicking fistula-in-ano in a 15-year-old female. Case Rep Surg. 2012;2012:310187.
6. Alrawashdeh W, Ajaz S, Hammond TM, Porrett TR, Lunniss PJ. Primary anal pilonidal disease. Colorectal Dis. 2008;10:303-4.
7. Testini M, Miniello S, Di Venere B, Lissidini G, Esposito E. Perineal pilonidal sinus. Case report. Ann Ital Chir. 2002;73:339-41.
8. Vallance S. Pilonidal fistulas mimicking fistulas-in-ano. Br J Surg. 1982;69:161-2.
9. Balcı S, Onur MR, Karaosmanoğlu AD, Karçaaltıncaba M, Akata D, Konan A, et al. MRI evaluation of anal and perianal diseases. Diagn Interv Radiol. 2019;25:21-7.

CARTA AL EDITOR

Variante genética HbaI de *APOE* como factor epidemiológico para el deterioro cognitivo post-COVID-19 en población amerindia de Oaxaca

HbaI genetic variant of APOE as an epidemiological factor for post COVID-19 cognitive impairment in the Amerindian population of Oaxaca

Carlos E. Cabrera-Pivaral

Departamento de Salud Pública, Centro Universitario de Ciencias de la Salud, Universidad de Guadalajara, Guadalajara, Jalisco, México

Señor Editor:

El deterioro cognitivo y el riesgo de demencia son comunes en los pacientes que tuvieron la infección por SARS-CoV-2 (COVID-19), diabéticos y adultos mayores. El número de personas con este padecimiento se ha proyectado que alcanzará 115.4 millones en el año 2050 a nivel global, actualmente como parte de la COVID-19 prolongada[1]. En población adulta mayor en México se ha reportado que el alelo E4 de *APOE* está asociado con los grados de deterioro cognitivo. Basados en lo anterior, se estudiaron 690 pacientes con diabetes tipo 2 originarios del Estado de Oaxaca, con ancestría zapoteca y que tuvieron COVID-19 corroborada por qRT-PCR *(quantitative real time polymerase chain reaction),* con un rango de edad de 30-45 años, de los cuales 286 presentaban deterioro cognitivo de leve a moderado evaluado mediante la escala 3MSE. El riesgo de desarrollo se estimó mediante el cálculo de la razón de momios con intervalo de confianza del 95% acorde al cociente de Wolf. Mediante la técnica de PCR-FRLP *(polymerase chain reaction - restriction fragment length polymorphism)* se estimaron los genotipos para *APOE* con la enzima HbaI[2,3]. Se detectaron los tres alelos que conducen a cambios de aminoácido en los residuos 122 y 158 de la apolipoproteína E: el alelo E3 (112cis-158arg), el alelo E2 (112cis-158cis) y el alelo E4 (112arg-158arg)[2,3]. Así, el genotipo más frecuente en la población analizada fue el homocigoto E3/E3 y E3/E4. Se encontró una asociación positiva como factor de riesgo para el deterioro cognitivo al genotipo E3-E4, E2-E3 y para los portadores del alelo E4; como factor protector, al genotipo E3-E3, el alelo E3 y los homocigotos (Tabla 1).

Este es el primer reporte que muestra la participación del gen *APOE* en el síndrome de COVID-19 prolongada, particularmente el deterioro cognitivo post-COVID-19. En México, los genotipos con los alelos E2 y E4 están implicados con diabetes y alteraciones metabólicas[3,4]. Los presentes resultados son similares a los reportado para los alelos E4 y E2 de *APOE* en estudios previos[3,4], por lo cual, en los pacientes con COVID-19 y que son diabéticos, ser portador del alelo E4 o del genotipo E2-E3 incrementa el riesgo de deterioro cognitivo como una manifestación de la COVID-19 prolongada.

Agradecimientos

El autor agradece a CB-Xpert Laboratorio de Patología Clínica, Miahuatlán de Porfirio Díaz, Oaxaca, México, Servicios Médicos Profesionales Particulares A.C., por su apoyo en la realización del trabajo.

Correspondencia:
Carlos E. Cabrera-Pivaral
E-mail: carlos.pivaral@academicos.udg.mx

Fecha de recepción: 13-07-2022
Fecha de aceptación: 13-11-2022
DOI: 10.24875/CIRU.22000362

Cir Cir. 2025;93(2):234-235
Contents available at PubMed
www.cirugiaycirujanos.com

Tabla 1. Variantes de *APOE* en el deterioro cognitivo por Covid-19

Genotipo	Diabéticos tipo 2 con Covid-19 sin DC	Diabéticos tipo 2 con Covid-19 con DC	ORR	p	x^2	IC95%
E2-E2	4	2	1.14	0.6853	0.0001179	0.6452, 2.014
E2-E3	2	14	2.231	0.0001003	13.19 corregida	1.812, 2.746
E2-E4	2	4	1.617	0.2083	1.586	0.9119, 2.867
E3-E3	252	146	0.6699	0.000000932	24.06	0.5699, 0.7873
E3-E4	140	102	0.843	0.05731	3.614	0.7045, 1.009
E4-E4	4	18	6.039	0.0002274	13.59 corregida	1.64, 2.535
Alelo						
E2	12	22	0.3769	0.04874	3.884	0.1378, 1.031
E3	646	408	0.7695	0.008624	6.899	0.6385, 0.9273
E4	150	142	1.228	0.04919	3.869	1.009, 1.495

Financiación

El autor declara que el artículo fue financiado por la Fundación Mexicana de Enfermedades Genéticas y Medicina Genómica A.C.

Conflicto de intereses

El autor declara no tener conflicto de intereses.

Responsabilidades éticas

Protección de personas y animales. El autor declara que los procedimientos seguidos se conformaron a las normas éticas del comité de experimentación humana responsable y de acuerdo con la Asociación Médica Mundial y la Declaración de Helsinki.

Confidencialidad de los datos. El autor declara que ha seguido los protocolos de su centro de trabajo sobre la publicación de datos de pacientes.

Derecho a la privacidad y consentimiento informado. El autor ha obtenido el consentimiento informado de los pacientes o sujetos referidos en el artículo. Este documento obra en su poder.

Bibliografía

1. Shih IF, Paul K, Haan M, Yu Y, Ritz B. Physical activity modifies the influence of apolipoprotein E ε4 allele and type 2 diabetes on dementia and cognitive impairment among older Mexican Americans. Alzheimers Dement. 2018;14:1-9.
2. Hixson JE, Vernier DT. Restriction isotyping of human apolipoprotein E by gene amplification and cleavage with HhaI. J Lipid Res. 1990;31:545-8.
3. Martínez-López E, Curiel LF, Hernández NZ, Moreno LE, Ramos ME, Román S, et al. Influence of ApoE and FABP2 polymorphisms and environmental factors in the susceptibility to gallstone disease. Ann Hepatol. 2015;14:515-23.
4. Genís-Mendoza AD, Martínez-Magaña JJ, Bojórquez C, Téllez-Martínez JA, Jiménez-Genchi J, Roche A, et al. Programa de detección del alelo APOE-E4 en adultos mayores mexicanos con deterioro cognitivo. Gac Med Mex. 2018;154:555-60.

LETTER TO THE EDITOR

Elective surgery in patients with asymptomatic COVID-19 infection: the other side of the coin

Cirugía electiva en pacientes asintomaticos con COVID-19: la otra cara de la moneda

*Sol Ramírez-Ochoa[1,2], Jorge I. Michel-González[1,2], Daniela Deossa-Piedrahita[1,2], José L. Sánchez-Reynoso[1,2], Shaúl A. Navarro-Lara[1,2], Octavio Ponce-Orozco[1,2], Fernando Burciaga-Zavala[1,2], Carlos J. Moreno-Bernardino[1,2], Ricardo A. Villanueva-Zavala[1,2], and Enrique Cervantes-Pérez[1,3]**

[1]Department of Internal Medicine, Hospital Civil de Guadalajara "Fray Antonio Alcalde"; [2]Health Sciences University Center, Universidad de Guadalajara, Guadalajara; [3]Centro Universitario de Tlajomulco, Universidad de Guadalajara, Tlajomulco de Zúñiga. Jalisco, México*

To the Editor:

Global health systems have been significantly impacted by the coronavirus disease-19 pandemic. During the initial peak disruption, millions of elective procedures were postponed or canceled, and for a variety of reasons, it was anticipated that elective surgery case volumes would continue to fall. A notable worry is the safety of the patient. Early research has shown that severe acute respiratory syndrome coronavirus 2 (SARS-CoV-2) surgical patients had higher mortality rates and cardiovascular problems, possibly more than non-surgical SARS-CoV-2 hospitalized patients. The relative risk of these problems in SARS-CoV-2 patients compared to uninfected controls, however, it was not clearly characterized[1].

A combination of lower virulence of circulating variations, vaccination programs, and natural immunity from prior infection are likely to be responsible for the observed trends toward less severe infection and fewer sequelae associated with SARS-CoV-2 infection, compared with 2020. It is pre-mature to assume that this will result in a decrease in perioperative problems from SARS-CoV-2 infection and a consequent change the recommended window of time between infection and elective surgery[2]. Although it is positive that all infections tend to be less severe in hospitalized patients with acute medical illnesses, it is unclear how this applies to perioperative patients and the resulting impact on morbidity and mortality after surgery. Evidence from surgical patients does not support the claim that the gap between asymptomatic SARS-CoV-2 infection and elective surgery might be reduced to 5 days.

The prospective CovidSurg Week research provides the most reliable data on the timing and safety of surgery following SARS-CoV-2 infection worldwide. These data comprised patients receiving both elective (n = 97,442) and emergency (n = 42,778) surgery during October and November 2020 in 116 countries. Seven weeks after infection, the unfavorable effects of SARS-CoV-2 infection remained in both asymptomatic and symptomatic individuals having both major and minor procedures. This is mirrored in multidisciplinary consensus guidelines issued by the Centre for Perioperative Care, which advocate a 7-week wait following SARS-CoV-2 infection, including in patients without symptoms, before surgery. The lack of data regarding the impact of vaccination or the Omicron variation on perioperative outcomes is highlighted in a fairly recent update to these guidelines, which also challenges the notion that a mild or asymptomatic infection does not raise the risk of perioperative complications[3,4]. Given evolving viral pathogenicity, rising vaccination rates, and innate immunity, it is conceivable that there may come a time in the future when no delay is necessary for vaccinated patients with asymptomatic infection. Besides, it's possible that even people with the symptomatic disease will be treated similarly to those who have upper

***Correspondence:**
Enrique Cervantes-Pérez
E-mail: enrique.cervantes@academico.udg.mx

Date of reception: 22-12-2022
Date of acceptance: 03-09-2023
DOI: 10.24875/CIRU.22000642

Cir Cir. 2025;93(2):236-237
Contents available at PubMed
www.cirugiaycirujanos.com

or lower respiratory tract infections, with delays only as long as they are needed for the patient to become asymptomatic and return to baseline health. It is unknown, though, whether or when we will reach this position or in what circumstances. The most recent study evaluated the outcomes of asymptomatic SARS-CoV-2 polymerase chain reaction (PCR)-positive patients who underwent general anesthesia and surgery and were compared with controls. The study found that surgery among asymptomatic PCR-positive patients was not associated with increased mortality[5].

The choice to postpone surgery may be impacted by a number of competing hazards, which may differ between nations and health systems. We must encourage the use of consensus recommendations that incorporate the best available data. Nevertheless, there are still gaps in the literature as it pertains to the dynamic international clinical setting.

Funding

The authors declare that they have not received funding.

Conflicts of interest

The authors declare no conflicts of interest.

Ethical considerations

Protection of humans and animals. The authors declare that no experiments involving humans or animals were conducted for this research.

Confidentiality, informed consent, and ethical approval. The study does not involve patient personal data nor requires ethical approval. The SAGER guidelines do not apply.

Declaration on the use of artificial intelligence. The authors declare that no generative artificial intelligence was used in the writing of this manuscript.

References

1. Clancy PW, Knio ZO, Zuo Z. Positive SARS-CoV-2 detection on intraoperative nasopharyngeal viral testing is not associated with worse outcomes for asymptomatic elective surgical patients. Front Med (Lausanne). 2022;9:1065625.
2. Lieberman N, Racine A, Nair S, Semczuk P, Azimaraghi O, Freda J, et al. Should asymptomatic patients testing positive for SARS-CoV-2 wait for elective surgical procedures? Br J Anaesth. 2022;128:e311-4.
3. COVIDSurg Collaborative, GlobalSurg Collaborative. Timing of surgery following SARS-CoV-2 infection: an international prospective cohort study. Anaesthesia. 2021;76:748-58.
4. El-Boghdadly KC, Cook TM, Goodacre T, Kua J, Blake L, Denmark S, et al. SARS-CoV-2 infection, COVID-19 and timing of elective surgery: a multidisciplinary consensus statement on behalf of the Association of Anaesthetists, the Centre for Peri-operative Care, the Federation of Surgical Specialty Associations, the Royal College of Anaesthetists and the Royal College of Surgeons of England. Anaesthesia. 2021;76:940-6.
5. Aydın O, Ergen P, Vahaboglu H. Safety of surgery among asymptomatic SARS-CoV-2 pcr-positive patients: a single-center retrospective cohort study. World J Surg. 2023;47:573-7.

CARTA AL EDITOR

Tratado sobre pandemias: discusiones preliminares

Pandemic treaty: preliminary discussions

Miguel Gallegos

Facultad de Ciencias de la Salud, Universidad Católica del Maule, Talca, Chile; Facultad de Psicología, Universidad Nacional de Rosario, Santa Fe, Argentina; Centro Interdisciplinario de Investigaciones en Ciencias de la Salud y el Comportamiento, Consejo Nacional de Investigaciones Científicas y Técnicas, Buenos Aires, Argentina

Los efectos de la pandemia de COVID-19 todavía siguen vigentes, no solo respecto a la circulación del virus y las secuelas post-COVID-19, sino también en cuanto a la discusión de cómo estar mejor preparados para futuras crisis de salud pública internacional. En 2021 se abrió una discusión acerca de los instrumentos vigentes de la política internacional para afrontar las pandemias[1,2], en la que se planteó la necesidad de revisar el Reglamento Sanitario Internacional (RSI), cuya función precisamente consiste en orientar las acciones durante emergencias de salud pública internacional[1].

Por la magnitud de las consecuencias de la reciente pandemia se han reactivado las dudas y las críticas sobre la capacidad del RSI para afrontar una crisis de salud internacional. Se ha señalado la poca eficacia del RSI para el cumplimiento de los acuerdos por parte de los países, así como la escasa autoridad de la Organización Mundial de la Salud (OMS) para logar el acatamiento de las directrices[2,3]. En consecuencia, diferentes líderes mundiales y la propia OMS realizaron un llamado para discutir la elaboración de un nuevo tratado sobre pandemias. Varios autores ya fijaron diferentes ideas acerca de la orientación y el contenido que debería contener el nuevo documento de política internacional (Tabla 1).

Tabla 1. Temas de consenso para abordar un nuevo tratado sobre pandemias

Extender la perspectiva de los derechos humanos y de salud pública.
Promover una perspectiva de «Salud Global» o «Una Salud».
Ampliar consensos y compromisos globales por parte de los gobiernos.
Garantizar la equidad en el acceso y la distribución de los recursos sanitarios.
Fomentar un mayor intercambio de información científica.
Establecer compromisos jurídicamente vinculantes para los gobiernos.
Exención de los derechos de propiedad intelectual para la producción de tecnología sanitaria.
Fortalecer los sistemas de salud y el financiamiento específico para crisis sanitarias.
Mejorar el sistema de información y comunicación de riesgos de salud pública.
Revisar el sistema de alarma de emergencia internacional.
Promover una mayor coordinación y gobernanza internacional en salud.
Enfatizar en las acciones de prevención de las pandemias.
Favorecer la coordinación con otros organismos internacionales.
Proporcionar mayor autoridad a la Organización Mundial de la Salud.

Correspondencia:
Miguel Gallegos
E-mail: maypsi@yahoo.com.ar

Fecha de recepción: 07-02-2024
Fecha de aceptación: 23-03-2024
DOI: 10.24875/CIRU.24000077

Cir Cir. 2025;93(2):238-239
Contents available at PubMed
www.cirugiaycirujanos.com

Si bien estos son algunos de los consensos más visibles entre los diferentes autores, también se ha llamado la atención sobre otros temas cruciales que deberían incorporarse en la discusión, tales como la mayor participación de la sociedad civil, la perspectiva de género, la discusión sobre el cambio climático, la ampliación de la visión del Sur Global y estimular una perspectiva crítica de la salud que limite las visiones hegemónicas y colonialistas[4,5]. En conclusión, el debate se encuentra abierto y resulta necesario dotar de mayor diversidad a la elaboración del nuevo tratado sobre pandemias.

Financiamiento

El autor declara no haber recibido financiamiento para este estudio.

Conflicto de intereses

El autor declara no tener conflicto de intereses.

Consideraciones éticas

Protección de personas y animales. El autor declara que para esta investigación no se han realizado experimentos en seres humanos ni en animales.

Confidencialidad, consentimiento informado y aprobación ética. El estudio no involucra datos personales de pacientes ni requiere aprobación ética. No se aplican las guías SAGER.

Declaración sobre el uso de inteligencia artificial. El autor declara que no utilizó ningún tipo de inteligencia artificial generativa para la redacción de este manuscrito.

Bibliografía

1. Labonté R, Wiktorowicz M, Packer C, Ruckert A, Wilson K, Halabi S. A pandemic treaty, revised international health regulations, or both? Global Health. 2021;17:128.
2. Singh S, Bartos M, Abdalla S, Legido-Quigley H, Nordström A, Sirleaf EJ, et al. Resetting international systems for pandemic preparedness and response. BMJ. 2021;375:e067518.
3. Gostin LO, Meier BM, Stocking B. Developing an innovative pandemic treaty to advance global health security. J Law Med Ethics. 2021;49:503-8.
4. Phelan AL, Carlson CJ. A treaty to break the pandemic cycle. Science. 2022;377:475-7.
5. Fukuda-Parr S, Buss P, Ely Yamin A. Pandemic treaty needs to start with rethinking the paradigm of global health security. BMJ Glob Health. 2021;6:e006392.